The Dissertation Committee for María Fé Lanfranco Gallofré certifies that this is the approved version of the following dissertation:

THE SEROTONIN (5-HT) 2C RECEPTOR (5-HT_{2C}R) AND ITS DOWNSTREAM SIGNALING COMPONENTS: DISTINCT ADAPTATIONS IN CORTICAL CIRCUITS ASSOCIATED WITH COCAINE EXPOSURE

Committee:

Kathryn A. Cunningham, Ph.D.
Supervisor

Xiaodong Cheng, Ph.D.

William P. Clarke, Ph.D.

Kenneth M. Johnson, Ph.D.

Cheryl S. Watson, Ph.D.

Dean, Graduate School

THE SEROTONIN (5-HT) 2C RECEPTOR (5-HT_{2C}R) AND ITS DOWNSTREAM SIGNALING COMPONENTS: DISTINCT ADAPTATIONS IN CORTICAL CIRCUITS ASSOCIATED WITH COCAINE EXPOSURE

by

María Fé Lanfranco Gallofré, BSc

Dissertation

Presented to the Faculty of the Graduate School of

Biomedical Sciences at Galveston

The University of Texas Medical Branch

in Partial Fulfillment of the Requirements

for the Degree of

Doctor of Philosophy

The University of Texas Medical Branch

May, 2009

Dedication

To my grandmother, parents and brothers;

In memory to my grandparents Graciela, Orlando and Juan

ACKNOWLEDGMENTS

I would like to express my sincere gratitude to Dr. Kathryn A. Cunningham for her inspiration, enthusiasm, guidance, and assistance during my education and in the production and presentation of this work. I also thank my dissertation committee members Dr. Xiaodong Cheng, Dr. William P. Clarke, Dr. Kenneth M. Johnson and Dr. Cheryl S. Watson for their constant support and input throughout these years. I also thank Drs. William Clarke and Kelly Berg for kindly providing the plasmid containing the cDNA for the 5-HT_{2C}R non-edited isoform used in our studies. Dr. Elaine Sanders-Bush and Dr. Ronald Emeson kindly provided the plasmids containing cDNA for the A, B, D, AD, ABD, ABCD and ABECD edited isoforms and total RNA from the VGV- and INI- expressing mutant mice (129S6 background) used in our studies. I would like to thank Dr. Concepcion Diaz-Arrastia, MD, Assistant Professor, Gynecologic Oncology at the University of Texas Medical Branch (UTMB) for providing access to the 7500 Fast real-time PCR equipment for our studies. I thank Dr. José Morón-Concepción from the Center for Addiction Research and Dept. of Pharmacology and Toxicology at UTMB for providing the synaptosomal fractionation protocol. I would also like to express my appreciation to Dr. Patricia Seitz and Adriane dela Cruz for their thoughtful comments and advice on these experiments and presentation of the data. I would like to thank Sonja Stutz and Bob Fox for their technical assistance and James Grady for his help with the statistical analysis of

these experiments. This research was supported by the National Institute on Drug Abuse grants DA006511, DA000260, DA016905, DA020087 (KAC); NS33323 (RBE) and by the Peter F. McManus Charitable Trust (KAC).

THE SEROTONIN (5-HT) 2C RECEPTOR (5-HT_{2C}R) AND ITS DOWNSTREAM SIGNALING COMPONENTS: DISTINCT ADAPTATIONS IN CORTICAL CIRCUITS ASSOCIATED WITH COCAINE EXPOSURE

Publication No._____

María Fé Lanfranco Gallofré, Ph.D.
The University of Texas Medical Branch, 2009

Supervisor: Kathryn A. Cunningham

Repeated intermittent cocaine administration results in a progressive augmentation of motor stimulant responses to subsequent drug challenge. Neuronal adaptations underlying this enduring behavioral transformation, known as behavioral sensitization, have been proposed to mediate the incentive motivational effects of cocaine that contribute to increased anxiety, craving and paranoia observed in cocaine addicts. Neuroadaptations in the serotonin $(5\text{-HT})_{2C}$ receptor (5-HT_{2C}R) system, which exerts an inhibitory influence over the limbic-corticostriatal circuitry and has been implicated in modulating cocaine-evoked behaviors, may play a key role in the development and maintenance of behavioral sensitization. However, the sensitivity of 5-HT_{2C}R is diminished after withdrawal from a sensitizing cocaine regimen, suggesting that 5-HT_{2C}R function

or its downstream signaling components are significantly altered. Cortical brain areas, including motor cortex and prefrontal cortex (PFC), are important sites of action for 5-HT_{2C}R control of cocaine-induced behaviors and are strongly implicated in cocaine-craving and cocaine-seeking behaviors. We investigated changes in four neuroadaptations that could contribute to functional 5-HT_{2C}R subsensitivity following repeated cocaine administration: 1) 5-HT_{2C}R protein expression and subcellular localization; 2) 5-HT_{2C}R mRNA editing; 3) expression and subcellular localization of postsynaptic-density (PSD) protein-95 (PSD-95); and 4) phosphorylation of p44/p42-mitogen-activated protein kinases (p44/p42-MAPK), which influences activity of molecules involved in 5-HT_{2C}R trafficking. We found decreased 5-HT_{2C}R protein expression in total homogenate and PSD compartment of motor cortex and an apparent shift in edited 5-HT_{2C}R mRNA isoforms in the PFC at day 3 of withdrawal from a repeated cocaine regimen. Acute cocaine administration resulted in redistribution of PSD-95 and p42-MAPK to the PSD in motor cortex, but not in PFC. Cocaine challenge following a sensitizing cocaine regimen increased phospho-p42-MAPK in total homogenate only in motor cortex. Our results suggest distinct regulatory mechanisms for 5-HT_{2C}R function in motor cortex and PFC, with motor cortex being more responsive to the pharmacological effects of cocaine. The combination of these neuroadaptations could strengthen the cortico-striatal circuit and activate the reward pathway, exacerbating the behavioral effects of cocaine and contributing

to the expression of sensitization, which could parallel the tendency for cocaine use to escalate to addiction in humans.

Table of Contents

List of Tables

List of Figures

Abbreviations

5-HT:	Serotonin
5-HT$_{2C}$R:	5-HT$_{2C}$ receptor
ACC:	Anterior cingulate cortex
CBF:	Glucose metabolism and cerebral blood flow
CC:	Cocaine pretreated-cocaine challenge
CNS:	Central nervous system
CPP:	Conditioned place preference
CREB:	cAMP response element binding transcription factor
CS:	Cocaine pretreated-saline challenge
CT:	Crossing threshold
DA:	Dopamine
DAG:	Diacylglycerol
ΔCt:	Delta Ct, average crossing threshold
DOI:	(±)-1-(4-iodo-2,5-dimethoxyphenyl)-2-aminopropane
ERK:	Extracellular signal-regulated kinases
fMRI:	magnetic resonance imaging
GABA:	γ-aminobutyric acid
GPCR:	G-protein coupled receptor
GRK:	G-protein receptor kinase
IL:	Infralimbic prefrontal cortex
IP:	Intraperitoneal
IP$_3$:	Inositol-1,4,5-trisphosphate
MAGUK:	Membrane-associated guanylate kinase
MAPK:	Mitogen-activated protein kinase
MGB:	Minor groove binder
MOP:	Primary motor area
MOS:	Secondary motor area
MPP3:	MAGUK p55 subfamily member 3

NAc:	Nucleus accumbens
pCPA:	para-chlorophenylalanine
PDZ domain:	PSD-95/Disks-large (dlg) protein in Drosophila/Zone Occluden-1 (ZO-1) domain
PET:	Positron emission transmission
PFC:	Prefrontal cortex
PIP_2:	Phosphatidylinositol 4,5-bisphosphate
PKC:	Protein kinase C
PLC-β:	Phospholipase C-β
PrL:	Prelimbic prefrontal cortex
PSD-95:	Postsynaptic density-95
qRT-PCR:	Quantitative (real-time) reverse transcription polymerase chain reaction
SC:	Saline pretreated-cocaine challenge
SS:	Saline pretreated-saline challenge
SSRI:	Selective 5-HT reuptake inhibitor
TES:	Treatment Effectiveness Score
VTA:	Ventral tegmental area

CHAPTER 1: INTRODUCTION

Drug addiction is a chronic, relapsing neuropsychiatric disorder characterized by compulsive drug-seeking and drug-taking despite negative consequences (Everitt and Robbins, 2005; Kalivas and O'Brien, 2008; Thomas et al., 2008). Typically, initial drug use occurs as a component of exploration, novelty or pleasure-seeking, with a subpopulation of drug users exhibiting vulnerability to the transition from occasional drug use to drug abuse and dependence (Baler and Volkow, 2006; Nic Dhonnchadha and Cunningham, 2008). During this transition there is a motivational shift in which the drug is no longer taken for its pleasurable effects, but to avoid withdrawal and intense craving, leading to further drug use or relapse (Baler and Volkow, 2006). The serotonergic and dopaminergic neurotransmitter systems modulate cognition, emotion, mood, and reward; perturbations of these neurotransmitter systems are thought to contribute to several common neuropsychiatric disorders, including drug addiction (Koob et al., 1998). Several investigators have suggested that repeated administration of drugs of abuse leads to long-term behavioral, neurochemical and molecular adaptive responses in the brain. Such changes may play a major role in the formation of deep-rooted drug-seeking habits. The consequences of these adaptations include persistent addictive behaviors, stimulant-induced psychoses, maintenance of compulsive drug use and a high rate of relapse observed in drug addicts even after long periods of abstinence (Post and Rose, 1976; Robinson and Becker, 1986; Wolf et al., 2004; Hyman et

al., 2006; Le and Koob, 2007). Therefore, to further understand the etiology of addiction and improve therapeutic options, there is considerable interest to elucidate the biochemical mechanisms underlying these neuroadaptations.

Cocaine

One psychoactive drug with high abuse potential is the psychostimulant cocaine, a naturally occurring alkaloid found in the leaves of the *Erythroxylum coca* plant which grows in the Andes Mountains in South America. The cocaine alkaloid was originally isolated by the German chemist Friedrich Gaedcke in 1855. Later, Albert Niemann of the University of Gottingen noted the anesthetic properties of cocaine, and developed and improved the purification process (Goldstein et al., 2009). By the late 1800s, cocaine was widely used for its analgesic properties and was sold over-the-counter until 1916 (Goldstein et al., 2009). By the early twentieth century, the addictive properties of cocaine were well known, and, in 1970, cocaine was officially made illegal and classified as a Schedule II drug in the United States under the Controlled Substances Act.

Cocaine in its purest form is known as cocaine hydrochloride (HCl), which is water soluble, and is well absorbed intranasally through the mucosal membrane (“snorting”) and by intravenous injection. Cocaine can also be used as a “freebase”. Cocaine base form is not water soluble, and it is thus unsuitable for drinking, snorting or injecting. However, cocaine base vaporizes at lower temperatures, which makes it suitable for inhalation.

In a recent National Survey on Drug Use and Health (NSDUH, 2007), it was estimated that 19.9 million Americans (8.0% of the population) were considered to have a substance abuse or substance dependence disorder. Among those, 2.1 million (10% of drug abusers) were reported to be active cocaine users aged 12 or older (0.8% of the population) (2007 NSDUH Survey). Therefore, cocaine remains a significant public health problem.

Behavioral effects of cocaine in humans

Low doses of cocaine (< 100 mg) have been reported by users to induce euphoria, increase a sense of well-being and self-confidence, heighten energy and diminish fatigue and alertness. On the other hand, some cocaine users have reported anxiety, decreased appetite, feelings of restlessness, irritability, and sleep disturbances (Gawin, 1989; Gawin, 1991; Gold, 1992). Furthermore, there are medical complications associated with cocaine intoxication, including cardiac arrhythmia, seizures and myocardial infarction. While higher doses (several 100 mg) are used to intensify the high, users may also experience aggressiveness, disorientation, hallucinations, paranoia, muscle twitches, tremors and vertigo (Gold, 1992; for review, Goldstein et al., 2009).

Tolerance to the euphoric effects associated with short-term cocaine use may develop. Under this scenario, users frequently increase their doses to obtain the same euphoric effects of cocaine; however, users may also become more sensitive to cocaine's anesthetic and convulsant effects without increasing the dose taken, which may explain some cocaine-related deaths (Afonso et al., 2007;

for review, Goldstein et al., 2009). Prolonged cocaine use leads to addiction and a state of increasing irritability, mood disturbance, restlessness, and full-blown paranoid psychosis (Karch, 1999; Goldstein et al., 2009). Other major medical complications and health problems include auditory hallucinations, gastrointestinal problems, heart disease, heart attacks, respiratory failure, strokes and seizures (Afonso et al., 2007; for review, Goldstein et al., 2009).

While there are some medications approved by the Food and Drug Administration (FDA) to treat alcohol, nicotine or opioid addiction (Nutt and Lingford-Hughes, 2008), there are currently no approved medications to successfully treat cocaine addiction. While cognitive and behavioral therapies (*e.g.*, 12-step program) may provide an alternative treatment for cocaine addiction, a synergistic approach involving both pharmacological manipulation and behavioral intervention may be more successful in maintaining recovery from cocaine addiction (Volkow and Li, 2004). Therefore, there is considerable interest in understanding the neurobiological and pathophysiological processes leading to cocaine addiction.

Behavioral effects of cocaine in animals

Animal models of addiction are valuable tools for understanding the neurobiology of addiction. The following paradigms have been extensively used to investigate the reinforcing and rewarding effects of cocaine.

Locomotor activity: This paradigm is used to assess the stimulant effects of a drug. It is also an indirect measure of activation of the neuronal substrates targeted by drugs of abuse. For example, acute administration of low doses of cocaine (*e.g.*, 10-15 mg/kg) induces motor stimulatory effects, as well as an increase in rearing and mild sniffing behaviors in rodents (Post and Rose, 1976; Cunningham et al., 1992b). As the dose increases (>20 mg/kg), these behaviors are replaced by focused stereotypes and convulsions (Post and Rose, 1976). In addition to the acute effects of cocaine, repeated intermittent administration of cocaine results in the development of a phenomenon known as behavioral sensitization, which is characterized by an augmentation of the behavioral effects of the drug upon re-administration (Robinson and Becker, 1986; Kalivas and Stewart, 1991; Robinson and Berridge, 1993). This phenomenon has been hypothesized to parallel the shift from drug-liking to drug-wanting observed in humans (Robinson and Berridge, 1993; Kalivas et al., 1998).

Conditioned Place Preference (CPP): The CPP paradigm is based on classical Pavlovian conditioning in which drug administration is paired with a distinct environment and administration of vehicle with another distinct environment. After several drug pairings, drug-free animals are allowed access to both environments, and the time spent in each environment is measured. The time the animal spends in the drug-paired environment provides a measure of the reinforcing effect of a drug (Itzhak and Martin, 2002; Hyman et al., 2006). For example, after cocaine conditioning (20 mg/kg), Swiss Webster mice showed an

increase in time spent in the drug-paired compartment as compared to baseline (Itzhak and Martin, 2002). Furthermore, our laboratory has shown cocaine-induced CPP after one drug conditioning (dela Cruz et al. *submitted*), which exemplifies that cocaine is potently associated to cues and serves as a stimulus to evoke conditioning of a CPP.

Self-administration: Drugs with high abuse potential, such as cocaine, are readily self-administered intravenously. In the simplest version of a self-administration paradigm, animals acquire a drug infusion (intravenous) after performing a given task (*e.g.*, pressing a lever). However, there are several modifications [*e.g.*, varying the schedule of reinforcement, adding an environmental stimulus (noise, light, scent)] that may be included in the paradigm to address other aspects of cocaine addiction. For example, by requiring more lever presses for a single cocaine injection, we can measure how reinforcing a drug is in this paradigm. The point at which the effort required exceeds the reinforcing value of a drug is called the "breaking point" (for review, Shippenberg and Koob, 2008). Therefore, the higher the breaking point, the greater the motivation to take the drug (for review, Shippenberg and Koob, 2008). For example, rats reliably self-administer cocaine during a 1 hr sessions under the schedule of one infusion of cocaine (0.25 mg/kg/infusion) for each lever press (Fletcher et al., 2002; Fletcher et al., 2004). When that schedule of reinforcement was progressively increased (1-118 lever presses for cocaine infusion), it was

found that animals that self-administered cocaine presented higher breaking points compared to saline (Fletcher et al., 2002; Fletcher et al., 2004).

Extinsion/reinstatement procedure: This model of addiction is used to assess the incentive motivation for drugs of abuse. In this model, animals trained to self-administer drugs subsequently undergo extinction training, during which lever-presses do not result in drug delivery. Animals are then tested for reinstatement of extinguished cocaine-seeking behavior elicited by either cocaine-conditioned stimuli or cocaine priming (cocaine re-administration) (Burmeister et al., 2004).

By using these animal models, researchers have proposed that medications which decrease self-administration of cocaine without altering the choice for natural reinforcers would be useful to decrease cocaine use and subsequent relapse.

Cocaine: Mechanisms of action

The mechanisms of action underlying the rewarding and reinforcing effects of cocaine depends upon its ability to block the reuptake of dopamine (DA), serotonin (5-HT) and norepinephrine, thereby increasing the concentration of these neurotransmitters at the synapse. Ligand binding studies have shown that cocaine binds with greatest affinity to the 5-HT reuptake transporter (0.14 μM), followed by the dopamine (0.64 μM) and norepinephrine (1.60 μM) reuptake transporters (Ritz et al., 1990). Blockade of the norepinephrine reuptake

transporter results in an overstimulation of the α- and β-adrenergic receptors leading to an increase in arterial and left ventricular pressure, contractility and heart rate (Brownlow and Pappachan, 2002). Cocaine has also been shown to inhibit 5-HT_3R function by acting as a competitive antagonist for 5-HT binding site (dissociation constant of 7 μM, IC50 of 4.2 μM) (Carta et al., 2003). Furthermore, the serotonin (5-HT) 3 receptor (5-HT_3R) is the only ligand-gated ion channels from the serotonin receptor family, and although this receptor is expressed at relatively low densities in the brain, it is thought to have a presynaptic localization, thus regulating neurotransmitter release to the synapse (Carta et al., 2003).

Cocaine's interaction with the sigma (σ) receptor was first reported by Sharkey and collaborators in 1988. Cocaine activates σ1 receptor subtype, which is widely distributed in peripheral organ (*e.g.,* heart, kidney and lung) and localized in the brain stem motor regions and limbic structures (Matsumoto et al., 2003). Activation of this receptor by cocaine, might lead to convulsions and seizures observed in overdosed addicts (Matsumoto et al., 2003).

Finally, as a local anesthetic, cocaine blocks the fast voltage-gated Na^+ channels in neuronal membranes, and by preventing the fast inward Na^+ current, cocaine inhibits depolarization of the cell membrane thereby blocking the initiation and conductance of nerve impulses (Brownlow and Pappachan, 2002; Goldstein et al., 2009). Cocaine vasoconstriction effects are mediated by the

blockade of the norepinephrine reuptake transporter (for review, Goldstein et al., 2009).

Even though all of these neurotransmitter systems contribute to the physiological and psychological effects of cocaine, the neurochemical actions of cocaine that attracted most attentions is in its actions on DA neurotransmission. The rewarding effects of most drugs of abuse are mediated in large part by activation of the limbic-corticostriatal circuitry. A key component of this circuit originates in dopaminergic cell bodies in the ventral tegmental area (VTA) and terminates in limbic [*e.g.*, nucleus accumbens (NAc)], prefrontal cortex (PFC) and striatal regions [*e.g.,* dorsal striatum and caudate] [**Fig 1.1**, DA pathway (black)]. This DA pathway has been extensively implicated as a modulator of the rewarding properties of both natural stimuli (*e.g.*, food, sex drive, drink; for review, Kelley and Berridge, 2002) and addictive drugs (Volkow and Li, 2004; Valjent et al., 2004a). This pathway is innervated and modulated by the 5-HT neurotransmitter system, and our laboratory is particularly interested in the role of 5-HT in regulating neuronal transmission of the limbic-corticostriatal circuit to modulate addictive behavior. Serotonin mediates its physiological and psychological effects through several 5-HT receptors (5-HT_XR). These receptors have been classified into seven subfamilies, comprised of 14 different receptor subtypes on the basis of their function, pharmacology and molecular properties (Giorgetti and Tecott, 2004; Hannon and Hoyer, 2008). With the exception of the 5-HT_3R, which is a ligand-gated ion channel, all of the 5-HT receptors are

members of the G-protein coupled receptor (GPCR) family (Hannon and Hoyer, 2008). We are primarily interested in the role of the 5-HT_{2C} receptor (5-HT_{2C}R) subtype in modulating the behavioral effects of cocaine. Furthermore, this receptor has been implicated in mediating 5-HT actions that contribute to normal and psychiatric disorders including anxiety, depression and psychosis (Dubovsky and Thomas, 1995). Recently, 5-HT_{2C}R has been implicated in mediating addictive processes, especially for cocaine (Cunningham et al., 1986; Callahan and Cunningham, 1994; Filip and Cunningham, 2003; Cunningham et al., 2004; Filip et al., 2004; Bubar and Cunningham, 2006; Filip et al., 2006; Liu and Cunningham, 2006).

In theory, pharmacological manipulation of the DA pathway would seem to be an appealing target as therapeutical medication; however, in practice, dopaminergic ligands have not shown to be ideal for therapeutic medications in cocaine addiction due to their interference with normal physiological and behavioral functions dependent on the DA pathway (Carroll et al., 1999; Vetulani, 2001; Matsumoto et al., 2003; Carroll, 2005). Therefore, alternative neurotransmitter systems that modulate the DA pathway, such as the 5-HT system, are interesting targets for novel therapeutics for cocaine addiction.

Regional distribution of the 5-HT_{2C}R in brain

The understanding of the role of the 5-HT_{2C}R in addictive processes begins with an appreciation of the localization of 5-HT_{2C}R. The 5-HT_{2C}R was initially identified in high levels in epithelial cells of the choroid plexus, a non-

neuronal cell-type in the central nervous system (CNS) that is associated with the production of cerebrospinal fluid (Julius et al., 1988b). Full characterizations of the regional distribution and abundance of the 5-HT_{2C}R indicated prominent representation in neurons in brain but not peripheral tissues (Julius et al., 1988a; Molineaux et al., 1989; Mengod et al., 1990a; Backstrom et al., 1995; Clemett et al., 2000). For example, Julius and collaborators (1988) identified 5-HT_{2C}R in choroid plexus and in other brain regions (*e.g.*, hypothalamus, hippocampus and cortex) but absent in cerebellum or in liver, kidney, intestine, heart, and lung. Agreement between localization of the protein and mRNA for the 5-HT_{2C}R suggests that the 5-HT_{2C}R is predominantly localized postsynapticly; however, presynaptic localization of the 5-HT_{2C}R has not been ruled out (Clemett et al., 2000). Initial studies demonstrated that γ-aminobutyric acid (GABA) neurons, but not DA neurons, within the VTA expressed 5-HT_{2C}R mRNA (Eberle-Wang et al., 1997). However, recent studies have shown the 5-HT_{2C}R is not only expressed in GABA neurons, but also DA neurons within the VTA (Bubar and Cunningham, 2007) (**Fig. 1.1**), which suggests a much more sophisticated modulatory role for the 5-HT_{2C}R in dopaminergic neurotransmission than previously expected. Immunohistochemical and radioactive *in situ* hybridization studies are in accordance that 5-HT_{2C}R mRNA and protein are widely expressed in the NAc and PFC (Pasqualetti et al., 1999; Clemett et al., 2000). Furthermore, in humans, 5-HT_{2C}R mRNA expression was restricted to a non-pyramidal subpopulation of cells (presumably GABA interneurons) located in layer V of all neocortical areas (Pasqualetti et al., 1999). Additionally, our laboratory has shown that the 5-HT_{2C}R

protein is primarily expressed in parvalbumin-containing GABA interneurons in the deep layers (layers V/VI) of the rat PFC (Liu et al., 2007), which innervate glutamate-containing pyramidal neurons.

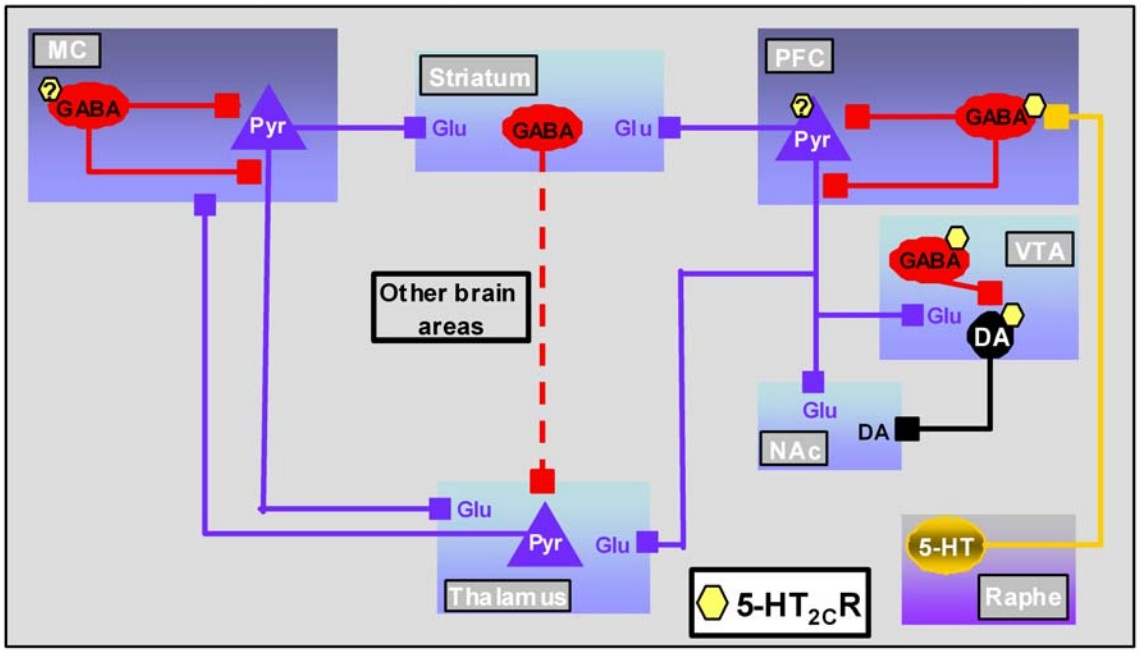

Figure 1.1. Schematic representation of the sites of action for the 5-HT_{2C}R to modulate motor cortex and PFC output to the VTA and NAc. The projection from 5-HT neurons in the raphe nuclei (Raphe) to the PFC is represented by the yellow line. The 5-HT_{2C}R located in the PFC is represented by yellow hexagons. Pyramidal glutamate (Pyr) projections from the PFC to the VTA and NAc are represented by purple lines. DA projections from the VTA to the NAc are represented by a black line. Stimulation of PFC 5-HT_{2C}R on GABA interneurons (represented by red lines) would function to reduce excitatory glutamate output as well as subsequent DA neurotransmission within the mesoaccumbens DA pathway (VTA and NAc). Adapted from Liu et al., 2007.

The pyramidal efferent neurons in layers V–VI of PFC primarily project to the VTA and NAc as well as other subcortical regions involved in autonomic, motor and limbic functions (Gabbott et al., 2005) and modulate dopaminergic neurotransmission. Intracellular recording studies have shown that GABA

hyperpolarizes neuronal membranes, thus supporting its role as an inhibitory neurotransmitter. Thus, release of GABA via activation of the depolarizing actions of 5-HT_{2C}R on GABA interneurons would be expected to reduce excitatory output from the PFC to the limbic-corticostriatal circuit, allowing 5-HT_{2C}R from the PFC to indirectly regulate glutamate and DA levels in the NAc (**Fig. 1.1**) (Liu et al., 2007). Altogether, these studies demonstrate that the 5-HT_{2C}R is expressed in the limbic-corticostriatal circuit.

Most addiction research has focused on the messoacumbens DA pathway (**Fig. 1.1**) as the reward circuit and the key target for neuroadaptations associated with cocaine use disorders; however due to recent imaging studies during the last decade(s) has expanded the focus to include additional corticolimbic circuits. Imagining technologies such as positron emission transmission (PET) and magnetic resonance imaging (fMRI) provided new grounds for the study of addictive process directly in humans (Volkow and Li, 2004). For example, fMRI, which measures changes in brain activity (when tissue is stimulated oxyhemoglobin is transformed to deoxyhemoglobin producing distinct magnetic profiles) have shown that the activity of cortical brain areas is increased when presented with drug-related stimuli (or if given drug) (Goldstein and Volkow, 2002; Volkow, 2004; Volkow and Li, 2004). Thus, cortical brain areas become interesting targets for the study of neuroadaptations associated with repeated cocaine exposure.

The rodent motor cortex and prefrontal cortex (PFC): Function and association with addiction

Serotonergic neurotransmission in cortical synapses contributes to affective and perceptual states, and these cortical synapses represent a major site of action for cocaine. A brain area that has been shown to be involved in cognitive and affective processes associated with motivation, stimulus-reinforcement, error detection and reward-based decision making is the PFC (Goldstein and Volkow, 2002; Volkow and Li, 2004; Goldstein et al., 2007). Glucose metabolism and cerebral blood flow (CBF) have been used in brain imaging studies as an index of regional brain activity to investigate the intoxication, craving, binging and withdrawal effects of cocaine (for review, Goldstein and Volkow, 2002). For example, human cocaine abusers when exposed to visual cocaine-associated cues (*e.g.,* injections of cocaine) presented greater glucose metabolism in the PFC, suggesting that PFC activation reflects a recognition of previous drug-paired context which could lead to craving and relapse (Childress et al., 1999; Garavan et al., 2000; Wexler et al., 2001; Garavan and Hester, 2007; Garavan et al., 2008). However, cocaine intoxication showed lower CBF throughout the brain, including cortex. The discrepancies observed between CBF and glucose metabolism data could be attributed to the vasoconstriction effects of cocaine. Altogether, these results suggested that the PFC is involved in processes associated with cocaine-craving and relapse.

The motor cortex is essential for the translation of biologically relevant environmental and pharmacological stimuli to adaptive motor responses,

including those adaptations seen after repeated cocaine administration (Kosten et al., 2006). In this study, all cocaine-dependent subjects were classified according to their Treatment Effectiveness Score (TES) as non-relapser when their TES score was above the mean (correlates to little cocaine in urine sample), and the remaining subjects were classified as relapsers (Kosten et al., 2006). After this separation, fMRI was utilized to examine the association between brain activity during exposure to cocaine-related cues and the incidence of relapse (Kosten et al., 2006). This study showed that relapsers had greater activation of sensory, motor and limbic cortical areas during cue exposure compared to non-relapsers (Kosten et al., 2006). These results suggest that cocaine-dependent patients may have difficulty inhibiting their initial motor responses in the presence of strong sensory stimulation by cocaine cues. Thus, activation of the motor cortex may reflect the initiation of motor action associated with cocaine-seeking. Under normal conditions, it has been postulated that well-learned behaviors rely on “habit” circuitry (comprised by thalamus, striatum and motor cortex), thereby freeing higher level cortical processing to integrate new information while the behavior is ongoing (Jog et al., 1999; Canales, 2005). If habitual behavior begins to produce unfavorable results, PFC executive function may intrude on the habit, causing the organism to modify the behavior (Kalivas, 2008). However, after repeated cocaine use, there is a decline in prefrontal executive function, and the habitual engagement of cocaine-seeking and cocaine consumption appears to be progressively strengthened (Everitt and Robbins, 2005). Thus, the interest in potentially differential neuroadaptations,

based on motor cortex involvement in habitual behavior, is well founded. A key component for treating cocaine addiction is the ability to convert compulsive drug-seeking into a manageable craving (reduce relapse) (Kalivas and O'Brien, 2008). While the characterization of traditional neural circuits (*e.g.*, messoaccumben DA pathway) involved in addiction has provided valuable insights, focus on alternative mechanisms and circuitry will offer a clear understanding of underlying neuroanatomical substrates of addictive disorders, with an end result to identify new targets for therapeutic development (Kalivas, 2008).

Cortical 5-HT_{2C}R: Structural organization

The cerebral cortex houses two primary neuronal species: the glutamate-containing pyramidal neurons and GABA interneurons (Molnar and Cheung, 2006). Importantly, the GABA interneurons form numerous synapses on pyramidal projection neurons and play a crucial regulatory function over cortical pyramidal output (Molnar and Cheung, 2006). The motor cortex consists of the precentral motor cortex, the primary motor area (MOP) and the secondary motor area (MOS) (Gabbott et al., 2005) (**Fig. 1.2**). The motor cortex receives afferent projections from the centrolateral nucleus of the thalamus (Haber and Calzavara, 2009), while afferent projections leave the motor cortex to innervate the striatum and the thalamus (**Fig. 1.1**; Haber and Calzavara, 2009).

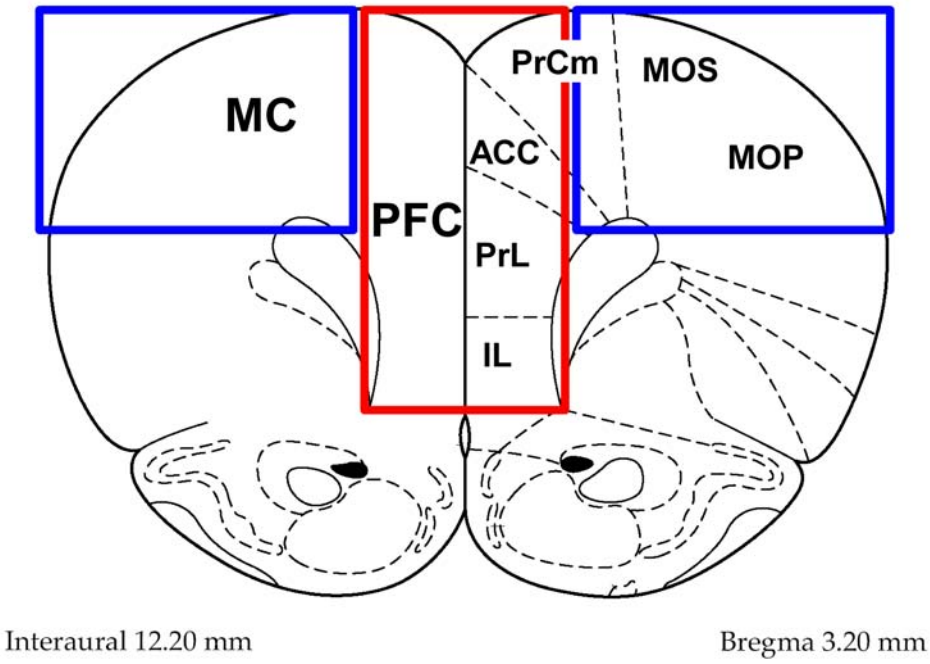

Figure 1.2. Schematic drawing of the anatomy of motor cortex and PFC. The blue box shows the area delimited as motor cortex (MC), while the box in red, the area delimited as prefrontal cortex (PFC). ACC, anterior cingular cortex; PrL, prelimbic cortex; IL, infralimbic cortex; PrCm, precentral motor cortex, MOS, secondary motor area; MOP, primary motor area [bregma 3.20 mm; adapted from Paxinos and Watson (2004)].

The rat PFC consists of the anterior cingulate cortex (ACC), the prelimbic prefrontal cortex (PrL), and the infralimbic prefrontal cortex (IL) (Dalley et al., 2004, **Fig. 1.2**). The most prominent subcortical afferents to the PFC arise in the mediodorsal nucleus of the thalamus (Fuster, 1997). The PFC also receives input from the dorsal raphe nuclei, VTA, hypothalamus as well as other cortical regions, while efferent pathways leave the PFC to reciprocally innervate those same regions (Fuster, 1997; Gabbott et al., 2005). A reduction in glutamatergic output from PFC would reduce GABA output from the striatum, thus inhibiting the inhibitory input to the thalamus and as a result reducing excitatory input to the

motor cortex (**Fig 1.1**). Thus, the motor cortex and PFC constitute interesting targets for the study of neuroadaptations associated with repeated cocaine exposure.

Physiological action of the 5-HT_{2C}R in brain

Neurochemical studies have shown that the 5-HT_{2C}R exerts a tonic inhibitory influence on the limbic-corticostriatal circuitry (Gobert et al., 2000; Di Matteo et al., 2001; De Deurwaerdere et al., 2004). For example, in single-cell recording studies, the moderately selective 5-$HT_{2C/2B}$R agonist RO 60-0175 dose-dependently reduced the basal activity of DA neurons in the VTA, whereas administration of the selective 5-HT_{2C}R antagonist SB 242084 dose-dependently increased the firing rate of VTA DA neurons (Di Giovanni et al., 1999; Di Matteo et al., 1999). Moreover, acute administration of the selective 5-HT reuptake inhibitor (SSRI) fluoxetine, which increases extracellular 5-HT concentration, caused a dose-dependent inhibition of the firing rate of DA neurons in the VTA, most likely acting through the 5-HT_{2C}R (Di Matteo et al., 2001). Finally, in microdialysis experiments, intraperitoneal (IP) injection of RO 60-0175 (1 and 3 mg/kg) decreased DA efflux in the NAc, whereas administration of SB 242084 (5 and 10 mg/kg) or the 5-$HT_{2B/2C}$R antagonist SB 206553 (1-10 mg/kg) increased DA outflow in the striatum and NAc (Di Giovanni et al., 1999; Di Matteo et al., 1999; Navailles et al., 2006; Navailles et al., 2008). Furthermore, Navailles and collaborator (2006) showed that the inhibitory effect of RO 60–0175 on DA release in NAc was significantly and dose-dependently blocked by intra-VTA

injections of the 5-HT_{2C}R antagonist SB 242084 (0.1-0.5 µg/0.2 µL). Together, these studies strongly suggest that the 5-HT_{2C}R acts in an inhibitory capacity to modulate the limbic-corticostriatal circuitry.

Signaling pathways associated with 5-HT_{2C}R

The 5-HT_{2C}R activates diverse downstream elements by coupling to preferentially to $G_{\alpha q/11}$–proteins (for review see Bonasera and Tecott, 2000; Hoyer et al., 2002; Higgins and Fletcher, 2003; Berg et al., 2008a). One such downstream effector is phospholipase C-β (PLC-β), a membrane-bound enzyme which catalyzes the cleavage of the inositol lipid, phosphatidylinositol 4,5-bisphosphate (PIP_2), into diacylglycerol (DAG) and inositol-1,4,5-trisphosphate (IP_3). IP_3 promotes Ca^{2+} release from intracellular storage sites, resulting in subsequent membrane depolarization. In addition, an increase in intracellular Ca^{2+} induces multiple responses, including activation of Ca^{2+}-calmodulin-dependent protein kinases, which phosphorylate key protein substrates in the cell. The other cleavage product, DAG, activates protein kinase C (PKC), which is involved in the regulation of numerous cellular functions, such as cell proliferation, differentiation and apoptosis. Furthermore, DAG can be hydrolyzed by a specific lipase to release arachidonic acid, resulting in the formation of prostaglandins and prostacyclins (for review see Bonasera and Tecott, 2000; Hoyer et al., 2002; Higgins and Fletcher, 2003; Berg et al., 2008a). Thus, activation of 5-HT_{2C}R leads to the formation of diverse downstream elements that induce changes in the regulation of many cellular processes.

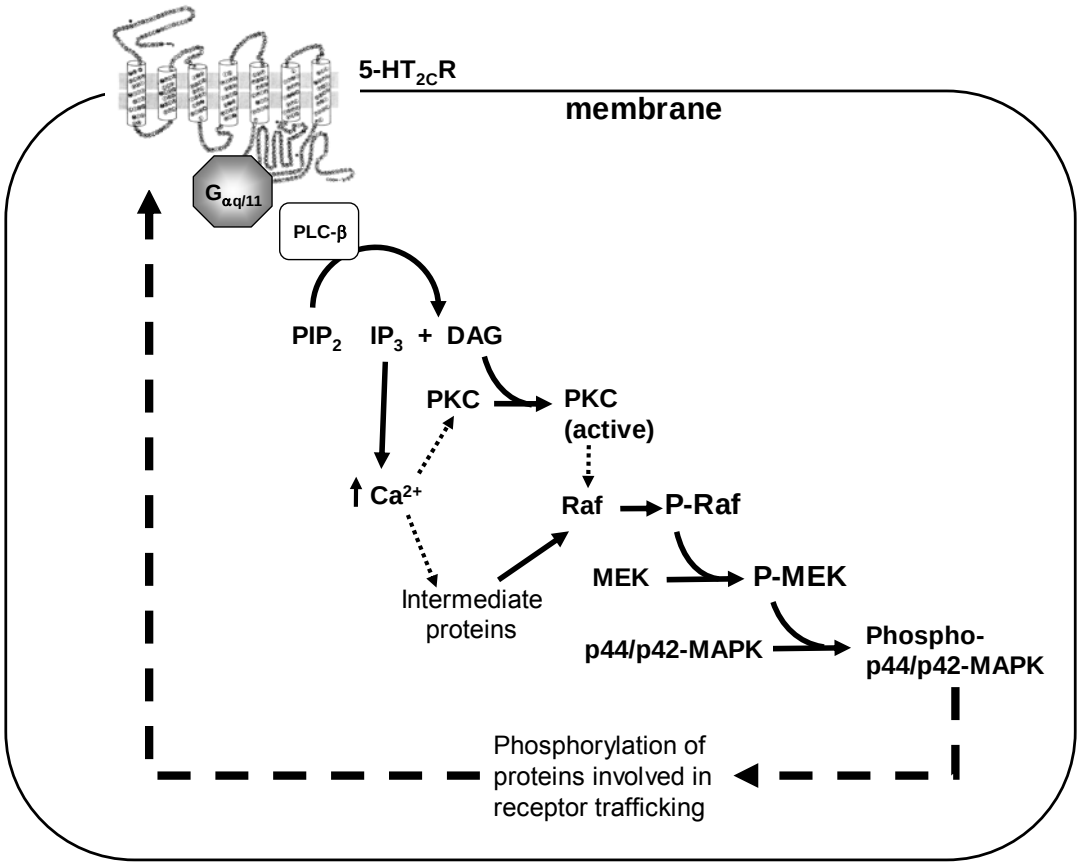

Figure 1.3. Association between the 5-HT_{2C}R signaling pathway and p44/p42-MAPK pathway. Adapted from Werry et al. 2005.

One important pathway that is activated by PKC, with intracellular Ca^{2+} as a cofactor, is the mitogen-activated protein kinase p42 and 44 (p44/p42-MAPK), also known as extracellular signal-regulated kinases 1 and 2 ($ERK_{1/2}$) pathway (Raymond et al., 2001; Werry et al., 2005; Werry et al., 2008a; Werry et al., 2008b). The p44/p42-MAPK pathway is distinguished by a characteristic core cascade of 3 kinases: MAPK kinase kinase (Raf), MAPK kinase/ERK kinase (MEK) and p44/p42 MAP Kinase (p44/p42-MAPK) (**Fig. 1.3**). Raf, which is phosphorylated by PKC, activates MEK via phosphorylation of serine-218 and serine-222 residues (Werry et al., 2005). MEK is a dual specificity kinase that

activates members of the MAPK family by phosphorylation of threonine and tyrosine residues that are separated by one amino acid (TEY motif). For example, p44-MAPK (ERK1) is phosphorylated at threonine-183 and tyrosine-185, while p42-MAPK (ERK2) at threonine-202 and tyrosine-204.

The p44/p42-MAPK pathway regulates a broad range of fundamental cellular processes, including cell proliferation, differentiation and survival by phosphorylating specific proteins (Schaeffer and Weber, 1999). For instance, p44/p42-MAPK regulates some components of the seven transmembrane receptor regulatory apparatus, such as G-protein receptor kinases (GRKs) and β-arrestins; two molecules that have been previously associated with protein trafficking and receptor internalization (Pitcher et al., 1999; Elorza et al., 2003; Werry et al., 2005).

GRK2 belongs to a family of serine/threonine protein kinases that phosphorylate agonist-occupied GPCR (Pitcher et al., 1999; Elorza et al., 2003). GRK2-phosphorylated GPCRs bind to an inhibitory protein known as β-arrestin2 and this interaction prevents receptor-mediated G-protein activation, and promotes subsequent receptor internalization (Pitcher et al., 1999; Elorza et al., 2003). GRK2 exists as a phosphoprotein and its activity depends on its phosphorylation state. Site-directed mutagenesis studies (namely, Ser670Ala) revealed that GRK2 presented a site for p44/p42-MAPK phosphorylation, which impaired GRK2 activity and subsequent GPCR phosphorylation (Pitcher et al., 1999). On the other hand, in vitro studies showed that phosphorylation of the

5-HT_{2C}R by GRK2 at two serine residues interrupts the interaction between the receptor and other intracellular binding proteins, affecting the rate of resensitization (for review, Melikian, 2004; Werry et al., 2005).

Binding partners associated with 5-HT_{2C}R: Postsynaptic density-95 (PSD-95)

The functional activity of the 5-HT_{2C}R is regulated by desensitization and resensitization processes which themselves are regulated by the interaction between the receptor and scaffolding proteins, such as postsynaptic density protein-95 (PSD-95). PSD-95, one of the major postsynaptic density proteins, belongs to the family of membrane-associated guanylate kinase (MAGUK) scaffolding proteins (Hunt et al., 1996; Gavarini et al., 2006). PSD-95 is a cytoplasmic protein that contains three repeated PSD-95/Disks-large (dlg) protein in Drosophila/Zone Occluden-1 (ZO-1) (PDZ) domains, important for protein-protein interaction (Hunt et al., 1996; Becamel et al., 2002; Becamel et al., 2004; Gavarini et al., 2004; Gavarini et al., 2006). At the synapse, PSD-95 is found associated with receptors and cytoskeletal elements and it has been implicated in synaptic plasticity and maturation of excitatory synapses (El-Husseini et al., 2000; El-Husseini et al., 2002; Ehrlich et al., 2007). *In vitro* studies have shown that PSD-95 recognizes PDZ domains located at the C-terminal of the 5-HT_{2C}R, promoting constitutive and agonist-induced internalization and trafficking (Becamel et al., 2002; Becamel et al., 2004; Gavarini et al., 2004; Gavarini et al., 2006). More recently, the functional activity of the 5-HT_{2C}R has been shown to be modulated according to the repertoire of PDZ proteins co-expressed with the

receptor (Gavarini et al., 2006). Gavarini and collaborators (2006) showed that 5-HT_{2C}R/PSD-95-co-transfected cells exhibited robust and transient Ca^{2+} peaks of similar amplitudes and decay rates as cells expressing only 5-HT_{2C}R to a first 5-HT application, suggesting that PSD-95 does not modify the efficacy of 5-HT_{2C}R signaling triggered by a single 5-HT challenge. However, in 5-HT_{2C}R/PSD-95-co-transfected cells, the amplitude of Ca^{2+} responses evoked by a second 5-HT application was markedly reduced, relative to cells transfected with the receptor alone, suggesting that PSD-95 evokes an inhibition of 5-HT_{2C}R response recovery.

5-HT_{2C}R mRNA-editing

The 5-HT_{2C}R is unique in that the 5-HT_{2C}R is the only GPCR currently known to undergo mRNA editing (Burns et al., 1997). RNA editing is a type of post-transcriptional modification in higher eukaryotes that inserts, deletes (Benne et al., 1986; Cruz-Reyes et al., 1998; Igo, Jr. et al., 2002) or modifies (Samuel, 2003) single or small numbers of ribonucleotides in pre-mRNA, thus altering the coding properties and information content of mRNA molecules (Bass, 2002; Hoopengardner et al., 2003; Maydanovych and Beal, 2006). Editing of the 5-HT_{2C}R was discovered by comparing genomic DNA to cDNA sequences obtained after reverse transcribing RNA from rat striatum (Burns et al., 1997). The cDNA library predicted the presence of valine (V), serine (S), and valine (V) at positions 157, 159 and 161, respectively, whereas genomic DNA predicted isoleucine (I), asparagine (N), and isoleucine (I) at these 3 positions. The

5-HT_{2C}R pre-mRNA was discovered to undergo RNA editing in four closely spaced adenosines (designated A, B, C and D) located within a 13 base region of the RNA in rat (**Fig. 1.4**; Burns et al., 1997; Gurevich et al., 2002a). In humans, an additional adenosine editing site has been detected in the N codon at position 158, denoted as site E (previously known as C' site) (**Fig. 1.4**). Editing at the E site alone converts the N to an aspartic acid (D) and, in combination with the C site, to a glycine (G) (Niswender et al., 1998; Niswender, 1998; Fitzgerald et al., 1999).

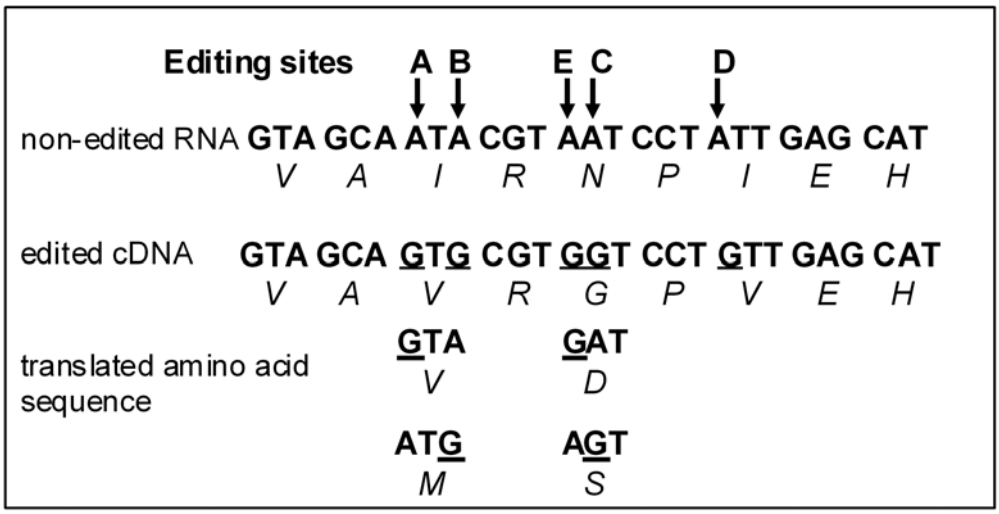

Figure 1.4. RNA editing sites of 5-HT_{2C}R transcript. cDNA nucleotide and predicted amino-acid sequences for the non-edited and fully-edited transcripts are shown with the editing sites indicated by arrows (↓). Picture adapted from Sanders-Bush et al (2003).

The convention when referring to any specific 5-HT_{2C}R isoform is to present the resultant amino acid sequence of potentially edited sites as a subscript following the receptor subtype. In theory, there are 32 possible RNA editing combinations, leading to 24 possible resultant protein isoforms; however

fewer isoforms are routinely detected and their pattern of expression is influenced by variables such as species and brain area (Burns et al., 1997; Niswender et al., 1998; Fitzgerald et al., 1999; Sanders-Bush et al., 2003). For instance, four of the most common 5-HT_{2C}R variants in the whole rodent brain are 5-$HT_{2C\text{-}VNV}$R, 5-$HT_{2C\text{-}VSV}$R, 5-$HT_{2C\text{-}VNI}$R and 5-$HT_{2C\text{-}VSI}$R, corresponding approximately to 47, 11, 18 and 10 percent of total 5-HT_{2C}R mRNA, respectively (Burns et al., 1997).

The RNA editing region is located within the second intracellular (i2) loop of the receptor, two amino acid residues downstream of the highly conserved E/DRY motif, which has been strongly linked to G-protein coupling (Burns et al., 1997; Berg et al., 2001; Marion et al., 2004; Berg et al., 2008a), as evidenced by lowered agonist potencies to activate PLC (Burns et al., 1997; Niswender et al., 1999; Wang et al., 2000). For example, in studies in which the ability of various 5-HT_{2C}R isoforms to stimulate PLC signal transduction cascade by measuring the accumulation of [^{3}H]-inositol monophosphates (^{3}H-IP) was tested, the human partially-edited isoform 5-$HT_{2C\text{-}VSV}$R exhibited a 5-fold decrease in potency for 5-HT compared to the non-edited isoform 5-$HT_{2C\text{-}INI}$R (Niswender et al., 1999). Furthermore, in those same studies, the fully-edited human 5-$HT_{2C\text{-}VGV}$R isoform presented a more substantial rightward shift in the dose-response curve for 5-HT, with an EC_{50} value of 59 nM versus 2.3 nM for the 5-$HT_{2C\text{-}INI}$R (Niswender et al., 1999). Stimulation of the partially-edited 5-$HT_{2C\text{-}VSV}$R and fully-edited 5-$HT_{2C\text{-}VGV}$R isoforms with the 5-HT_{2C}R partial agonist (±)-1-(4-iodo-2,5-

dimethoxyphenyl)-2-aminopropane (DOI) produced a 9- and 43-fold less potent signal activation respectively, when compared to the 5-$HT_{2C\text{-}INI}$R (Niswender et al., 1999). These results strongly suggested that the ability of 5-HT_{2C}R agonists to activate PLC more efficiently is dependent on the degree of editing of the 5-HT_{2C}R. On the other hand, few studies have focused on the effects of 5-HT_{2C}R antagonists on 5-HT_{2C}R RNA editing. For example, studies showed that the 5-HT_{2C}R antagonist ketanserin or mesulgerine presented similar affinity for both the 5-$HT_{2C\text{-}INI}$R and 5-$HT_{2C\text{-}VSV}$R, suggesting that antagonist binding to its receptor is not affected by RNA editing (Quirk et al., 2001). In addition, the i2 loop may participate in desensitization associated with β-arrestin2 binding and receptor downregulation (Marion et al., 2004). Evidence also suggests that residues within the i2 regulate the capacity of receptors to isomerize, thereby controlling the formation of active receptor conformations and constitutive receptor activity (Berg et al., 2008a).

The 5-HT_{2C}R also presents constitutive activity, and this activity is dependent upon the degree of 5-HT_{2C}R mRNA editing (Herrick-Davis et al., 1999; Niswender et al., 1999; Berg et al., 2001). Constitutively active receptors are defined as receptors that stimulate downstream signaling events in the absence of agonist occupation. For example, when ^{3}H-IP production was measured in COS-7 cells transfected with different 5-HT_{2C}R isoforms (human or rat) in the absence of 5-HT_{2C}R ligands, there was a 5-fold greater level of ^{3}H-IP in 5-$HT_{2C\text{-}INI}$R expressing cells when compared to cells that expressed the

5-$HT_{2C\text{-}VGV}$R isoform (Herrick-Davis et al., 1999). This suggests that 5-HT_{2C}R RNA editing events serve to modulate basal 5-HT_{2C}R activity.

More recently, the I156V substitution, a naturally occurring mRNA partially-edited 5-HT_{2C}R isoform, has been shown to alter the functional selectivity of both ligand-dependent and ligand-independent 5-HT_{2C}R signaling (Berg et al., 2008b). This single substitution is sufficient to produce profound changes in agonist selectivity, favoring signaling via PLC over phospholipase A2. In keeping with this concept, Werry and collaborators (2008) showed that the partially-edited 5-$HT_{2C\text{-}VSV}$R and the fully-edited 5-$HT_{2C\text{-}VGV}$R retained the ability to couple to the p44/p42-MAPK pathway, but with a loss of efficacy compared to the non-edited 5-$HT_{2C\text{-}INI}$R isoform. This suggests that editing of the 5-HT_{2C}R may play a role in providing agonist-specific information to the signal transduction machinery of the cell (Berg et al., 2008b; Werry et al., 2008b). Thus, RNA editing has a profound influence over the fate of p44/p42-MAPK signaling following 5-HT_{2C}R stimulation.

Editing regulation is sensitive to changes in synaptic concentrations of 5-HT (Gurevich et al., 2002a; Englander et al., 2005; Iwamoto et al., 2005). For example, 5-HT depletion consequent to treatment with para-chlorophenylalanine (pCPA), a potent and irreversible inhibitor of tryptophan hydroxylase, the rate limiting step in 5-HT synthesis, significantly increased the expression of 5-HT_{2C}R mRNA isoforms that encode receptors with higher sensitivity to agonist stimulation (i.e., 5-$HT_{2C\text{-}VNV}$R) (Gurevich et al., 2002a). Furthermore, treatment

with the 5-$HT_{2A/2C}$R agonist DOI twice a day for four days significantly increased expression of the fully-edited (5-$HT_{2C\text{-}VGV}$R) or partially-edited (i.e., 5-$HT_{2C\text{-}VSI}$R, 5-$HT_{2C\text{-}ISV}$R) 5-HT_{2C}R mRNA isoforms (Gurevich et al., 2002a). Thus, prolonged stimulation of the 5-HT_{2C}R caused alterations in 5-HT_{2C}R RNA editing, resulting in the expression of RNA isoforms encoding receptors that least efficiently activate G-protein, and exhibit reduced agonist-stimulated activity.

In summary, the non-edited 5-$HT_{2C\text{-}INI}$R isoform has been shown to maintain its high affinity for G-protein coupling, resulting in a high level of constitutive activity. Editing of 5-HT_{2C}R mRNA serves to reduce the efficiency of the interaction between the receptor and its G-protein, which results in low levels of constitutive activity (Burns et al., 1997; Marion et al., 2004).

Cocaine and the 5-HT_{2C}R: Effects of acute systemic administration of 5-HT_{2C}R ligands

Administration of 5-HT_{2C}R ligands has been shown to influence cocaine-induced DA outflow in the NAc (Navailles et al., 2006). For example, acute systemic administration of the 5-$HT_{2B/2C}$R antagonist SB 206553 (5 mg/kg) or the selective 5-HT_{2C}R antagonist SB 242084 (1 mg/kg) potentiated accumbal DA outflow induced by systemic intraperitoneal injection of cocaine (10 and 15 mg/kg) (Navailles et al., 2006). Interestingly, administration of the 5-HT_{2C}R agonist RO 60-0175 (1 mg/kg IP) had no effect on cocaine-induced accumbal DA release when cocaine was given at 15 mg/kg (Navailles et al., 2006). Altogether,

these results strongly support an inhibitory role for the 5-HT_{2C}R over the neurochemical effects of cocaine.

Table 1.1. Description of 5-HT_2R ligands

5-HT_2R Ligands	Compound	Description
Agonist	RO 60-0175	Preferential 5-$HT_{2B/2C}$R Agonist
	MK 212	5-HT_{2C}R Agonist
Inverse Agonist	SB 2066553	5-$HT_{2B/2C}$R Inverse Agonist
Antagonist	SB 242084	Selective 5-HT_{2C}R Antagonist
	SDZ SER-082	5-HT_{2C}R Antagonist
	RS 102221	5-HT_{2C}R Antagonist

Administration of 5-HT_{2C}R ligands has been shown to influence the behavioral effects of cocaine (Cunningham and Callahan, 1994; Callahan and Cunningham, 1995; McMahon et al., 2001; Filip and Cunningham, 2003; Filip et al., 2004). For example, acute systemic administration of the moderately selective 5-$HT_{2B/2C}$R agonist RO 60-0175 (0.1-3 mg/kg) (Grottick et al., 2000) or MK 212 (2 mg/kg) reduced (Filip et al., 2004), whereas the 5-HT_{2C}R antagonist SDZ SER-082 (0.25–1 mg/kg) (Filip et al., 2004) or SB 242084 (0.5 mg/kg IP) (Fletcher et al., 2002) enhanced cocaine-evoked hyperactivity in a dose-dependent manner. In addition, an acute systemic injection of SB 206553 (4 mg/kg IP) potentiated cocaine-induced (15 mg/kg IP) hyperactivity (McCreary

and Cunningham, 1999). Altogether, these studies strongly support the inhibitory role of the 5-HT_{2C}R over the behavioral effects of cocaine.

Studies have shown that 5-HT_{2C}R ligands have an effect on the reinforcing effects of cocaine across a range of cocaine doses. For example, pretreatment with RO 60-0175 produced a dose-dependent reduction in rates of responding for cocaine (lower “breaking point”), when compared to vehicle treated animals (Grottick et al., 2000). Furthermore, the 5-HT_{2C}R antagonist SB 242084 significantly increased rates of responding at the lowest doses of cocaine (higher “breaking point”) compared to vehicle treated animals (Fletcher et al., 2002). These results strongly suggest that 5-HT_{2C}R agonists inhibit, while 5-HT_{2C}R antagonists enhanced the reinforcing effects of cocaine.

5-HT_{2C}R ligands also change the effectiveness of cocaine to reinstate responding on a lever that previously delivered cocaine (Grottick et al., 2000). For example, after two weeks of extinction, rats that learned to self-administrate cocaine were injected with vehicle or RO 60-0175 (0.3-3.0 mg/kg sc) 15 min before a vehicle or cocaine injection (15 mg/kg IP). In this experiment, RO 60-0175 (3 mg/kg) pretreatment significantly attenuated the reinstatement of cocaine responding elicited by a priming injection of cocaine (Grottick et al., 2000). Conversely, 5-HT_{2C}R antagonist SB 242084 (0.5 mg/kg) enhanced cocaine-evoked reinstatement of responding on a previously active lever (Fletcher et al., 2002). These studies suggest that 5-HT_{2C}R ligands are capable of modulating cocaine-primed reinstatement of cocaine-seeking behavior.

Together, these results strongly suggest that 5-HT_{2C}R agonists reduce, while 5-HT_{2C}R antagonists enhance hyperactivity, reinforcing effects and reinstatement of drug-seeking evoked by cocaine, supporting the idea that 5-HT_{2C}R plays a modulatory role in the *in vivo* effects of cocaine.

Cocaine and the 5-HT_{2C}R: Effects of acute systemic administration of 5-HT_{2C}R ligands after intermittent repeated cocaine administration

Behavioral sensitization can be divided in two phases known as *induction* and *expression*. The *induction phase* is defined as the transient sequence of cellular and molecular events precipitated by psychostimulant administration that leads to the enduring changes in neural function responsible for behavioral augmentation (Pierce and Kalivas, 1997), whereas the *expression phase* is defined as the enduring neural alterations arising from the initiation process that directly mediate the augmented behavioral response (Pierce and Kalivas, 1997). Several investigators have focused their attention on the role of 5-HT_XR system in the development and the expression of cocaine sensitization (De La Garza and Cunningham, 2000; Filip et al., 2001; Przegalinski et al., 2001; Filip et al., 2004). For example, pretreatment with a nonselective 5-$HT_{2A/2C}$R antagonist ketanserin or 5-HT_{2C}R antagonist SDZ SER-082 or 5-HT_{2C}R agonist MK-212 before each daily injection of cocaine did not affect the development of cocaine sensitization (Filip et al., 2001; Filip et al., 2004); whereas when the expression of sensitization was assessed, only ketanserin dose-dependently reduced cocaine-evoked hyperactivity (Filip et al., 2001). Subsequent to treatment with cocaine (10 mg/kg/day) for five days, the 5-HT_{2C}R agonist MK 212 or the

5-HT_{2C}R antagonist SDZ SER-082 were no longer effective in reducing or enhancing cocaine-evoked hyperactivity, respectively (Filip et al., 2004), suggesting that 5-HT_{2C}R activity is diminished significantly during withdrawal from a regimen of intermittent repeated exposure to cocaine. The lack of effect of the 5-HT_{2C}R agonist and antagonist suggest that either the function of this receptor, or its downstream signaling components, is significantly altered after cocaine administration (Filip et al., 2004). The loss of 5-HT_{2C}R inhibitory actions may promote DA release in VTA (Di Giovanni et al., 1999; De Deurwaerdere et al., 2004), contributing to the expression of sensitization and increasing the tendency to self-administer cocaine in rats, which could parallel the tendency in humans to increase drug use. For this reason it is important to understand the neuroadaptations associated with the 5-HT_{2C}R to gain a better understanding of the mechanisms that contribute to the development of cocaine use disorders.

Cocaine and the 5-HT_{2C}R: Sites of action

Sites of action for the 5-HT_{2C}R in the brain have been explored utilizing intracranial microinjection techniques to understand more specifically how the 5-HT_{2C}R acts within the limbic cortico-striatal circuit. Traditionally, these studies have focused on VTA, NAc and PFC because these brain areas have been directly implicated in mediating the behavioral effects of cocaine. Furthermore, the 5-HT_{2C}R is densely expressed in these brain regions.

Intra-VTA microinfusion of RO 60-0175 (3 and 10 μg/side) significantly attenuated cocaine-induced locomotion (Fletcher et al., 2004); however,

intra-VTA infusion of the selective 5-HT_{2C}R antagonist RS 102221 (0.05-0.5 µg/side) did not alter cocaine-evoked hyperactivity (McMahon et al., 2001). In agreement with this finding, intra-VTA microinfusion of RO 60-0175 (5 µg/0.2 µL) significantly attenuated cocaine-induced DA release in NAc (Navailles et al., 2008), whereas intra-VTA infusion of the selective 5-HT_{2C}R antagonist SB 242084 (0.1 or 0.5 µg/0.2 µL) did not alter cocaine-evoked accumbal DA release (Navailles et al., 2008). Intra-NAc infusion of MK 212 (0.05 and 0.15 µg/side) or RO 60-0175 (5 µg/side) significantly enhanced, whereas intra-NAc microinfusion of RS 102221 (0.05, 0.15 or 0.5 µg/side) dose-dependently blocked, the hyperactivity induced by systemic cocaine administration (McMahon et al., 2001; Filip and Cunningham, 2002). Intra-NAc microinfusion of RO 60-0175 (0.1 µM) significantly potentiated cocaine-induced DA release in NAc (Navailles et al., 2008), whereas intra-NAc infusion of the selective 5-HT_{2C}R antagonist SB 242084 (0.1 µM) reduced cocaine-evoked accumbal DA release (Navailles et al., 2008). Intra-PFC infusion of MK 212 (0.05 and 0.15 µg/side) and RS 102221 (5 µg/side) decreased and increased cocaine-evoked horizontal activity, respectively (Filip and Cunningham, 2003). Although there seems to be a discrepancy between intracranial and systemic administration of 5-HT_{2C}R, these differences may be explained by looking at the neuronal subpopulations in which the 5-HT_{2C}R is expressed. Thus, intracranial studies suggest that the 5-HT_{2C}R within the VTA, NAc and PFC differentially control the DA mesocorticoaccumbens pathway, and that 5-HT_{2C}R in cortical areas exert an

inhibitory control over the behavioral response to cocaine, which parallels the effects of a systemic injection of a 5-HT_{2C}R agonist.

Effects of cocaine on 5-HT_{2C}R signaling pathways

Behavioral studies suggest subsensitivity of the 5-HT_{2C}R following repeated cocaine administration suggesting that cocaine has profound effects on the 5-HT_{2C}R and/or signaling pathways associated with the 5-HT_{2C}R. Studies have shown that acute cocaine administration has profound effects on p44/p42-MAPK pathway activation in rodents. For example, immunohistochemical studies revealed that acute cocaine administration at a dose of 20 mg/kg increased the levels of phospho-p44/p42-MAPK in the dorsal striatum and NAc (core and shell) when compared to saline-treated mice (Valjent et al., 2004a; Valjent et al., 2004b; Mattson et al., 2005; Valjent et al., 2006). Furthermore, mice injected with the MEK inhibitor SL327 1 hr before an acute systemic cocaine injection showed a reduction in phospho-p44/p42-MAPK when compared to controls (Radwanska et al., 2005). In the same study, the expression of immediate-early genes cFos and JunB in NAc and amygdala was prevented when mice were pretreated with SL327 before acute cocaine administration (Radwanska et al., 2005). This suggests that p44/p42-MAPK plays an important role in the molecular adaptations associated with acute administration of cocaine.

Repeated intermittent cocaine administration has been shown to alter phospho-p44/p42-MAPK abundance and activity in rodents. Rats previously

pretreated with cocaine (15 mg/kg/daily for 7 days) presented 90% higher levels of phospho-p44/p42-MAPK 20 min after cocaine challenge in NAc when compared to rats pretreated with saline and challenge with cocaine (Mattson et al., 2005). Furthermore, p44/p42-MAPK activity was detected by measuring phosphorylation of a specific p44/p42-MAPK substrate in the NAc and striatum (Mattson et al., 2005). Briefly, p44/p42-MAPK activity levels were assessed 20 min following a cocaine challenge injection. It was shown that a challenge injection of cocaine significantly increased p44/p42-MAPK activity levels by 80% in rats repeatedly pretreated with cocaine when compared to rats pretreated with saline. In another study, rats that received a pretreatment of cocaine twice a day for ten days presented a 37% increase in p44/p42-MAPK activity in VTA when compared to control animals (Berhow et al., 1996). Briefly, VTA was removed from decapitated rats 12-14 hr after the last cocaine injection. In-gel assay of p44/p42-MAPK catalytic activity was used to study the effects of cocaine on the enzyme. In this assay, MBP, an MAPK substrate, is phosphorylated in the presence of [γ32P] ATP by p44/p42-MAPK activity within the resolving gel. These results reveal that p44/p42-MAPK plays a role in the molecular adaptations associated with repeated intermittent cocaine administration.

If psychostimulants are capable of affecting p44/p42-MAPK pathway activation, it follows that they might also have an effect on proteins that affect 5-HT_{2C}R turnover and trafficking (**Fig. 1.5**). We decided to focus on proteins of the p44/p42-MAPK pathway because this pathway responds to

psychostimulants, and it is also considered to be a multifunctional signaling integrator involved in the regulation of several cellular processes.

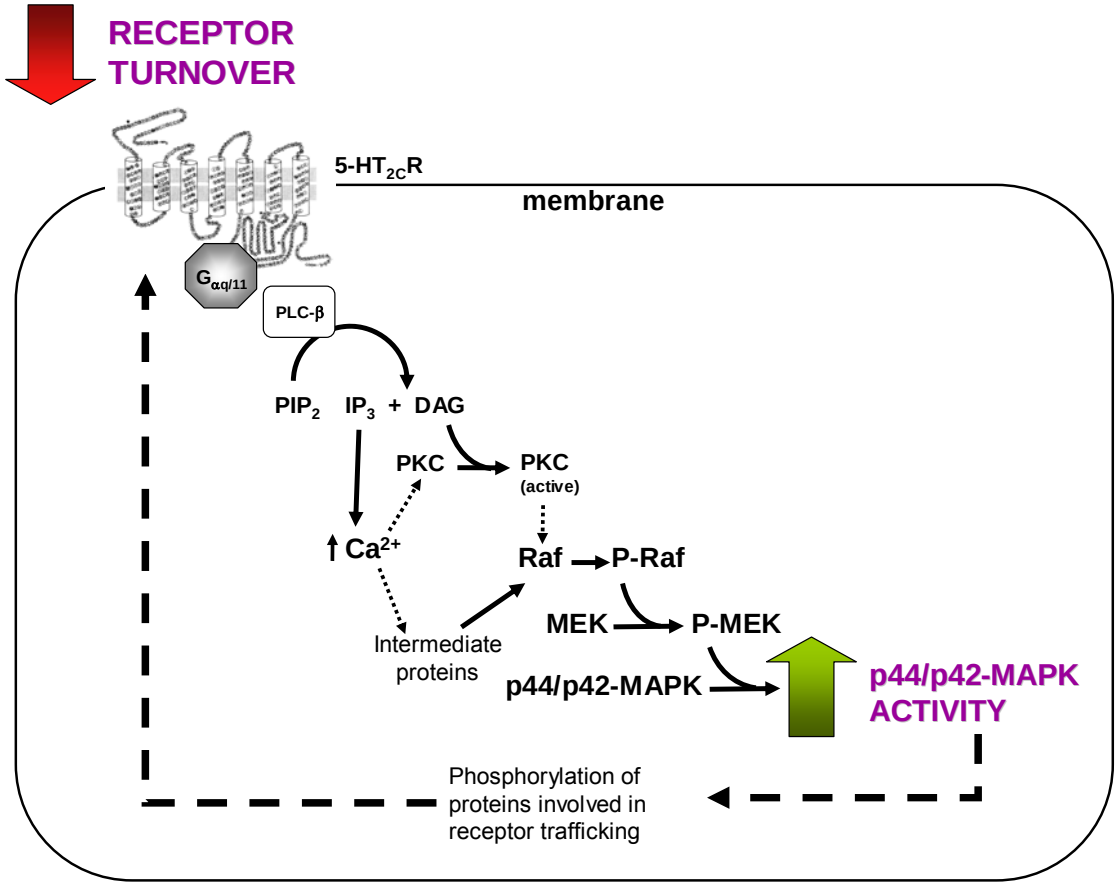

Figure 1.5. Schematic representation of the rationale for the study of the association of 5-HT$_{2C}$R and p44/p42-MAPK pathway following repeated intermittent cocaine administration. Adapted from Werry et al. 2005

Effects of cocaine on RNA editing of the 5-HT$_{2C}$R

Limited information has been gathered about the effects of psychostimulants, such as cocaine, on 5-HT$_{2C}$R mRNA editing (Iwamoto and Kato, 2002). Since cocaine is an inhibitor of 5-HT reuptake, resulting in an

increase in extracellular 5-HT, we would expect to see changes in the relative abundance of the 5-HT_{2C}R isoforms in the brain in response to repeated intermittent cocaine exposure. Prolonged stimulation of the 5-HT_{2C}R would result in the expression of RNA isoforms encoding receptors that exhibit reduced agonist-stimulated activity. Hence, mRNA editing may be an alternative mechanism by which serotonergic signal transduction may be regulated and play a critical role in modulating multiple cellular functions.

Overall summary

This project will is focused on four possible neuroadaptations, which may explain the reduced sensitivity of the 5-HT_{2C}R after repeated intermittent cocaine administration: 1) changes in expression and subcellular localization of the 5-HT_{2C}R; 2) changes in expression and subcellular localization of PSD-95; 3) changes in phosphorylation of p44/p42-MAPK pathway, which may in turn influence the activity of molecules involved in 5-HT_{2C}R trafficking, such as β-arrestin2 and GRK2; 4) changes in 5-HT_{2C}R mRNA editing which contribute to the formation of 5-HT_{2C}R isoforms with reduced efficiency to couple G-proteins, which affects the activation of the 5-HT_{2C}R intracellular signaling pathway.

CHAPTER 2: SPECIFICITY AND SELECTIVITY IN RAT CORTEX OF COMMERCIALLY-AVAILABLE SEROTONIN (5-HT) 2C RECEPTOR (5-HT_{2C}R) ANTIBODIES

INTRODUCTION

The 5-HT_{2C}R (previously known as 5-HT_{1C}R) influences numerous CNS functions (*e.g.,* sleep, mood, cognition and motility), while disturbances of this neurotransmitter system are implicated in obesity and the pathogenesis of psychiatric disorders (*e.g.,* addiction, anxiety, depression, and schizophrenia) (Giorgetti and Tecott, 2004; Bubar and Cunningham, 2008; Hannon and Hoyer, 2008). The 5-HT_{2C}R couples preferentially to the $G_{\alpha q/11}$ and receptor activation leads to an increase in the formation of inositol phosphates and release of Ca^{2+} from intracellular storage compartments (for reviews, Bonasera and Tecott, 2000; Hoyer et al., 2002; Higgins and Fletcher, 2003; Hannon and Hoyer, 2008).

Sites of 5-HT_{2C}R mRNA synthesis have been established in the CNS via *in situ* hybridization methods (Hoffman and Mezey, 1989; Molineaux et al., 1989; Mengod et al., 1990a; Mengod et al., 1990b; Pompeiano et al., 1994; Eberle-Wang et al., 1997), In particular 5-HT_{2C}R mRNA in corticals regions such as prefrontal (most prominent at the ACC), parietal, occipital cortices (Molineaux et al., 1989; Pasqualetti et al., 1999) and somatosensory cortex (Molineaux et al., 1989) have been found to be restricted to layer V (Hoffman and Mezey, 1989). The regional distribution of the 5-HT_{2C}R protein density has been characterized with radioligand binding autoradiography in the CNS (Pazos et al., 1984a; Pazos et al., 1984b; Pazos and Palacios, 1985; Pazos et al., 1987). The 5-HT_{2C}R

protein was initially identified in high levels in epithelial cells of the choroid plexus, a non-neuronal cell type in the CNS that is associated with the production of cerebrospinal fluid (Pazos et al., 1984b; Julius et al., 1988a; Julius et al., 1988b). The 5-HT_{2C}R protein also resides in neurons in cortical (*e.g.,* frontal cortex, frontoparietal motor cortex, somatosensory cortex, ACC) and limbic regions (*e.g*., amygdala, hippocampus) as well basal ganglia and thalamus (Molineaux et al., 1989; Abramowski et al., 1995; Clemett et al., 2000). Therefore, ligand-binding studies have advanced our knowledge of density, ligand affinities and the brain distribution of 5-HT_{2C}R binding sites. However, radioligand techniques do not provide sufficient resolution for localization of the receptor to both cellular and subcellular compartments (Pazos et al., 1998). Altogether, *in situ* hybridization and radioligand binding autoradiography suggest overlapping and distinct brain regions for 5-HT_{2C}R mRNA and protein expression suggesting a possible postsynaptic and presynaptic localization of the 5-HT_{2C}R.

Immunohistochemical studies validated the same pattern of expression to cortico-limbic areas previously identified with radioligand binding studies (Abramowski et al., 1995; Clemett et al., 2000). For example, immunoreactivity for the 5-HT_{2C}R protein was observed in the frontal, cingulate, parietal and occipital cortices (layers IV-VI presented a more intense immunoreactivity than layer I-III), in agreement with radioligand binding studies (Abramowski et al., 1995; Pazos et al.,1985a). Thus, immunological approaches employing selective antibodies are also useful in exploring the subcellular localization and trafficking

of neuronal proteins and molecular partners of the protein of interest, and are likely to enhance our understanding of 5-HT_{2C}R role in the CNS (Clemett et al., 2000).

Immunohistochemical studies using the N-19 anti-5-HT_{2C}R antibody [sc-15081, Santa Cruz Biotechnology] identified 5-HT_{2C}R localization in the VTA and other brain areas in C57BL wild-type mice which was undetectable in the same regions in 5-HT_{2C}R knockout mice (Bubar et al., 2005). The latter result agreed with ligand autoradiographical studies in which a reduced density of the 5-HT_{2C}R in the VTA was observed in 5-HT_{2C}R knockout mice (Lopez-Gimenez et al., 2002). Furthermore, the N-19 anti-5-HT_{2C}R antiboby presented immunoreactivity in CHO cells transfected with 5-HT_{2C}R, but not in CHO cells transfected with 5-HT_{2A}R, demonstrating the selectivity and suitability of this antibody in immunocytochemistry and immunohistochemistry studies (Bubar et al., 2005). Studies employing this same antibody demonstrated that the 5-HT_{2C}R is expressed in GABA interneurons and probably pyramidal glutamatergic neurons in the PFC (Liu et al., 2007); and in GABA interneurons and DA neurons in the VTA (Bubar and Cunningham, 2007). This same antibody (Bubar et al., 2005; Bubar and Cunningham, 2007; Liu et al., 2007) and others (Abramowski and Staufenbiel, 1995; Clemett et al., 2000) have been validated for the use in immunohistochemical studies, however the utility of the N-19 anti-5-HT_{2C}R antibodies and other commercially-available anti-5-HT_{2C}R antibodies for Western blot is still unknown.

Individual laboratory-produced anti-5-HT_{2C}R antibodies raised against various domains of the 5-HT_{2C}R have also been useful in exploration of cellular distribution of the the 5-HT_{2C}R *in vitro* by Western blot (Abramowski et al., 1995; Backstrom et al., 1995; Backstrom and Sanders-Bush, 1997) and regional localization of the 5-HT_{2C}R *ex vivo* by immunohistochemical approaches (Abramowski et al., 1995; Clemett et al., 2000). However the cellular distribution of the 5-HT_{2C}R has been hampered by the fact that the laboratory-produced anti-5-HT_{2C}R antibodies are not widely available, and the specificity and selectivity of commercially-available anti-5-HT_{2C}R antibodies have not been extensively characterized for use in Western blot, immunoprecipitation or immunohistochemical analyses *ex vivo*. For example, when commertially-available antibodies have been used in Western blots, there has been a lack of consensus as to the precise immunoreactive band that should be quantified for assessment of 5-HT_{2C}R expression (**Table 2.1**). Therefore, there is a need to reliably characterize these anti-5-HT_{2C}R antibodies and to establish consistent methods for their use. Accurate characterization of these antibodies will greatly assist their use in understanding the role of the 5-HT_{2C}R in physiology and pathology. Furthermore, precise detection of the 5-HT_{2C}R cellular and subcellular localization under physiological or pathological conditions, or even following pharmacological manipulations would ultimately allow a better understanding of 5-HT_{2C}R function.

Table 2.1. Description of commercially-available anti-5-HT_{2C}R antibodies

Abbrev.	Anti- 5-HT_{2C}R Antibody	Commercial Source	Cat No.	Lot No.	Epitope	Expected MW (KDa)	Blocking peptide
D-12	Mouse Monoclonal (SR2C D-12)	Santa Cruz Biotechnology, Inc	sc-17797	J1606	aa 374-458, C-terminus	46	No
N-19	Goat Polyclonal (SR2C N-19)	Santa Cruz Biotechnology, Inc	sc-15081	L0904 G102	19 aa sequence, N-terminus	46	Yes
C-20	Goat Polyclonal (SR2C C-20)	Santa Cruz Biotechnology, Inc	sc-1464	J1800	C-terminus	60	Yes
CH	Rabbit Polyclonal	Millipore (Chemicon)	AB5655	0601020283	aa 40-54, extracellular domain	Not specified	No

The purpose of the present study was to establish the utility and validity of four commercially-available anti-5-HT_{2C}R antibodies (**Table 2.1**) for use in Western blot studies on subcellular fractions isolated from brain and peripheral organ tissue. In particular, the 5-HT_{2C}R was analyzed in brain synaptosomes and a subfraction, the postsynaptic density (PSD), an electron-dense structure of the submembrane cytoskeleton involved in receiving and transducing synaptic signals (Cotman, 1974; Gundelfinger and Tom, 2000). Since previous studies have suggested a postsynaptic localization of the 5-HT_{2C}R (Clemett et al., 2000; Lopez-Gimenez et al., 2002; Liu et al., 2007), the PSD is an appropriate cellular compartment to address the specificity and selectivity of the commercial antibodies. First, we compared immunoreactive band patterns produced by the anti-5-HT_{2C}R antibodies to determine the common and unique bands in PSD samples taken from the rat cortex. Second, since the 5-HT_{2C}R is widely expressed in brain and spinal cord, but not peripheral systems (Julius et al., 1988a; Julius et al., 1988b), we then compared membrane fractions derived from

brain and peripheral organs to assess whether the immunoreactive bands identified in cortical PSD were unique to samples isolated from brain tissue. Because the 5-HT_{2C}R contains 3 potential N-linked glycosylation sites [one at the N-terminus and two contiguous in the 3rd intracellular loop of the receptor; (Julius et al., 1988a; Backstrom et al., 1995; Abramowski and Staufenbiel, 1995; Abramowski et al., 1995; Mancia et al., 2007)], a third set of studies used enzymatic deglycosylation of samples prior to Western blotting to determine whether the immunoreactive bands identified in the PSD-enriched samples represent posttranslationally modified forms of the 5-HT_{2C}R. We predicted that if the diverse immunoreactive bands correspond to posttranslationally modified 5-HT_{2C}R protein then the removal of the posttranslational modification would lead to a shift in the molecular weight of the immunoreactive bands that in theory should be identified by all the anti-5-HT_{2C}R antibodies at the same molecular weight. Lastly, because the PSD-95 is an important binding partner for 5-HT_{2C}R (Becamel et al., 2002; Becamel et al., 2004; Gavarini et al., 2004; Gavarini et al., 2006), we immunoprecipitated synaptosomal membrane proteins with each of the anti-5-HT_{2C}R antibodies and then probed the resultant Western blots for PSD-95 and the precipitating antibody. If 5-HT_{2C}R co-immunoprecipitates with PSD-95 and vice versa, the likelihood of the anti-5-HT_{2C}R antibodies of accurately detecting the 5-HT_{2C}R protein would increase.

MATERIAL AND METHODS

Animals

Adult male Sprague-Dawley rats (virus antibody-free; 250-300g, Harlan, Indianapolis, IN) weighing 225-280 g at the beginning of the experimental procedures were used. All rats were kept in the colony room for a minimum of 7 days after arrival, during which time they were handled and weighed daily to acclimate them to the handling procedures used during experiments. All rats were housed four/cage with food and water *ad libitum*. The animal colony was maintained at a constant temperature (21-23^{o}C) and humidity (45-50%) on a 12 hr light-dark cycle (lights on 0700-1900 hr). All experimental protocols were carried out in accordance with the Guide for the Care and Use of Laboratory Animals (National Institutes of Health, 1986) and with the approval by the Institutional Animal Care and Use Committee (IACUC).

Drugs

Chloral hydrate was dissolved in physiological saline and administered at a dose of 800 mg/kg. The solution was injected at room temperature.

Antibodies

Table 2.1 lists suppliers and key features of each of the 5-HT_{2C}R antibodies employed in the present study. Western blot membranes were incubated with primary antibody as follows. All anti-5-HT_{2C}R antibodies were incubated overnight: mouse monoclonal **D-12** [SR-2C, sc-17797, Lot No. J1606, Santa Cruz; at 1:100 dilution]; affinity purified goat polyclonal **N-19** [sc-15081, Lot

No. I1508, Santa Cruz; 1:250]; affinity purified goat polyclonal **C-20** [sc-1464, Lot No. J1800, Santa Cruz; 1:200]; rabbit polyclonal **CH** [AB5655, Lot No. 0601020283, Chemicon International, Temecula, CA; 1:500]. Other primary antibodies were incubated at room temperature (RT) for 1 hr: monoclonal mouse anti-PSD-95 [Chemicon International; 1:2,000]; monoclonal mouse anti-syntaxin [Chemicon International; 1:5,000]; monoclonal mouse anti-SNAP-25 [Chemicon International; 1:1,000]; monoclonal mouse anti-β-actin [Chemicon International; 1:5000]. Secondary antibodies (used at 1:20,000 dilution) included infrared (IR)-labeled goat anti-mouse (IRDye™680; 926-32220, Lot No. B61017-02, LI-COR® Biosciences, Lincoln, NK); goat anti-rabbit (IRDye™800; 827-08365, Lot No. B61023-01, LI-COR® Biosciences) and donkey anti-goat (IRDye™800CW; 605-731-125, Lot No. 17309, Rockland Immunochemicals, Inc., Gilbertsville, PA).

Tissue preparation

Membrane fractionation: brain and peripheral tissues

Rats were anesthetized [chloral hydrate solution (800 mg/kg)], decapitated, and brain (motor cortex, PFC and cerebellum), liver, kidney and lung were microdissected immediately on a cool tray (4^{o}C) (Heffner et al., 1980). Samples were flash frozen in liquid nitrogen and stored at -80^{o}C for subsequent protein extraction. All tissues were homogenized in 300 µL extraction buffer (pH 7.4) containing 10 mM HEPES, 1 mM EDTA, 2 mM EGTA, 500 µM DTT, protease inhibitor cocktail (10 µL/mL; Sigma, St. Louis, MO, Cat. No. P8340) and

phosphatase inhibitor cocktails 1 and 2 (10 µL/mL each; Sigma, Cat. No. P2850 and P5726, respectively). The homogenate was centrifuged at 1,000 g for 10 min at 4°C to pellet the nuclear fraction. The supernatant (S_1) was removed and the pellet (nuclear pellet) was washed by resuspending in extraction buffer and recentrifuging. The S_1 from the first spin was centrifuged at 20,000 g at 4°C for 30 min to pellet the membrane bound protein fraction. The membrane-enriched pellet was washed once, then resuspended in 200 µL 1% SDS solution. Total protein concentration was determined for each fraction using a BCA protein determination kit (Pierce, Rockford, IL).

Postsynaptic density (PSD)-enriched fractionation

PSD-enriched fractionation was performed as previously described (Phillips et al., 2001; Liu et al., 2007; Moron and Devi, 2007). Motor cortex and PFC were homogenized in 0.32 M sucrose solution containing 0.1 mM $CaCl_2$ and protease and phosphatase inhibitor cocktails (10 µL/mL each). An aliquot (**total homogenate**) was set aside and the remaining homogenate was diluted with 6 mL 2 M sucrose and 2.5 mL 0.1 mM $CaCl_2$. The resulting solution was mixed by inversion, transferred to a 25 mL ultracentrifuge tube (Beckman Coulter, Fullerton, CA), overlaid with enough 1 M sucrose solution to fill the remaining volume of the ultracentrifuge tube, then ultracentrifuged (LE-80K Ultracentrifuge, Beckman Coulter) in a fixed angle rotor (50.2 Ti Rotor) at 100,000 g for 3 hrs at 4^{o}C. Synaptosomes were located at the interface of the 1.25 M and the 1 M sucrose phase and were removed by careful pipetting. An aliquot

(**synaptosomal fraction**) was taken and the remaining solution (approximately 2.5 mL) was diluted with 15.6 mL hypotonic solution [13.5 mL 0.1 mM $CaCl_2$, 0.3 mL 1 M Tris pH 6 buffer, 1.5 mL 10% Triton X-100, 150 µL each of protease and phosphatase inhibitor cocktails]. This solution was mixed by inversion and incubated on a shaker for 20 min at 4°C. The synaptic junctions were collected by centrifugation at 48,000 g for 20 min at 4°C (J2-HS centrifuge, Beckman Coulter). The supernatant was discarded; the pellet was resuspended in 15.6 mL hypotonic solution and incubated on a shaker for 20 min at 4°C. Synaptic junctions were collected by centrifugation at 48,000 g for 20 min at 4°C. The supernatant was discarded and the pellet was resuspended in 10 mL of pH 8 buffer [20 mM Tris, 1% Triton X-100] to disrupt the pre-to-post synaptic connection. The solution was incubated on a shaker for 20 min at 4°C. The PSD-enriched fraction was collected by centrifugation at 48,000 g for 20 min at 4°C, washed once in 10 mL pH 8 buffer with incubation on a shaker for 20 min at 4°C and recentrifuged. The supernatant was discarded; the remaining pellet was resuspended in 1% SDS. All aliquots collected were frozen at -80°C for later protein analysis.

Western blotting

Equal amounts of protein (10 µg from each fraction, reduced with an appropriate volume of Laemmli sample buffer with DTT and heated for 20 min at 70°C) were separated by SDS-PAGE using 4-12% BisTris pre-cast gels (Invitrogen, San Diego, CA) for 2-3 hrs at 120V. Following gel electrophoresis,

proteins were transferred to a PVDF membrane (BioRad, Hercules, CA) via a wet-transfer electroblotting apparatus (BioRad) for 3 hr at 100V. Western blot assays were conducted as follows: membranes were blocked with Odyssey blocking buffer (LI-COR® Biosciences; 1:1 in Tris Buffered Saline (TBS), pH 7.4) for 1-2 hr followed by incubation with primary antibody for 1 hr to overnight (see above). Membranes were rinsed 4 x 10 min in TBS + 0.1% Tween-20 (TBS-T), incubated with secondary antibody for 45 min, then rinsed 4 x 10 min in TBS-T prior to incubation with TBS for a period of 2 hr. Fluorescent dyes were detected with the Odyssey® Infrared Imaging System (LI-COR® Biosciences).

Deglycosylation assay

The PSD-enriched fraction derived from PFC was suspended in resuspension buffer [10 mM NaCl, 5 mM EDTA, 10 mM NaH_2PO_4, 0.25 % Triton X-100, pH 7.4; protease and phosphatase inhibitors (10 µL/mL)]. The deglycosylation reaction was carried out using 1 µL of N-Glycosidase F (PNGase F, 500 U/µL; Cat. No. P07045, New England Biolabs, Ipswich, MA) according to manufacturer's directions. The enzyme cleaves bonds between asparagine and N-acetylglucosamine, thus separating the oligosaccharide from the polypeptide. To follow the progress of the reaction, aliquots were taken 0, 30 min, 60 min and overnight. A parallel reaction that utilized 1 µL of RNAse B (5 µg/µL; Cat. No. P78175, New England Biolabs) as substrate served as a positive control. The deglycosylation reaction was stopped by addition of loading buffer and

immediately boiling for 5-10 min. Samples were separated by SDS-PAGE using 4-12% BisTris pre-cast gels (Invitrogen) for 3 hrs at 120V.

Co-immunoprecipitation assays

Pooled synaptosomes (100 µg) from PFC were centrifuged at 14,000 g for 40 min at 4^{o}C (TOMY High Speed Refrigerated Microcentrifuge TX-160, Palo Alto, CA). The resultant synaptosomal pellet was resuspended in 400 µL of lysis buffer [10 mM NaCl, 5 mM EDTA, 10 mM NaH_2PO_4, 1% Triton X-100, pH 7.4; protease and phosphatase inhibitors (10 µL/mL each)] by pipetting, then incubated for 20 min at 4^{o}C in a nutating mixer (VWR Internationals, West Chester, PA). 3 µg of antibody and 80 µL of protein G agarose beads (pre-washed 3x in lysis buffer) were added simultaneously to the suspension and the solution was incubated overnight at 4^{o}C with shaking. The suspension was centrifuged at 1,000 g for 10 min. The supernatant was discarded and the pellet (beads) was washed twice (centrifuged at 1,000 g for 1 min) with lysis buffer containing 0.25 % Triton X-100, then once with PBS containing 5 mM EDTA. The resultant pellet was resuspended in 20 µL of elution buffer (0.1 M glycine-HCl pH 2.5) and incubated at RT for 5 min (mixed by pipetting). Neutralization buffer (1 M Tris pH 7; 1/10 of the Elution buffer volume) was added to adjust the eluate to physiological pH. Samples were centrifuged and the supernatant was collected. Loading buffer was added and the resulting supernatant was separated by SDS-PAGE using 10% BisTris pre-cast gels (Invitrogen) for 2-3 hrs at 120V. A

sample incubated with Protein G agarose beads but no primary antibody was used as a control.

Data Analysis

Membranes were imaged using the Odyssey® Infrared Imaging System (LI-COR® Biosciences) at 700 and/or 800 nm at 169 µm resolution. The integrated intensity of each band was analyzed with the Odyssey® Infrared Imaging System Application version 2.1 Software. Following background subtraction, the ratio of 5-HT_{2C}R band intensity to actin band intensity was determined for each sample to normalize for the amount of protein loaded (see Results for details of band selection). A one-way Analysis of Variance [ANOVA, GLM procedure with SAS System for Windows V.8.2 (SAS Institute Inc., Cary, NC)] was used to assess differences in 5-HT_{2C}R protein expression among tissue samples. Since the PSD-enriched fraction used in **Fig. 2.2** was extracted from motor cortex, we decided to use the 5-HT_{2C}R density in motor cortex for preplanned comparisons. When an overall significant F ratio was observed, individual means were compared for 5-HT_{2C}R density using Dunnett's procedure with an experimentwise error rate $\alpha = 0.05$.

RESULTS

We have used synaptosomal and PSD-enriched fractions isolated from motor cortex and PFC to characterized four antibodies (**Table 2.1**) raised against different regions of the 5-HT_{2C}R protein. Our goal was to determine what proteins

and their subsets are recognized by these reagents, and to describe the best conditions under which to use them to study expression of the 5-HT_{2C}R.

Validation of synaptosomal enrichment

Western blots bands detected by antibodies were compared to appropriate marker proteins. PSD-95, a PSD marker (Banker et al., 1974; Hunt et al., 1996), indicated that PSD-95 was found in all fractions, with the highest levels seen in synaptic junction and PSD-enriched fraction (**Fig. 2.1**). In contrast, syntaxin, which selectively labels the presynaptic active zone (Bennett and Scheller, 1994), was detected in the total homogenate and synaptosomal fractions, and was reduced or absent in the synaptic junction and the PSD-enriched fractions, respectively (**Fig. 2.1**). SNAP-25, another presynaptic active zone marker, was observed at higher levels in total homogenate and in the synaptosomal fraction but was reduced in synaptic junction and PSD-enriched fractions (**Fig. 2.1**). Thus, our fractionation protocol yielded an enrichment of postsynaptic density proteins with a reduction of presynaptic active zone proteins, in agreement with previously published data (Phillips et al., 2001; Liu et al., 2007; Moron and Devi, 2007).

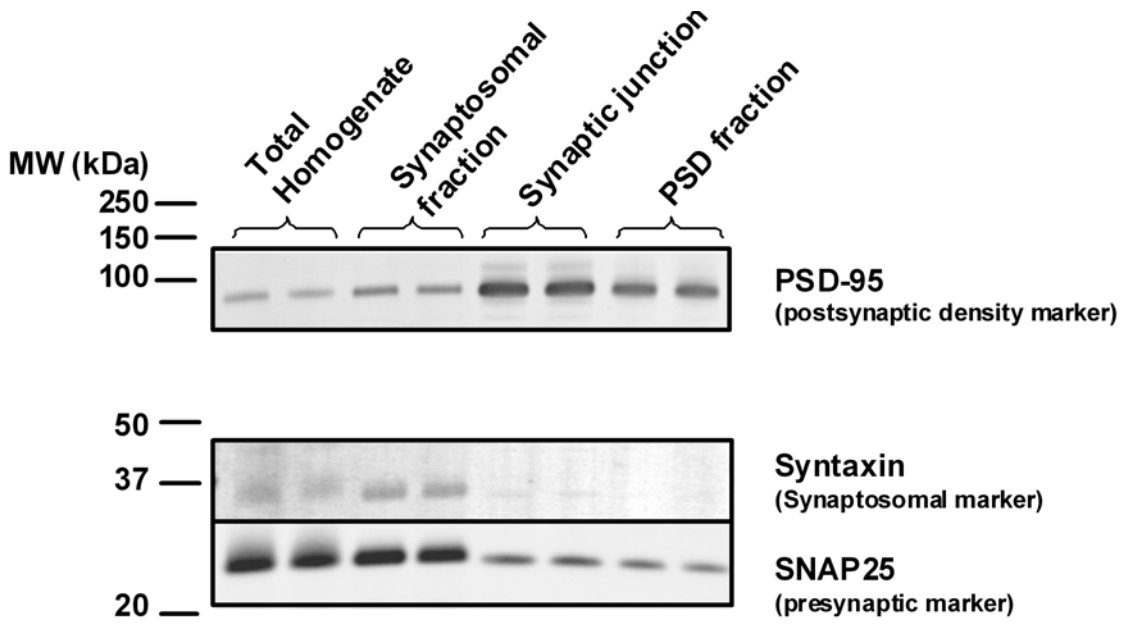

Figure 2.1. Validation of synaptosomal enrichment. Total homogenate, synaptosomal fraction, synaptic junction and PSD-enriched fraction isolated from motor cortex of naive rats were analyzed by Western blot using antibodies against PSD-95, syntaxin and SNAP-25. Data presented are from a single blot that was stripped and re-probed. Location of the MW markers is shown to the left of the blots.

Validation of 5-HT_{2C}R antibodies using the PSD-enriched fraction

The 5-HT_{2C}R, which contains 460 amino acids, presents a theoretical MW of 51,916 Da (Julius et al. 1988). However, experimenters using individual laboratory-produced anti-5-HT_{2C}R antibodies have reported immunoreactive bands with apparent MWs of 41, 51 and 56-62 kDa in membrane fractions of rat choroid plexus (Backstrom et al., 1995; Abramowski and Staufenbiel, 1995) and 45-97 kDa in the 3T3/2C cell line (Backstrom and Sanders-Bush, 1997).

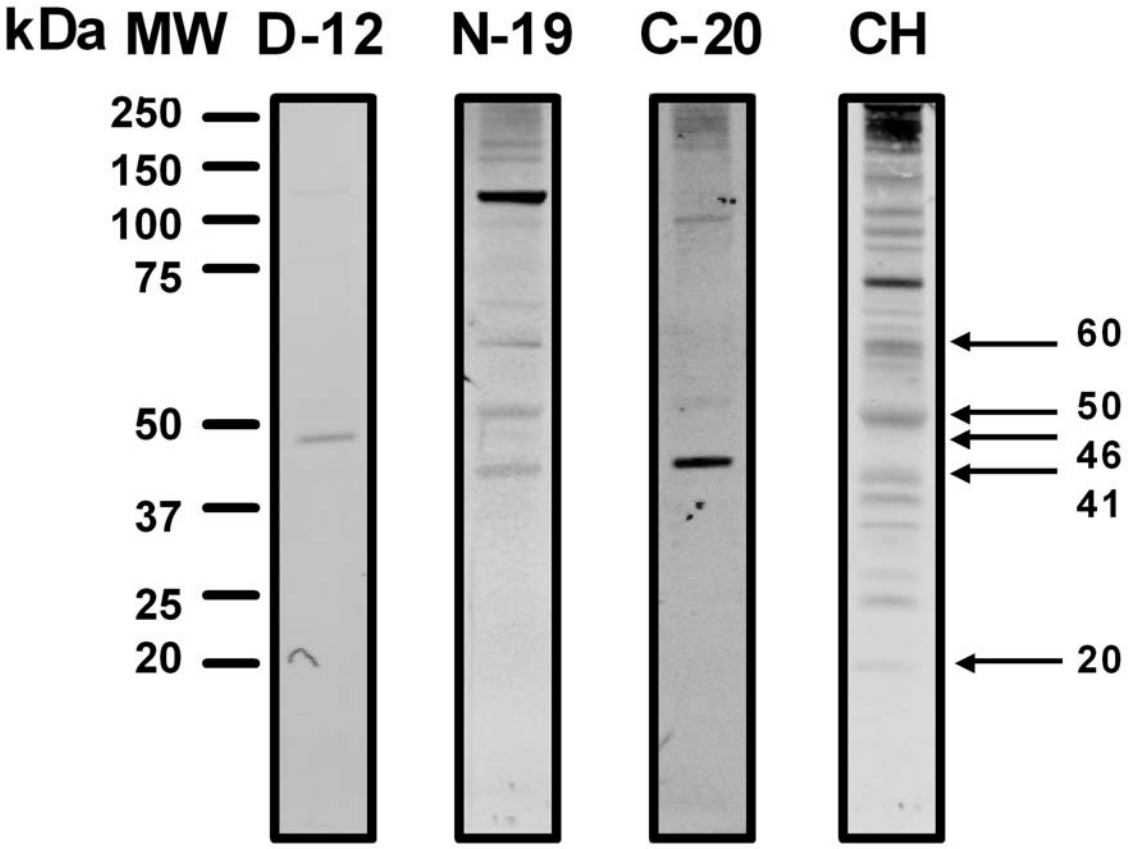

Figure 2.2. Band patterns of 5-HT_{2C}R. PSD-enriched fractions from motor cortex of naïve rats (10 µg of protein) from motor cortex were analyzed by Western blot using antibodies against the 5-HT_{2C}R (see **Table 2.1**). Lane 1: D-12 (1:100); 2: N-19 (1:250); 3: C-20 (1:200); and 4: CH (1:500). Data presented are from a single blot. Location of the MW markers is shown to the left of the blots.

Fig. 2.2 illustrates Western blot analysis with four commercially-available anti-5-HT_{2C}R antibodies selected for this study. Western blot analysis of the PSD-enriched fraction with the D-12 antibody indicated a unique band with an apparent MW of 46 kDa and an additional very faint immunoreactive band above 100 kDa (**Fig.2.2**, lane 1). The N-19 antibody detected 3 immunoreactive bands of intermediate intensity of apparent molecular sizes 41, 50 and 60 kDa. The

N-19 antibody detected a very faint band at 46 kDa and also a very strong immunoreactive band above 100 kDa (**Fig. 2.2**, lane 2). The C-20 antibody detected a very strong immunoreactive band at 41 kDa and one fainter band at 50 kDa (**Fig. 2.2,** lane 3) as well as multiple bands in the >100 kDa range. The CH antibody detected the most immunoreactive bands, many of intermediate intensity including at 41, 50 and 60 kDa. Of note are an additional fainter band of ~20 kDa (**Fig. 2.2**, lane 4) and multiple high molecular weight bands. A particularly strong band was seen at ~70 kDa.

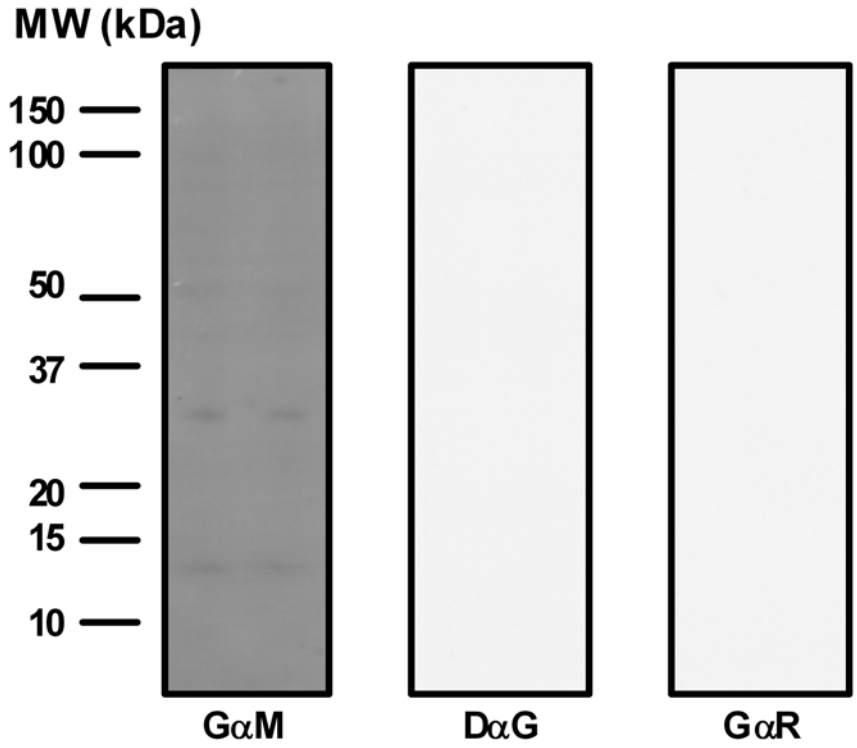

Figure 2.3. Cross-reactivity of fluorescently-labeled secondary antibodies. 5 µg of PSD-enriched fraction was analyzed by Western blot against [GαM] goat anti-mouse; [DαG] donkey anti-goat; and [GαR] goat anti-rabbit secondary antibodies in the absence of anti-5-HT_{2C}R antibodies. Data presented are from a single blot. Location of the MW markers is shown to the left of the blots.

It is noteworthy that only the D-12 and N-19 anti-5-HT_{2C}R antibodies detected immunoreactive bands at the MWs reported by the manufacturer (**Table 2.1**). To assess whether the multiple bands observed were due to nonspecific binding of secondary antibody, we performed a Western blot in the absence of primary antibodies (**Fig. 2.3**). Our results showed that the immunoreactive bands observed in the PSD-enriched fraction were not due to nonspecific secondary antibody binding.

Tissue distribution of the 5-HT_{2C}R

The regional distribution and abundance of the 5-HT_{2C}R have been previously characterized (Backstrom et al., 1995; Clemett et al., 2000) and indicate a lack of 5-HT_{2C}R protein expression in peripheral tissues (Julius et al., 1988a; Julius et al., 1988b; Molineaux et al., 1989). We assessed the specificity of the four commercially-available anti-5-HT_{2C}R antibodies in total membrane fractions of three brain regions (motor cortex, PFC, cerebellum) and three peripheral organs (liver, kidney, lung) (**Fig. 2.4**). We decided to pursue a total membrane fractionation protocol for this experiment because previous experiments using the individual laboratory-produced 5-HT_{2C}R antibodies were performed in total membrane fractions (Abramowski et al.,1995; Abramowski and Staufenbiel, 1995; Backstrom et al., 1995; Backstrom and Sanders-Bush, 1997; Parker et al., 2003). In agreement with MWs previously reported for the 5-HT_{2C}R (Backstrom, et al., 1995; Canton, et al., 1996), the D-12 (**Fig. 2.4A**) and CH (**Fig. 2.4D**) antibodies detected intensely immunoreactive bands at apparent MWs 46

and 41 kDa, respectively, in motor cortex and PFC, but less so in cerebellum and liver, and negligible in lung, kidney membranes. The N-19 anti-5-HT_{2C}R antibody detected an intensely immunoreactive band of apparent MW 60 kDa (**Fig. 2.4B**), one fainter band at 46 kDa in motor cortex and PFC, but not in cerebellum, lung, kidney or liver samples. These results obtained for the D-12, N-19 and CH antibodies agree with our findings on the expression of 5-HT_{2C}R in the PSD-enriched fraction derived from motor cortex (**Fig. 2.2**).

All of the bands chosen for analysis in this experiment corresponded to immunoreactive bands observed in the PSD-enriched fraction (**Fig. 2.2**). We quantified the immunoreactive bands for the D-12 (46 kDa), N-19 (60 kDa) and CH (41 kDa) anti-5-HT_{2C}R antibodies. A unique immunoreactive band seen for the C-20 antibody was difficult to quantify due to the high cross-reactivity of this antibody with proteins from peripheral organ membrane fractions (**Fig. 2.4C**). Rather, the 41 kDa immunorective band, which was the most intense band detected in the PSD-enriched fraction (**Fig. 2.2**) was analyzed for this study (**Fig. 2.4C**). A one-way ANOVA revealed a statistically significant difference between motor cortex and liver, kidney or lung when the D-12 anti-5-HT_{2C}R antibody was used ($F_{(5,21)}$ = 10.278, p = 0.0001). No statistically significant differences were observed between the motor cortex and PFC or cerebellum ($p > 0.05$). When the N-19 anti-5-HT_{2C}R antibody was used statistically significant differences among tissue samples were observed between motor cortex and liver, kidney or lung ($F_{(5,21)}$ = 16.584, p = 0.0001).

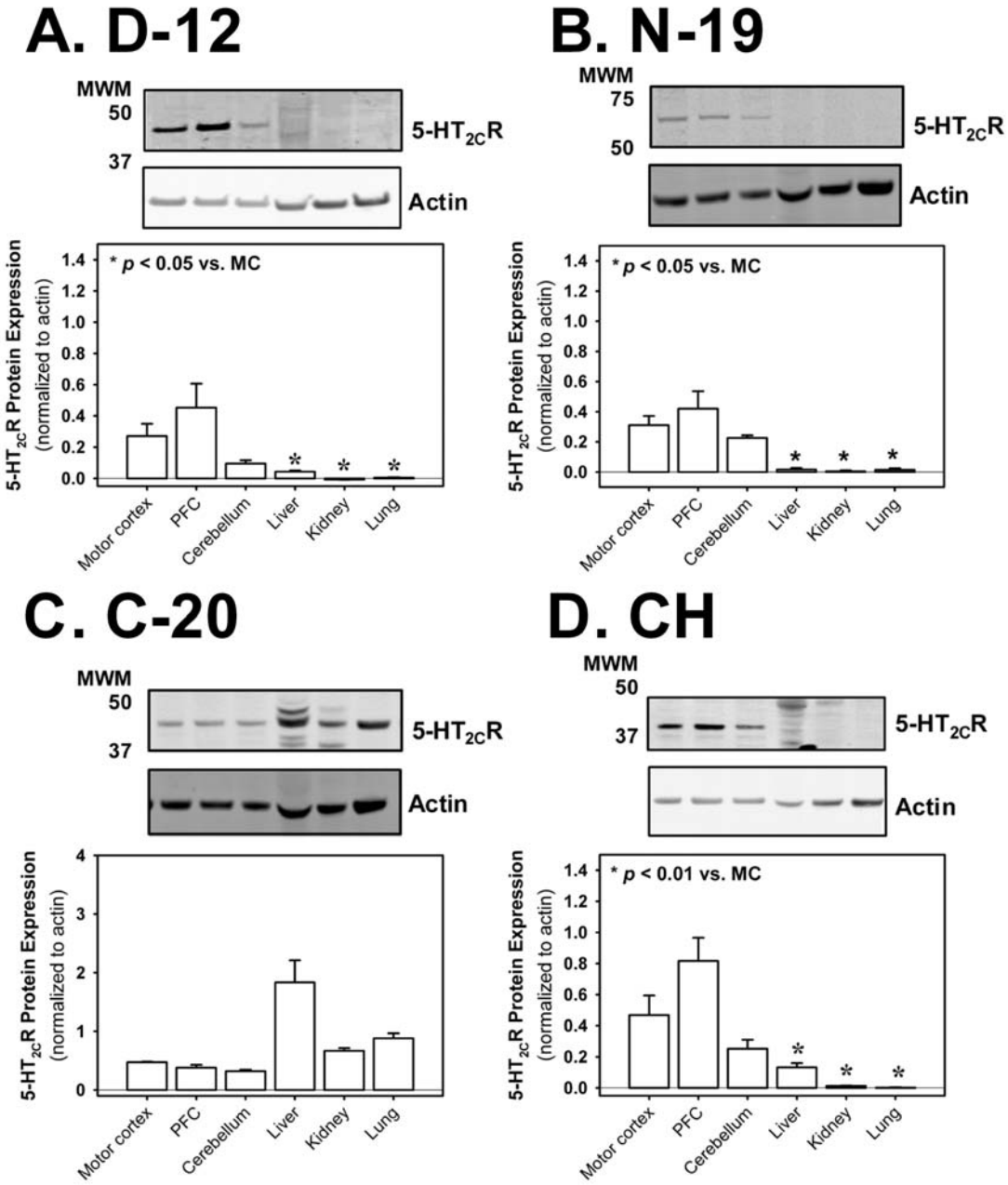

Figure 2.4. Specificity of anti-5-HT$_{2C}$R antibodies for brain. Membrane fractions from motor cortex, PFC, cerebellum, kidney, liver and lung (n = 3-4 samples/each) were analyzed by Western blot using four commercially-available anti-5-HT$_{2C}$R antibodies. [A] D-12; [B] N-19; [C] C-20; [D] CH anti-5-HT$_{2C}$R antibodies. Western blot data was normalized to actin. Experiments were repeated twice. Results are expressed as mean ± SEM.

A statistically significant differences was observed between the motor cortex and PFC ($p < 0.05$), but not for cerebellum ($p > 0.05$). Finally, when the CH anti-5-HT_{2C}R antibody was used, a one-way ANOVA revealed statistically significant differences between the motor cortex and kidney, liver or lung membrane samples ($F_{(5,22)} = 2.920$, $p < 0.0001$). A statistically significant difference was not observed between the motor cortex and the PFC or cerebellum ($p > 0.05$). Because of the high levels of 5-HT_{2C}R immunoreactivity detected in peripheral tissue membrane fractions by the C-20 antibody, leading us to be less confident of selective recognition of the receptor protein, the remaining experiments were conducted only with the D-12, N-19 and CH antibodies.

Deglycosylation assay

To assess whether the multiple bands observed following Western blot assays correspond to multiple posttranslationally modified versions of the 5-HT_{2C}R, appropriate immunoreactive bands were monitored in samples of PSD-enriched fractions from PFC under deglycosylation conditions compared to untreated samples (controls) using the D-12 (46 kDa), N-19 (60 kDa) and CH (41 kDa) anti-5-HT_{2C}R antibodies. RNAse B, which presents a single glycosylation site, was used as a positive control for enzymatic activity. Under conditions of exposure to PNGase F, the deglycosylation enzyme produced the expected shift in MW for RNAse B from ~23 to 17 kDa indicating the separation of the oligosaccharide from the polypeptide (**Fig. 2.5A**).

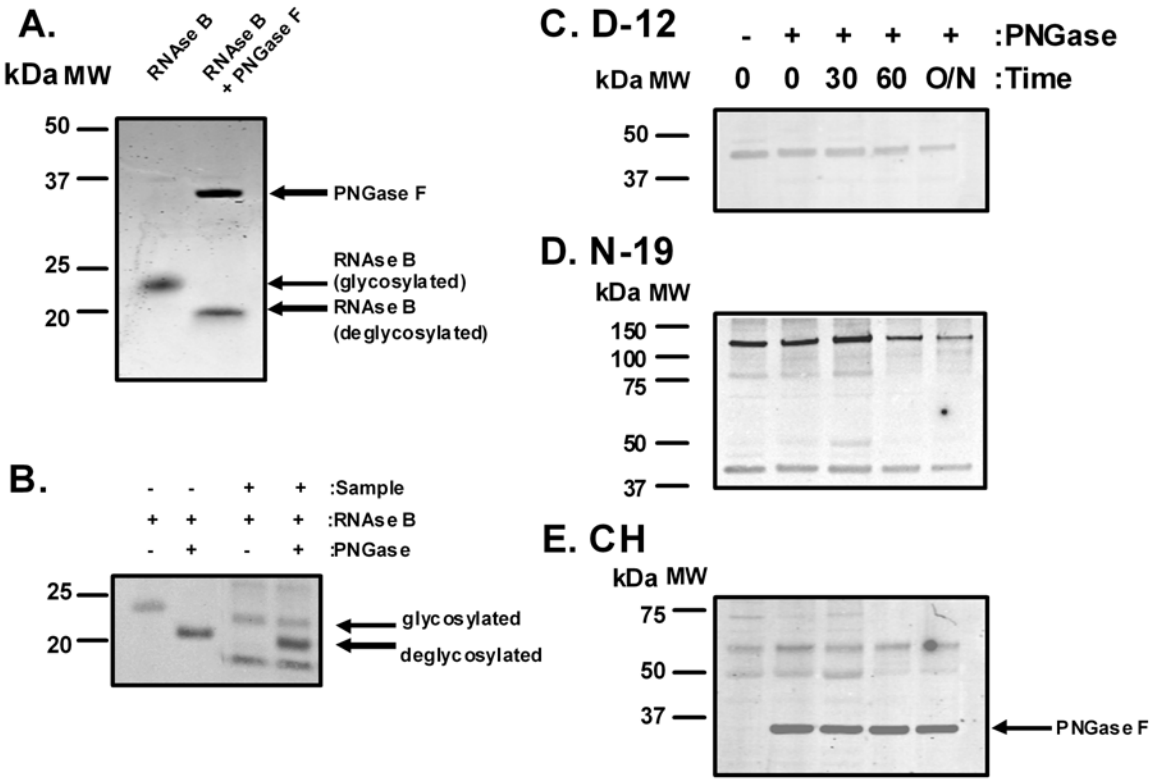

Figure 2.5. Comparison of deglycosylated and untreated samples. PSD-enriched fractions from the PFC were treated with the N-glycosidase F (PNGase, 500 U/μL) to cleave the oligosaccharide from the receptor protein. [A] Migration pattern of RNAse B (positive control) in the presence and absence of PNGase F (Commassie blue). [B] Validation of enzymatic PNGase F activity in PSD-enriched fraction; Western blots using [C] D-12, [D] N-19 and [E] CH anti-5-HT_{2C}R antibodies. Several aliquots (0, 30, 60 min and overnight) were taken to follow the progress of the reaction.

However, **Fig. 2.5C-E** shows that incubation of PSD samples with PNGase F, even for progressive time periods, did not cause MW shifts in any of the immunoreactive bands detected by any of the 3 antibodies. Furthermore, the CH antibody cross-identified the enzyme itself, suggesting that the CH antibody is nonspecific and that particular care should be taken when using this antibody in Western blot studies **Fig. 2.5E**. To determine whether these results were due

to insufficient enzyme concentration or to inhibitors in the sample buffer that might affect enzyme activity (Material and Methods), RNAse B (1 µg) was included in the reaction mixture with PSD-enriched samples as an internal control and incubated for a total of 90 min. The results in **Fig. 2.5B** show that the RNAse B was successfully cleaved, thus indicating that there was sufficient catalytic activity of 1 µg of PNGase F under the assay conditions and that the reaction was not inhibited by the buffers used.

Co-immunoprecipitation assays

PSD-95 is a protein that is physically associated with 5-HT_{2C}R (Becamel et al., 2002; Becamel et al., 2004; Gavarini et al., 2004; Gavarini et al., 2006), therefore identification of PSD-95 in eluted samples immunoprecipitated with the 5-HT_{2C}R antibodies D-12, N-19 or CH would further validate that the protein recognized by the commercially-available 5-HT_{2C}R antibodies is authentic 5-HT_{2C}R. We performed co-immunoprecipitation assays to assess whether the D-12, N-19 and CH anti-5-HT_{2C}R antibodies were capable of immunoprecipitating PSD-95 (Becamel et al., 2002; Becamel et al., 2004; Gavarini et al., 2004; Gavarini et al., 2006).

Co-immunoprecipitation studies using the anti-5-HT_{2C}R antibodies

The synaptosomal fraction of pooled PFC tissue (n = 6 tissues pooled) was used for co-immunoprecipitation studies employing the anti-5-HT_{2C}R antibodies. The anti-PSD-95 antibody detected the expected immunoreactive band of 95 kDa in samples immunoprecipitated with each of the anti-5-HT_{2C}R

antibodies as well as with the anti-PSD-95 antibody (**Fig. 6**). As expected synaptosomal samples immunoprecipitated with anti-PSD-95 antibody exhibited an intense immunoreactive band at 95 kDa. Less intense immunoreactive bands were also observed for the D-12 and CH anti-5-HT_{2C}R antibodies, and a faint immunoreactive band was observed for the N-19 anti-5-HT_{2C}R antibody (**Fig. 6A**).

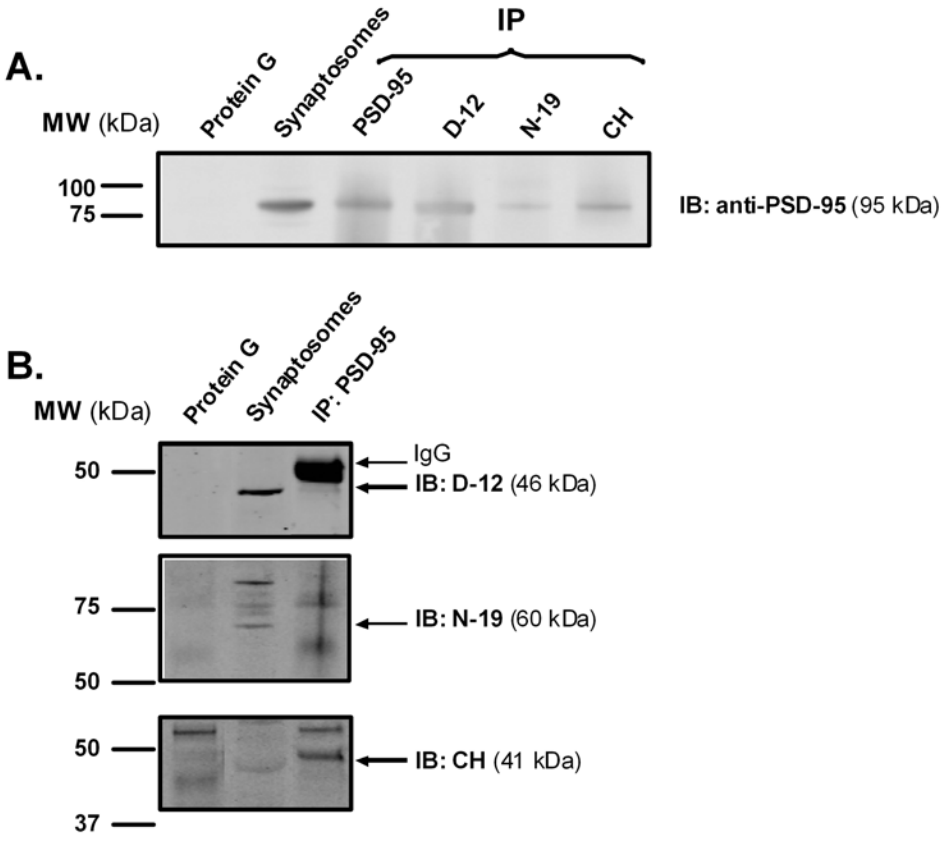

Figure 2.6. Co-immunoprecipitation studies with anti-5-HT_{2C}R antibodies. [A] synaptosomal fraction immunoprecipitated with PSD-95, D-12, N-19 and CH antibodies and immunoblotted with anti-PSD-95 antibody; [B] synaptosomal fraction immunoprecipitated with anti-PSD-95 antibody and immunoblotted with the anti-5-HT_{2C}R antibodies.. For [A] and [B] Lane 1: negative control (protein G agarose beads); and lane 2: synaptosomes (10 µg)

The D-12 anti-5-HT_{2C}R antibody detected the appropriate immunoreactive band of 46 kDa in synaptosomal samples immunoprecipitated with the anti-PSD-95 antibody (**Fig. 6B**, upper lane). The N-19 did not detect the antibody-appropriate immunoreactive bands of 60 kDa in samples immunoprecipitated with the anti-PSD-95 antibody, which was unexpected (**Fig. 6B**, middle lane). However, this findings agrees and correlates with the faint detection of PSD-95 following immunoprecipitation by N-19 antibody (**Fig. 6A**). It is possible that the eluted 5-HT_{2C}R protein immunoprecipitated with anti-PSD-95 antibody is below the detection limit for the N-19 anti-5-HT_{2C}R antibody. In any case, this result suggests that N-19 is not suitable for immunoprecipitation studies under the conditions employed here. The CH antibody did not detect an immunoreactive band at 41 kDa (the band detected by CH that was unique to brain samples; **Fig. 2.4D**) in the synaptosomal sample immunoprecipitated with anti-PSD-95 antibody (**Fig. 6B**, lower lane). In addition, the CH antibody exhibited nonspecific binding with the controls (Protein G Agarose beads), further suggesting that this antibody is not a good candidate for immunoprecipitation studies. The D-12 and the N-19 anti-5-HT_{2C}R antibodies did not show nonspecific binding with proteins associated to the Agarose beads (**Fig. 6B**, protein G lane). The results obtained with the D-12 and the N-19 anti-5-HT_{2C}R antibodies are consistent with previous studies in which an interaction between PSD-95 and 5-HT_{2C}R was observed (Becamel et al., 2002; Becamel et al., 2004; Gavarini et al., 2004; Gavarini et al., 2006). Taken together, these data support the hypothesis that the D-12 and N-19 anti-5-HT_{2C}R antibodies are useful to detect authentic 5-HT_{2C}R protein, but that

only the D-12 is suitable for immunoprecipitation studies under the conditions employed here.

Cross-reactivity of primary and secondary antibodies in co-immunoprecipitation studies

Cross-reactivity between primary and secondary antibodies was assessed by testing the nonspecific binding of these antibodies in the absence of sample. Primary antibodies (3-4 µg of D-12, N-19, CH, C-20 and PSD-95) were subjected to the same gel electrophoresis protocol used for samples then transferred to a PVDF membrane via wet-transfer electroblotting. Immunoblotting then was conducted in the absence of the primary antibody to assess cross-reactivity of the secondary antibodies with any of the primary antibodies used in this study (Material and Methods). Our data showed as expected that the goat-anti mouse secondary antibody only detected primary antibodies raised in mouse (D-12 and PSD-95 antibodies) with no cross-reactivity with antibodies raised in goat (N-19 and C-20 antibodies) or rabbit (CH antibody) (**Fig. 2.7A**). The donkey anti-goat secondary antibody not only detected primary antibodies raised in goat (N-19 and C-20 antibodies), but also exhibited a reduced cross-reactivity with primary antibodies raised in mouse (D-12 and PSD-95 antibodies) (**Fig. 2.7B**). Finally, the goat-anti rabbit secondary antibody only detected primary antibodies raised in rabbit (CH antibody) with no cross-reactivity with antibodies raised in goat (N-19 and C-20 antibodies) or mouse (D-12 and PSD-95 antibody) (**Fig. 2.7C**). Thus, when performing co-immunoprecipitation experiments particular care

should be taken in deciding the combination of primary antibodies that are going to be used in the study.

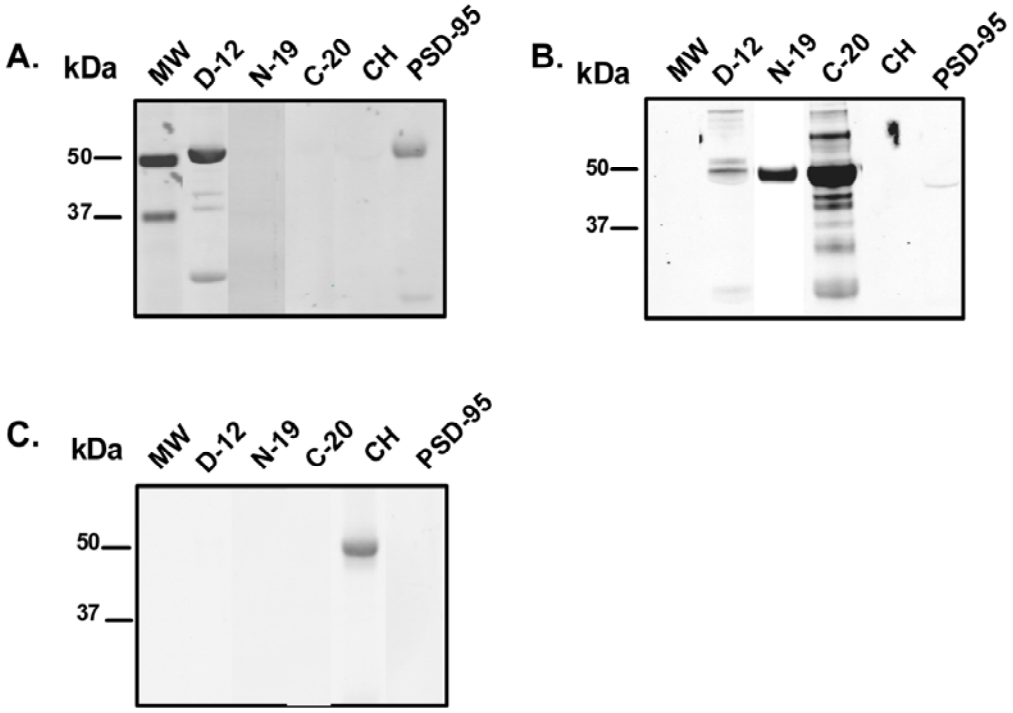

Figure 2.7. Cross-reactivity of fluorescently-labeled secondary antibodies with the primary antibodies for co-immunoprecipitation studies. 4 µg of primary antibodies [D-12, N-19, C-20, CH and PSD-95 primary antibodies] were analyzed by Western blot using the [A] goat anti-mouse; [B] donkey anti-goat; [C] goat anti-rabbit secondary antibodies. Data presented are from a single blot. Location of the MW markers is shown to the left of the blots.

We also assessed cross-reactivity among the primary antibodies. D-12 (**Fig. 2.8A**) and PSD-95 (**Fig. 2.8E**) antibodies did not cross-react with the other primary antibodies. The polyclonals goat N-19 (**Fig. 2.8B**) and C-20 (**Fig. 2.8C**) antibodies exhibited an apparent nonspecific binding with antibodies raised in mouse (D-19 and PSD-95 antibodies); however this result could be attributed to the fact that the donkey anti-goat secondary antibody, which is used to detect the

N-19 and the C-20 antibodies cross-reacted with antibodies raised in mouse (**Fig. 2.7B**) and not due to a true nonspecific binding of the N-19 or the C-20 antibodies themselves. The CH primary antibody (**Fig. 2.8D**) exhibited species-dependent interactions: high cross-reactivity with the antibodies raised in goat (the N-19 and the C-20 antibodies) but little cross-reactivity with the antibodies raised in mouse (D-12 and PSD-95) (**Fig. 2.8D**). These data suggest that particular care should be taken when assessing detection of immunoreactive bands near or close to the IgG band (approximately 50 kDa) due to a the potential for false positive results.

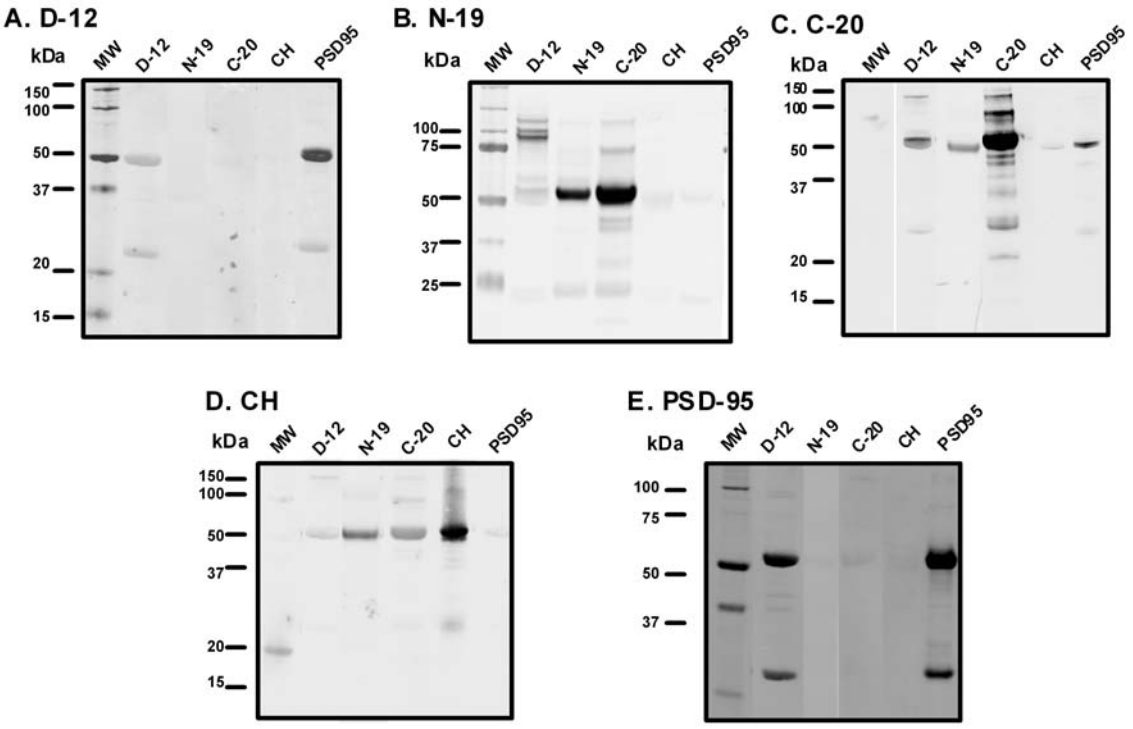

Figure 2.8. Cross-reactivity between primary antibodies for co-immunoprecipitation studies. 3 µg of primary antibodies (D-12, N-19, C-20, N-19 and PSD-95 antibodies) was analyzed by Western blot using the [A] D-12; [B] N-19; [C] C-20; [D] CH; and [E] PSD-95 primary antibodies. Data presented are from a single blot. Location of the MW marker is shown to the left of the blots.

DISCUSSION

Our results confirm the expression of the 5-HT_{2C}R in cortical synaptosomal and PSD-enriched fractions using Western blot analysis and characterize the four commercially-available 5-HT_{2C}R antibodies (**Table 2.1**) as described above. We found that the D-12 and N-19 anti-5-HT_{2C}R antibodies from Santa Cruz Biotechnology were suitable for Western blot analysis of the 5-HT_{2C}R. However, only the D-12 was suitable for immunoprecipitation studies. These observations pave the way for further quantitative analyses of trafficking and regulation of synaptic 5-HT_{2C}R protein following pharmacological manipulation.

Several studies have reported multiple immunoreactive bands for the 5-HT_{2C}R (Backstrom et al., 1995; Abramowski and Staufenbiel, 1995; Abramowski et al., 1995; Backstrom and Sanders-Bush, 1997). Immunoreactive proteins of apparent MW 51 and 56-62 kDa have been reported for the choroid plexus (Backstrom et al., 1995; Abramowski and Staufenbiel, 1995; Abramowski et al., 1995; Backstrom and Sanders-Bush, 1997). Western blotting of extracts from mouse NIH/3T3 fibroblast cells stably transfected with 5-HT_{2C}R cDNA revealed a number of immunoreactive bands ranging from 45 to 100 kDa (Backstrom et al., 1995). In this study, the anti-5-HT_{2C}R antibody did not cross-react with other proteins of untrasfected NIH/3T3 cells (Backstrom et al., 1995). In a related study, Western blotting of extracts from fibroblasts transiently transfected with cDNA derived from the truncated isoform of the 5-HT_{2C}R (whose

predicted size was 19.1 kDa) revealed bands at 17, 19, 30, and 39-40 kDa (Canton et al., 1996) (an untransfected control was not included in the study). All the immunoreactive bands (20, 41, 46, 50, 60 kDa) in the cortical PSD-enriched fraction labeled with the commercially-available anti-5-HT_{2C}R antibodies (**Fig. 2.2**) have been previously reported by other investigators using individual laboratory-produced anti-5-HT_{2C}R antibodies in protein extracts from other brain areas or from cell lines. We found that only the 41, 46 and 60 kDa bands detected by the CH, D-12 and N-19 anti-5-HT_{2C}R antibodies, respectively, were unique to brain samples and not found in peripheral tissues (lung, liver and kidney) (**Fig. 2.4**). Thus, further narrowing down the immunoreactive bands to quantify when studying the 5-HT_{2C}R with the D-12, N-19 and CH anti-5HT_{2C}R antibodies.

All of these studies suggest that multiple immunoreactive forms of the 5-HT_{2C}R exist and that the expression of protein variants depend upon the brain area or cell type under study. This multiplicity has been attributed to the fact that this receptor, like many others, undergoes alternative splicing and several posttranslational modifications; these alterations affect the electrophoretic migration and the resultant band pattern for the 5-HT_{2C}R. For example, the rodent 5-HT_{2C}R has at least two glycosylation sites (Backstrom et al., 1995; Abramowski and Staufenbiel, 1995), and the human 5-HT_{2C}R has four potential glycosylation sites (Tohda et al., 2006). Human, rat and mouse 5-HT_{2C}R transcripts also give rise to two known splice variants of the 5-HT_{2C}R including

the transcript encoding the full-length protein and an additional transcript that translates into a dramatically truncated protein (Canton et al., 1996; Xie et al., 1996). The deleted portion of the truncated receptor includes the region encoding the putative second intracellular loop and the fourth transmembrane domain of the 5-HT_{2C}R transcript and leads to a frameshift in the downstream sequence generating a premature stop codon and a uniquely short C-terminus of 19 (Canton et al., 1996) and 96 amino acids (Xie et al., 1996) in rodents and in humans, respectively. This truncated form of the 5-HT_{2C}R (in rat) would still contain two of five potential glycosylation sites predicted by the Oxford Protein Production Facility (OPPF) Protein Analysis Linker (OPAL) webpage (OPPF, University of Oxford). However, only one of the two sites presented high probability (~75%) of being glycosylated; and this site is located at the N-terminus of the 5-HT_{2C}R. This variability in protein forms and the inconsistency in the reported sizes of the 5-HT_{2C}R have contributed to the difficulty of validating anti-5-HT_{2C}R antibodies.

The anti-5-HT_{2C}R antibodies used in the present study have been raised against either the N-terminus (N-19 and CH) or the C-terminus of the receptor (D-12 and C-20) (**Table 2.1**). There are two current models that describe the topology of the 5-HT_{2C}R. The first model proposes the conventional extracellular localization of the N-terminus predicted for most GPCRs (Julius et al., 1988a; Hurley et al., 1999). The second model derives from computational and hydrophobicity analyses which suggest that the N-terminus of the 5-HT_{2C}R

contains a hydrophobic domain that might interact with the plasma membrane (Hurley et al., 1999). The amino acid sequence of this hydrophobic domain is conserved among mouse, rat and human 5-HT_{2C}R (Hurley et al., 1999), suggesting that the hydrophobic domain may serve an important function. In addition, the N-terminus of the 5-HT_{2C}R presents a potential N-linked glycosylation site in position 39 (Julius et al., 1988a) which may affect antibody-epitope recognition either by steric interference or by being required for receptor recognition by the antibody. Sequence homology between the 5-HT_{2A}R and 5-HT_{2C}R within the N-terminal region determined by sequence alignment analysis resulted in very low homology (<18%), with only 9 amino acids conserved between the rat 5-HT_{2A}R and 5-HT_{2C}R N-terminal sequences (Roth et al., 1998) and less than 4% homology between the 5-HT_{2C}R and the 5-HT_{2B}R with two conserved amino acids (Roth et al., 1998), therefore not likely giving rise to opportunities for cross-recognition. Thus, the N-terminus becomes an appealing candidate for antibody production due to the low homology presented among the members of the 5-HT_2R family. However, any combination of these factors might account for the complexity of successful antibody production against the N-terminus of 5-HT_{2C}R. It is interesting that a similar immunoreactive band pattern (60, 50 and 41 kDa) was observed for the antibodies raised against the N-terminus of the receptor for each the N-19 and CH anti-5-HT_{2C}R antibodies.

Antibodies raised against the C-terminus of the receptor (*e.g.*, D-12 and C-20) present their own recognition difficulties. For example, a BLAST analysis

reveals that a 90 amino acids segment of the C-terminus of the 5-HT_{2C}R has 34-38% identity with the 5-HT_{2A}R and 32-34% identity with the 5-HT_{2B}R (data not shown), suggesting that antibodies raised against this portion of the C-terminus may have the potential to cross-react with the 5-HT_{2A}R or 5-HT_{2B}R proteins (Roth et al., 1998). Furthermore, antibodies raised against conserved sequences of the 5-HT_{2C}R might make the antibody less specific for its target protein. For example, the 5-HT_{2C}R contains PDZ domain that might be shared by other proteins or other members of the 5-HT_2R receptor family, such as the 5-HT_{2A}R which has also been shown to interact with PSD-95 through PDZ domains (Becamel et al., 2004; Gavarini et al., 2006).

In situ hybridization studies have shown 5-HT_{2C}R mRNA expression in cerebral cortex and other brain areas (*e.g.,* amygdala, hippocampus) in rats and human (Julius et al., 1988a; Hoffman and Mezey, 1989; Molineaux et al., 1989). These findings were further corroborated with ligand binding autoradiography (Pazos et al., 1987; Mengod et al., 1990a) and immunocytochemistry (Abramowski et al., 1995; Clemett et al., 2000) and Western blot studies (Backstrom et al., 1995; Abramowski and Staufenbiel, 1995) in which 5-HT_{2C}R protein expression in cerebral cortex and other brain areas (*e.g.,* hypothalamus, amygdala, hippocampus) was detected. Furthermore, the regional distribution and abundance of the 5-HT_{2C}R mRNA expression have been previously characterized in organs of rats and results indicate that peripheral tissues lack 5-HT_{2C}R. For example, 5-HT_{2C}R mRNA was identified in choroid plexus and in

multiple brain regions (*e.g.,* hypothalamus, hippocampus and cortex), but not cerebellum nor found in liver, kidney, intestine, heart, or lung (Julius et al., 1988a; Canton et al., 1996). In light of these earlier results, our data examining 5-HT_{2C}R protein distribution eliminates the C-20 as a useful antibody for Western blot detection. Even though the remaining antibodies had some cross-reactivity with peripheral tissue, they detected immunoreactive bands that were unique in the brain [D-12 (46 kDa), N-19 (60 kDa) and CH (41 kDa)], and were therefore much better candidates.

Discrepancies in the literature concerning the mRNA and protein expression of 5-HT_{2C}R in the cerebellum have been noted. For example, none (Canton et al., 1996; Pasqualetti et al., 1999) to very low levels of 5-HT_{2C}R mRNA expression (Hoffman and Mezey, 1989; Molineaux et al., 1989) has been reported for cerebellum. Likewise, 5-HT_{2C}R protein expression in cerebellum was not detected using Western blot assays (Backstrom et al., 1995) but was detected with ligand binding autoradiography (Pazos and Palacios, 1985) and immunohistochemical studies [(Abramowski et al., 1995) but see (Clemett et al., 2000)]. The sensitivity of these types of assays and/or specificity of the mRNA probes may account for these differences in detection. Our studies showed a low level of 5-HT_{2C}R protein expression in cerebellum with all 3 acceptable antibodies (D-12, N-19 and CH anti-5-HT_{2C}R; **Fig. 2.4**), which is consistent with *in situ* hybridization (Hoffman and Mezey, 1989; Molineaux et al., 1989) and immunohistochemical studies (Clemett et al., 2000) in which expression of

5-HT_{2C}R mRNA and protein, respectively, was detected in low abundance in the cerebellum.

Our data also agree with previous observations concerning localization and abundance of 5-HT_{2C}R mRNA and protein expression in cortical brain areas. In our experiments, we observed higher 5-HT_{2C}R protein expression in the PFC than in motor cortex for all four anti-5-HT_{2C}R antibodies, although the difference was not statistically significant. Previous studies also have reported a regional distribution of the 5-HT_{2C}R with higher 5-HT_{2C}R protein expression in layer V of the PFC (Clemett et al., 2000; Liu et al., 2007) and lower expression in other cortical areas (Hoffman and Mezey, 1989) suggesting that the tested antibodies are suitable for 5-HT_{2C}R detection in cortex.

Previous deglycosylation studies using individual laboratory-produced 5-HT_{2C}R antibodies demonstrated shifts of the MW of multiple immunoreactive bands from 51 and 56-62 to 41-42 kDa (Backstrom et al., 1995; Abramowski and Staufenbiel, 1995; Abramowski et al., 1995) upon digestion with PNGase. These results suggest that some of the multiple bands observed are due to the presence of glycosylated forms of the receptor. In contrast, our deglycosylation studies showed no shift in the MW of immunoreactive bands following PNGase treatment for all of the 3 antibodies used, suggesting that other posttranslational modifications may account for the apparent MW of the immunoreactive bands detected by the D-12 (46 kDa), N-19 (60 kDa) or CH (41 kDa) antibodies (**Fig. 2.5**). Another possible reason for the discrepant results is that glycosylation of

the receptor is required for or interferes with proper recognition of the protein by the commercially-available anti-5-HT_{2C}R antibodies used here while the antibodies used in the previous studies (Backstrom et al., 1995; Abramowski and Staufenbiel, 1995; Abramowski et al., 1995) recognize both forms of the receptor.

Our immunoprecipitation assays (**Fig. 2.6**) indicate that all of the commercially-available anti-5-HT_{2C}R antibodies are capable of co-immunoprecipitating PSD-95 and vice versa, although with different efficiency, suggesting that the proteins detected have the potential to be authentic 5-HT_{2C}R (**Fig. 2.6A**) (Becamel et al., 2002; Becamel et al., 2004; Gavarini et al., 2004; Gavarini et al., 2006). However, the fact that the CH antibody detected immunoreactive bands in the control samples (containing the Protein G agarose beads and pooled synaptosomes from PFC, used to assess whether the beads themselves can precipitate proteins), suggests that the target protein binds to the beads without the aid of the antibody (nonspecific binding). The D-12 antibody did not detect bands nonspecifically, supporting its suitability for immunoprecipitation studies. The N-19 antibody has previously been characterized for immunohistochemistry studies (Bubar and Cunningham, 2006; Liu, et al., 2007) and the data presented here further extends its utility to Western blot studies. However, its weak ability to immunoprecipitate PSD-95 may limit is suitability for immunoprecipitation studies, at least under the experimental conditions used here.

Antibody selection for the detection of 5-HT_{2C}R for Western blot and immunoprecipitation studies remains challenging. We recommend an initial assessment of the ability of the antibody to detect the receptor in a subcellular compartment of interest, to see if location-based increases in concentration are verified by the antibody signal. In addition, a comparison of immunoblotting in tissue extracts from the brain area of interest to that seen in peripheral organs (that do not express 5-HT_{2C}R) would then allow evaluation of immunoreactive bands common to brain vs. other organs samples, which would then allow identification of unique immunoreactive bands in brain. Co-immunoprecipitation with several binding partners of the 5-HT_{2C}R would increases the likelihood that the anti-5-HT_{2C}R antibody is actually detecting authentic 5-HT_{2C}R. However, it would be very helpful if commercial antibody purveyors always provided the peptide antigens to which their antibodies were raised, as this is a typical way to verify which band is specific to the epitope (**Table 2.1**).

Herein we have reported the utility of two anti-5–HT_{2C}R antibodies for Western blot studies that will further our understanding in detail of the cellular, subcellular, tissue and brain region localization of the 5-HT_{2C}R under physiological and pathological conditions. Consistent with previous studies, we have demonstrated the expression of the 5-HT_{2C}R in PSD-enriched fractions from cortical brain suggesting a postsynaptic localization of the 5-HT_{2C}R (Lopez-Gimenez, et al., 2002; Clemett, et al., 2000), an observation that paves the way

for further quantitative analyses of the migration and regulation of this 5-HT_{2C}R protein at the synapse following pharmacological manipulation.

CHAPTER 3: AN INNOVATIVE REAL-TIME PCR METHOD TO MEASURE CHANGES IN RNA EDITING OF THE SEROTONIN 2C RECEPTOR (5-HT_{2C}R) IN BRAIN

INTRODUCTION

The 5-HT_{2C}R is involved in normal physiology and behavior, as well as in mental health disorders, including addiction, depression, obsessive-compulsive disorder and schizophrenia (for reviews, Giorgetti and Tecott, 2004; Bubar and Cunningham, 2008). The 5-HT_{2C}R is found in brain (Pasqualetti et al., 1999; Clemett et al., 2000) and is the only GPCR currently known to undergo mRNA editing (Burns et al., 1997; Sanders-Bush et al., 2003), a type of post-transcriptional modification that inserts, deletes (Benne, 1996; Cruz-Reyes et al., 1998; Igo, Jr. et al., 2002) or modifies (Samuel, 2003) single or small numbers of ribonucleotides in pre-mRNA. These changes alter the coding properties and information content of mRNA molecules (Bass, 2002; Hoopengardner et al., 2003; Maydanovych and Beal, 2006).

The 5-HT_{2C}R pre-mRNA is a substrate for base modification via hydrolytic deamination of five closely spaced adenosines (A) to yield inosines within a 13 base region of the RNA [(designated A, B, E, C, and D; **Fig. 3.1**) (Burns et al., 1997; Niswender et al., 1998; Gurevich et al., 2002a)]. In the course of translation, the ribosome recognizes the resultant inosine (I) as a guanosine (G), resulting in an A→G substitution. This leads to the formation of proteins that differ by up to 3 amino acids, thereby modulating receptor:G-protein coupling, constitutive activity and receptor trafficking (Herrick-Davis et al., 1999; Wang et

al., 2000; Berg et al., 2001; Marion et al., 2004). In theory, there are 32 possible nucleotide combinations of these editing sites, resulting in 24 possible protein isoforms. In practice, fewer isoforms are routinely detected and the pattern of expression varies by species and brain region (Fitzgerald et al., 1999; Niswender et al., 1999; Sanders-Bush et al., 2003).

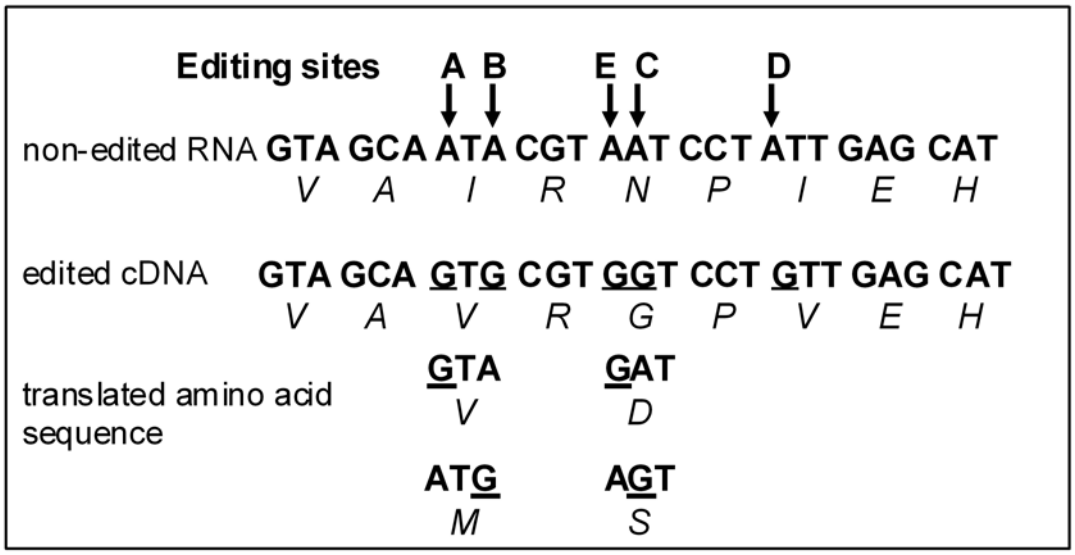

Figure 3.1. RNA editing sites of 5-HT$_{2C}$R transcript. cDNA nucleotide and predicted amino-acid sequences for the non-edited and fully-edited transcripts are shown with the editing sites indicated by arrows (↓). Picture adapted from Sanders-Bush et al (2003).

The profile of edited 5-HT$_{2C}$R isoforms is significantly modified following 5-HT depletion (Iwamoto and Kato, 2002; Gurevich et al., 2002a; Englander et al., 2005) and drug exposure (Iwamoto and Kato, 2002; Gurevich et al., 2002a; Englander et al., 2005) as well as in a rat model of depression (Iwamoto et al., 2005). In humans, changes in 5-HT$_{2C}$R RNA editing profiles have been observed in the prefrontal cortex of depressed suicide victims (Gurevich et al., 2002b; Schmauss, 2003; Dracheva et al., 2008a; Dracheva et al., 2008b) and

schizophrenics (Sodhi et al., 2001; Dracheva et al., 2003). Thus, basal patterns of 5-HT_{2C}R isoform expression may play a role in vulnerability to and/or expression of various psychiatric disorders. Furthermore, it is conceivable that abnormal 5-HT_{2C}R function based upon altered patterns of 5-HT_{2C}R isoform expression may be normalized by therapeutic treatment with psychiatric medications (Niswender et al., 2001; Sanders-Bush et al., 2003).

The quantitative measurement of final protein products of edited 5-HT_{2C}R transcripts is an important analytic endpoint for study; however, antibodies capable of discriminating among 5-HT_{2C}R proteins with the minor sequence differences caused by RNA editing are not currently available. Until options are available to study isoform-specific proteins, there is obvious utility in accurately detecting and quantifying changes in the levels of mature mRNA isoforms in *ex vivo* samples. The two most commonly used methods to quantify edited RNA isoforms in *ex vivo* brain samples are direct sequencing (Burns et al., 1997; Gurevich et al., 2002b) and pyrosequencing (Iwamoto et al., 2005; Sodhi et al., 2005). These methods yield unambiguous results, but are labor intensive and involve multiple intermediate steps that can increase error and introduce sampling bias. In general, these methods involve an initial reverse transcription of isolated RNA, cloning of the cDNA, bacterial transformation and amplification, colony selection (both methods) followed by amplification and DNA isolation (direct sequencing only), then sequencing of the DNA from each colony. Because each colony analyzed represents a single RNA transcript (Sodhi et al.,

2005), this sequencing process must be performed on numerous colonies for each individual subject in order to characterize the editing profile for that subject. To determine the percentage of the total population of the 5-HT_{2C}R isoform of interest, it is necessary to measure the entire isoform profile for each test subject. As a result of the time and expense involved, the number of sequences characterized is often small compared to the actual number of mRNA molecules. For example, sequencing methods have been employed to characterize entire RNA editing profiles by analyzing 51-60 (Gurevich et al., 2002a) or more than 50 5-HT_{2C}R cDNA sequences for each animal (Iwamoto et al., 2005). Thus, there is a pressing need for a precise, rapid assay that avoids sampling bias and extracts data from the entire 5-HT_{2C}R mRNA population. In practice such an assay would be beneficial particularly in *ex vivo* analyses of changes in the RNA editing of the 5-HT_{2C}R that occur after pharmacological, behavioral or genetic manipulation with a larger number of subjects.

We have adapted quantitative (real-time) reverse transcription polymerase chain reaction (qRT-PCR) as a method to detect and quantify changes in edited 5-HT_{2C}R RNA isoforms by utilizing TaqMan® probes modified with a minor groove binder (MGB) (Kutyavin et al., 2000). As a proof of concept, four TaqMan® MGB probes were designed for detection of four closely-related 5-HT_{2C}R edited transcripts (**Table 3.1**). The non-edited, fully-edited ABECD and partially-edited AD 5-HT_{2C}R RNA isoforms were chosen as examples of low abundance isoforms relative to the partially-edited ABD isoform which is the most

abundant in the rodent brain (Burns et al. 1997). In addition, the AD isoform differs from the ABD isoform by only a single nucleotide while the fully-edited ABECD isoform differs by two nucleotides. This set of probes was chosen to allow us to assess the ability of the TaqMan® MGB assay to detect both high and low abundance isoforms and to discriminate among closely related isoforms. The probes were tested against a complementary set of standard cDNA templates generated by PCR amplification from well-characterized plasmids expressing the respective 5-HT_{2C}R isoforms to accurately control the amount of given cDNA template in the reaction (and thereby determine whether the results were as expected). We then analyzed RNA samples isolated from whole brains of wild-type mice and mutant mice limited in expression to a single isoform each. The findings strongly suggest that the TaqMan® MGB assay exhibits appropriate specificity and sensitivity to analyze changes in levels of specific edited 5-HT_{2C}R mRNA isoforms in both *in vitro* and *ex vivo* systems.

Table 3.1. Names and sequences of TaqMan® MGB probes for RNA isoforms of 5-HT_{2C}R

TaqMan® MGB Probe	5-HT_{2C}R isoform detected	Edited Sites	TaqMan® MGB Probe Sequence	Amino Acid Sequence
ABECD	ABECD	A, B, E, C and D	[FAM] TAGCAGTGCGTGGTCCTGTTGA [MGB/NFQ]	VGV
ABD	ABD	A, B, and D	[FAM] TAGCAGTGCGTAATCCTGTTGA [MGB/NFQ]	VNV
AD	AD	A and D	[FAM] TGTAGCAGTACGTAATCCTGTTGA [MGB/NFQ]	VNV
non-edited	non-edited	None	[FAM] TAGCAATACGTAATCCTATTG [MGB/NFQ]	INI

MATERIALS AND METHODS

Animals

Eight week old naïve adult male C57BL/6J mice (n=4; Harlan Sprague-Dawley, Inc., Indianapolis, Ind., USA) weighing 15-20 g were used. The animals were housed four per cage in a temperature (21–23ºC) and humidity (40–50%) controlled environment and lighting was maintained under a 12-h light-dark cycle (lights on 7:00 a.m. to 7:00 p.m.). Mice were euthanized by cervical dislocation, their brains rapidly removed and placed in a cool tray (4^{o}C). Whole brains were cut into small pieces, stored in RNAlater (Ambion) and kept at -80^{o}C until RNA extraction was performed. Total whole brain RNA also was obtained from 129S6 mice and genetically modified mice (n=1 each) that solely express either the fully-edited ABECD (VGV) or the non-edited (INI) isoform (129S6 genetic background). Mice solely expressing the VGV isoform were generated by mutating the five edited adenosine residues by homologous recombination to mimic RNA editing at all five sites. Mice solely expressing the INI isoform were generated by introducing 11 point mutations in the intron 5 portion of the $5HT_{2C}R$ pre-mRNA duplex opposite the five adenosine editing sites in order to disrupt RNA duplex formation and inhibit $5HT_{2C}R$ RNA editing. Confirmation that the introduced mutations resulted in the sole expression of RNA transcripts encoding VGV and INI isoforms was confirmed by sequence analysis of RT-PCR amplicons derived from whole brain RNA obtained from each mutant mouse strain (poster# 465.9/H21, 2007 Society for Neuroscience (SFN) Scientific Meeting; *manuscript submitted*).

Materials

6-carboxyfluorescein (FAM)-labeled TaqMan® MGB probes were custom synthesized by Applied Biosystems. Primers and unlabeled competing probes were synthesized by SigmaGenosys (Sigma-Aldrich, St. Louis, MO). We designed a TaqMan® assay for the housekeeping gene cyclophilin (accession number M_19533; bases 224-293); primer and probe sequences were: SN primer = 5'-TGT GCC AGG GTG GTG ACT T-3'; ASN primer = 5'-TCA AAT TTC TCT CCG TAG ATG GAC TT-3'; Probe = [FAM] ACA CGC CAT AAT GGC ACT GGT GG [TAMRA]. TaqMan® Universal PCR Master Mix, TaqMan® Reverse Transcription Kit and Gene Amp XL PCR kit were purchased from Applied Biosystems.

Preparation of standard templates

Sense (SN) and antisense (ASN) primer sequences flanking the 5-HT_{2C}R editing region (accession number M21410; bases 1014-1192) were designed using Primer3 Software (Whitehead Institute, Cambridge, MA) with stringent parameters to reduce primer dimerization and to minimize the difference between primer melting temperatures (Tms within 2^{o}C). SN and ASN sequences were 5'-CCT GTC TCT GCT TGC AAT TCT-3' and 5'-GCG AAT TGA ACC GGC TAT G-3', respectively.

A plasmid containing cDNA for the complete non-edited 5-HT_{2C}R was kindly provided by Drs. William Clarke and Kelly Berg (University of Texas Health Science Center at San Antonio). A standard template for the non-edited isoform

was produced using conventional PCR with Taq DNA polymerase (Fisher Scientific, Houston, TX) and the primers described above. Plasmids containing cDNA for the A, B, D, AD, ABD, ABCD and ABECD edited isoforms were developed by RT-PCR amplification of total RNA from adult mouse brain using oligonucleotide primers in exon 5 (5'-ATT AGA ATT CTA TTT GTG CCC CGT CTG G-3') and intron 5 (5'-GGG CAA ATA TTC TGA AAA GAT GTT-3') that flanked the edited region of the 5-HT_{2C}R pre-mRNA. The 376 bp PCR amplicon was subcloned into the pBlueScript II KS (-) plasmid (Stratagene, La Jolla, CA) between the EcoR I and Hind III sites and individual cDNA isolates were subjected to DNA sequence analysis to identify clones containing the required patterns of editing. Because the cDNA fragments in these clones did not extend upstream to the primers selected for this study, we utilized an extra long SN primer (60 bases) to extend the sequences during amplification. The SN primer was 5'-CCT GTC CCT GCT TGC TAT TCT TTA TGA TTA TTT ACC TAG ATA TTT GTG CCC CGT CTG GAT-3'; the ASN primer was as described above. The underlined nucleotides correspond to the region of hybridization of the sense primer to the clone DNA. Because of the length of this sense primer, the PCR reaction was carried out with the Gene Amp XL PCR kit (Applied Biosystems) according to manufacturer's directions.

Following PCR, all amplimers were characterized by agarose gel electrophoresis for the correct size (180 bp), then excised, gel purified and sequenced by the Sealy Center for Molecular Science (UTMB) to confirm the

identities of the 5-HT_{2C}R isoforms. The DNA concentrations of standard template stock solutions were estimated by absorbance at 260 nm, then by comparison to quantitative DNA standards in polyacrylamide gel electrophoresis (Recombinant DNA Lab, UTMB). The concentrations of the standard stock solutions were as follows: non-edited (30 ng/μL), A (30 ng/μL), B (30 ng/μL), D (30 ng/μL), AD (100 ng/μL), ABD (100 ng/μL), ABCD (60 ng/μL), and ABECD (100 ng/μL). Stocks were aliquoted and frozen at -20^{o}C. These amplimers were used as templates to standardize reaction conditions and to test the sensitivity and discriminative ability of the TaqMan® MGB probes.

RNA extraction and reverse transcription

Tissue was homogenized in 500 μL of TRI Reagent® (Applied Biosystems), using a Tissue-Tearor™ homogenizer. RNA was then isolated using the RiboPure kit (Applied Biosystems) according to the manufacturer's directions. Any residual genomic DNA was removed by treatment with TURBO DNA-free™ (Applied Biosystems); a final incubation step of 70^{o}C for 10 min was used to inactivate the DNAse. The final RNA concentration was determined by absorbance at 260 nm. The reverse transcription reaction was performed on 0.25-0.5 μg of RNA using the TaqMan® Reverse Transcription Kit (Applied Biosystems) with random hexamer primers according to the manufacturer's directions. The reverse transcription program consisted of an annealing step (25°C, 10 min) followed by elongation (48°C, 30 min) and a final enzyme inactivation step (95°C, 5 min).

TaqMan® MGB assay

TaqMan® MGB probes for four 5-HT_{2C}R mRNA isoforms (ABECD, ABD, AD and non-edited; **Table 3.1**) were designed with the assistance of Dr. Joy Sheng of Applied Biosystems Technical Support. The SN and ASN primers flanking the editing region (described above) were used in real-time PCR assays with each TaqMan® MGB probe to assess the different 5-HT_{2C}R mRNA edited isoform levels. Initial real-time PCR reactions were comprised of 10 µL of Universal TaqMan Master Mix, 125 nM sense and antisense primers, 150 nM probe and 6 µL of sample containing target template in a final reaction volume of 20 µL. Assays were performed in a 7500 Fast Real-Time PCR System (Applied Biosystems). The initial TaqMan® assay amplification program (according to manufacturer's directions) consisted of an activation step (95°C, 10 min) followed by 40 cycles of denaturation (95°C, 15 s), annealing and elongation (60°C, 1 min). Conditions for the assay were varied during the optimization process and are described in the ***Results*** section. All data were analyzed using the 7500 Fast System Detection Software (SDS) version 1.3.1 (Applied Biosystems).

The relative quantitation method was used to compare differences between samples (Livak and Schmittgen, 2001; Wong and Medrano, 2005; Schefe et al., 2006). Results are expressed in terms of Crossing Threshold (Ct), which is defined as the PCR cycle at which sample fluorescence crosses a threshold set above baseline fluctuations (background noise) and within the logarithmic portion of the amplification plot. The difference in crossing thresholds

(ΔCt) was calculated for each cDNA being studied: ΔCt = Ct (5-HT_{2C}R isoform of interest) – Ct (cyclophilin). Mean ± SEM was determined for each group. The magnitude of the differences between groups was calculated as: ΔΔCt = ΔCt (5-HT_{2C}R isoform of interest) – ΔCt (5-HT_{2C}R most abundant isoform); relative mRNA expression was estimated by $2^{-\Delta\Delta Ct}$.

Sensitivity of the TaqMan® MGB probes

Probe sensitivity was tested by performing real-time PCR assays for each probe with matching standard template stock solutions serially diluted 10^6-to 10^{12}-fold. Serial dilutions of target templates were tested until the resultant Ct value of the sample was not significantly different from that of no template controls (NTCs). Each sample (6.0 µL per reaction) was tested in triplicate against its respective TaqMan® MGB probe. The slope of the standard template dilution curve was determined by plotting Ct values measurements as a function of the log DNA concentration. Efficiency (E) of each assay was determined according to the equation $E = 10^{(-1/slope)}-1$ (Wong and Medrano, 2005).

Specificity of TaqMan® MGB probes

Probe specificity was determined by performing a series of real-time PCR assays using each probe with templates that differed by 1-5 nucleotides from the perfectly matched template. Standard templates were diluted 10^6-fold. [Initial concentrations were 15 ng/µL (D and non-edited) or 50 ng/µL (ABECD, ABCD, ABD, and AD)]. The real-time PCR program was that recommended by Applied Biosystems (see above). The Ct values for mismatched templates were

compared to those for perfectly matched templates. To simplify these comparisons, we have defined the following term:

Ct Difference = (Ct of mismatched template) – (Ct of matched template)

The percentage of cross-hybridization was calculated by:

$$\textbf{Cross-hybridization} = [1 / (2^{\text{Ct Difference}})] \times 100\%$$

By using these equations, a Ct Difference of 5 cycles correlates to 3.125% cross-hybridization. This should provide a sufficient level of discrimination between closely related isoforms and we have adopted this criterion as our minimum acceptable value for probe specificity.

Optimization of reaction conditions

Parameters that were varied from the standard conditions included: 1) annealing temperature (60.0, 60.5, 61.0 and 62.0°C); 2) probe concentration (25, 50, 100, 125 and 150 nM final concentration); 3) addition of PCR enhancers: ammonium chloride [5, 10 and 20 mM (Decker et al., 2002)]; tetra-methyl ammonium chloride [60 mM (Chevet et al., 1995)]; formamide [1, 2.5 and 5% (Varadaraj and Skinner, 1994)]; and DMSO [1, 2.5 and 5% (Varadaraj and Skinner, 1994)]; 4) addition of competitors (see below).

Effects of unlabeled competing probes ("Competitors")

Unlabeled competing probes (competitors) are oligonucleotides that differ from the complementary target sequence for each respective TaqMan® MGB

probe at a single (editing site) nucleotide. [We have used the same nomenclature (**Table 3.1**) regarding editing sites for competitor probes as for the TaqMan® MGB probes.] A fixed concentration of each TaqMan® MGB probe was tested against various concentrations of competitor (ranging from 0.0125 to 1 μM final concentration). The D, ABD, ABCD, and ABCD standard templates were used as mismatched templates for the TaqMan® MGB non-edited, AD, ABD and ABECD probes, respectively. Each real-time PCR reaction consisted of: 10 μL of Universal TaqMan® Master Mix, 125 nM SN and ASN primers, 100 nM TaqMan® MGB probe, 6 μL of standard templates (10^6-fold dilution of standard stocks) and 2 μL 0.125-10 μM of 10x stock solution of competitors in a final reaction volume of 20 μL. These concentrations of standard templates yielded Ct values of 18-22, which are lower (indicating higher template concentrations) than those we have found in brain samples, thus representing a more stringent test of specificity. Assays were performed according to the manufacturer's directions (Applied Biosystems).

Effects of mixed templates on TaqMan® MGB probe assays

In order to simulate conditions expected for *ex vivo* experiments, we tested the non-edited probe against various standard template mixtures. In these experiments, the real-time PCR reaction mix consisted of: 10 μL of Universal TaqMan® Master Mix, 125 nM sense and antisense primers, 100 nM TaqMan® MGB non-edited probe and 6 μL of standard template mixture [1.5 μL each of A, B, D and non-edited standard templates (10^8-fold dilution)] in a final reaction

volume of 20 µL. Assays were performed according to manufacturer's directions (Applied Biosystems).

Effects of competitors on assays with mixed templates

Extensive tests on the non-edited probe, which has five possible single-mismatch competitors, were performed. Equal concentrations of competitors for the A, B, C, D and E edited isoforms were combined to form a cocktail (0.25 µM final total concentration; 0.05 µM each). The final real-time PCR reaction mix consisted of: 10 µL of Universal TaqMan® Master Mix, 125 nM sense and antisense primers, 100 nM TaqMan® MGB non-edited probe, 2 µL competitor cocktail mix and 6 µL template mixture [1.5 µL each of A, B, D and non-edited standard templates (10^8-fold dilution)] in a final reaction volume of 20 µL. Assays were performed as described above.

Validation of TaqMan® MGB probe assays using RNA from whole mouse brains

Following reverse transcription, samples were diluted in 4 volumes of nuclease-free water (Applied Biosystems). TaqMan® MGB probe assays were performed as described above on the resultant cDNA samples both in the presence and absence of competitors. The relative quantification method was used to analyze the data. Competitor cocktails were prepared for each probe in 20 µL final volumes from 15 µM stock solutions as follows: non-edited = 4 µL each of A, B, E, C and D; AD = 4 µL each of A, D, ABD and ACD; ABD = 4 µL each of AD, AB and ABCD; and ABECD = 4 µL each of ABCD and ABEC.

Competitor cocktails were then diluted 8 or 16 times in nuclease-free water. The resultant final concentrations for each competitor in the respective dilutions were 0.375 and 0.188 μM. Two μL of the diluted competitor cocktails were used in the real-time PCR reaction, producing final concentrations of each individual competitor of 37.5 and 18.8 nM, respectively.

Data Analysis

All samples were run in triplicate and statistical analyses were performed on the Ct values using non-parametric one-way ANOVA (NPAIRWAY1 comparison with SAS System for Windows V.8.2 (SAS Institute Inc., Cary, NC)) with a Kruskal-Wallis test and Dunn's post-test with an experimentwise error rate α = 0.05. When statistical analyses were performed on the Ct Differences, a one-way ANOVA (Instat for Win95/NT V.3.01; GraphPad Software, San Diego, CA) was used with a Dunnett post-test with an experimentwise error rate α = 0.05. The SEM for the Ct Difference was calculated by error propagation using the following equation: $SEM = \sqrt{(SEM_1^2 + SEM_2^2)}$ (Livak and Schmittgen, 2001).

RESULTS

The five editing sites of the 5-HT_{2C}R mRNA are illustrated in **Fig. 3.1**; the sequences and nomenclature of the TaqMan® MGB probes utilized in this study are outlined in **Table 3.1**. Our first task was to validate that each probe sensitively detects its target (complementary; matching) template and then to

determine how well each discriminates templates that are not perfectly complementary (mismatched templates). The assay parameters were optimized on matched and mismatched templates under a variety of conditions to simulate expected *ex vivo* conditions and then were validated in RNA from mouse brain.

Validation of TaqMan® MGB Probes: Sensitivity and Specificity

Sensitivity of the probes

As shown in **Fig. 3.2**, there were strong correlations between the log [concentration] and resultant Ct values for each probe tested with its respective matching standard template. All correlation coefficients (r^2 value) were ≥ 0.9999 ($p \leq 0.0001$). Linearity was maintained even when standard templates were diluted between 10^6- and 10^{11}-fold, demonstrating a wide dynamic range and yielding accurate Ct values until at least 34 cycles. Ct values > 35 approach those of non-template controls, and thus were considered nonspecific. Efficiencies of the probes were as follows: E_{ABECD} = 0.988 (slope = -3.35); E_{ABD} = 0.879 (slope = -3.65); E_{AD} = 0.813 (slope = -3.87); and $E_{non\text{-}edited}$ = 0.926 (slope = -3.51). These values are well within or exceed the expected range of 0.65 – 0.9 for efficiencies of TaqMan® assays (Schefe et al., 2006). The efficiency of this TaqMan® MGB probes are well within expected values for TaqMan® PCR assays (Wong and Medrano, 2005; Schefe et al., 2006; Yao et al., 2006). If the objective of an experiment is to compile quantitative isoform profiles, measurements of individual isoforms would need to be adjusted to account for differences in efficiencies of the TaqMan® 5-HT_{2C}R MGB probes. However,

when the experimental goal is to determine changes in a given isoform(s) in response to treatment, there would be no need to correct for efficiency differences. Such experiments are the ideal application of the proposed method.

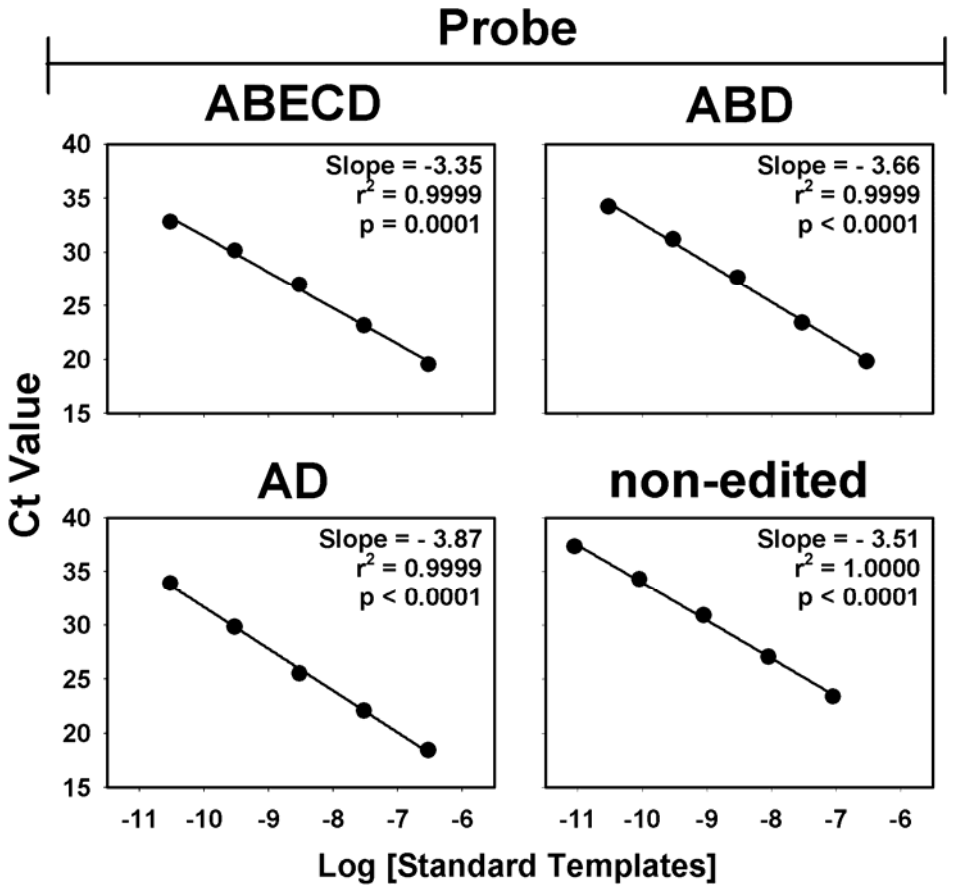

Figure 3.2. Sensitivity of the TaqMan® MGB probes. Ct values for each probe are plotted as a function of serial dilutions of the respective matching standard template.

Specificity of probes

Results of assays utilizing matched templates compared to those utilizing mismatched templates for all four probes are summarized in **Table 3.2**. Our results demonstrated that each probe unequivocally discriminated templates that

differed by two or more nucleotides: the Ct Difference in most cases was > 10 cycles. For example, the cross-hybridization observed for the AD probe with the ABD template (one mismatch) was 80-87% and for the D template (also one mismatch) was 32-45%. However, a cross-hybridization of < 1.2% was observed for the same probe with the ABCD template (two mismatches) (**Table 3.2**). These results indicated an even greater discrimination between the probe and templates with two mismatches than that previously reported by Yao et al. (2006; 4 cycles, equivalent to 6.25% cross-hybridization). However, cross-hybridization with templates containing only a single mismatch was still considerable.

Optimization of Assay Conditions

In an attempt to determine whether discrimination of single mismatches could be improved, we measured the effects of several variations of the assay conditions on Ct Difference.

Annealing temperature and PCR enhancers

To test whether increased annealing temperature would differentially affect probe binding to matched versus mismatched templates, we tested 60 to 62°C in increments of 0.5°C. An annealing temperature of 60.5°C achieved small, probe-dependent increases in Ct Difference; however, annealing temperatures > 61.0°C were deleterious (data not shown). Consequently, we continued to perform the assays at the original 60.0°C annealing temperature.

Table 3.2. Specificity of 5-HT_{2C}R TaqMan® MGB probes. Results obtained from real-time PCR assays utilizing various mismatched standard templates (from 1 to 5 mismatches) are compared to those utilizing matched templates for all four probes. Ct Difference = Ct (mismatched template) – Ct (matched template); Cross-hybridization = [1 / ($2^{Ct\ Difference}$)] x 100%. Each Ct value is the average of 3 replicates (mean ± SEM).

Standard Template	# of Mismatches	Ct Value	P Values (vs. Matched Template)	Ct Difference	Cross-hybridization (%)
ABECD	**0**	18.177 ± 0.060			
ABCD	**1**	19.095 ± 0.050	p > 0.05	0.918 ± 0.078	50.139 - 55.869
ABD	**2**	28.455 ± 1.320	p > 0.05	10.278 ± 1.321	0.032 - 0.201
AD	**3**	undetected		> 15.000	< 0.003
D	**4**	undetected		> 15.000	< 0.003
non-edited	**5**	undetected		> 15.000	< 0.003
ABD	**0**	18.442 ± 0.138			
AD	**1**	19.405 ± 0.067	p > 0.05	0.963 ± 0.153	46.137 - 57.038
ABCD	**1**	19.964 ± 0.221	p > 0.05	1.522 ± 0.161	31.143 - 38.931
ABECD	**2**	24.039 ± 0.705	p > 0.05	5.597 ± 0.718	1.256 - 3.398
D	**2**	undetected		> 15.000	< 0.003
non-edited	**3**	undetected		> 15.000	< 0.003
AD	**0**	18.559 ± 0.080			
D	**1**	19.936 ± 0.230	p > 0.05	1.377 ± 0.244	32.311 – 45.597
ABD	**1**	18.765 ± 0.080	p > 0.05	0.206 ± 0.113	80.163 – 87.478
ABCD	**2**	29.128 ± 0.830	p > 0.05	10.569 ± 0.834	0.037 – 1.173
non-edited	**3**	29.609 ± 2.410	p > 0.05	11.050 ± 2.411	0.009 – 0.253
ABECD	**3**	undetected		> 15.000	< 0.003
non-edited	**0**	20.005 ± 0.240			
D	**1**	22.466 ± 0.190	p > 0.05	2.461 ± 0.306	14.690 – 22.453
AD	**2**	undetected		> 15.000	< 0.003
ABD	**3**	undetected		> 15.000	< 0.003
ABCD	**4**	undetected		> 15.000	< 0.003
ABECD	**5**	undetected		> 15.000	< 0.003

We compared the effects of several PCR enhancers (small molecules used to destabilize nonspecific base pairing) on discrimination of matched versus mismatched templates. Addition of ammonium ions (60 mM tetra-methyl ammonium chloride) to the reaction mix improved discrimination by approximately one cycle for the ABECD probe only (data not shown). Inclusion of

formamide (1-5%) or DMSO (1-5%) dose-dependently disrupted interactions of probes with both matched and mismatched templates (data not shown). In summary, effects of PCR enhancers on Ct values were small, probe-dependent and did not improve the discrimination between matched and mismatched templates.

Probe concentration

Applied Biosystems (Foster City, CA) recommends a final probe concentration between 150 and 200 nM for TaqMan® assays. Since high concentrations would be expected to increase amounts of binding (by mass action), we tested several lower probe concentrations (25, 50, 100, 125 and 150 nM) to determine whether a decrease in the final concentration of the probe would reduce cross-hybridization with singly mismatched templates. Probes were tested against 10^6-fold dilutions of their respective standard template stocks (Material and Methods). **Table 3.3** shows that, for template concentrations resulting in Ct values between 18-22 cycles, lowering the probe concentration to 100 or 125 nM increased the Ct values of singly mismatched templates only slightly without dramatically increasing Ct values of the matched template. For example, in the case of the ABECD probe, decreasing probe concentration from 150 nM (Ct value = 18.217) to 100 nM (Ct value = 18.323) increased the Ct value for the matched template by 0.106 cycles. For the singly mismatched (ABCD) template the Ct values increased from 19.694 to 19.886 (0.242 cycles). Thus

lowering the probe concentration only improved the discrimination (Ct Difference) of the assay by 0.136 cycles.

There were no significant changes in Ct values at probe concentrations of 100 and 125 nM relative to the initial condition of 150 nM. Decreasing probe concentration below 100 nM resulted in significant increases in Ct values of both matched templates and mismatched templates, with no improvement in the Ct Difference. Even at concentration < 100 nM there were only a few Ct Differences that were statistically different than those seen at 150 nM. [For the ABECD probe ($F_{(4,14)}$ = 2.029, p < 0.1660); for the ABD probe ($F_{(4,14)}$ = 13.892, p = 0.0004); for the AD probe ($F_{(4,14)}$ = 1.762, p = 0.2131); for the non-edited probe ($F_{(4,14)}$ = 5.122, p < 0.0166); **Table 3.3.**]

It was anticipated that *ex vivo* samples would contain lower abundance 5-HT_{2C}R isoforms (Ct values > 25 but < 34; unpublished data); thus, a subset of the experiment of the experiment using lower template concentrations was performed to determine the effect of decreased probe concentrations (**Table 3.4**). Decreasing the probe concentration from 150 to 100 nM had little effect on Ct Difference under these conditions. As above, only probe concentrations ≤ 100 nM resulted in any Ct Differences statistically different than those seen at 150 nM. [For the ABECD probe ($F_{(2,8)}$ = 0.1186, p = 0.8902); for the ABD probe ($F_{(2,8)}$ = 3.433, p = 0.1014); for the AD probe ($F_{(2,8)}$ = 0.0847, p = 0.9199) and for the non-edited probe ($F_{(2,8)}$ = 28.283, p = 0.0009).]

Table 3.3. Effects of TaqMan® MGB probe concentration on template detection at a higher template concentration. Ct values were measured at final probe concentrations of 25, 50, 100, 125 and 150 nM with matched and mismatched 5-HT_{2C}R isoform standard templates (10^6-fold dilution). Differences in Ct values were determined as Ct Difference = Ct (mismatched template) – Ct (matched template) at the given [Probe]. Each Ct value is the average of 3 replicates; results are expressed as mean ± SEM. * $p < 0.05$ vs. 150 nM probe concentration; ** $p < 0.01$ vs. 150 nM probe concentration.

Probe	Standard Template	Final [Probe] (nM)	Ct Value	Ct Difference		Cross-hybridization (%)
ABECD	ABECD	**150**	18.217 ± 0.060			
	(match)	**125**	18.302 ± 0.130			
		100	18.323 ± 0.190			
		50	19.225 ± 0.080			
		25	20.541 ± 0.460			
	ABCD	**150**	19.694 ± 0.170	1.477 ± 0.180		33.986 – 40.697
	(mismatch)	**125**	19.886 ± 0.040	1.584 ± 0.136		30.355 – 36.653
		100	19.936 ± 0.220	1.613 ± 0.291		26.720 – 39.998
		50	21.514 ± 0.090	2.289 ± 0.120		18.829 – 22.236
		25	22.786 ± 0.130	2.245 ± 0.478		15.149 – 29.382
ABD	ABD	**150**	20.830 ± 0.084			
	(match)	**125**	20.654 ± 0.160			
		100	20.402 ± 0.122			
		50	20.526 ± 0.132			
		25	21.295 ± 0.146			
	ABCD	**150**	22.016 ± 0.071	1.186 ± 0.110		40.725 – 47.434
	(mismatch)	**125**	21.891 ± 0.083	1.237 ± 0.180		37.339 – 48.063
		100	22.054 ± 0.122	1.652 ± 0.173		28.224 – 35.948
		50	22.593 ± 0.130	2.067 ± 0.185	*	20.993 – 27.130
		25	23.946 ± 0.072	2.651 ± 0.163	**	17.825 – 23.100
AD	AD	**150**	19.101 ± 0.170			
	(match)	**125**	19.256 ± 0.140			
		100	19.055 ± 0.090			
		50	19.365 ± 0.050			
		25	19.926 ± 0.090			
	ABD	**150**	19.241 ± 0.030	0.140 ± 0.173		80.497 – 100.00
	(mismatch)	**125**	20.041 ± 0.030	0.785 ± 0.143		52.559 – 64.082
		100	19.928 ± 0.150	0.873 ± 0.175		48.364 – 61.642
		50	20.277 ± 0.130	0.912 ± 0.139		48.263 – 58.520
		25	20.872 ± 0.460	0.946 ± 0.469		37.501 – 71.501
non-edited	non-edited	**150**	21.432 ± 0.054			
	(match)	**125**	21.241 ± 0.049			
		100	21.130 ± 0.006			
		50	22.224 ± 0.375			
		25	23.443 ± 0.049			
	D	**150**	22.994 ± 0.081	1.562 ± 0.097		31.666 – 36.224
	(mismatch)	**125**	22.953 ± 0.085	1.712 ± 0.098		28.520 – 43.669
		100	23.126 ± 0.006	1.996 ± 0.008		24.931 – 25.209
		50	24.371 ± 0.527	2.147 ± 0.647		14.419 – 35.355
		25	26.948 ± 0.379	3.505 ± 0.382	**	6.759 – 11.478

Table 3.4. Effects of TaqMan® MGB probe concentration on template detection at a lower template concentration. Ct values were measured at final probe concentrations of 50, 100, and 150 nM with matched and mismatched 5-HT_{2C}R isoform standard templates (10^8-fold dilution). Ct Difference = Ct (mismatched template) – Ct (matched template) at each respective [Probe]. Cross-hybridization = [1 / ($2^{Ct\ Difference}$)] x 100%. Each Ct value is the average of 3 replicates and results are expressed as mean ± SEM. * $p < 0.05$ vs. 150 nM probe concentration.

Probe	Standard Template	Final [Probe] (nM)	Ct Value		Cross-hybridization (%)
ABECD	ABECD (match)	**150**	26.172 ± 0.120		
		100	25.871 ± 0.230		
		50	26.214 ± 0.030		
	ABCD (mismatch)	**150**	27.957 ± 0.460		20.877 – 40.332
		100	27.414 ± 0.380		25.226 – 46.684
		50	27.960 ± 0.010		29.159 – 30.481
ABD	ABD (match)	**150**	25.648 ± 0.920		
		100	26.574 ± 0.150		
		50	26.662 ± 0.180		
	ABCD (mismatch)	**150**	27.410 ± 0.260		15.195 – 57.197
		100	27.616 ± 0.220		40.388 – 58.398
		50	28.201 ± 0.080		32.737 – 39.447
AD	AD (match)	**150**	25.967 ± 0.070		
		100	26.250 ± 0.050		
		50	26.880 ± 0.050		
	ABD (mismatch)	**150**	27.624 ± 0.340		24.931 – 40.332
		100	27.607 ± 0.020		37.605 – 40.528
		50	28.294 ± 0.880		20.377 – 69.112
non-edited	non-edited (match)	**150**	28.392 ± 0.151		
		100	28.703 ± 0.209		
		50	28.703 ± 0.372		
	D (mismatch)	**150**	31.365 ± 0.174		10.859 – 14.937
		100	30.082 ± 0.287	*	30.062 – 49.175
		50	33.679 ± 0.165	*	2.396 – 4.213

.

Since lowering the concentration of the probe to 100 nM did not alter the Ct values of the matched template when compared to the Ct values obtained with 150 nM of probe in either set of experiments (**Table 3.3** and **Table 3.4**), we decided to use 100 nM as the final probe concentration to conserve resources and decrease the cost of the reaction.

Single Mismatch Discrimination

Addition of competitors

None of the above modifications achieved our desired discrimination criterion of Ct Difference > 5 cycles for singly mismatched templates. Since commercial real-time PCR single nucleotide polymorphism assays utilize two probes (labeled with two different fluors, one for each allele) to successfully distinguish between single nucleotide mismatches, we reasoned that the addition of an unlabeled probe complementary to the singly mismatched template (competitors) should compete with the labeled probe to diminish cross-hybridization. The theoretical basis for this is classical kinetics: the perfectly matched probe should have a greater affinity for its complement than a slightly mismatched one and should effectively compete for binding at equilibrium.

In **Fig. 3.3,** we tested this hypothesis by measuring the effect of increasing concentration of a single competitor on the Ct values of matching template (●) and a singly mismatched template (○) for each TaqMan® MGB probe (template dilution of 10^6-fold). The added competitor dramatically increased the Ct value with the mismatched template (○) in a concentration-dependent manner but had

little effect on detection of the matched template (●). For example, in the absence of the ABCD competitor, the Ct value for the ABECD probe with its target template is 19.43 ± 0.39 and with the singly mismatched ABCD template is 20.73 ± 0.17. However, in the presence of 0.05 μM of the ABCD competitor, the respective values are 20.06 ± 0.13 and 23.54 ± 0.56, respectively (**Fig. 3.3A**). The inclusion of the ABCD competitor thus increased the Ct Difference from approximately 1.3 to 3.5 cycles (**Fig. 3.3B**) representing a decrease in the percentage of cross-hybridization from 40.6 to 8.8%. By converting all the Ct Differences to percentage cross-hybridization, the same data can be represented in a fashion that is analogous to a classical displacement curve (**Fig. 3.3C**) and clearly demonstrates the efficacy of this approach. It should be noted that the final concentration necessary to achieve the criterion of a 5 cycle Ct Difference (as interpolated from **Fig. 3.3C**) is probe-dependent and varies between approximately 0.05 and 0.25 μM for this concentration of target template. These concentrations of template are higher than those we expect to encounter in experimental samples and therefore constitute a stringent test of the ability of the competitors to improve the specificity of the reaction.

While the addition of competitors do not measurably affect Ct values for the matched template, high final concentrations [> 0.04 μM (ABECD probe), 0.05 μM (ABD probe), 0.025 μM (AD probe), and 0.25 μM (non-edited probe)] begin to decrease the plateau level of the relative fluorescence readings, resulting in

decreased signal to noise (S/N) ratio (data not shown) and thus should be avoided.

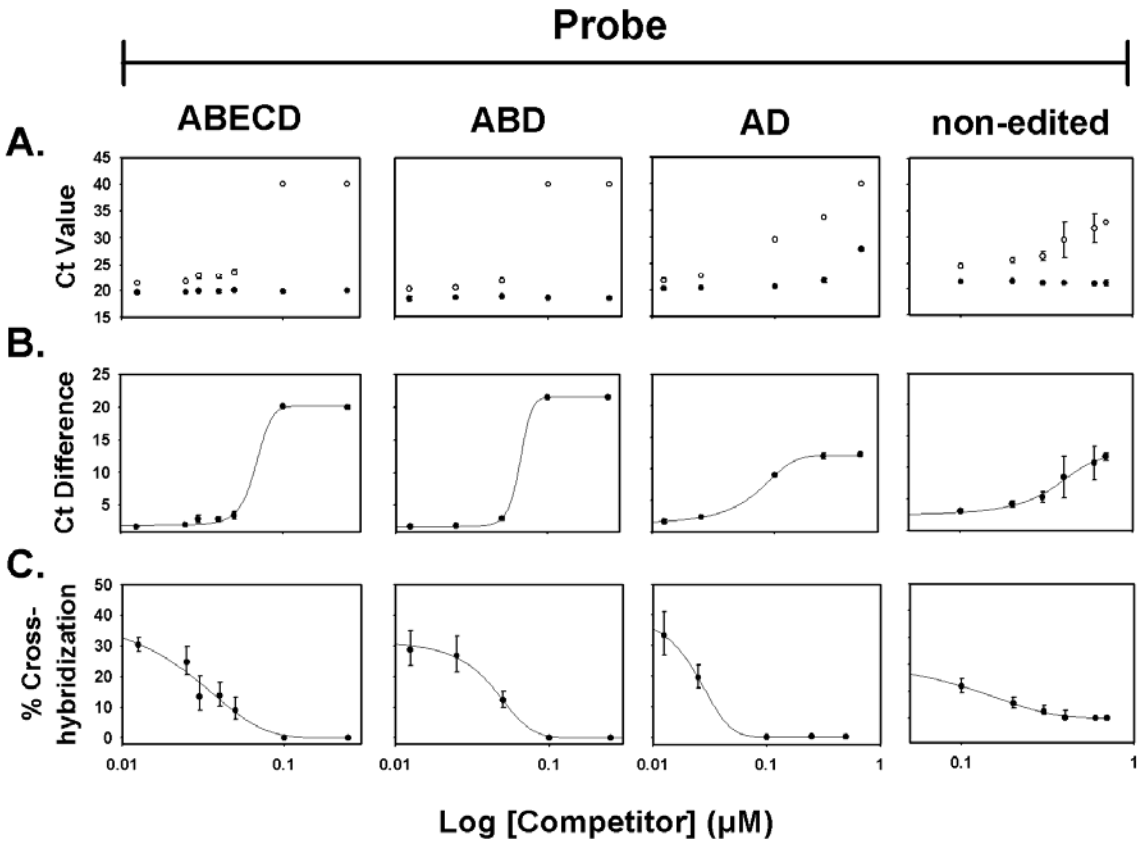

Figure 3.3. Effects of competitors on TaqMan® MGB assay. [A] Ct values for matched (●) and singly mismatched (○) templates in the presence of increasing concentrations of competitors complementary to the singly mismatched template. Competitors are: ABCD (for the ABECD probe); ABCD (for the ABD probe); ABD (for the AD probe); D (for the non-edited probe). [B] Ct Difference calculated at each concentration of competitor from the data shown in [A]. [C] % of Cross-hybridization as a function of [competitor]. Experiments were repeated 2-4 times for each probe, with each sample run in triplicate. Results are expressed as mean ± SEM. Where error bars are not seen, SEM is smaller than the size of the symbol.

Mixed templates

Previous studies have shown that multiple 5-HT_{2C}R isoforms can be found within a tissue sample (Burns et al., 1997; Niswender et al., 1998; Niswender et al., 2001). To more closely model this scenario, we conducted a series of assays with mixtures of standard templates (**Table 3.5**). If a TaqMan® MGB probe is most specific for its perfectly matched template, addition of mismatched template(s) to the mix should result in little cross-hybridization and thus have negligible effects on the measured Ct values of the probe target. We tested the non-edited probe and focused on mixtures of matched (non-edited template) and singly mismatched templates (A, B and D templates) because single mismatches represent the most stringent tests for accurate discrimination (**Table 3.5**). In addition, preliminary data from our laboratory with *ex vivo* samples (data not shown) have indicated that 5-HT_{2C}R is present in relatively low abundance (Ct values > 25 but < 34). Therefore, we set up the mixture of templates with lower concentrations of individual standard templates (total concentration equal to that in **Table 3.4**) to more closely model expected *ex vivo* samples.

Similar to results reported in **Table 3.2**, the non-edited probe, in the absence of its own target template, exhibited small amounts of cross-hybridization with the A, B and D standard templates, either individually (A < 0.1%, B < 0.1% and D < 6%; upper section, **Table 3.5**) or in combination (*e.g.,* A + B < 0.1%, A + D < 2%; upper section, **Table 3.5**).

Table 3.5. Effects of standard template mixtures on template detection by the non-edited probe. Ct values for the non-edited probe were measured for the non-edited template alone and for various combinations of A, B, and D templates, with or without the non-edited template. Ct Difference = Ct – Ct (non-edited template only). In the upper section, Ct Difference reflects cross-hybridization due to the presence of the mismatched templates: Cross-hybridization = [1 / ($2^{Ct\ Difference}$)] x 100%. In the lower section, cross-hybridization is not calculated because binding of the probe to the matched template predominates. Each Ct value is the average of 3 replicates; results are expressed as mean ± SEM.

Template Combination	Ct Value	Ct Difference	Cross-hybridization (%)
No Matching Template			
None	> 35.000		
A	> 35.000	> 10.000	< 0.1
B	> 35.000	> 10.000	< 0.1
D	29.383 ± 0.073	4.204 ± 0.094	5.084 – 5.789
A + B	> 35.000	> 10.000	< 0.1
A + D	32.021 ± 0.692	6.842 ± 0.695	0.538 – 1.411
B + D	31.301 ± 0.250	6.112 ± 0.260	1.199 – 1.719
A + B + D	30.686 ± 0.560	5.507 ± 0.563	1.488 – 3.248
With Matching Template			
non-edited	25.176 ± 0.059	0.000 ± 0.084	
non-edited + A	25.298 ± 0.050	0.119 ± 0.078	
non-edited + B	25.521 ± 0.172	0.342 ± 0.182	
non-edited + D	25.083 ± 0.140	-0.095 ± 0.152	
non-edited + A + B	25.248 ± 0.331	0.069 ± 0.337	
non-edited + A + D	25.172 ± 0.127	-0.007 ± 0.140	
non-edited + B + D	25.283 ± 0.069	0.104 ± 0.091	
non-edited + A + B + D	25.401 ± 0.038	0.222 ± 0.070	

As in **Table 3.2**, the Ct difference reflects cross-hybridization due to the presence of the mismatched templates. Data in the lower section of **Table 3.5** indicate that the non-edited probe continued to distinguish its target (non-edited) template even in the presence of the A, B and D standard templates: Ct values were not significantly different from the Ct with the non-edited template alone, suggesting that, at these concentrations, there is little or no cross-hybridization of this probe to other templates when its matched template is present in the reaction mix [$X^2_{(DF=7,\ n=23)} = 9.160$, $p = 0.241$].

Mixed templates: Addition of multiple competitors

Data in **Fig. 3.3** show the effects of a single competitor on the Ct value of a probe with a singly mismatched template. We expect to encounter multiple 5-HT_{2C}R isoforms *in vivo* that differ from the target template by a single mismatch (Burns et al., 1997; Englander et al., 2005; Du et al., 2006). Thus, depending on the concentration of isoforms with single mismatches to a given probe, experimental assays may require the presence of several competitors to blanket the spectrum of potential cross-hybridization. We tested the effects of all the relevant competitors (those targeting the A, B, E, C and D edited sites), individually and in combination (same combinations as in **Table 3.5**), on the Ct values obtained with the non-edited probe and its target template. To minimize inhibition of plateau fluorescence levels, we began with a cocktail comprised of a low concentration of competitors (0.05 μM of each, resulting in a total final concentration of 0.25 μM). Even at these concentrations, the competitors

decreased cross-hybridization of the non-edited probe with the D standard template (the only template in **Table 3.5** that exhibited < 5 cycle Ct Difference) from 5-6% to 2.47-3.45% (Ct Difference = 5.097 ± 0.240) and did not affect the Ct values of the target template (data not shown). Though the initial cross-hybridization is low at these template concentrations, these results are consistent with **Fig. 3.3**, and suggest that addition of multiple competitors improves the specificity of the assay while not changing detection of the target.

Validation of TaqMan® MGB probes in *ex vivo* assays

5-HT$_{2C}$R isoform expression in mouse brains

The RNA from whole brains derived from transgenic mouse strains (129S6 genetic background) solely expressing the fully-edited ABECD (VGV) or the non-edited (INI) isoforms of 5-HT$_{2C}$R were used to validate the specificity (cross-reactivity) of our four TaqMan® MGB probes in an *ex vivo* experimental system. Only the fully-edited ABECD isoform was detected by the ABECD probe in VGV-expressing mutant mice which solely express the ABECD transcript (**Fig. 3.4A**). This complete lack of cross-reactivity demonstrates that the ABD, AD or non-edited probes (2, 3 and 5 nucleotide mismatches, respectively) do not cross-hybridize with ABECD isoform cDNA. Similarly, only the non-edited isoform was detected using the non-edited probe in INI-expressing mutant mice which solely express the non-edited transcript (**Fig. 3.4B**).

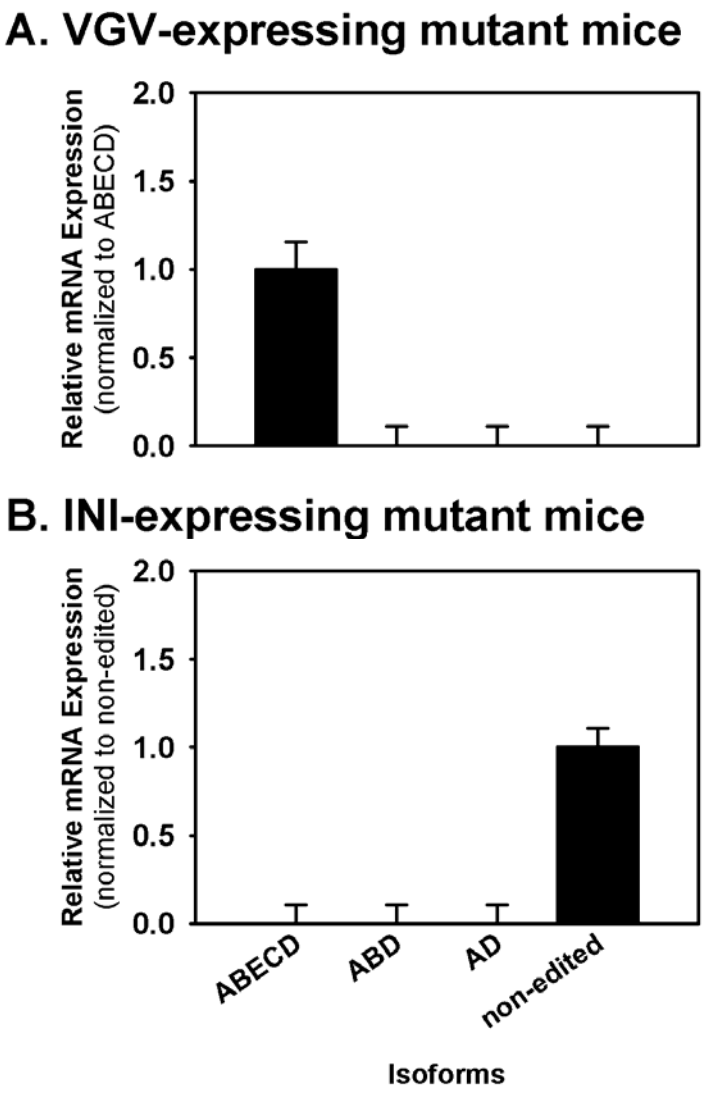

Figure 3.4. Specificity of TaqMan® MGB probes in RNA from whole brain from genetically-modified 129S6 mouse strains. [A] VGV-expressing mutant and [B] INI-expressing mutant mice. Data are normalized to cyclophilin and plotted relative to expression of [A] ABECD and [B] non-edited isoforms. The average crossing threshold (ΔCt) was calculated for each isoform studied: ΔCt = Ct (isoform of interest) – Ct (cyclophilin). Relative expression between groups was determined by: $2^{-\Delta\Delta Ct}$ where $\Delta\Delta$Ct = ΔCt (isoform of interest) - ΔCt (ABECD or non-edited isoform). Experiments were repeated twice for each probe, with each sample run in triplicate. Results are expressed as mean $\pm$ SEM.

A similar lack of cross-reactivity by the ABECD, ABD or AD probes (5, 3 and 2 nucleotide mismatches, respectively) was observed in INI-expressing mutant mice. These results are consistent with our previous results in the well defined system using standard templates (**Table 3.5**) and indicate that the TaqMan® MGB assay accurately detects the expected 5-HT_{2C}R isoforms.

Fig. 3.5 shows differential expression of the four 5-HT_{2C}R isoform transcripts in brains of 129S6 and C57BL/6J mice. In 129S6 mice, the ABD isoform is the most prevalent; this agrees with results obtained by pyrosequencing for that strain (ABD+AD isoforms = 38%; Dr. Emeson, preliminary data) (**Fig. 3.5**; closed bars). The rank order (ABD+AD >>> non-edited > ABECD) and low expression levels of the non-edited and ABECD isoforms obtained by pyrosequencing for this strain (Dr. Emeson, preliminary data) are similar to the results obtained with the TaqMan® MGB assay. These data are also consistent with previously published data obtained with RNA from whole brain of C57BL/J6 mice: the ABD edited isoform is the most prevalent (**Fig. 3.5,** open bars**;** compare to Du et al., 2006); the relative abundance of AD edited 5-HT_{2C}R transcript is significantly lower than that observed for the ABD edited isoform; and the ABECD edited isoform as well as the non-edited isoforms are found in lower levels than the ABD isoform. More precise comparison to published data is not likely to be possible because editing of 5-HT_{2C}R can be affected by minor genetic differences (such as supplier), age and life experience of the mice. The proposed technique successfully detected four 5-HT_{2C}R edited

mRNA variants in 129S6 and C57BL/6J wild-type mouse brains, in amounts and rank order similar to published data, suggesting that the method herein is suitable for the detection of these closely related mRNA sequences.

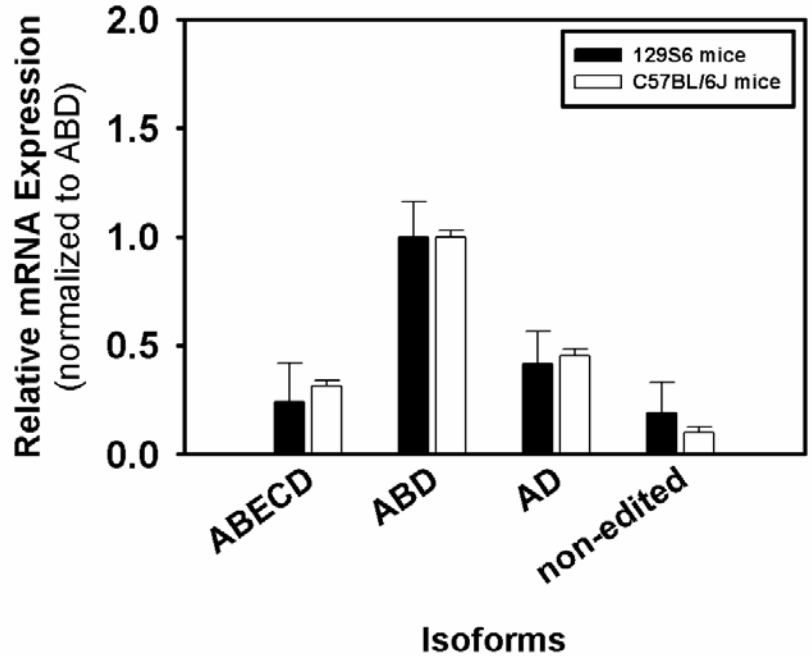

Figure 3.5. Specificity of TaqMan® MGB probes in RNA from whole brain from mouse strains. The data from the 129S6 (closed bars) and C57BL/6J mouse strains (open bars) are normalized to cyclophilin and plotted relative to expression of the ABD isoform for each mouse strain. The average crossing threshold (ΔCt) was calculated for each isoform studied: ΔCt = Ct (isoform of interest) – Ct (cyclophilin). Relative expression between groups was determined by: $2^{-\Delta\Delta Ct}$ where $\Delta\Delta$Ct = ΔCt (isoform of interest) - ΔCt (ABD isoform). Experiments were repeated twice for each probe, with each sample run in triplicate. In all instances, results are expressed as mean $\pm$ SEM.

5-HT$_{2C}$R isoform relative expression measured in the presence of competitors

Preliminary data indicated that the Ct values obtained *ex vivo* are higher (data not shown) than those Ct values shown in **Table 3.2**, therefore we utilized lower concentrations of competitor for this experiment. **Fig. 3.6** illustrates the effects of two concentrations of competitor cocktails (18.8 or 37.5 nM) employed in determinations of the relative expression of ABECD, ABD, AD and non-edited 5-HT$_{2C}$R transcripts in whole brain from 129S6 and C57BL/6J mice. For the 129S6 strain (**Fig. 3.6A**), addition of competitor cocktail did not change the relative expression of the four isoforms compared to control (absence of competitor): ABECD [$X^2_{(DF=2,\ n=9)}$ = 7.200, p = 0.0036], ABD [$X^2_{(DF=2,\ n=9)}$ = 5.600, p = 0.0500], AD [$X^2_{(DF=2,\ n=9)}$ = 5.600, p = 0.0500] and non-edited probes [$X^2_{(DF=2,\ n=9)}$ = 4.622, p = 0.1000]. However, for the C57BL/6J strain (**Fig. 3.6B**), the relative expression of the AD [$X^2_{(DF=2,\ n=12)}$ = 9.8462, p < 0.001] and ABECD isoforms [$X^2_{(DF=2,\ n=12)}$ = 9.2692, p < 0.001] decreased significantly in the presence of the higher concentration of the competitor cocktail. The relative expression of the ABD [$X^2_{(DF=2,\ n=12)}$ = 7.7308, p = 0.0066] and non-edited isoforms [$X^2_{(DF=2,\ n=12)}$ = 2.000, p = 0.3967] was unaffected by addition of competitor cocktails. These data suggest that the precision of measurement of the AD and ABECD isoforms in brains of C57BL/6J mice is improved by addition of competitors but addition of competitors is not required for the measurement of ABECD, ABD, AD and non-edited isoforms in whole brains of 129S6 mice.

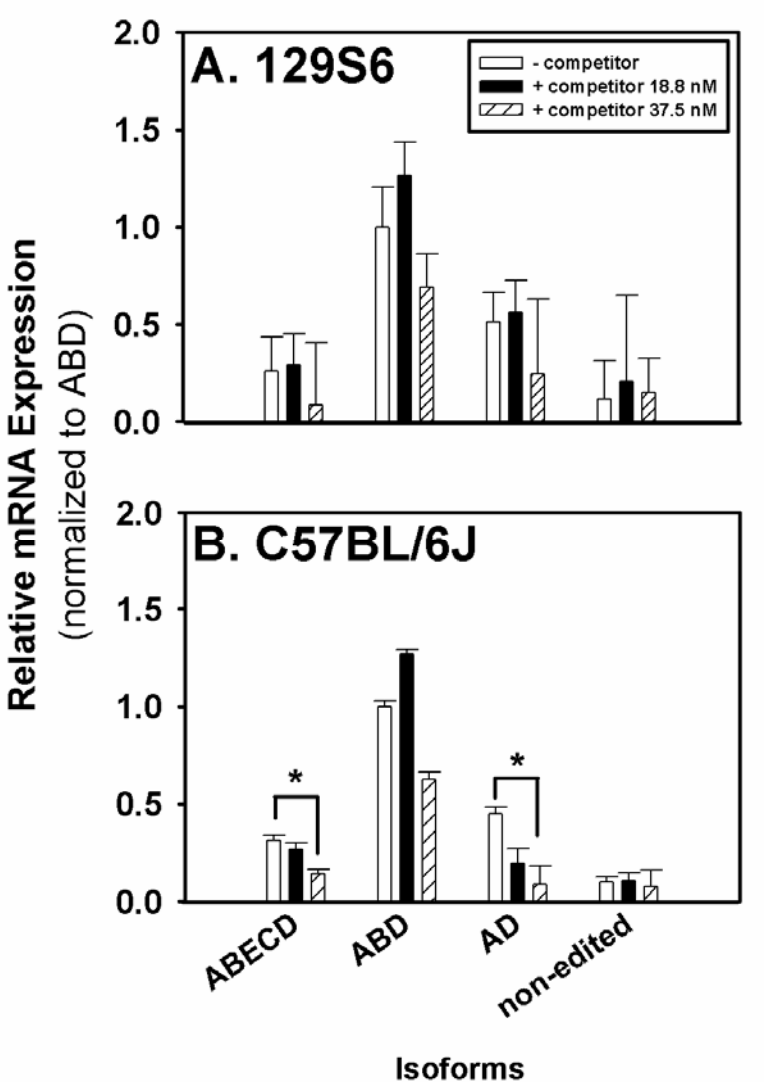

Figure 3.6. Effect of competitors on 5-HT$_{2C}$R RNA isoform profiles of mouse strains. Relative expression levels in [A] 129S6 and [B] C57BL/6J mouse strains in the absence and presence of competitors. The relative quantification method was used to compare 5-HT$_{2C}$R samples (www.appliedbiosystems.com/). The average crossing threshold (ΔCt) was calculated for each isoform studied: ΔCt = Ct (isoform of interest) – Ct (cyclophilin). Relative expression between groups was determined by: $2^{-\Delta\Delta Ct}$ where $\Delta\Delta$Ct = ΔCt (isoform of interest) - ΔCt (ABD isoform of control (no competitor)). Experiments were repeated twice for each probe, with each sample run in triplicate. In all instances, results are expressed as mean $\pm$ SEM. * $p < 0.001$ vs. no competitor.

DISCUSSION

A precise and rapid assay to establish changes in levels of relative expression of specific brain 5-HT_{2C}R RNA isoforms is needed to move forward our understanding of the biology of RNA editing in the brain. We have advanced this goal by adapting a qRT-PCR method to detect and quantify relative changes in edited 5-HT_{2C}R RNA isoforms by utilizing MGB TaqMan® probes. Probes for a series of four closely-related 5-HT_{2C}R isoforms were designed to test the sensitivity and discriminative ability of the proposed assay. After confirming these characteristics against standardized templates, we tested the *ex vivo* cross-reactivity of the four TaqMan® MGB probes (ABECD, ABD, AD and non-edited) against cDNA samples derived from transgenic mouse strains solely expressing the ABECD or non-edited 5-HT_{2C}R isoform. We found that both the ABECD and the non-edited isoforms were detected accurately by their respective probes without cross-reactivity, demonstrating that this technique can sensitively measure target isoforms and discriminate closely-related isoforms extracted from tissue samples.

The *ex vivo* sensitivity and specificity of these probes was further verified in RNA isolated from whole brain of 129S6 and C57BL/6J mice. The relative values of the four isoforms measured were similar to those predicted from DNA sequencing data in both 129S6 (Emeson, preliminary data) and C57BL/6J mouse brain (Du et al., 2006), suggesting that the described method is suitable for the detection of closely-related mRNA sequences in *ex vivo* samples. The current

TaqMan® MGB assay detected a rank order of isoform abundance of ABD >>> ABECD ≈ non-edited ≈ AD (**Fig. 3.5**). DNA sequencing analysis of RNA from C57BL/6J mouse whole brain indicated a rank order of abundance of ABD >>> non-edited ≈ AD ≈ ABECD (Du et al., 2006). Both the TaqMan® (present results) and DNA sequencing (Du et al., 2006) techniques detected the ABD isoform as the most abundant isoform with the other 3 isoforms present in much lower amounts. This consistency between the TaqMan® method and published data on the relative abundance of different isoforms is reassuring and suggests the usefulness of the TaqMan® MGB probes to measure disease- or treatment-related changes in individual isoforms *ex vivo.*

The discriminatory ability of the TaqMan® MGB probes can be enhanced by the addition of unlabeled competitors, either singly or as a cocktail (**Fig. 3.3** and **Table 3.5**). This simple adjustment represents a major advancement in the utility of the method for routine applications. Addition of competitors did not alter the Ct values of the ABECD and non-edited isoforms in VGV- and INI-expressing mutant mice, respectively suggesting that addition of competitors do not interfere with the detection of the target sample (data not shown). For C57BL/6J mouse brain, there were small differences in the amount of ABECD and AD isoforms detected with the addition of 37.5 nM competitor (**Fig. 3.6**), although the rank order of abundance was not changed [ABD >>> ABECD ≈ non-edited ≈ AD]. These data strongly suggest that the observed decrease in detection of the ABECD and AD isoforms in cDNA samples from whole brain of C57BL/6J mice

upon the addition of the competitor cocktail is due to a reduction of cross-reactivity of the respective probes to other 5-HT_{2C}R isoforms. In cDNA samples from whole brain of 129S6 mice, increasing concentrations of competitors did not alter Ct values for the four isoforms suggesting that the need for competitor cocktails is specific to the system under study. For probes not characterized herein, appropriate concentrations of competitor cocktails will need to be estimated using standard templates at concentrations approximating the Ct values of each isoform in the particular *ex vivo* system under study. When a series of experiments is initiated, it will be an easy matter to compare Ct values for each isoform of interest obtained with and without competitors to establish the necessity (and concentration) of competitor cocktail (as in **Fig. 3.6**). Since high concentrations decrease plateau fluorescence, there are limits to the total amount of competitors (singly or as a cocktail) that can be added to a reaction. For example, concentrations of competitors above 0.25 μM for the non-edited probe utilized with standard templates altered the detection of high concentrations of the target template (**Fig. 3.3**). However, lower concentrations of competitors, such as the ones used in **Fig. 3.6**, may prove to be sufficient for *ex vivo* systems.

The labor-intensive direct DNA sequencing (*e.g.,* Burns et al., 1997; Gurevich et al., 2002a) and pyrosequencing methods (Iwamoto et al., 2005; Sodhi et al., 2005) provide unambiguous results and have been used as a “gold standard” in the measurement of the entire profile of mRNA editing. This new

TaqMan® MGB method addresses several drawbacks for the study of editing *ex vivo*. With the TaqMan® MGB assay, measurements are performed directly on cDNA reverse transcribed from isolated RNA. Elimination of the subsequent processing steps increases the speed of data collection and eliminates several sources of error. In direct sequencing and pyrosequencing, each sequenced colony represents a single transcript of RNA within a single sample. While several hundred sequences per sample is a large number to analyze, it is, statistically speaking, a very small number of mRNA molecules. Sodhi and collaborators (2005) also point out the statistical bias that can result from small sampling size per subject; such concerns would be moot with the present approach because the proposed qRT-PCR method samples the entire population of mRNA transcripts unlike the small subset of transcripts assessed in sequencing methods. Measurement of the entire population of mRNA transcripts in a sample would reduce or eliminate the errors generated due to sampling bias, resulting in more precise measurements and greater statistical discrimination among experimental groups (Wong and Medrano, 2005; Yao et al., 2006). By focusing on only the isoforms of interest based upon the experimental question in hand, the proposed method will bypass the need to characterize the entire isoform profile, thus requiring only a single measurement (rather than hundreds) for each experimental subject. This, in turn, will facilitate the use of a greater number of subjects per study group.

The choice of specific mRNA species for normalization will depend upon the nature of the study being conducted. Normalization to a classical housekeeping gene, such as cyclophilin or actin, is useful to allow expression of isoform level proportionate to cell number. In the present studies, we have normalized our *ex vivo* data to cyclophilin and then set the value of the most abundant isoform to 100% (ABECD and non-edited in **Fig. 3.4**; ABD in **Figs. 3.5-3.6**). Setting the normalized value of the expected isoform to 100% clearly conveys the results with no additional manipulations necessary. An additional normalization step using total 5-HT_{2C}R mRNA could describe expression of isoforms as a percentage of total 5-HT_{2C}R mRNA but such analysis would require that measurements of total 5-HT_{2C}R and all individual isoforms be corrected to account for differences in efficiencies among TaqMan® MGB probes. Data obtained with those probes would need to be adjusted in order to calculate percentages appropriately (Schefe et al., 2006; Rebrikov and Trofimov, 2006; Schmittgen and Livak, 2008). However, there are several caveats to this approach. First, and most importantly, such corrections are not necessary when the goal is to measure disease- or treatment-related changes in individual isoforms because the average reaction efficiency to measure a single isoform *ex vivo* will be the same whether analyzed before or after a given manipulation (Schmittgen and Livak, 2008). Second, the algorithms to correct for probe-to-probe and sample-to-sample differences in efficiency vary among the available online software packages (*e.g.*, LinRegPCR, GenEx, and REST; http://www.efficiency.gene-quantification.info; University of Amsterdam,

Amsterdam, The Netherlands) (Rebrikov and Trofimov, 2006). There is currently no consensus for the choice of one correction method over the others. Third, the multiple calculations performed during the correction process can vastly increase the amount of error in the final comparisons. Such manipulations are essential when the goal is to obtain absolute values (*i.e*., copy numbers) or to measure complete 5-HT_{2C}R isoform profiles, but are not necessary when the goal is to measure disease- or treatment-related changes in individual isoforms *ex vivo* (Schmittgen and Livak, 2008).

The TaqMan® MGB method allows relative quantification of edited isoforms of 5-HT_{2C}R mRNA in a rapid and cost-effective manner. Purchase of MGB-labeled probes (about $250 each for 6000 pmol from Applied Biosystems) represents an initial expense but is sufficient for measuring a large number of samples (5,000 reactions at a final probe concentration of 100 nM). Once assays for isoforms of particular genes have been developed, large quantities of data can be obtained in a relatively short time (Wong and Medrano, 2005; Yao et al., 2006). This method will be particularly useful to study changes in levels of specific isoforms in response to pharmacological, behavioral or genetic manipulations *ex vivo* without the necessity of measuring an entire profile for each experimental sample. Following an initial survey of isoform profiles by DNA sequencing, assays can be designed to specifically target one (or a few) isoform(s) of interest and rapidly assess changes in expression levels following treatment or to correlate with disease state, behavioral activity, or other

parameter. In addition, the qRT-PCR method also will enable investigators to study the impact of treatment-elicited changes in less abundant isoforms because of the increased precision of the assay.

Another approach to the quantitative assessment of 5-HT_{2C}R edited isoform profiles has been published recently (Poyau et al., 2007). Following reverse transcription and nested PCR (in which the second round of PCR incorporates different fluorescent labels onto the forward and reverse cDNA strands), these authors used capillary electrophoresis (CE) to separate the single stranded products. Results were quantified by comparison to similarly prepared standards. The CE method approach is very promising for entire isoform profiles, particularly if researchers have access to the appropriate equipment. This method, however, may require significantly more time and technical expertise than the present TaqMan® MGB method, especially when only one or a few isoforms need to be measured.

In summary, the method to measure RNA edited isoforms described here for brain is a novel and innovative application of TaqMan® technology with the potential to broaden our knowledge of the function and regulation of RNA editing for the brain 5-HT_{2C}R. The general technique can be adapted easily to the study of other multiply-edited RNAs and should facilitate the development of a knowledge base to address broader issues of the physiological roles of RNA editing. With the advent of increasing numbers of qRT-PCR equipment and core facilities, this technique has the potential for widespread application by

laboratories without in-house DNA sequencing or capillary electrophoresis equipment. With the discovery of ever-increasing numbers of edited mRNAs in brain or other tissues, a rapid method to measure changes in multiply-edited RNA isoforms following pharmacological, behavioral or genetic manipulations should have wide applicability. The increased capabilities afforded by this new application will accelerate the pace of discovery in discerning the role of RNA editing in normal physiology and in disease processes.

CHAPTER 4: NEUROADAPTATIONS OF THE 5-HT_{2C}R AND ITS INTRACELLULAR SIGNALING MOLECULES FOLLOWING ACUTE AND REPEATED COCAINE ADMINISTRATION

INTRODUCTION

Repeated intermittent administration of cocaine results in a progressive augmentation of the motor stimulant response to subsequent drug challenge (Cunningham et al., 1992b; Hooks et al., 1994; Pierce and Kalivas, 1997; Filip et al., 2001). This phenomenon, also known as behavioral sensitization, was initially used as an animal model for the development of psychosis (Hooks et al., 1994; Kalivas et al., 1998). More recently, however, the neuronal adaptations underlying sensitization have been proposed as an important model for the incentive motivational effects of drugs of abuse (Robinson and Berridge, 1993) which contributes to the increased anxiety, craving and paranoia observed in drug addicts. Behavioral sensitization is an enduring behavioral transformation, and neuroadaptations in the 5-HT_{2C}R system may play a role in the behavioral sequelae precipitated by repeated cocaine administration.

The 5-HT_{2C}R predominantly exerts an inhibitory influence over the limbic-corticostriatal circuitry (Gobert et al., 2000; Di Matteo et al., 2001; De Deurwaerdere et al., 2004). The 5-HT_{2C}R has been implicated in modulating the hyperactive (McMahon et al., 2001; Filip et al., 2004) and the reinforcing effects (Fletcher et al., 2002) as well as the reinstatement of drug-seeking evoked by cocaine. However, the sensitivity of 5-HT_{2C}R is significantly diminished after a

period of withdrawal from a regimen of intermittent repeated exposure to cocaine (Filip et al., 2004). For example, the 5-HT_{2C}R agonist and antagonist lose the ability to reduce or enhance, respectively, cocaine-evoked hyperactivity after a repeated intermittent cocaine regimen. Thus, reduction in 5-HT_{2C}R ligand efficacy suggests that the 5-HT_{2C}R function or its downstream signaling components are significantly altered after cocaine administration (Filip et al., 2004). This loss of inhibition would be expected to enhance the activation of the limbic-corticostriatal circuitry evidenced by an increase in DA outflow from VTA (Di Giovanni et al., 1999; De Deurwaerdere et al., 2004) contributing to the expression of sensitization and increasing the tendency to self-administer cocaine in rats, which could parallel the tendency for cocaine use to escalate to addiction in humans (Gawin, 1991; Segal and Kuczenski, 1997).

The 5-HT_{2C}R couples preferentially to $G_{\alpha q/11}$ leading to an increase in the formation of inositol phosphates and to a release of intracellular Ca^{2+} in response to 5-HT_{2C}R stimulation (Bonasera and Tecott, 2000; Higgins and Fletcher, 2003; Hannon and Hoyer, 2008). Moreover, the 5-HT_{2C}R has also been shown to couple to $G_{12/13}$ which regulates structural changes in the cell via the Rho signaling pathway (McGrew et al., 2004). The 5-HT_{2C}R can also activate phospholipase A_2 (PLA_2), phospholipase D (PLD) (via $G_{12/13}$ coupling) and p44/p42-MAPK signaling pathways. Consequently, activation of the 5-HT_{2C}R can produce a plethora of cellular events, that are functionally regulated.

Receptor downregulation is a common adaptative response among GPCRs to sustained agonist exposure *in vitro* (Barker and Sanders-Bush, 1993) and *in vivo* studies (Pranzatelli et al., 1993; Fone et al., 1998; Van Oekelen et al., 2003). In a broaden definition, downregulation is the process of reducing or suppressing a response to a stimulus; as such we are going to look at four mechanism by which the 5-HT_{2C}R can be downregulated: 1) a reduction in protein expression of the 5-HT_{2C}R; 2) a redistribution of the 5-HT_{2C}R to subcelullar compartments 3) an increase in the expression of edited 5-HT_{2C}R mRNA isoforms; 4) changes in the expression and distribution of PSD-95 and p44/p42-MAPK, two molecules associated with the desensitization and resensitization processes of the 5-HT_{2C}R. We first ***tested the hypothesis that the reduced 5-HT_{2C}R sensitivity is due to 5-HT_{2C}R reduction or a change in subcellular localization of the 5-HT_{2C}R after a short-term withdrawal from a repeated intermittent cocaine regimen.*** Previous studies have suggested a postsynaptic localization of the 5-HT_{2C}R (Clemett et al., 2000; Lopez-Gimenez et al., 2002; Liu et al., 2007), making this compartment the logical focus in which to assess 5-HT_{2C}R protein expression. Additionally, the rewarding and reinforcing effects of cocaine depend upon its ability to block the reuptake of DA, 5-HT and norepinephrine thereby increasing the concentration of these neurotransmitters at the synapse and prolonging the stimulation of postsynaptic receptors in synapse. Furthermore, synapses are highly organized sites of neuronal cell-cell contact and signal transduction that are characterized by intense membrane trafficking (Banker et al., 1974; Hunt et al., 1996). Finally, a high concentration of

proteins that are involved in receiving and transducing synaptic signals (*e.g.*, neurotransmitter receptors and ion channels) are highly concentrated in the PSD, an electron-dense specialized structure of the submembrane cytoskeleton (Banker et al., 1974; Hunt et al., 1996). Thus, the synapse becomes the most likely place in which changes in 5-HT_{2C}R protein distribution may occur.

One mechanism that regulates 5-HT_{2C}R function is mRNA editing of the receptor. mRNA editing which is sensitive to changes in synaptic concentrations of 5-HT (Niswender et al., 1999; Gurevich et al., 2002a; Englander et al., 2005; Iwamoto et al., 2005) regulates receptor constitutive activity, receptor:G-protein coupling efficiency, agonist functional selectivity (Berg et al., 2001; Berg et al., 2008b); and receptor subcellular localization and trafficking (Marion et al., 2004). For example, the non-edited 5-$HT_{2C\text{-}INI}$R isoform demonstrates high affinity for G-protein coupling resulting in high levels of constitutive activity. Editing of 5-HT_{2C}R mRNA serves to reduce the efficiency of the interaction between the receptor and its G-protein resulting in low levels of constitutive activity (Burns et al., 1997; Marion et al., 2004). Most recently, functional selectivity, a process by which an agonist presents selectivity for a specific signaling pathway coupled to a single receptor, has been shown to be dependent on the degree of editing of the receptor (Berg et al., 2008b). For example, mRNA editing reduces or eliminates the coupling to $G_{12/13}$ and its subsequent pathway activation (McGrew et al., 2004). Hence, mRNA editing is another mechanism that regulates

serotonergic signal transduction and could play a critical role in modulating multiple cellular functions.

The 5-HT_{2C}R mRNA editing profiles have been investigated in depression (Niswender et al., 2001; Schmauss, 2003; Englander et al., 2005; Iwamoto et al., 2005), and schizophrenia (Rauser et al., 2001; Dracheva et al., 2003; Iwamoto and Kato, 2003; Sodhi et al., 2005), but limited information on the involvement of 5-HT_{2C}R mRNA editing events in addiction is available (Iwamoto and Kato, 2002). Since cocaine inhibits 5-HT reuptake and increases extracellular levels of 5-HT, we would expect to see changes in the relative abundance of the 5-HT_{2C}R isoforms in the brain in response to repeated, intermittent cocaine exposure. An increase in 5-HT_{2C}R mRNA editing, which results in the production of receptors with lower affinity for their G-proteins, could contribute to the reduced response observed in the presence of agonist stimulation after chronic cocaine administration. Thus, ***we tested the hypothesis that repeated intermittent cocaine administration will promote changes in the expression of the most prevalent 5-HT_{2C}R mRNA isoforms in the motor cortex and PFC.***

The functional activity of the 5-HT_{2C}R is also regulated via desensitization and resensitization processes. These processes are modulated according to the repertoire of PDZ proteins co-expressed with the receptor (Gavarini et al., 2006). One such PDZ protein is PSD-95 which plays an important role in the organization of protein networks in the PSD (Ehrlich et al., 2007).

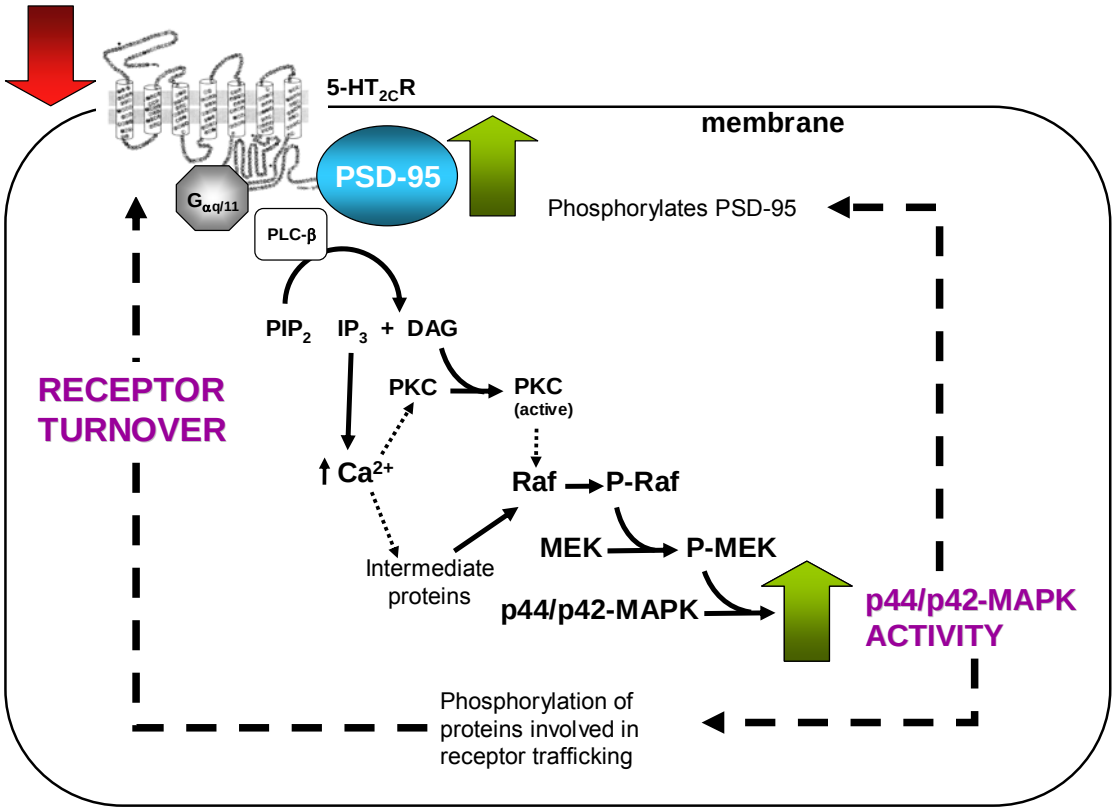

Figure 4.1. Association between the 5-HT$_{2C}$R signaling pathway, PSD-95 and p44/p42-MAPK pathway. A schematic representation of the rationale for the study of the association of 5-HT$_{2C}$R, PSD-95 and p44/p42-MAPK pathway following repeated intermitent cocaine administration. Adapted from Werry et al. 2005

Dysregulation of PSD-95 induced by repeated cocaine administration could alter the signaling profile of many signaling pathways including that for the 5-HT$_{2C}$R (Yao et al., 2004). For example, *in vitro* studies have shown that PSD-95 recognizes PDZ domains located at the C-terminal of the 5-HT$_{2C}$R; and that the interaction between 5-HT$_{2C}$R and PSD-95 reduces agonist-evoked intracellular Ca^{2+} release as well as constitutive and agonist-induced internalization and trafficking (Backstrom et al., 2000; Parker et al., 2003; Becamel et al., 2004; Gavarini et al., 2006) (**Fig 4.1**). In fact, *in vitro* studies have

shown that overexpression of PSD-95 in neuronal cell cultures desensitizes 5-HT_{2C}R signaling (Gavarini et al., 2006). Thus, ***we tested the hypothesis that repeated intermittent cocaine administration will promote a translocation of PSD-95 to the PSD thus decreasing functionality of the 5-HT_{2C}R system.***

Lastly, a fourth mechanism that could contribute to the functional 5-HT_{2C}R subsensitivity seen after repeated intermittent cocaine is via activation of the p44/p42-MAPK signaling pathway. The p44/p42-MAPK signaling pathway is an important downstream signaling pathway of the 5-HT_{2C}R (Raymond et al., 2001; Werry et al., 2005; Werry et al., 2008b). The most well-known MAPK variants are the p42-MAPK (42 kDa) and the p44-MAPK (44 kDa), known as extracellular signal-regulated kinase (ERK), ERK-2 and ERK-1, respectively. The p42-MAPK variant presents an 8-fold higher expression than p44-MAPK in frontal cortex (Ortiz et al., 1995); and even though both p42-MAPK and p44-MAPK have been identified in synaptosomes (Ortiz et al., 1995), only p42-MAPK localizes to the dendritic lipid raft and to the PSD subfractions from synaptosomes (Suzuki et al., 1995; Suzuki et al., 1999). Mice lacking the p44-MAPK (ERK-1 KO mice) are more prone to develop cocaine-induced psychomotor sensitization and to acquire cocaine-induced CPP, suggesting a more important role of p42-MAPK in behavioral sensitization (Ferguson et al., 2006). Furthermore, p42-MAPK has been shown to be activated by cocaine (Valjent et al., 2004a; Mattson et al., 2005; Valjent et al., 2006; Girault et al., 2007; Li et al., 2008). If cocaine is capable of inducing phosphorylation of p44/p42-MAPK, then changes in proteins

activity that are involved in 5-HT_{2C}R turnover and trafficking would be expected (Pitcher et al., 1999). Thus, ***we tested the hypothesis that repeated intermittent cocaine administration will promote the phosphorylation of p44/p42-MAPK to the PSD thus decreasing functionality of the 5-HT_{2C}R system.***

Thus, the purpose of the present study was to investigate four possible neuroadaptations that could contribute to functional 5-HT_{2C}R subsensitivity following repeated intermittent cocaine administration (**Fig. 4.1**): 1) changes in expression and subcellular localization of the 5-HT_{2C}R; 2) changes in 5-HT_{2C}R mRNA editing contributing to the formation of isoforms with reduced efficiency to couple G-protein; 3) changes in expression and subcellular localization of PSD-95; and finally 4) changes in phosphorylation of p44/p42-MAPK pathway, which could in turn influence the activity of molecules involved in 5-HT_{2C}R trafficking.

First, rats were treated with cocaine (15 mg/kg IP) or saline twice a day for 7 days, and then further subdivided into two more groups and challenge either with cocaine or saline. Motor cortex and PFC were collected for Western blot or qRT-PCR analyses. Then proteins of interest were analyzed in total homogenate, synaptosomes and the PSD-enriched fractions. Finally correlation studies were performed to assess relationships between ambulatory counts and protein or mRNA expression.

MATERIALS AND METHODS

Behavioral sensitization to cocaine

Animals

Adult male Sprague-Dawley rats (n=132; virus antibody-free; Harlan, Indianapolis, IN) weighing 225-280g at the beginning of the experimental procedures were used. All rats were kept in the colony room for a minimum of 7 days after arrival, during which time they were handled and weighed daily. All rats were housed four/cage with food and water *ad libitum*. The animal colony was maintained at a constant temperature (21-23^{o}C) and humidity (45-50%) on a 12 hr light-dark cycle (lights on 0700-1900 hr). All testing was conducted during the light phase. All experimental protocols were carried out in accordance with the Guide for the Care and Use of Laboratory Animals (National Institutes of Health, 1986) and with the approval by the Institutional Animal Care and Use Committee (IACUC).

Drugs

Cocaine-HCl (National Institutes on Drug Abuse, Research Triangle Park, NC, USA) was dissolved in 0.9% NaCl solution to a final concentration of 15 mg/kg. Chloral hydrate was dissolved in physiological saline to a final concentration of 800 mg/kg. All solutions were injected at room temperature.

Apparatus

Ambulation was quantified using an open-field activity system (San Diego Instruments, San Diego, CA) housed within sound-attenuating chambers,

consisting of a clear Plexiglas open field (40 x 40 x 40 cm) and a 4 x 4 photobeam matrix located 4 cm above the chamber floor. A horizontal row of 16 photobeams located 16 cm from the floor provided each chamber with the capability to measure rearing activity. Activity recorded in the inner 16 x 16 cm of the open field was counted as central activity, whereas the outer 16-cm band registered peripheral activity. Peripheral, central, and rearing activity counts were made by the control software (Photobeam Activity Software; San Diego Instruments) and stored for statistical evaluation. Video cameras above the chambers were used to monitor activity continuously without disruption of behavior.

Experimental protocols

Development of cocaine sensitization The ability of cocaine to induce sensitization was assessed by recording cocaine-induced locomotor hyperactivity and by rating cocaine-induced stereotypy (behavioral scoring scale) (Paris et al., 1991).

1) Behavioral protocol: Before placing rats into the locomotor chamber, all rats were removed from their home cage between 08:00 and 9:00 hr, weighed, and immediately returned to their home cage. All rats were habituated to the test chamber for 2 hrs per day for three days prior to the start of the experiment. On each test day, rats were placed in the locomotor monitors for 60 min before behavior was recorded. Rats (n=24 rats/group) were then injected intraperitoneally (IP) with cocaine (15 mg/kg) or saline and ambulation was

measured for 60 min immediately after the first daily injection. The second daily injection was administered in the home cages. This procedure, referred as “pretreatment”, was repeated for seven consecutive days.

2) Behavioral scoring scale: Immediately after the first daily injection, rats were placed into the locomotor monitors and the behavior of the rats was rated using the following scale. A value from 1 to 8 is assigned according to the predominant behavior at a given time: (1) asleep, resting, eyes closed; (2) inactive, resting with eyes open, little or no movement; (3) in-place, periodic sniffing, infrequent locomotion, grooming; (4) active, occasional locomotion and rearing/wall climbing, sniffing without a repetitive pattern, at normal levels of activity; (5) hyperactive, faster, non-stereotyped sniffing, locomotion, with frequent rearing/wall climbing, intermittent grooming; (6) slow-patterned, repetitive exploration of cage with hyperactivity; (7) fast-patterned, repetitive motor pattern in one corner and then rapid translocation to another corner and repetition of the behavior (includes jumping); (8) stereotypy, fast, perseverative behaviors with prominent sniffing and head bobbing with little or no locomotion. The behavior of each animal was rated following a 15 second observational period that scored 15 min after the first daily injection.

Challenge with cocaine duridownng withdrawal

1) Behavioral protocol 1: Two days after the last injection, all rats were challenged with saline and placed in the locomotor monitors. During locomotor

recording, behavior was scored for stereotypy as above. On the following day, rats were challenged with cocaine (15 mg/kg IP) and locomotor assessment and behavioral scoring were repeated. This phase was performed to test the induction of behavioral sensitization by repeated intermittent cocaine administration (**Fig. 4.2A**).

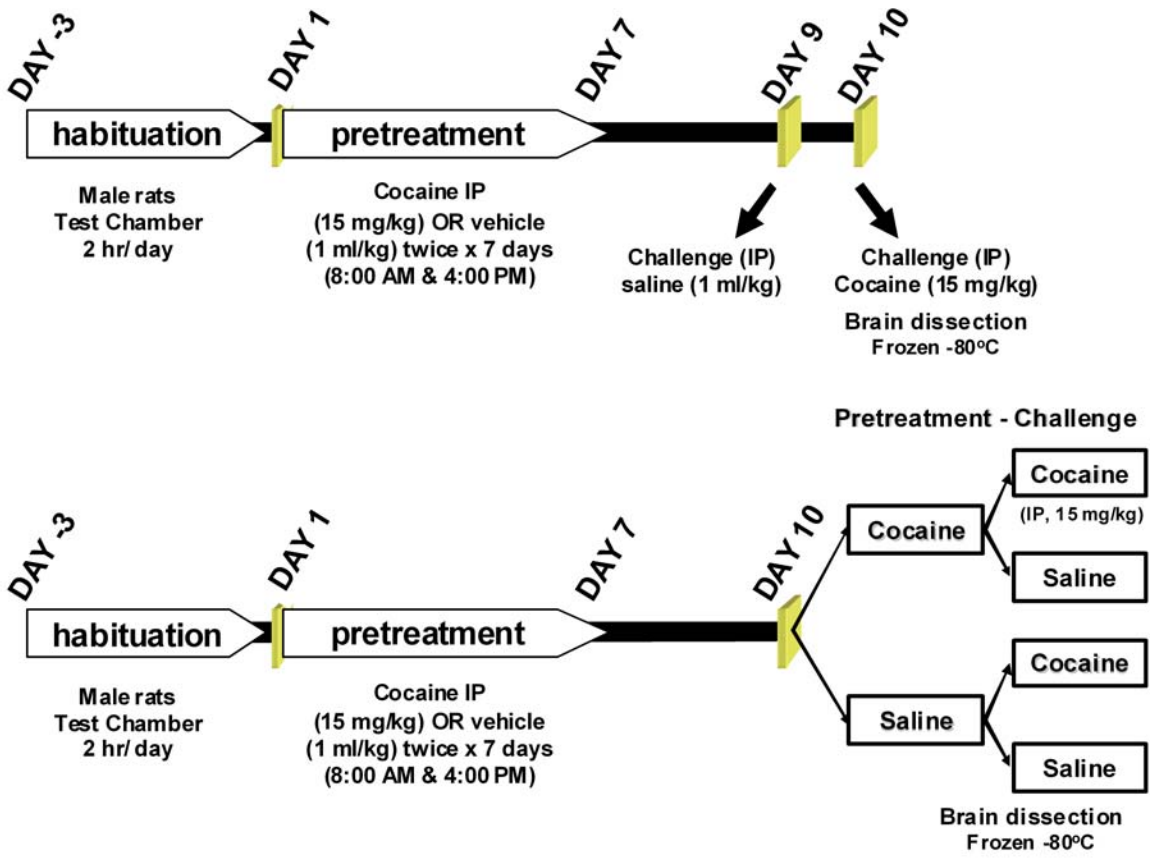

Figure 4.2. Outline for Behavioral Experiments: [A] behavioral protocol 1; [B] behavioral protocol 2.

2) Behavioral protocol 2: This protocol was used for all experiments after experiment 1. After seven days of pretreatment each group was subdivided in two (n=12 rats/subgroup). Three days later, animals received either a challenge injection of cocaine (15 mg/kg IP) or saline (1 ml/kg IP). From this subdivision, four groups were generated: saline pretreated-saline challenge (SS), saline pretreated-cocaine challenge (SC), cocaine pretreated-saline challenge (CS), and cocaine pretreated-cocaine challenge (CC) (**Fig. 4.2B**). By having these four groups, questions regarding the effects of the pretreatment as well as the effects of the challenge injection were answered. On challenge day, rats were injected with cocaine (15 mg/kg IP) or saline in the home cages and a score was assigned 15 min immediately after the injection. Animals were anesthetized and sacrificed by decapitation immediately after scoring. Motor cortex and PFC were rapidly microdissected on ice.

Preplanned comparisons:

1) *SS vs. SC:* This comparison studied neuroadaptations associated with acute cocaine administration.
2) *SS vs. CS:* This comparison studied neuroadaptations associated with repeated intermittent cocaine exposure after a short period of withdrawal (3 days).
3) *SC vs. CC:* This comparison studied the effects of previous cocaine exposure on cocaine exposure following a short-term withdrawal period (3 days).

Protein Analyses

Antibodies

The mouse monoclonal anti-5-HT_{2C}R antibody [SR-2C (**D-12**): sc-17797, Lot No. J1606] was used at a concentration of 1:100 at 4°C overnight; the monoclonal mouse anti-PSD-95 antibody (Chemicon International, Temecula, CA) was used at a concentration of 1:2000 at room temperature for 1 hr. The mouse monoclonal anti-phospho-p44/p42-MAPK antibody (9106, Lot No. 19, Cell Signaling technology, Inc., Danvers, MA) was used at a concentration of 1:2000 at 4°C overnight. The rabbit polyclonal anti-p44/p42 MAPK antibody (9102, Lot No. 27, Cell Signaling Technology, Inc., Danvers, MA) was used at a concentration of 1:2000 at 4°C overnight. The monoclonal mouse anti-β-actin antibody (Chemicon International, Temecula, CA) was used at a concentration of 1:5000 at room temperature for 1 hr to normalize protein loading on all Western blots. Secondary antibodies (1:20,000) used included Infrared (IR)-labeled goat anti-mouse (IRDye™680; 926-32220, Lot No. B61017-02, LI-COR® Biosciences, Lincoln, NK); goat anti-rabbit (IRDye™800; 827-08365, Lot No. B61023-01, LI-COR® Biosciences, Lincoln, NK).

Synaptosomal fractionation

After behavioral assessment, rats were immediately anesthetized with chloral hydrate (800 mg/kg IP) and then decapitated. Following decapitation, motor cortex and PFC tissue was microdissected on a cool tray (4°C) (Heffner et al., 1980). Motor cortex and PFC tissue was homogenized in 0.32 M sucrose

solution [0.1 mM $CaCl_2$] containing protease (SIGMA, Cat. No. P8340) and phosphatase inhibitor cocktails 1 and 2 (SIGMA, Cat. No. P2850 and P5726, respectively). An aliquot (total homogenate) was taken, and the remaining homogenate was diluted in 6 mL 2 M sucrose solution and 2.5 mL 0.1 mM $CaCl_2$. The solution was mixed by inversion and transferred to a 25 mL ultracentrifuge tube (Beckman Coulter, Fullerton, CA). The remaining tube volume was overlaid carefully with 1 M sucrose solution. It was ultracentrifuged (Beckman LE-80K Ultracentrifuge, Beckman Coulter, Fullerton, CA) in a fixed angle rotor (50.2 Ti Rotor) at 100,000 g for 3 hrs at 4^{o}C. The synaptosomes were located between the interface of the 1.25 M and the 1 M sucrose phase. An aliquot (synaptosomal fraction) was taken, and then, the remaining solution (approximately 2.5 mL) was diluted in 15.6 mL hypotonic solution [13.5 mL 0.1 mM $CaCl_2$, 0.3 mL 1 M Tris pH 6 buffer, 1.5 mL 10% Triton X-100, 150 uL protease and phosphatase inhibitor cocktails each]. The solution was then mixed by inversion and incubated on a shaker for 20 min at 4^{o}C. The synaptic junctions were collected by centrifugation at 48,000 g for 20 min at 4^{o}C (Beckman J2-HS centrifuge, Beckman Coulter, Fullerton, CA). The supernatant was discarded, and the pellet was resuspended in 15.6 mL hypotonic solution. The solution was incubated on a shaker for 20 min at 4^{o}C and centrifuged at 48,000 g for 20 min at 4^{o}C. The supernatant was discarded, and the pellet was first resuspended in 1 mL of pH 8 buffer [20 mM Tris, 1% Triton X-100, pH 8]. An aliquot (synaptic junction) was taken, and 9 mL of pH 8 buffer was added to the remaining solution. The solution was incubated on a shaker for 20 min at 4^{o}C. The PSD-enriched fraction was collected by

centrifugation at 48,000 g for 20 min at 4°C. The PSD-enriched pellet was resuspended in 10 mL pH 8 buffer, incubated on a shaker for 20 min at 4°C, and centrifuged at 48,000 g for 20 min at 4°C. The supernatant was discarded; the remaining pellet (PSD-enriched fraction) was resuspended in 1% SDS. All the aliquots collected were frozen at -80°C until protein analysis was conducted. Total protein concentration was determined for each fraction using a BCA protein determination kit (Pierce, Rockford, IL).

Western blot assay

Equal amounts of protein (5-10 µg from each fraction; reduced with an appropriate volume of Laemmli sample buffer with DTT for 20 min at 70°C) were separated by SDS-PAGE using a 4-12% BisTris pre-cast gels (Invitrogen, San Diego, CA) for 2-3 hrs at 120V. Following gel electrophoresis, proteins were transferred to a PVDF membrane (BIORAD, Hercules, CA) via wet-transfer electroblotting (BIORAD, Hercules, CA) for 3 hr at 100V. Western blot assay was conducted according to manufacturer's specifications with slight modifications (Odyssey® Western blot Analysis, www.licor.com): Briefly, the membrane was blocked with Odyssey blocking buffer (1:1 in Tris Buffered Saline (TBS)) for 1 hr, followed by incubation with the primary antibody (see Antibody section for incubation conditions). Membranes were rinsed 4 x 10 min in TBS + 0.1% Tween-20 (TBS-T), and incubated with the secondary antibody (diluted in TBT-T) for 45 min. Membranes were rinsed again 4 x 10 min in TBS-T prior to incubation

with TBS for 2 hr. The fluorescent dyes were detected with the Odyssey® Infrared Imaging System (LI-COR® Biosciences, Lincoln, NE) (See chapter 2).

Total 5-HT_{2C}R mRNA expression and mRNA Editing Analysis

qRT-PCR Reagents

FAM-labeled TaqMan® MGB probes were custom synthesized by Applied Biosystems (Applied Biosystems; Foster City, CA). Primers and unlabeled competing probes were synthesized by SigmaGenosys (Sigma-Aldrich, St. Louis, MO). A predesigned TaqMan® Gene Expression Assay (Rn00562748_m1, Applied Biosystems, Foster City, CA) was used to detect total 5-HT_{2C}R mRNA derived from rat. The location of the amplified region does not include the editing sites and thus provides a separate measure of total 5-HT_{2C}R mRNA. We designed a TaqMan® assay for the housekeeping gene, cyclophilin (accession number M_19533; bases 224-293); primer and probe sequences were: SN primer = 5'-TGT GCC AGG GTG GTG ACT T-3'; ASN primer = 5'-TCA AAT TTC TCT CCG TAG ATG GAC TT-3'; Probe = [FAM] ACA CGC CAT AAT GGC ACT GGT GG [TAMRA]. SN and ASN primer sequences flanking the 5-HT_{2C}R editing region (accession number M21410; bases 1014-1192) were designed using Primer3 Software (Whitehead Institute, Cambridge, MA) with stringent parameters to reduce primer dimerization and to minimize the difference between primer melting temperatures (Tms within 2^{o}C). SN and ASN sequences were 5'-CCT GTC TCT GCT TGC AAT TCT-3' and 5'-GCG AAT TGA ACC GGC TAT G-3', respectively. 5-HT_{2C}R edited TaqMan® MGB probes were as followed:

ABECD = [FAM] TAGCAGTGCGTGGTCCTGTTGA [MGB/NFQ]; ABD = [FAM] TAGCAGTGCGTAATCCTGTTGA [MGB/NFQ]; and AD = [FAM] TGTAGCAGTACGTAATCCTGTTGA [MGB/NFQ]; TaqMan® Genotyping PCR Master Mix, TaqMan® Reverse Transcription Kit and Gene Amp XL PCR kit were purchased from Applied Biosystems (Foster City, CA). Competitor cocktails were prepared for each probe in 20 µL final volumes from 15 µM stock solutions as follows: AD = 4 µL each of A, D, ABD and ACD; ABD = 4 µL each of AD, AB and ABCD; and ABECD = 4 µL each of ABCD and ABEC. Competitor cocktails were then diluted 16 times in nuclease-free water (188 µM final concentration for each competitor). Two µL of the diluted competitor cocktails were used in the qRT-PCR reaction, producing a final concentration of each individual competitor of 18.8 nM.

RNA extraction and reverse transcription

Motor cortex and PFC tissue was homogenized in 500 µL of TRI Reagent® (Applied Biosystems), using a Tissue-Tearor™ homogenizer. RNA was then isolated using the RiboPure kit (Applied Biosystems) according to the manufacturer's directions. Any residual genomic DNA was removed by treatment with TURBO DNA-free™ (Applied Biosystems); a final incubation step of 70^{o}C for 10 min was used to inactivate the DNAse. The final RNA concentration was determined by absorbance at 260 nm. The reverse transcription reaction was performed on 0.25 µg of RNA using the TaqMan® Reverse Transcription Kit (Applied Biosystems) with random hexamer primers according to the

manufacturer's directions. The reverse transcription program consisted of an annealing step (25°C, 10 min) followed by elongation (48°C, 30 min) and a final enzyme inactivation step (95°C, 5 min).

TaqMan® MGB assay

qRT-PCR reaction comprised of 10 µL of TaqMan® Genotyping Master Mix, 125 nM sense and antisense primers, 100 nM TaqMan® MGB probe, 2 µL of competitor cocktail and 6 µL of sample containing target template in a final reaction volume of 20 µL. Assays were performed in a 7500 Fast Real-Time PCR System (Applied Biosystems). The TaqMan® assay amplification program (according to manufacturer's directions) consisted of an activation step (95°C, 10 min) followed by 40 cycles of denaturation (95°C, 15 s), annealing and elongation (60°C, 1 min). All data were analyzed using the 7500 Fast System Detection Software (SDS) version 1.3.1 (Applied Biosystems).

The relative quantitation method was used to compare differences between samples (Schefe et al, 2006; Livak and Schmittgen, 2001; Wong and Medrano, 2005). Results are expressed in terms of Ct values (See Chapter 3). The ΔCt was calculated for each cDNA being studied: ΔCt = Ct (5-HT_{2C}R isoform of interest) – Ct (cyclophilin). Mean ± SEM was determined for each group. The magnitude of the differences between groups was calculated as: ΔΔCt = ΔCt (CS) – ΔCt (SS); relative mRNA expression was estimated by $2^{-\Delta\Delta Ct}$. Data was presented as relative expression of SS group.

Data Analysis

For behavioral studies, a two-way analysis of variance (ANOVA) for repeated measures (SAS System for Windows V.8.2 (SAS Institute Inc., Cary, NC)) was used to assess differences between treatment groups on measures of ambulation. *A priori* planned pairwise comparisons were made using Dunnett's T-test procedure (vs. Day 1) with the experimentwise error rate $\alpha = 0.05$. A non-parametric Friedman ANOVA by ranks χ_r^2 test was used to assess differences between treatment groups on measures of specific stereotypic responses.

For qRT-PCR studies, a non-parametric Wilcoxon two-sample by ranks χ_r^2 test (NPAR1WAY procedure, SAS System for Windows V.8.2 (SAS Institute Inc., Cary, NC)) with a Kruskal-Wallis test and Dunn's post-test with an experimentwise error rate $\alpha = 0.05$ was performed on the delta Ct values between the SS and CS groups. The relative gene expression was presented using the comparative CT method also referred to as the $2^{-\Delta\Delta CT}$ method. The SEM was calculated by error propagation using the following equation: $SEM = \sqrt{(SEM_1^2 + SEM_2^2)}$ (Schmittgen and Livak 2008).

For Western blot analysis, membranes were imaged using the Odyssey® Infrared Imaging System (LI-COR® Biosciences) at 700 and/or 800 nm at 169 µm resolution. The integrated intensity of each band was analyzed with the Odyssey Odyssey® Infrared Imaging System Application version 2.1 Software. Following background subtraction, the ratio of target band intensity to actin band

intensity was determined for each sample to normalize for the amount of protein loaded. Data are presented as the mean (± SEM) protein expression expressed as percent change from SS controls. A two-way repeated measures analysis of variance (ANOVA) utilizing restricted maximum likelihood estimation (REML) was used to obtain parameter estimates using the MIXED procedure in SAS System for Windows V.8.2 (SAS Institute Inc., Cary, NC). The outcome variable was protein expression on Western blot analysis and the grouping factors were the four treatment groups (SS, SC, CS and CC). Each set of measurements from the same batch were considered a correlated cluster of observations. By accounting for the inherent correlations that arise from multiple gels from the same experimental unit, the correct standard errors are used for statistical tests. Compound symmetry structures were used for the covariance structure. Treatment groups were compared [SS vs SC; SS vs. CS; SC vs CC] using individual lineal contrasts in the MIXED procedure. Data from two different experiments (experiment 1 and 2) were combined. To assess the appropriateness of combining these data we looked for similarity of effect across experiments. To do this we assessed the (experiment x treatment interaction and experiment x challenge interaction) in our preliminary models. If the treatment effect depended on which experiment was considered, this unfavorable phenomenom would manifest itself in a statistically significant interaction effect ($p < 0.05$, **Table 4.1**).

Table 4.1. Statistics for comparison across experiments

	experiment x treatment *p* value	**experiment x challenge** *p* value
PSD-95 protein expression		
Motor cortex		
Total homogenate	0.7280	0.8532
Synaptosomes	0.0885	0.1770
PSD-enriched fraction	**0.0445**	0.7077
PFC		
Total homogenate	0.9648	0.5491
Synaptosomes	**0.0018**	0.1533
PSD-enriched fraction	0.0521	0.4472
p42-MAPK protein expression		
Motor cortex		
Total homogenate	0.2263	0.1770
Synaptosomes	0.3465	0.4299
PSD-enriched fraction	0.0915	0.8398
PFC		
Total homogenate	0.9568	0.1565
Synaptosomes	0.1426	0.1192
PSD-enriched fraction	0.8860	**0.0038**
Phospho-p42-MAPK protein expression		
Motor cortex		
Total homogenate	0.0951	0.2329
PFC		
Total homogenate	0.1797	0.9715
Synaptosomes	**0.0006**	0.5649
PSD-enriched fraction	**<0.0001**	0.1025
p42-MAPK ratio		
Motor cortex		
Total homogenate	0.0512	0.7508
PFC		
Total homogenate	0.3348	0.6643
Synaptosomes	**0.0033**	0.3487
PSD-enriched fraction	**0.0002**	0.412

In all cases in which p value > 0.05 the data from experiments 1 and 2 were grouped. In all instances in which p value < 0.05, experiments were not grouped. It could be argued that the reason for this phenomenon is due to the learning curve for the synaptosomal fractionation procedure and/or for the differences between the times at which the animals were sacrificed. Although our goal was to sacrifice all animals 15 min after their challenge injection of either saline or cocaine, the average time in which most animals in experiment 1 were sacrificed was 14 min, whereas animals in experiment 2 were sacrificed 17 min after the last challenge injection of either saline of cocaine in average.

RESULTS

Development and expression of cocaine sensitization

The ability of cocaine to induce behavioral sensitization was determined via measurements of ambulation immediately following the first daily injections of cocaine (15 mg/kg IP) or saline. Mean total ambulatory counts from Day 1, 3, 5 and 7 are presented in **Fig. 4.3**. A two-way ANOVA with Day as a repeated measures revealed a main effect of pretreatment ($F_{(1,825)} = 478.19$; $p < 0.0001$), day of injection ($F_{(6,825)} = 7.40$; $p < 0.001$), and a pretreatment x day of injection interaction ($F_{(6,825)} = 10.30$; $p < 0.0001$) for mean total ambulatory counts summed across a 60 min session. Furthermore, cocaine (15 mg/kg IP) induced significantly higher levels of ambulation compared to saline on days 1 through 7 ($p < 0.001$). Animals also presented significantly higher levels of ambulation in

response to cocaine on days 3, 5 and 7 compared to day 1 of the repeated treatment [$F_{(6,405)}$ = 3.00, p < 0.0001, closed circles, **Fig. 4.3**], suggesting that behavioral sensitization had indeed developed. Ambulatory counts following saline administration differ between day 1 and every other test day [$F_{(6,419)}$ = 4.90; p < 0.0001; open circles, **Fig. 4.3**] indicating habituation to placement into the locomotor chambers.

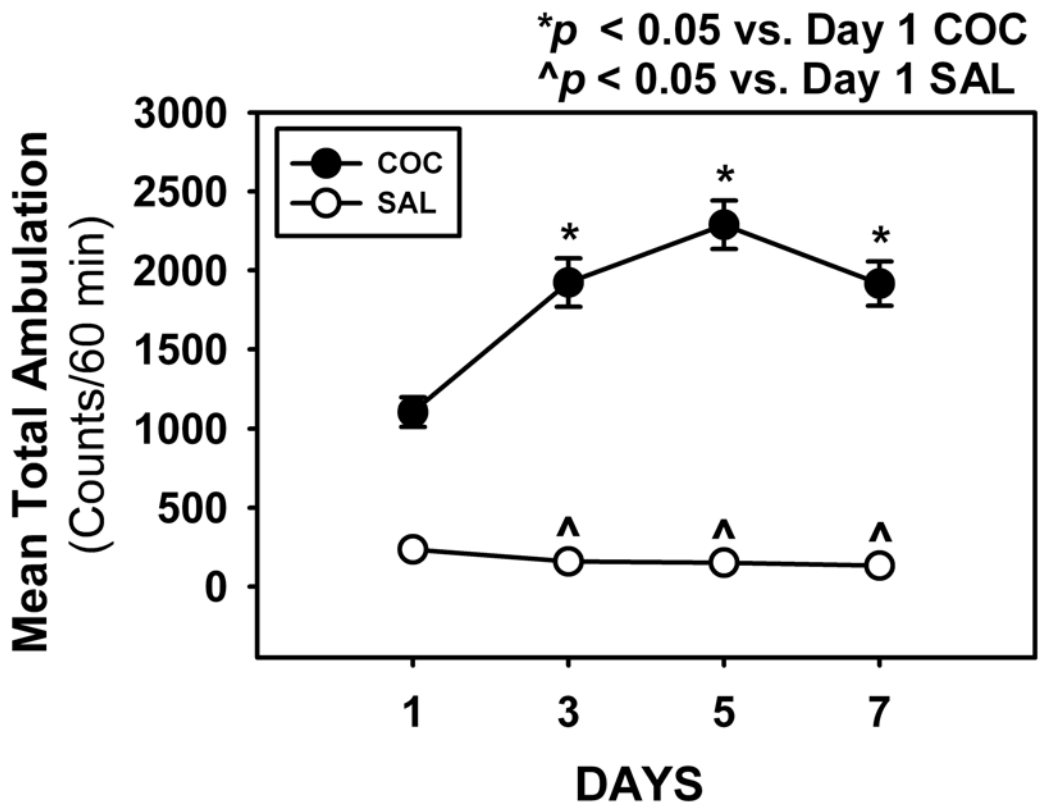

Figure 4.3. Chronic cocaine (15 mg/kg) regimen enhanced cocaine-evoked hyperactivity. Data represent the mean ambulatory activity counts (± SEM; n = 58-60 rats/group) summed over a 60 min session following injection of saline (1 ml/kg, IP) or cocaine (15 mg/kg, IP) on days 1, 3, 5 and 7 of a 7-day repeated regimen. * p < 0.05 vs. cocaine on day 1. ^ p < 0.05 vs. saline on day 1.

We assessed the expression of behavioral sensitization in a subset of animals that were treated with cocaine (15 mg/kg, filled bars) or saline (1 mg/kg, open bars) and challenged with saline on day 2 of withdrawal (**Fig. 4.4A,** left bar group) and cocaine (15 mg/kg) on day 3 of withdrawal (**Fig. 4.4A,** right bar group). During locomotor recording, the expression of stereotypy was determined a behavioral rating scale (see Methods). No differences in ambulation were observed between cocaine and saline-pretreated rats at day 2 of withdrawal following saline challenge (**Fig. 4.4A**, DF = 12.812, t = 1.454, p = 0.170). Repeated intermittent administration of cocaine resulted in an enhancement of the locomotor activating effects of cocaine when rats were challenged at day 3 of withdrawal from a chronic regimen of cocaine compared to rats pretreated with saline (**Fig. 4.4A**, DF = 10.866, t = 2.535, p = 0.022), demonstrating the expression of sensitization. In support of this, cocaine presented statistically significant higher behavioral scores following cocaine challenge (**Fig. 4.4B**, left bar group) when compared to those animals that received a saline pretreatment ($p < 0.01$). Thus, we have validated the behavioral sensitization protocol and reproduced previous results observed in this laboratory (Cunningham et al., 1992b; Callahan and Cunningham, 1994; De La Garza and Cunningham, 2000).

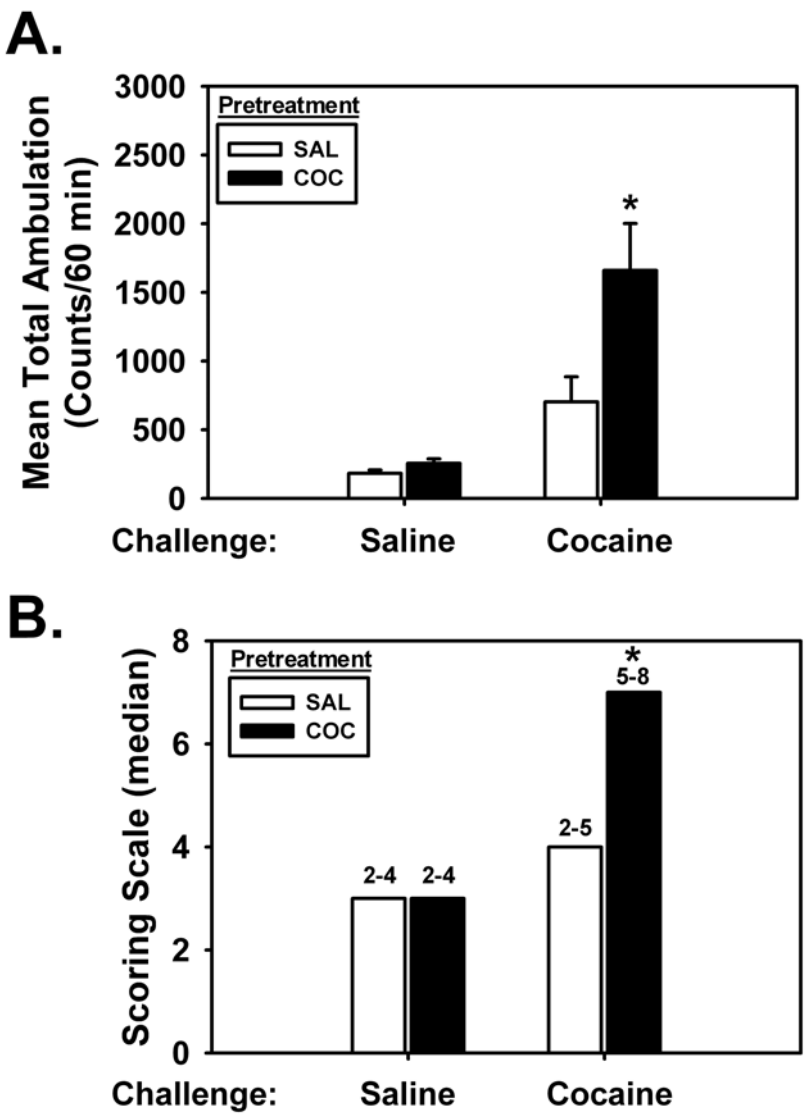

Figure 4.4. Sensitization to repeate intermittent cocaine administration. [A] Rats were treated for 7 days (twice/day) with saline (open bars; n=8 rats) or cocaine (filled bars; n=7 rats) and challenged on day 9 with saline (1ml/kg IP) and on day 10 with cocaine (15 mg/kg IP). Ambulation is presented as mean total number of counts (± SEM) (*$p < 0.05$ vs SC). [B] Behavior was rated once after a 15 sec observation period at 15 min after the challenge injection of saline or cocaine (15 mg/kg IP). Behavioral rating scores are depicted as medians for rats repeatedly treated with either cocaine (15 mg/kg; n = 8; filled bars) or saline (1 ml/kg; n = 8; open bars). (* $p < 0.05$ vs SC).

Neuroadaptations of the 5-HT_{2C}R and its intracellular signaling molecules associated with cocaine administration

Our objective was to identify the molecular neuroadaptations of the 5-HT_{2C}R and intracellular signaling pathways associated with this receptor in the cortical circuitry that may contribute to the reduced sensitivity of the 5-HT_{2C}R observed after intermittent repeated cocaine administration. To determine such adaptations, 5-HT_{2C}R (46 kDa), p42-MAPK (42 kDa), p44-MAPK (44 kDa), phospho-p42-MAPK, phospho-p44-MAPK and PSD-95 (95 kDa), molecules associated with 5-HT_{2C}R desensitization and resensitization processes (including membrane trafficking), were measured at day 3 of withdrawal from an intermittent repeated exposure to cocaine (15 mg/kg/twice a day, 7 days, IP) (Cunningham and Callahan, 1994). The treatment regimen and withdrawal interval were chosen to be consistent with previous work from this laboratory (Cunningham et al., 1992a; Cunningham et al., 1992b; De La Garza and Cunningham, 2000). Since one focus of this project was to investigate phosphorylation of p44/p42-MAPK, animals were sacrificed 15 min after the challenge injection of cocaine or saline at day 3 of withdrawal. This time-point was decided according to previous studies performed on cocaine-induced activation of p44/p42-MAPK (Valjent et al., 2000; Valjent et al., 2004b; Mattson et al., 2005).

For the synaptosomal fractionation protocol, tissue was pooled (n = 3-4 samples/per pool; there were at least 3 pooled samples per treatment) to provide sufficient tissue for ultimate analysis of the PSD-enriched fraction. We fractionated the original protein homogenate into synaptosomal and PSD

compartments by sucrose gradient and serial centrifugations (Phillips et al., 2001; Moron and Devi, 2007). Expression of PSD-95 (a PSD marker), syntaxin (a synaptosomal marker) and SNAP-25 (a presynaptic active zone marker) were used to assess the purity of the fractions (Chapter 2, Fig. 2.1). PSD-95, one of the major postsynaptic density proteins, is also involved in the scaffolding of membrane-bound receptors, such as 5-HT_{2C}R (Parker et al., 2003; Becamel et al., 2004; Gavarini et al., 2004; Gavarini et al., 2006), which makes it relevant to our studies.

The present chapter was subdivided in three sections (Sections I-III) according to the three proposed preplanned comparisons (see Material and Methods). Section I addressed the neuroadaptations associated with acute cocaine administration (SS vs SC). Section II addressed the neuroadaptations associated with repeated intermittent cocaine exposure after a short-term of withdrawal (3 days; SS vs CS). Finally, Section III addressed the effects of repeated intermittent cocaine exposure (cocaine sensitization regimen) on cocaine exposure following a short-term withdrawal period (3 days; SC vs CC).

<u>Section I</u>: Neuroadaptations of the 5-HT_{2C}R and its intracellular signaling molecules associated with acute cocaine administration

The molecular changes seen in motor cortex and PFC associated with a single administration of cocaine are presented here to allow comparison with changes observed with repeated cocaine administration (**Section III**).

5-HT$_{2C}$R protein expression and subcellular localization after acute cocaine administration

Motor cortex: Acute challenge with cocaine (15 mg/kg) at 3 days following repeated intermittent saline administration did not alter 5-HT$_{2C}$R protein expression in total homogenate of motor cortex (DF = 20, t = 1.29, p = 0.2123). However changes in the face of a lack of 5-HT$_{2C}$R protein expression in the total homogenate, a redistribution of 5-HT$_{2C}$R into any other subcellular compartment could occur. Hence we evaluated 5-HT$_{2C}$R protein expression in the PSD. A challenge injection of cocaine did not alter 5-HT$_{2C}$R protein expression in the PSD of motor cortex suggesting the 5-HT$_{2C}$R did not differentially redistribute to this subcellular compartment (DF = 20, t = -0.55, p = 0.5873) (**Table 4.2**).

Prefrontal cortex: Similarly, acute cocaine challenge (15 mg/kg) at 3 days following repeated intermittent saline administration did not alter either 5-HT$_{2C}$R protein expression in total homogenate (DF = 19, t = 0.89, p = 0.4003) or in the PSD-enriched fraction (DF = 20, t = 0.41, p = 0.6832) (**Table 4.2**).

Together, these results suggest that acute injection of cocaine is not sufficient to produce a change in protein expression or subcellular localization at the PSD in motor cortex and PFC under the current conditions. To assess whether there was a direct correlation between the protein expression of the 5-HT$_{2C}$R and the ambulatory counts observed for the saline-pretreated animals (basal levels of ambulation), we plotted the Day 7 over Day 1 of ambulatory

counts (Day 7 / Day 1 Ratio) vs. 5-HT_{2C}R protein expression (**Fig. 4.5**) (Boudreau and Wolf, 2005; Boudreau et al., 2007).

Table 4.2. Neuroadaptations associated with acute effects of cocaine (15 mg/kg) [SS vs SC groups]

Proteins detected	**Fraction**	**Motor cortex** (*p values*)	**PFC** (*p values*)
5-HT_{2C}R	Total homogenate	**NC** (0.2123)	**NC** (0.4003)
	PSD-enriched	**NC** (0.5873)	**NC** (0.6832)
PSD-95	Total homogenate	**NC** (0.3477)	**NC** (0.7397)
	Synaptosomes	⇑ (0.0369)	**NC** (0.1249)
	PSD-enriched	⇑ (0.0612)	**NC** (0.3855)
p42-MAPK	Total homogenate	**NC** (0.5538)	⇓ (0.0509)
	Synaptosomes	**NC** (0.7895)	**NC** (0.8713)
	PSD-enriched	⇑ (0.0370)	**NC** (0.9793)
Phospho p42-MAPK	Total homogenate	**NC** (0.5084)	**NC** (0.6628)
	Synaptosomes	**NC** (0.4711)	**NC** (0.5618)
	PSD-enriched	**NC** (0.4102)	**NC** (0.5320)
p42-MAPK ratio	Total homogenate	**NC** (0.5592)	**NC** (0.6922)
	Synaptosomes	**NC** (0.7088)	**NC** (0.2583)
	PSD-enriched	⇓ (0.0091)	**NC** (0.7396)
p44-MAPK	Total homogenate	**NC** (0.8545)	**NC** (0.7998)
	Synaptosomes	**NC** (0.6541)	**NC** (0.1402)
	PSD-enriched	**NC** (0.3814)	**NC** (0.9584)

Red arrow: statistically significant decrease
Green arrow: statistically significant increase
NC: no change

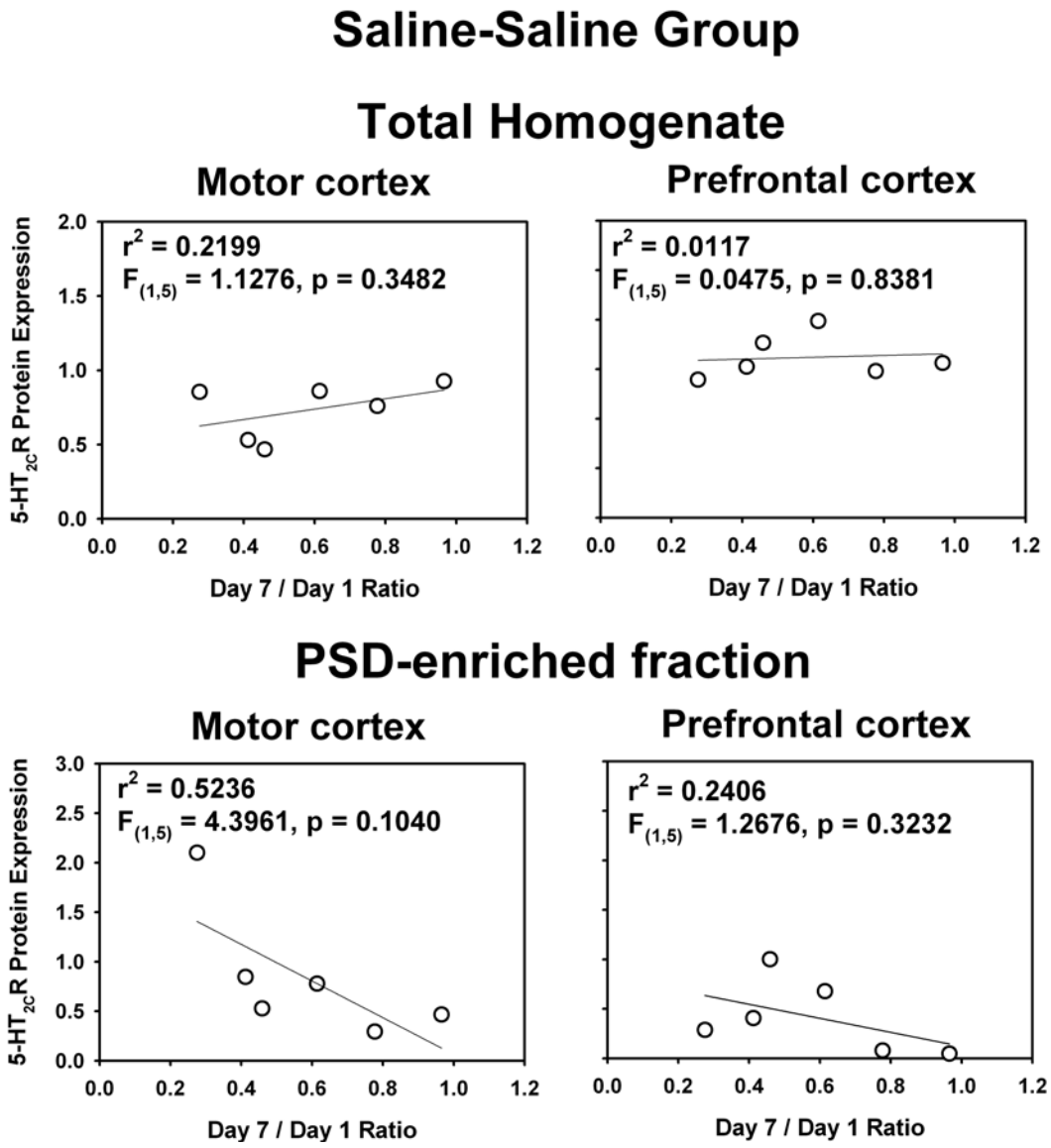

Figure 4.5. Correlation between behavior and 5-HT_{2C}R protein expression in total homogenate and PSD-enriched fraction motor cortex and PFC. Rats were treated twice for 7 days with saline and challenged on day 10 with saline (SS; 1ml/kg IP). Protein expression was normalized to actin. Protein samples were run in duplicates and the average protein expression was plotted against the ratio of Day 7 to Day 1 of ambulation.

Fig. 4.5 suggests that ambulatory counts correlates better with 5-HT_{2C}R protein expression in the PSD-enriched fraction than with total 5-HT_{2C}R protein content (without reaching statistical significance) suggesting that the basal levels

of ambulatory activity could arise from postsynaptic localization of the receptor. No correlations between 5-HT_{2C}R protein expression to Day 7 / Day 1 Ratio following acute cocaine challenge were observed in total homogenate and PSD-enriched fractions from either motor cortex or PFC (data not shown).

PSD-95 protein expression and subcellular localization after acute cocaine administration

Motor cortex: **Fig. 4.6** shows the effects of acute cocaine on PSD-95 protein expression and distribution after cocaine challenge (15 mg/kg) or saline. An acute challenge injection of cocaine (15 mg/kg) at 3 days following repeated intermittent saline administration was not associated with altered PSD-95 expression in total homogenate (DF = 36, t = -0.95, *p* = 0.3477; **Fig. 4.6A**). A challenge injection of cocaine promoted a statistically significant increase in PSD-95 localization to the synaptosomal compartment (DF = 36, t = 2.17, *p* = 0.0369; **Fig. 4.6B**) and a trend towards increased PSD-95 protein expression at the PSD (DF = 20, t = 1.54, *p* = 0.0612; **Fig. 4.6C**). The fact that we observed no changes in PSD-95 expression in total homogenate with an increase in the expression of PSD-95 at the synapse suggested redistribution of this scaffolding protein to these compartments in response to acute cocaine challenge.

Prefrontal cortex: An acute challenge injection of cocaine (15 mg/kg) at 3 days following repeated intermittent saline administration did not alter PSD-95 expression in total homogenate (DF = 32, t = -0.34, *p* = 0.7397; **Fig. 4.6A**).

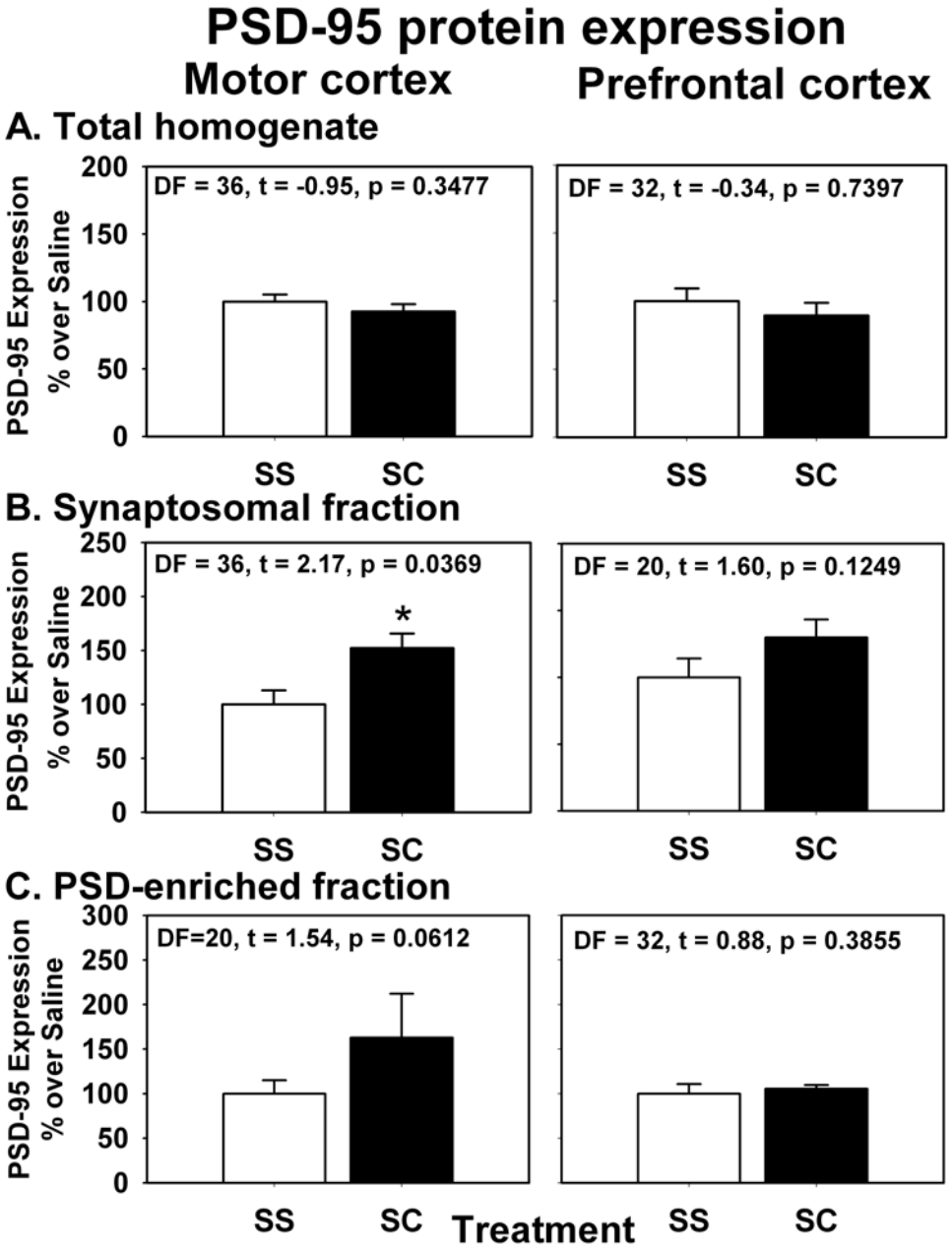

Figure 4.6. PSD-95 protein expression and subcellular localization in motor cortex and PFC following acute cocaine administration. Rats were treated twice a day for 7 days with saline and challenged on day 10 with saline (SS) or cocaine (SC). Western blot data was normalized to actin and plotted relative to SS group. Graphs presented are of experiments that were repeated 2-5 times for each antibody. Results are expressed as mean ± SEM.

A trend towards an increase in PSD-95 localization to the synaptosomal compartment (DF = 20, t = 1.06, *p* = 0.1249; **Fig. 4.6B**) was observed after an acute cocaine injection, without an alteration in PSD-95 expression at the PSD-enriched fraction (DF = 32, t = 0.88, *p* = 0.3855; **Fig. 4.6C**). No changes in PSD-95 protein expression in total homogenate combined with a change in PSD-95 in the synaptosomal or PSD compartments would suggest protein redistribution. The fact that we observed a trend towards an increase in PSD-95 in the synaptosomal with no changes in the PSD fraction suggests that PSD-95 is being redistributed to extra-synaptic compartments.

The fact that we observed this differential distribution of PSD-95 among subcellular compartments between motor cortex and PFC following acute cocaine administration suggests that the effects of cocaine on PSD-95 are brain-area dependent.

p44/p42-MAPK protein expression, subcellular localization and protein phosphorylation after acute cocaine administration

Motor cortex: Acutes effect of cocaine on p42-MAPK protein expression and distribution 15-20 min after the challenge injection of cocaine (15 mg/kg) or saline are summarized in **Table 4.2**. An acute cocaine challenge (15 mg/kg) did not alter p42-MAPK protein expression in total homogenate (DF = 36, t = -0.14, *p* = 0.5538, **Fig. 4.7A**). A challenge injection of cocaine did not alter p42-MAPK protein expression in the synaptosomes (DF = 36, t = -0.27, *p* = 0.7895, **Fig. 4.7B**).

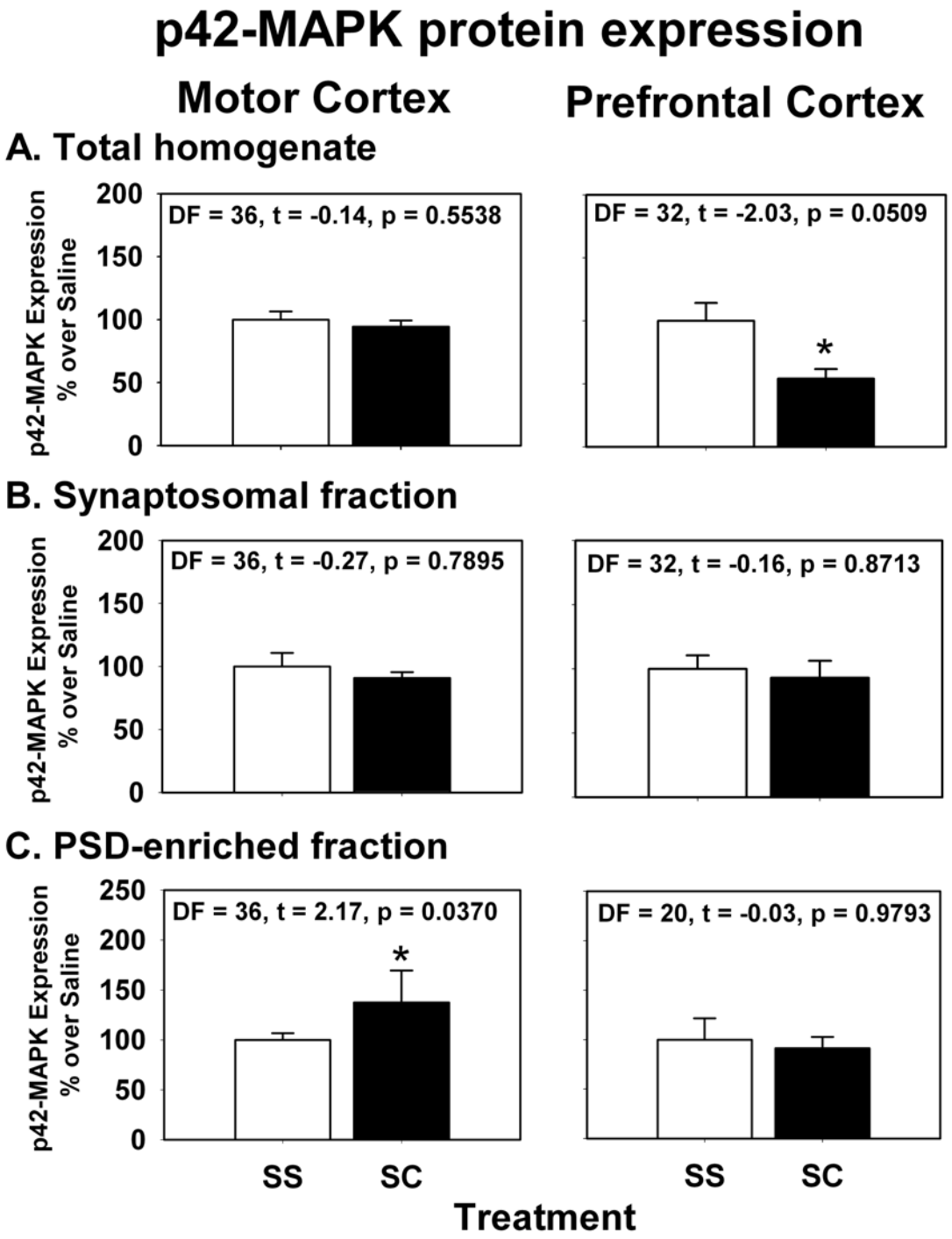

Figure 4.7. p42-MAPK protein expression in motor cortex and PFC following acute cocaine administration. Rats were treated twice for 7 days with saline and challenged on day 10 with saline (SS) or cocaine (SC). Western blot data was normalized to actin and plotted relative to SS group. Graphs presented are of experiments that were repeated 2-5 times for each antibody. Results are expressed as mean ± SEM.

An increase in p42-MAPK was observed in the PSD-enriched fraction following cocaine challenge (DF = 36, t = 2.17, *p* = 0.0370; **Fig. 4.7C**), suggesting that p42-MAPK in the motor cortex is responsive to the acute effects of cocaine. Since we did not observe changes in distribution of p42-MAPK to the synaptosomal compartment the observed increase in p42-MAPK in the PSD suggests that the p42-MAPK that was already stored in the synaptosome was translocated to the PSD.

Phosphorylation of p42-MAPK was unchanged following an acute injection of cocaine in total homogenate, synaptosomal and PSD-enriched fractions. When phospho-p42-MAPK to total p42-MAPK ratio was calculated (p42-MAPK ratio), a decrease in this ratio was observed only in the PSD-enriched fraction (DF = 19, t = -2.91, *p* = 0.0091; **Fig. 4.8**) suggesting that activated p42-MAPK might be replaced by inactive p42-MAPK. Finally, we observed no statistically significant changes in p44-MAPK protein expression (total homogenate) or distribution (synaptosomal and PSD-enriched fraction) (**Table 4.2**), suggesting that p42-MAPK is more susceptible to the acute effects of cocaine in the motor cortex than is p44-MAPK.

Prefrontal cortex: An acute cocaine challenge (15 mg/kg) produced an unexpected reduction in p42-MAPK protein expression in total homogenate (DF = 32, t = -2.03, *p* = 0.0509), suggesting a rapid degradation of this kinase in this brain area (**Fig. 4.7A**). A challenge injection of cocaine did not alter either the distribution of p42-MAPK to the synaptosomal (DF = 32, t = -0.16, *p* = 0.8713) or

PSD-enriched fractions (DF = 20, t = -0.03, *p* = 0.9793) (**Fig. 4.7B-C**). A decrease in p42-MAPK protein expression in total homogenate coupled with no changes in protein distribution to the synaptosomal or the PSD compartments suggests that other subcellular compartments might be depleted of p42-MAPK.

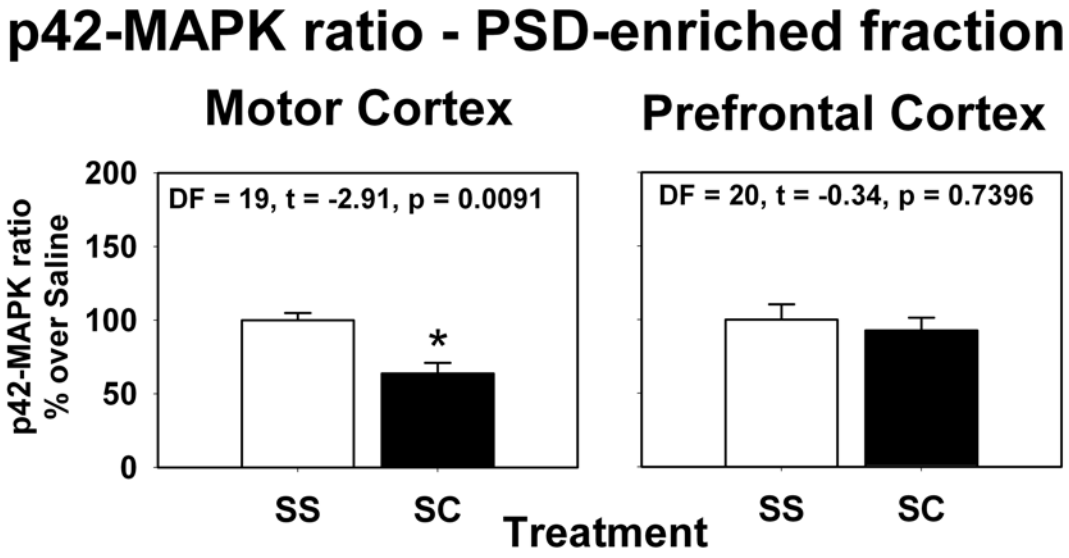

Figure 4.8. p42-MAPK ratio in PSD-enriched fraction in motor cortex and PFC following acute cocaine administration. Rats were treated twice for 7 days with saline and challenged on day 10 with saline (SS) or cocaine (SC). Western blot data was normalized to actin and plotted relative to SS group. Graphs presented are of experiments that were repeated 2-5 times for each antibody. Results are expressed as mean ± SEM.

Table 4.2 shows that phosphorylation of p42-MAPK and the p42-MAPK ratio (**Fig. 4.8**) remained unchanged following an acute injection of cocaine in total homogenate, synaptosomal and PSD-enriched tractions. Finally, we observed no statistically significant changes in p44-MAPK protein expression

(total homogenate) or distribution (synaptosomal and PSD-enriched fraction) (**Table 4.2**).

In summary, these results suggest that an acute injection of cocaine is not sufficient to produce a change in 5-HT_{2C}R protein expression (total homogenate) or distribution (synaptosomal and PSD compartments) either motor cortex or PFC. Furthermore, a trend towards a correlation between 5-HT_{2C}R protein expression and ambulation (Day 7 / Day 1 Ratio) was observed at the PSD-enriched fraction in motor cortex but not in PFC, suggesting that the basal levels of ambulatory activity could arise from postsynaptic localization of the receptor in motor cortex. Furthermore, acute cocaine challenge increased the distribution of PSD-95 to the synaptosomal and PSD fractions in motor cortex. In contrast, in the PFC, only a trend towards increased PSD-95 expression was observed in the synaptosomal compartment with no changes in the PSD-enriched subfraction, suggesting that the effects of cocaine on PSD-95 are brain-area dependent. Finally**,** p42-MAPK was redistributed to the PSD compartment in motor cortex but downregulated in the PFC.

<u>Section II</u>: Neuroadaptations of the 5-HT_{2C}R and its intracellular signaling molecules that contribute to reduced 5-HT_{2C}R sensitivity during withdrawal from repeated intermittent exposure to cocaine

Exposure to repeated cocaine administration is associated with a loss of functional influence of the 5-HT_{2C}R (Filip et al., 2004). One possible explanation for this loss of influence is reduced expression of 5-HT_{2C}R after cocaine pretreatment. To test the hypothesis that repeated intermittent cocaine is

associated with decrease in the overall expression of 5-HT_{2C}R protein, we performed Western blots on total protein homogenates from motor cortex and PFC (**Fig. 4.9**).

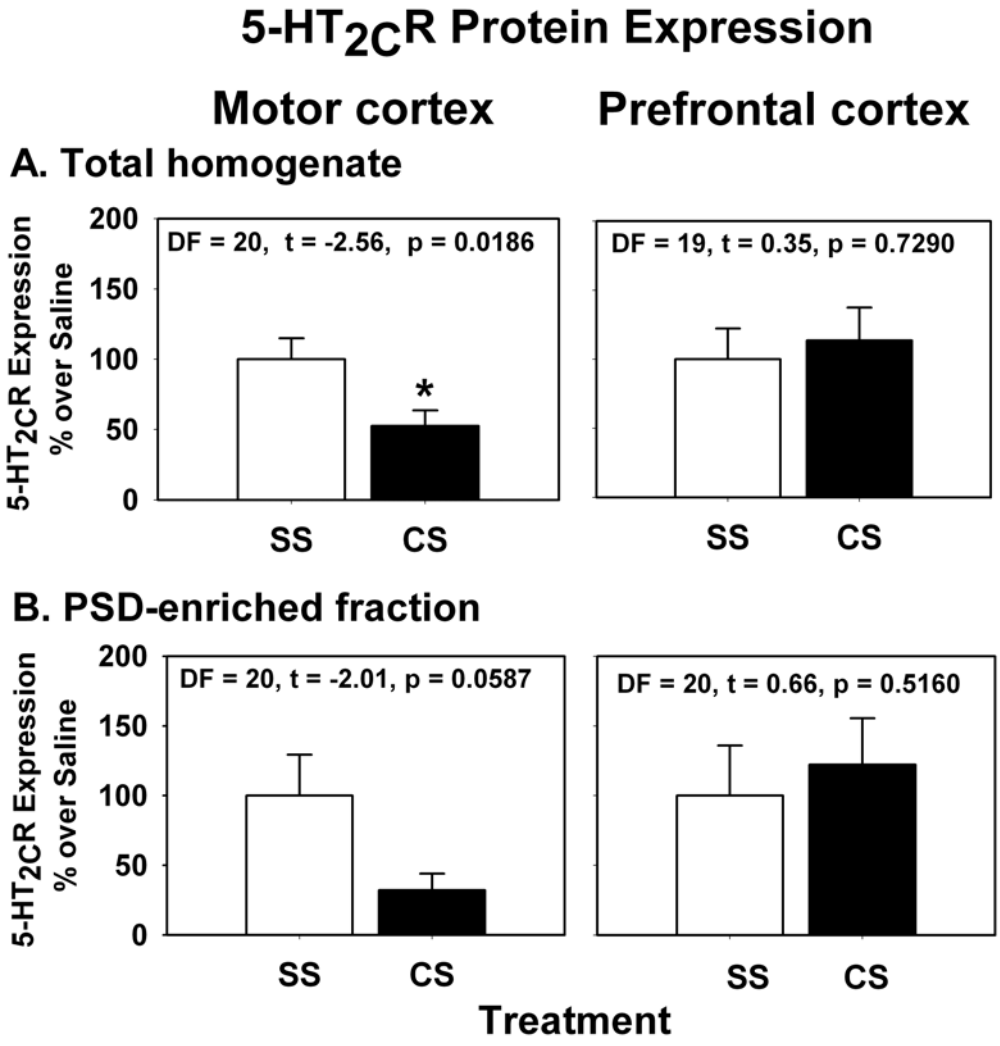

Figure 4.9. 5-HT_{2C}R protein expression and subcellular localization in motor cortex and PFC following repeated intermittent cocaine administration. Rats were treated twice for 7 days with saline or cocaine and challenged on day 10 with saline (SS (n=6) and CS (n=5); 1ml/kg IP). Western blot data was normalized to actin and plotted relative to SS group. Graphs represent an experiment that was repeated twice for each antibody. Results are expressed as mean ± SEM.

Motor cortex: A statistically significant reduction in 5-HT_{2C}R protein expression was observed in total homogenate at day 3 of withdrawal from a repeated intermittent cocaine administration (CS; t value = -2.59, DF = 20, *p* = 0.0186; **Fig. 4.9A**). The protein expression of 5-HT_{2C}R in the PSD-enriched fraction was also examined since previous studies have suggested a postsynaptic localization of the 5-HT_{2C}R. Pretreatment with cocaine tended to reduced 5-HT_{2C}R in the PSD compartment (t value = -2.01, DF = 20, *p* = 0.0587; **Fig. 4.9B**), a result that might be associated with the general decrese in protein expression of the receptor (**Fig. 4.9A**).

Prefrontal cortex: No statistically significant differences between SS and CS groups in total homogenate were observed at day 3 of withdrawal from repeated intermittent cocaine administration (t value = 0.35, DF = 19, *p* = 0.7290; **Fig. 4.9A**). Our results did not rule out the possibility of a differential distribution of the 5-HT_{2C}R among subcellular compartments without alteration of total protein expression (*e.g.,* internalization of the receptor from the membrane to intracellular compartments). Thus, we tested the hypothesis that intermittent repeated cocaine exposure promoted changes in subcellular localization of the 5-HT_{2C}R protein when compared to saline-treated animals in the PFC. Pretreatment with cocaine did not alter 5-HT_{2C}R distribution out of the PSD (**Fig. 4.9B**), suggesting that other molecular adaptations are involved in the functional 5-HT_{2C}R loss observed following repeated cocaine exposure.

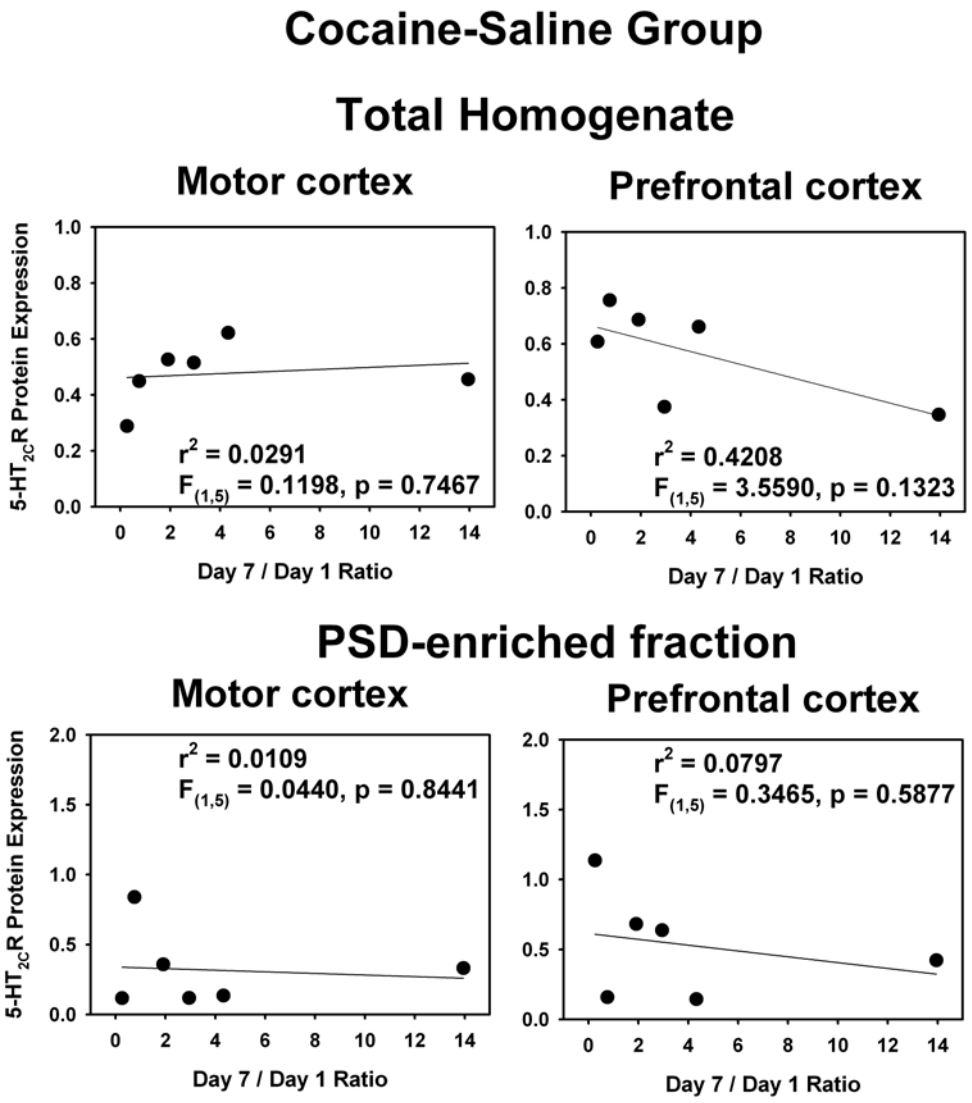

Figure 4.10. Correlation between 5-HT$_{2C}$R protein expression motor cortex and PFC with ambulation following repeated intermittent cocaine administration. Rats were treated twice for 7 days with saline or cocaine and challenged on day 10 with saline (SS and CS; 1ml/kg IP). 5-HT$_{2C}$R protein expression was plotted against the ratio of day 7 and day 1 of ambulation (ambulation). In all instances, results are expressed as mean ± SEM.

To assess whether the decrese in the expression of the 5-HT$_{2C}$R observed in motor cortex correlates with an increase in ambulation, we plotted 5-HT$_{2C}$R protein expression vs. Day 7 / Day 1 Ratio of rats that received repeated intermittent cocaine (CS group). **Fig. 4.10** shows no correlation between the

decrease in protein expression of the 5-HT_{2C}R in total homogenate or in the PSD-enriched fraction of motor cortex and ambulation. Furthermore, no correlation between protein expression of the 5-HT_{2C}R in total homogenate or in the PSD-enriched fraction of PFC and ambulation was observed.

Protein expression levels and protein phosphorylation of 5-HT_{2C}R downstream elements after repeated intermittent cocaine administration

Another mechanism by which the responsiveness of the 5-HT_{2C}R may be reduced is via alterations in the expression of binding partners associated with 5-HT_{2C}R desensitization and resensitization processes. PSD-95, one of the major PSD proteins, belongs to the family of membrane-associated guanylate kinase (MAGUK) scaffolding proteins (Hunt et al., 1996; El-Husseini et al., 2000; El-Husseini et al., 2002; Gavarini et al., 2006; Ehrlich et al., 2007). PSD-95 is a cytoplasmic protein that contains 3 repeated PDZ domains important for protein-protein interaction (Hunt et al., 1996; Parker et al., 2003). At the synapse, PSD-95 is found associated with receptors and cytoskeletal elements, and it has been implicated in synaptic plasticity and maturation of excitatory synapses (El-Husseini et al., 2000; El-Husseini et al., 2002; Ehrlich et al., 2007). *In vitro* studies showed that PSD-95 recognizes PDZ domains located at the C-terminal of the 5-HT_{2C}R, and that this interaction promotes constitutive and agonist-induced internalization and trafficking of the receptor (Becamel et al., 2004; Gavarini et al., 2006). Deletion of the 3 amino acids at the C-terminus of the 5-HT_{2C}R, which includes the PDZ-domain, delayed resensitization of 5-HT_{2C}R (Backstrom et al., 2000). This result suggests that interaction of the 5-HT_{2C}R with

its PDZ-binding partners is important for the receptor desensitization and resensitization processes. Thus, a dysregulation of PSD-95 expression might be a component that contributes to the reduced responsiveness of the 5-HT_{2C}R.

One important pathway that is activated by 5-HT_{2C}R downstream elements as well as by the DA neurotransmitter system is the p44/p42-MAPK pathway, as previously noted (Werry et al, 2005; Brown and Gerfen, 2006). p44/p42-MAPK regulates some components of the seven transmembrane receptor regulatory apparatus, such as GRKs and β-arrestins, and both of these molecules have been previously associated with protein trafficking and receptor internalization which are part of the desensitization / resensitization process (Pitcher et al., 1999; Elorza et al., 2003; Werry et al., 2005). *In vitro* studies have shown that phosphorylation of the 5-HT_{2C}R by GRK2 at two serine residues interrupts the interaction between the receptor and other intracellular binding proteins, affecting the rate of resensitization (Gavarini et al., 2004; Melikian, 2004). Therefore, activation of the p44/p42-MAPK pathway via serotonergic or dopaminergic routes could produce changes in the abundance of phospho-p44/p42-MAPK (active form of p44/p42-MAPK), which in turn could regulate 5-HT_{2C}R turnover.

PSD-95 protein expression and subcellular localization after repeated cocaine administration

Motor cortex: The effects of intermittent repeated cocaine exposure on PSD-95 protein expression (total homogenate) and subcellular localization (synaptosomal

and PSD-enriched fractions) are shown in **Table 4.3** and **Fig. 4.11**. **Table 4.3** demonstrates the effects of repeated intermittent cocaine administration on PSD-95 protein expression and distribution after the challenge injection of saline. Repeated intermittent cocaine administration did not alter PSD-95 expression in total homogenate (DF = 32, t = -0.57, p = 0.5704) and did not induce PSD-95 distribution to the synaptosomal compartment (DF = 36, t = -1.07, p = 0.2937). However, a trend towards an increase in PSD-95 at the PSD-enriched fraction was observed following repeated intermittent cocaine administration (DF = 20, t = 1.96, p = 0.0587), suggesting that redistribution of PSD-95 occurred within the synapse in motor cortex.

Prefrontal cortex: The effects of intermittent repeated cocaine exposure on PSD-95 protein expression (total homogenate) and subcellular localization (synaptosomal and PSD-enriched fractions) are shown in **Table 4.3** and **Fig. 4.11**. Repeated intermittent cocaine administration did not alter PSD-95 expression in total homogenate (DF = 32, t = -0.03, p = 0.9787). A trend towards an increase in PSD-95 expression was observed at the synaptosomal (DF = 20, t = 1.55, p = 0.1387) but not at the PSD-enriched compartments (DF = 32, t = 0.21, p = 0.8352), suggesting that PSD-95 is being distributed to extra-synaptic compartments rather than to the PSD.

Our observations of differential distribution of PSD-95 among subcellular compartments following repeated cocaine administration in motor cortex and PFC suggest that the effects of cocaine on PSD-95 are brain-area dependent.

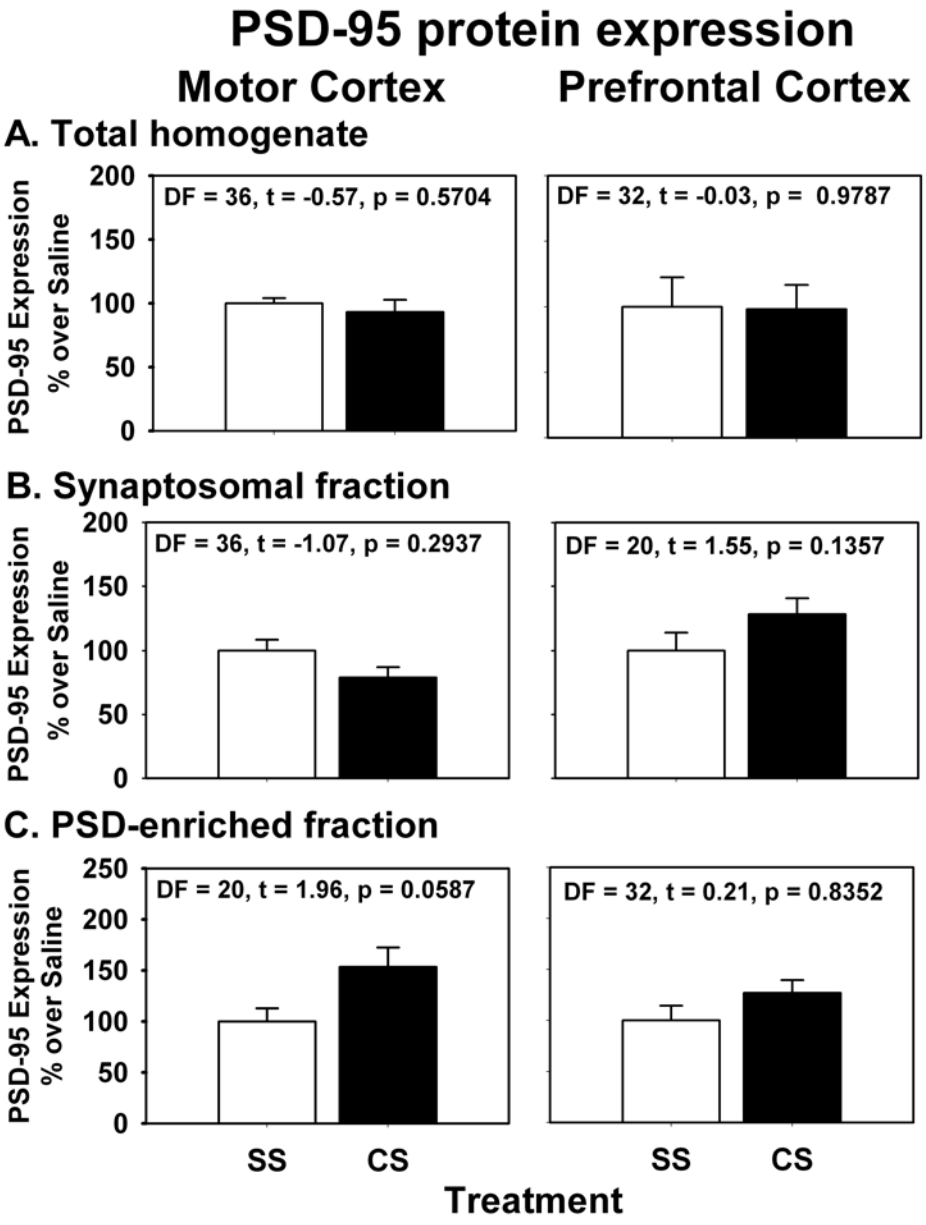

Figure 4.11. PSD-95 protein expression and subcellular localization in motor cortex and PFC following repeated cocaine administration. Rats were treated twice a day for 7 days with saline and challenged on day 10 with saline or cocaine (SS and SC). Western blot data was normalized to actin and plotted relative to saline-pretreated rats. Representative graphs from an experiment that was repeated 2-5 times for each antibody. Results are expressed as mean ± SEM.

Table 4.3. Neuroadaptations associated with repeated intermittent cocaine (15 mg/kg) administration [SS vs CS groups]

Proteins detected	**Fraction**	**Motor cortex** *(p values)*	**PFC** *(p values)*
5-HT_{2C}R	Total homogenate	⇓ (0.0186)	**NC** (0.6832)
	PSD-enriched	⇓ (0.0587)	**NC** (0.4209)
PSD-95	Total homogenate	**NC** (0.3840)	**NC** (0.7397)
	Synaptosomes	**NC** (0.2937)	**NC** (0.1357)
	PSD-enriched	⇑ (0.0587)	**NC** (0.8352)
p42-MAPK	Total homogenate	**NC** (0.8878)	**NC** (0.3633)
	Synaptosomes	**NC** (0.8559)	⇓ (0.0511)
	PSD-enriched	**NC** (0.9705)	⇓ (0.0862)
Phospho p42-MAPK	Total homogenate	**NC** (0.4642)	**NC** (0.1284)
	Synaptosomes	**NC** (0.9568)	**NC** (0.9093)
	PSD-enriched	**NC** (0.6130)	**NC** (0.5515)
p42-MAPK ratio	Total homogenate	**NC** (0.7253)	**NC** (0.2029)
	Synaptosomes	**NC** (0.3477)	**NC** (0.6545)
	PSD-enriched	**NC** (0.1969)	**NC** (0.1228)
p44-MAPK	Total homogenate	**NC** (0.6541)	**NC** (0.9818)
	Synaptosomes	⇑ (0.0310)	⇓ (0.0194)
	PSD-enriched	**NC** (0.2778)	**NC** (0.7263)

Red arrow: statistically significant decrease
Green arrow: statistically significant increase
NC: no change

p44/p42-MAPK protein expression, subcellular localization and protein phosphorylation after repeated cocaine administration

Motor cortex: **Table 4.3** shows a summary of the repeated intermittent effects of cocaine on p42-MAPK protein expression and distribution 15-20 min after the challenge injection of saline. Repeated intermittent cocaine administration altered neither p42-MAPK protein expression in total homogenate (DF = 36, t = -0.14, *p* = 0.8878; **Fig. 4.12A**) nor p42-MAPK distribution to synaptosomal (DF = 36, t = -0.18, *p* = 0.8559) or PSD compartments (DF = 36, t = -0.04, *p* = 0.9705).

Prefrontal cortex: **Fig. 4.12** and **Table 4.3** shows the effects of repeated intermittent cocaine exposure on p42-MAPK protein expression and phosphorylation in total homogenate, synaptosomal and PSD-enriched fractions in PFC. Repeated intermittent cocaine administration did not alter p42-MAPK protein expression in total homogenate (DF = 32, t = -0.93, *p* = 0.3633). A decrease in distribution of p42-MAPK was observed in the synaptosomal compartment (DF = 32, t = -2.03, *p* = 0.0511; **Fig. 4.12B**) with a trend towards decreased p42-MAPK at the PSD (DF = 20, t = -1.80, *p* = 0.0862: **Fig. 4.12C**), suggesting that postsynaptic p42-MAPK in the PFC is more susceptible to the effects of repeated intermittent cocaine administration.

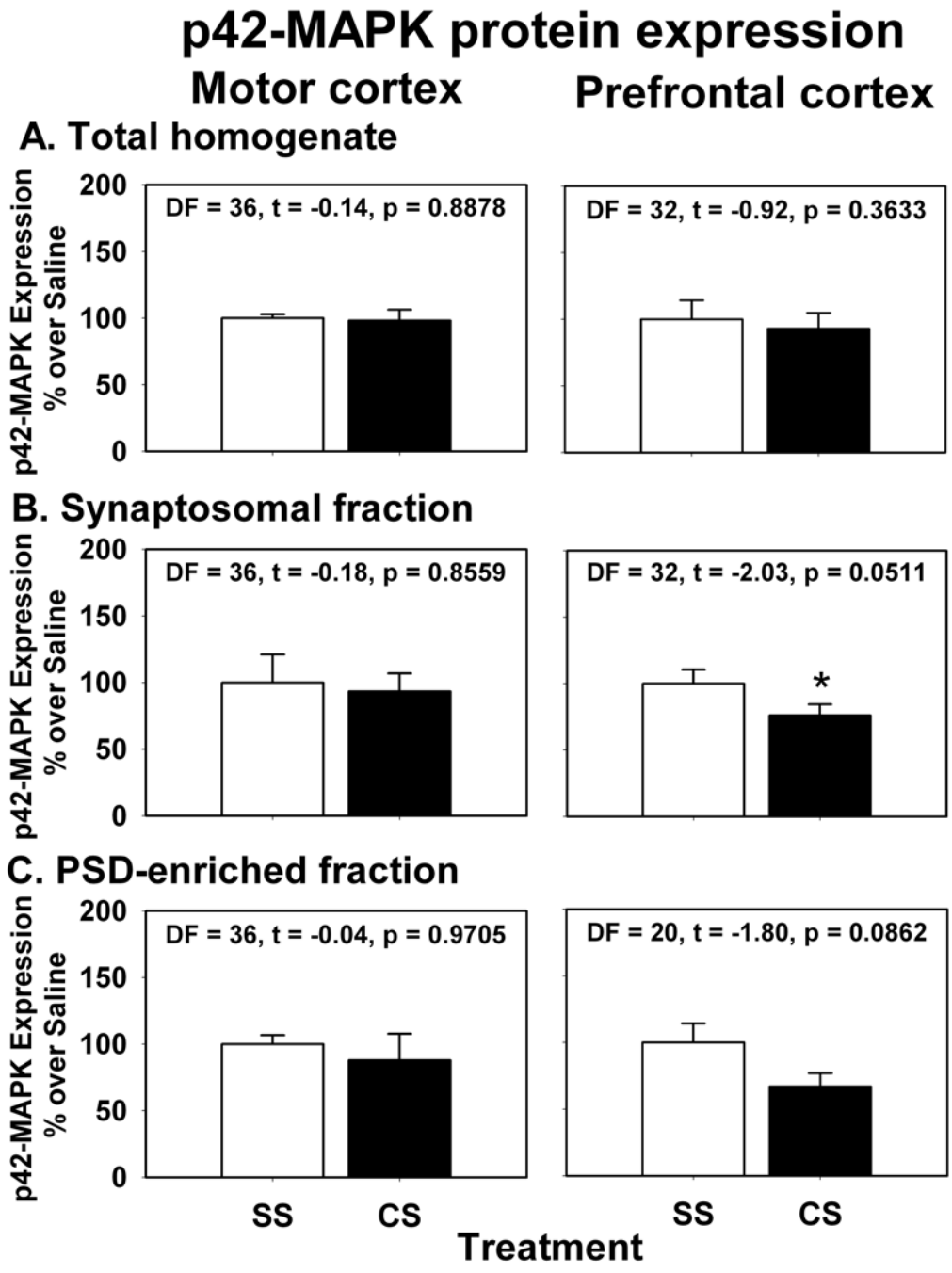

Figure 4.12. p42-MAPK protein expression and subcellular localization in motor cortex and PFC following repeated cocaine administration. Rats were treated twice for 7 days with saline or cocaine and challenged on day 10 with saline (SS and CS; 1ml/kg IP). Western blot data was normalized to actin and plotted relative to SS group. Graphs represent an experiment that was repeated 2-5 times for each antibody. Results are expressed as mean ± SEM.

Table 4.3 shows that phosphorylation of p42-MAPK protein remains unchanged following repeated cocaine administration in total homogenate, synaptosomal and PSD-enriched tractions in both brain areas. When phospho-p42-MAPK to total p42-MAPK ratio was calculated (p42-MAPK ratio), no statistically significant changes were observed in motor cortex and PFC. A statistically significant increase and decrease in p44-MAPK protein expression was observed in the synaptosomal fraction in motor cortex and PFC, respectively following repeated intermittent cocaine administration (**Fig. 4.13**).

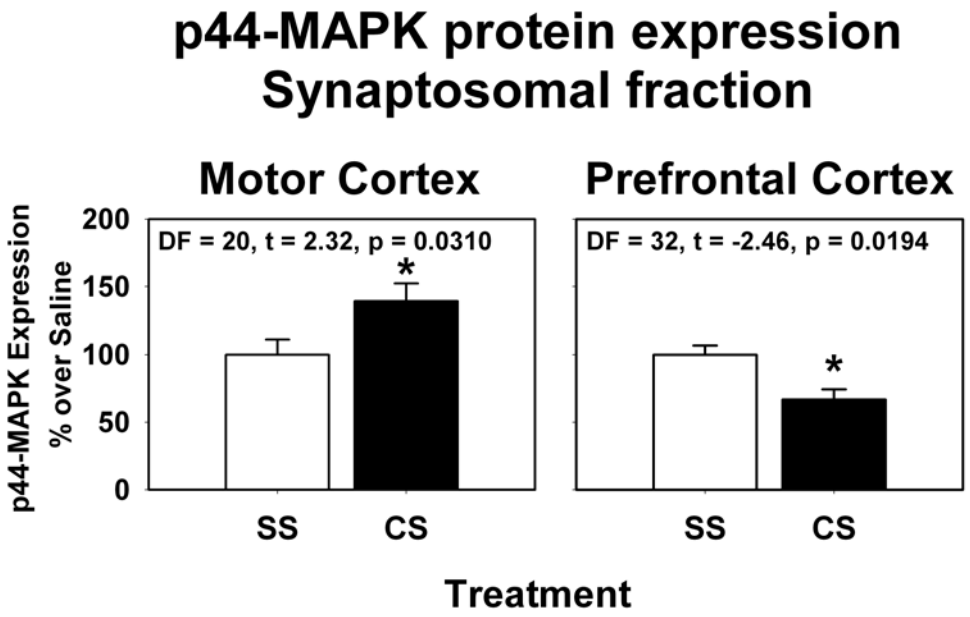

Figure 4.13. p44-MAPK protein expression in synaptosomal fraction in motor cortex and PFC following repeated intermittent cocaine administration. Rats were treated twice for 7 days with saline or cocaine and challenged on day 10 with saline (SS and CS; 1ml/kg IP). Western blot data was normalized to actin and plotted relative to SS group. Graphs represent an experiment that was repeated 2-5 times for each antibody. Results are expressed as mean ± SEM.

In summary, we observed a decrease in 5-HT_{2C}R protein expression in both total homogenate and PSD fraction following repeated intermittent cocaine administration. However, no changes in total expression or distribution were observed in the PFC, suggesting a brain-area dependent response to repeated intermittent cocaine administration. Repeated intermittent cocaine administration also produced a brain-area dependent redistribution of PSD-95 among subcellular compartments. For example, we observed a trend towards an increase in PSD-95 at the PSD in motor cortex, whereas a trend towards an increase in PSD-95 expression was observed at the synaptosomal fraction in the PFC. Finally, we did not observe any changes p42-MAPK protein expression (total homogenate) or distribution (synaptosomal and PSD fraction) in motor cortex whereas a reduction in p42-MAPK was observed in the synaptosomal and PSD compartments in the PFC with no changes in total protein expression.

Total mRNA expression and RNA editing of the 5-HT_{2C}R mRNA following short-term withdrawal after repeated intermittent cocaine administration

Motor cortex: A non-parametric Wilcoxon two-sample test comparing cocaine and saline pretreated groups revealed no significant differences in 5-HT_{2C}R mRNA expression after repeated intermittent cocaine administration (DF = 10, t = 1.1240, p = 0.2891; **Fig. 4.14**). Studies correlating 5-HT_{2C}R mRNA expression and the measurements of Day 7 / Day 1 Ratio (**Fig. 4.15**) revealed a direct relationship between the ratio of ambulation and ΔCt values obtained for 5-HT_{2C}R mRNA of saline-treated animals. As the Day 7 / Day 1 Ratio increases (higher ambulation), the delta Ct value increases (lower amount of mRNA of

5-HT_{2C}R) in motor cortex, suggesting that the basal levels of ambulatory counts correlates with lower levels of 5-HT_{2C}R mRNA expression.

Prefrontal cortex: A non-parametric Wilcoxon two-sample test comparing cocaine and saline pretreated groups revealed a trend towards a reduction in 5-HT_{2C}R mRNA following repeated intermittent cocaine regimen (DF = 10, t = 2.4381, p = 0.1184; **Fig. 4.14**). Most interestingly and unexpectedly, we observed an inverse correlation between the Day 7 / Day 1 Ratio and ΔCt values obtained for 5-HT_{2C}R mRNA in the PFC (**Fig. 4.15**). As the Day 7 / Day 1 Ratio increases (higher ambulation) the ΔCt value decreases (higher amount of 5-HT_{2C}R mRNA) in saline-treated rats in PFC.

It should be noted that in both motor cortex and PFC the correlations observed in saline-treated animals are lost following repeated intermittent cocaine administration, suggesting that repeated cocaine alters the 5-HT_{2C}R system (**Fig. 4.15**).

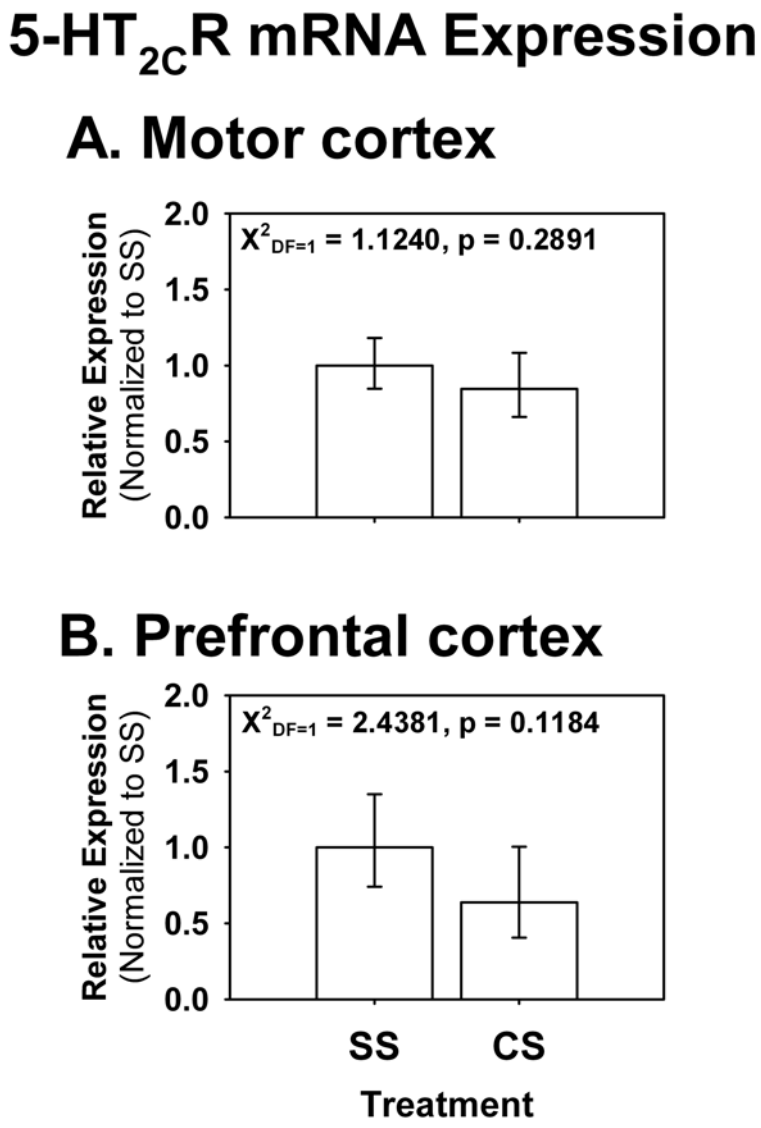

Figure 4.14. 5-HT_{2C}R mRNA expression in motor cortex and PFC following repeated intermittent cocaine administration. Rats were treated twice for 7 days with saline or cocaine and challenged on day 10 with saline (SS and CS; 1ml/kg IP). qRT-PCR data was normalized to cyclophilin and plotted relative to expression of saline pretreatment. ΔCt was calculated for total 5-HT_{2C}R mRNA: ΔCt = Ct (5-HT_{2C}R) – Ct (cyclophilin). Relative expression between groups was determined by: $2^{-\Delta\Delta Ct}$ where $\Delta\Delta$Ct = ΔCt (treatment) - ΔCt (SS (control)). Experiments were repeated twice. Results are expressed as mean $\pm$ SEM.

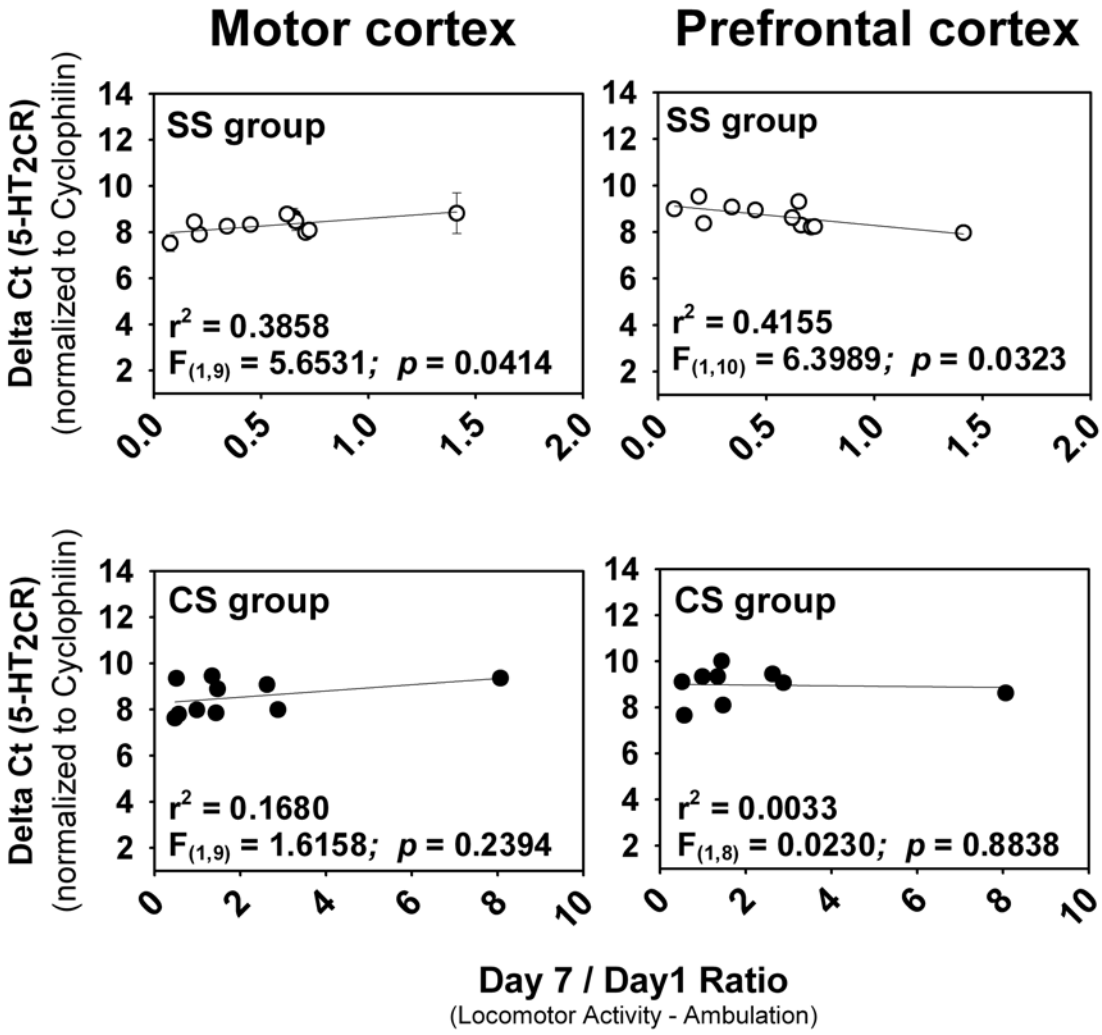

Figure 4.15. Correlation between 5-HT$_{2C}$R mRNA expression and ambulation in motor cortex and PFC. Rats were treated twice daily for 7 days with saline or cocaine and challenged on day 10 with saline (SS and CS; 1ml/kg IP). Relative expression of 5-HT$_{2C}$R mRNA expression was plotted against the ratio of day 7 and day 1 of ambulatory ambulation (Day 7 / Day 1 Ratio). In all instances, results are expressed as mean ± SEM.

Our previous results did not rule out the possibility of changes in the relative abundance of different isoforms of 5-HT$_{2C}$R mRNA; these isofoms result from RNA editing of the 5-HT$_{2C}$R pre-mRNA (Chapter 3). Previous studies have suggested that repeated administration of cocaine resulted in reduced 5-HT$_{2C}$R

function (Filip et al., 2004) and our results suggest that this decreased response occurs in the absence of changes in total 5-HT_{2C}R mRNA. These results could be explained by alterations in mRNA editing of the 5-HT_{2C}R, as previous work has demonstrated that the activation of downstream signaling molecules that couple to the receptor (*e.g.,* PLC) is dependent on the degree of editing (Herrick-Davis et al., 1999; Niswender et al., 1999; Berg et al., 2001). Thus, although total 5-HT_{2C}R mRNA was not altered by repeated cocaine exposure (**Fig. 4.14**), it is imperative to also examine the relative expression of edited 5-HT_{2C}R isoforms following the various treatment regimens. To test the hypothesis that repeated intermittent cocaine regimen increases the expression of 5-HT_{2C}R mRNA isoforms that are less efficiently coupled to G-protein, we performed qRT-PCR with TaqMan® MGB probes (Chapter 3) on total RNA from motor cortex and PFC (**Fig. 4.16-4.17**).

Three 5-HT_{2C}R RNA isoforms were chosen for study based on their relative abundance in rodent brain (Burns et al., 1997; Niswender et al., 1998; Herrick-Davis et al., 1999; Gurevich et al., 2002a): 5-$HT_{2C\text{-}VNV}$R (comprised by the AD and the ABD-edited 5-HT_{2C}R mRNA) and 5-$HT_{2C\text{-}VGV}$R (fully-edited ABECD 5-HT_{2C}R isoform).

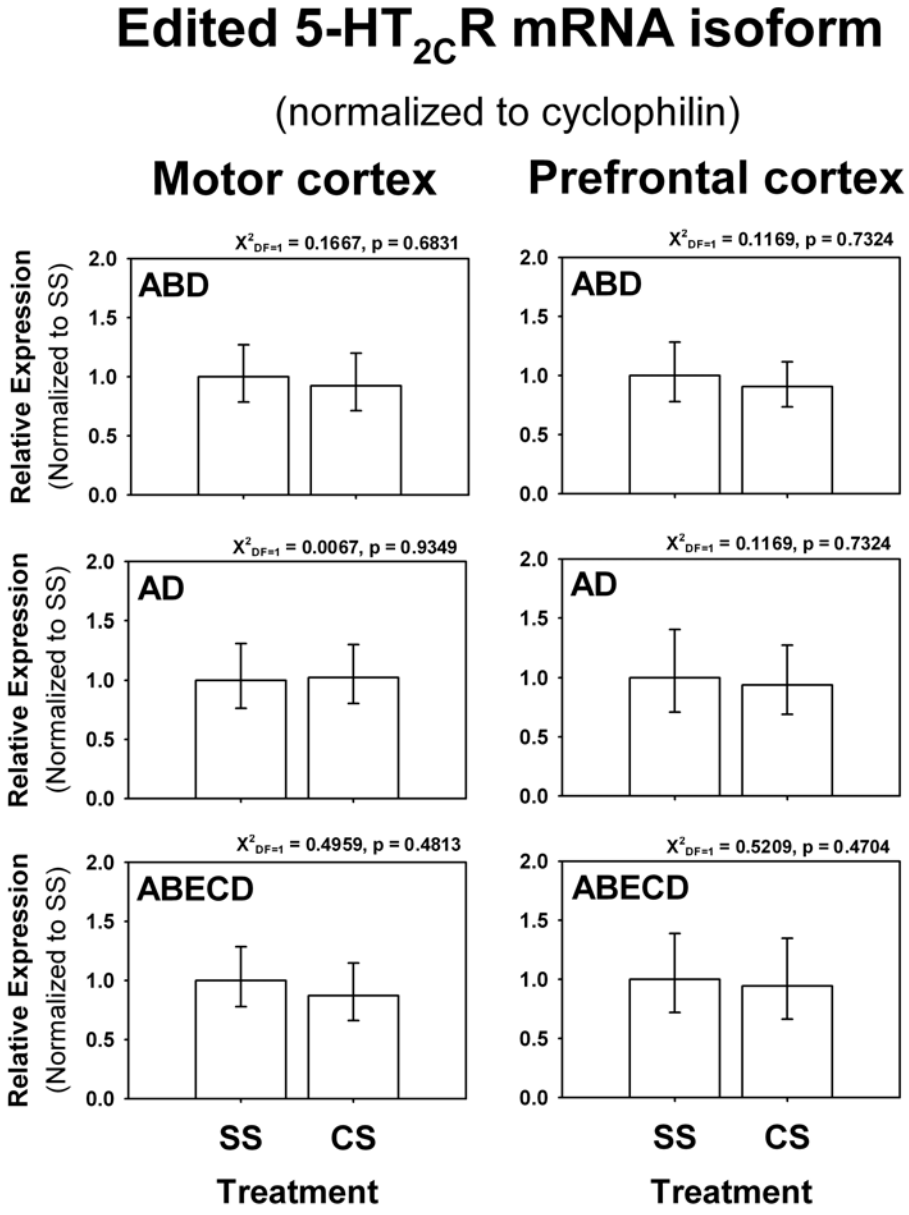

Figure 4.16. 5-HT$_{2C}$R mRNA expression in motor cortex and PFC following repeated intermittent cocaine administration. qRT-PCR data was normalized to cyclophilin and plotted relative to of SS group. ΔCt was calculated for each isoform: ΔCt = Ct (isoform) – Ct (cyclophilin). Relative expression was determined by: $2^{-\Delta\Delta Ct}$ where $\Delta\Delta$Ct = ΔCt (CS) - ΔCt (SS). Experiments were repeated twice. Results are expressed as mean $\pm$ SEM.

Each sample from motor cortex or PFC of a single rat (n=8-12 rats per treatment group) was run in triplicate to assess intra-assay reproducibility, and the experiment was run twice to assess inter-assay reproducibility.

Since cocaine increases 5-HT levels at the synapse by inhibiting 5-HT reuptake, we expected to detect an increase in the ABECD, ABD and the AD-edited 5-HT_{2C}R isoforms, as the fully-edited ABECD couples to G-protein with least efficiency, followed by the ABD and then by the AD-edited 5-HT_{2C}R isoforms (Burns et al., 1997; Niswender et al., 1999; Gurevich et al., 2002a). When the samples were normalized to the housekeeping gene cyclophilin, no statistically significant changes in the expression of the chosen 5-HT_{2C}R mRNA isoforms were observed in the motor cortex or PFC following repeated cocaine administration (**Fig. 4.16**). However, since a trend toward a reduction in total 5-HT_{2C}R mRNA expression was observed in PFC (**Fig. 4.14**, p = 0.1184), the data collected were also normalized to total 5-HT_{2C}R. This analysis demonstrated that the relative expression of the AD-edited, ABD-edited and fully-edited ABECD 5-HT_{2C}R were elevated in PFC, without reaching statistical significance (**Fig. 4.17**). The fully-edited ABECD isoform, which is the least efficiently coupled, presented a trend towards an increase in the PFC (p = 0.0790), suggesting a shift in this isoform profile. Since our data showed a trend towards a reduction in total 5-HT_{2C}R in the PFC with no changes in the amount of the 5-HT_{2C}R isoforms detected for the AD, ABD and ABECD-edited 5-HT_{2C}R isoforms (**Figs. 4.16-4.17**), it is tempting to speculate that decreased expression of other 5-HT_{2C}R isoforms may contribute to the reduce sensitivity observed following repeated intermittent cocaine administration.

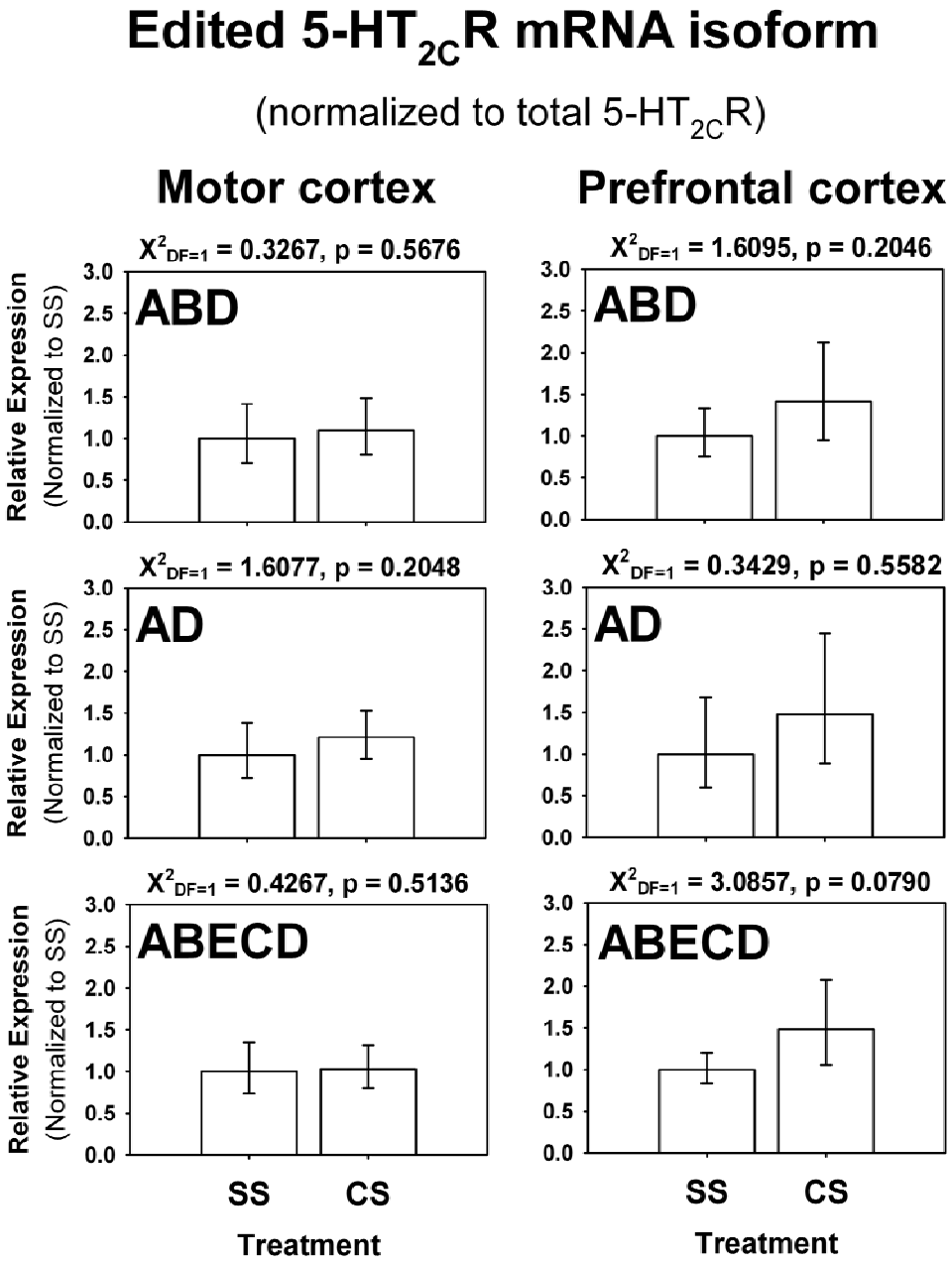

Figure 4.17. Edited 5-HT$_{2C}$R mRNA isoforms normalized against total 5-HT$_{2C}$R expression in motor cortex and PFC following repeated intermittent cocaine administration. Data were normalized to total 5-HT$_{2C}$R mRNA and plotted relative to expression of SS group. ΔCt was calculated for each isoform: ΔCt = Ct (isoform) – Ct (5-HT$_{2C}$R). Relative expression was determined by: $2^{-\Delta\Delta Ct}$ where $\Delta\Delta$Ct = ΔCt (CS) - ΔCt (SS). Experiments were repeated twice. Results are expressed as mean $\pm$ SEM.

When correlation studies between AD-edited, ABD-edited and ABECD-edited 5-HT_{2C}R mRNA isoforms and behavior (Day 7 / Day 1 Ratio) were performed, we observed no relationship between the levels of each edited isoform and the behavioral outcome (**Fig. 4.18**).

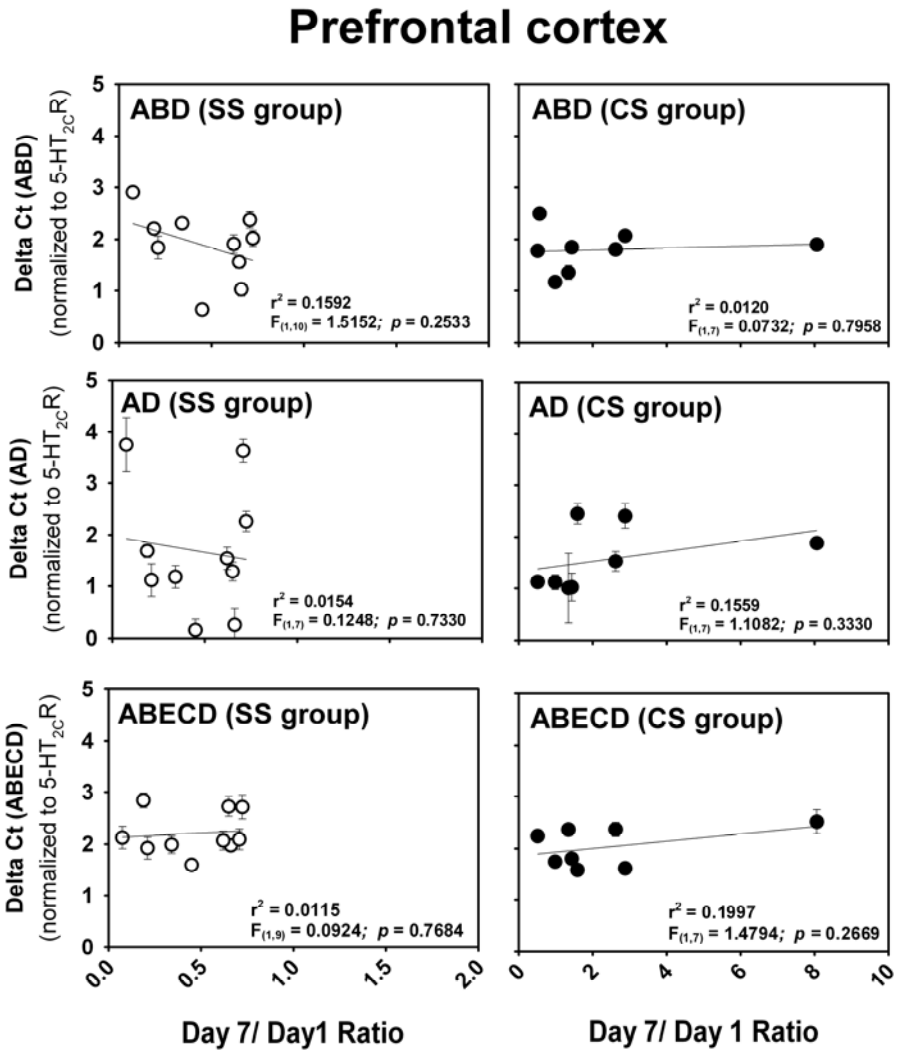

Figure 4.18. Correlation between edited-5-HT_{2C}R mRNA isoforms in PFC with ambulation. Rats were treated twice for 7 days with saline or cocaine and challenged on day 10 with saline (SS and CS; 1ml/kg IP). Relative expression of edited 5-HT_{2C}R isoforms normalized to total 5-HT_{2C}R mRNA expression was plotted against the ratio of day 7 and day 1 of ambulation (ambulation). Results are expressed as mean ± SEM.

<u>Section III</u>: Neuroadaptations of the 5-HT_{2C}R and its intracellular signaling molecules that contribute to reduced 5-HT_{2C}R sensitivity during cocaine challenge following day 3 of withdrawal from repeated intermittent exposure to cocaine

Results for the effects of a challenge injection of cocaine (15 mg/kg) following day 3 of withdrawal from repeated intermittent cocaine administration are summarized in **Table 4.4**.

<u>Motor cortex:</u> A challenge injection of cocaine at day 3 of withdrawal from a sensitizing cocaine regimen did not alter 5-HT_{2C}R protein expression or distribution at the PSD. Furthermore, a challenge injection of cocaine produced a non-significant reduction of PSD-95 in the synaptosomal fraction without affecting distribution of PSD-95 to the PSD compartment. Furthermore, an increase in phospho-p42-MAPK was observed only in the total homogenate after a challenge injection of cocaine (DF = 36, t = 2.47, p = 0.0186). Finally, we observed a non-significant increase in p42-MAPK ratio in the total homogenate (DF = 36, t = 1.93; p = 0.0619) and in the PSD-enriched fraction (DF = 19, t = 1.75, p = 0.0970), suggesting that p42-MAPK activity is susceptible to the sensitizing effects of cocaine.

<u>Prefrontal cortex:</u> **Table 4.4** shows that a challenge injection of cocaine at day 3 of withdrawal from a sensitizing cocaine regimen was not associated with alteractions in 5-HT_{2C}R, PSD-95, p42-MAPK, phospho-p42-MAPK or p44-MAPK proteins expression (total homogenate) or subcellular localizations (synaptosomal and PSD-enriched fractions) in the PFC.

Table 4.4. Neuroadaptations associated with a challenge injection of cocaine (15 mg/kg) following a period of withdrawal from repeated intermittent cocaine (15 mg/kg) administration [SC vs CC groups]

Proteins detected	Fraction	Motor cortex (*p values*)	PFC (*p values*)
5-HT_{2C}R	Total homogenate	**NC** (0.5525)	**NC** (0.7489)
	PSD-enriched	**NC** (0.3861)	**NC** (0.4209)
PSD-95	Total homogenate	**NC** (0.5828)	**NC** (0.4989)
	Synaptosomes	⇓ (0.0596)	**NC** (0.4437)
	PSD-enriched	**NC** (0.6265)	**NC** (0.2081)
p42-MAPK	Total homogenate	**NC** (0.3811)	**NC** (0.2076)
	Synaptosomes	**NC** (0.8152)	**NC** (0.8544)
	PSD-enriched	**NC** (0.4845)	**NC** (0.8072)
Phospho-p42-MAPK	Total homogenate	⇑ (0.0186)	**NC** (0.9936)
	Synaptosomes	**NC** (0.2537)	**NC** (0.3875)
	PSD-enriched	**NC** (0.4004)	**NC** (0.4746)
p42-MAPK ratio	Total homogenate	⇑ (0.0619)	**NC** (0.1845)
	Synaptosomes	**NC** (0.3859)	**NC** (0.1845)
	PSD-enriched	⇑ (0.0970)	**NC** (0.4910)
p44-MAPK	Total homogenate	**NC** (0.5237)	**NC** (0.5314)
	Synaptosomes	**NC** (0.4230)	**NC** (0.1750)
	PSD-enriched	**NC** (0.8440)	**NC** (0.7489)

Red arrow: statistically significant decrease
Green arrow: statistically significant increase
NC: no change

DISCUSSION

Behavioral assessment

Behavioral sensitization describes the augmented motor-stimulant response that occurs following repeated intermittent cocaine exposure and is hypothesized to underlie the neuronal adaptations that contribute to the transition from drug use to addiction (Goldstein and Volkow, 2002; Baler and Volkow, 2006). Thus, there is considerable interest in elucidating the neuroadaptations associated with cocaine-induced sensitization. In agreement with previous studies, our sensitizing cocaine regimen produced behavioral sensitization (Cunningham et al., 1992a; Cunningham et al., 1992b; De La Garza and Cunningham, 2000).

We investigated the role of molecular neuroadaptations on two brain areas (motor cortex and PFC) in the induction and expression of behavioral sensitization. The *induction phase* is defined as the transient sequence of cellular and molecular events precipitated by psychostimulant administration that leads to the enduring changes in neural function responsible for behavioral augmentation (Pierce and Kalivas, 1997). The induction of behavioral sensitization is thought to occur in the VTA and PFC (Pierce and Kalivas, 1997; White and Kalivas, 1998; Wolf, 1998; Vanderschuren and Kalivas, 2000). For example, ibotenic acid lesions of the VTA or the PFC (Pierce et al., 1998) blocked the induction of cocaine-induced sensitization. The *expression phase* is defined as the enduring neural alterations arising from the initiation process that directly mediate the

augmented behavioral response (Pierce and Kalivas, 1997). The expression of sensitization is dependent on NAc with a modulatory role played by the PFC (Pierce and Kalivas, 1997; White and Kalivas, 1998; Wolf, 1998; Vanderschuren and Kalivas, 2000). For example, ibotenic acid injections to the PFC suppress the expression of cocaine-induced sensitization (Kalivas, 1995; Steketee, 2003; Steketee, 2005). Thus, the PFC plays a role in modulation of the induction and the expression of cocaine-induced behavioral sensitization. However, little is known about the involvement of other cortical areas, such as the motor cortex, in cocaine-induced sensitization.

5-HT_{2C}R protein expression and subcellular localization after acute and repeated cocaine administration

Our results suggest a downregulation of the 5-HT_{2C}R protein following repeated intermittent cocaine administration in both total homogenate and in the PSD in motor cortex, but not in PFC; the latter result agrees with previous studies in which a sensitizing regimen of the psychostimulant (+)-3,4-methylenedioxymethamphetamine [(+)-MDMA] did not change 5-HT_{2C}R protein expression in the PFC (*Bubar, unpublished observations*). Downregulation of the 5-HT_{2C}R in response to both agonist and antagonist stimulation has been well documented in *in vitro* (Barker and Sanders-Bush, 1993) and *in vivo* studies (Pranzatelli et al., 1993; Fone et al., 1998; Van Oekelen et al., 2003). For example, prolonged exposure to 100 μM of the 5-HT_{2C}R antagonist mianserin or 5-HT_{2C}R agonist DOI caused a decrease in receptor binding in primary cultures of epithelial cells from choroid plexus (as determined by [3H] mesulergine binding

to membrane fractions) with no change in the apparent affinity (K_D) (Barker and Sanders-Bush, 1993). Pranzatelli and collaborators (1993) showed that a single injection of 5-HT_{2C}R agonist (*e.g.,* DOI, quipazine) or 5-HT_{2C}R antagonist (*e.g.,* mianserin, ritanserin) was not sufficient to alter 5-HT_{2C}R protein expression in spinal cord, suggesting that long term exposure is required for receptor downregulation. This last finding agrees with our results in which no differences in expression or distribution of the 5-HT_{2C}R were detected following a single challenge of cocaine.

No correlation between ambulatory counts and 5-HT_{2C}R protein expression was observed in the total homogenate in motor cortex or PFC. This result could be related to the heterogeneity in compartments found in the total homogenate (*e.g.,* plasma membrane, endoplasmic reticulum, golgi apparatus, endocytic vesicles). For example, the 5-HT_{2C}R has been found to be located in intracellular compartments such as endocytic vesicles and at the plasma membrane (Marion et al., 2004; Chanrion et al., 2008), and analyzing the total homogenate does not account for these differences. However, a better correlation between 5-HT_{2C}R protein expression and ambulatory counts was observed in the PSD-enriched fraction from motor cortex and PFC in saline-treated rats suggesting that the basal levels of ambulatory counts inversely correlates with levels of 5-HT_{2C}R protein expression in the PSD.

The expression of mRNA and protein for 5-HT_{2C}R has been shown to agree on the subcellular localization of the 5-HT_{2C}R. For example, 5-HT_{2C}R

mRNA expression was found to be restricted to layer V of all the neocortical areas, including prefrontal, parietal and occipital cortices (Pasqualetti et al., 1999), and the labeled cells in this layer presented a rounded, but not pyramidal-like shapes, presumably GABA interneurons (Pasqualetti et al., 1999). Immunohistochemical staining for the 5-HT_{2C}R suggests that this receptor is located in GABA interneurons in cortex (Clemett et al., 2000; Liu et al., 2007). Inhibitory GABA interneurons are known to form numerous synapses on pyramidal glutamatergic neurons, thus modulating cortical excitatory output (Molnar and Cheung, 2006). A decrease in the expression of 5-HT_{2C}R in GABA interneurons in motor cortex would result in decreased inhibitory influence over excitatory output from glutamatergic projections (Vanderschuren and Kalivas, 2000); thus facilitating the activation of the DA neurotransmission and further exacerbating the sensitized response (**Fig. 1.1**).

5-HT_{2C}R mRNA expression and RNA editing events after repeated cocaine administration

Rats that exhibited lower levels of 5-HT_{2C}R mRNA in the motor cortex presented higher levels of 5-HT_{2C}R mRNA in the PFC and vice versa, which could suggest a balance or a homeostatic mechanism for the regulation of basal levels of ambulation. This idea is supported by correlation studies between 5-HT_{2C}R mRNA expression and the Day 7 / Day 1 Ratio which showed that basal levels of ambulatory activity in rats is inversely proportional to 5-HT_{2C}R mRNA expression in motor cortex but directly proportional to 5-HT_{2C}R mRNA expression in PFC.

Our observation of decrease protein expression in the absence of altered mRNA expression in motor cortex is not surprising, since previous reports have shown that long-term application of 5-HT_{2C}R antagonist or 5-HT_{2C}R agonist in cell culture models promoted a downregulation of receptor protein in the membrane fraction (assessed by ligand binding studies) with no changes in mRNA levels of the 5-HT_{2C}R (Barker and Sanders-Bush, 1993). These comparisons suggest degradation of the 5-HT_{2C}R protein, a compensatory mechanism often seen in signaling pathways.

The ability of 5-HT_{2C}R agonists to activate PLC efficiently depends on the degree of RNA editing of the 5-HT_{2C}R (Herrick-Davis et al., 1999; Niswender et al., 1999; Berg et al., 2001). Our data showed that the relative expression of the AD-edited, ABD-edited and fully-edited 5-HT_{2C}R mRNA isoforms was elevated (though not with statistical significance) only in the PFC when normalized to total 5-HT_{2C}R mRNA. It is conceivable that the combination of these minor changes would have an additive effect on 5-HT_{2C}R responsiveness. It has been reported that the combination and abundance of mRNA edited isoforms is expressed in a brain area-dependent manner (Burns et al., 1997; Niswender et al., 1998; Herrick-Davis et al., 1999; Gurevich et al., 2002a; Englander et al., 2005; Iwamoto et al., 2005; Du et al., 2006), and therefore it is possible that 5-HT_{2C}R response *in vivo* would result in a combination of the responses of each individual isoform expressed. Furthermore, our results did not rule out the possibility of changes in other edited 5-HT_{2C}R isoforms not studied herein. Thus,

the motor cortex and the PFC might have different regulatory mechanisms for 5-HT_{2C}R function, with the motor cortex more vulnerable to the pharmacological effects of cocaine.

The 5-HT_{2C}R has been shown to be expressed in GABA interneurons and possibly in glutamatergic neurons in the PFC (Liu et al., 2007) and inhibitory GABA interneurons modulate cortical excitatory output (see Chapter 1); (Molnar and Cheung, 2006). A potential shift in the population of 5-HT_{2C}R edited isoforms to those isoforms that are least efficiently coupled to G-protein would result in a reduction of inhibitory influence of GABA interneurons in the PFC. Therefore, activated 5-HT_{2C}R edited isoforms via 5-HT would have a reduced signaling response than the original population of isoforms (in the absence of repeated cocaine treatment) resulting in increased glutamatergic output, thus facilitating the activation of the DA neurotransmission.

PSD-95 protein expression and subcellular localization after acute and repeated cocaine administration

Motor cortex: PSD-95 drives synaptic maturation and receptor delivery or stabilization at the synapse and, thus plays an important role in synaptic plasticity *in vivo* and *in vitro* (El-Husseini et al., 2000; El-Husseini et al., 2002; Ehrlich et al., 2007). For example, overexpression of PSD-95 in hippocampal cultured neurons leads to an increase in size and number of dendritic spines (El-Husseini et al., 2000) while the knockdown of PSD-95 by RNAi in brain slices arrested the normal development of synaptic structure (*e.g.,* spine density and morphology)

and function (Ehrlich et al., 2007). In agreement with previous studies, our results suggest no changes in PSD-95 total expression (total homogenate) in motor cortex or PFC following acute or repeated cocaine administration (Yao et al., 2004). However, cocaine exposure (either acute or repeated) induced a redistribution of PSD-95 to the PSD in motor cortex, but not in the PFC, suggesting that these two brain areas respond differentially to cocaine administration. In support of this observation, differential modification in the structure and spine density in prelimbic and motor cortex were observed following morphine self-administration suggesting unequal modification of the cerebral cortex by another drug of abuse (Ballesteros-Yanez et al., 2007). Furthermore, our results also suggest that the motor cortex might be more susceptible to the effects of cocaine, even after only a single exposure.

At day 3 of withdrawal from repeated intermittent cocaine administration we observed an elevation of PSD-95 in the PSD-enriched fraction isolated from motor cortex. Gavarini and collaborators (2006) showed that overexpression of PSD-95 in mice cortical neurons increased the desensitization of the 5-HT_{2C}R Ca^{2+} response. Our results suggest a decrease in protein expression of 5-HT_{2C}R with an increase in PSD-95 at the PSD-enriched fraction in motor cortex following a sensitizing regimen of cocaine, therefore it is conceivable that PSD-95 could be removing the receptor from the cell surface. Further studies with other 5-HT_{2C}R binding partners [*e.g.,* MAGUK p55 subfamily member 3 (MPP3] need to be

performed to gain a more complete picture of the regulation of 5-HT_{2C}R by its binding partners in the PSD.

Prefrontal cortex: After acute and repeated cocaine administration we observed a trend towards an increase in PSD-95 in the synaptosomal fraction. As mentioned in Chapter 1, the PFC is an heterogeneous structure that can be subdivided into ACC, PrL, and IL (Dalley et al., 2004) that has been implicated in the behavioral and molecular changes associated with behavioral sensitization to cocaine (Steketee, 2003; McFarland et al., 2003; McFarland et al., 2004; Steketee, 2005). Previous work in which synaptosomal fractions were isolated from the dorsal but not the ventral PFC indicated a significant elevation of PSD-95 following a sensitizing regimen of cocaine (Ghasemzadeh et al., 2008a; Ghasemzadeh et al., 2008b). In the light of this, it is possible that our assay of the whole PFC might obscure significant changes in PSD-95 expression seen in subregions of the PFC after acute and repeated cocaine administration.

p44/p42-MAPK protein expression, subcellular localization and protein phosphorylation after repeated cocaine administration

One important pathway that is activated by 5-HT_{2C}R downstream elements, as well as by the DA neurotransmitter system, is the p44/p42-MAPK pathway (Werry et al., 2005; Fumagalli et al., 2005; Brown and Gerfen, 2006).

p42-MAPK protein expression in motor cortex and PFC: Our findings suggest that p42-MAPK is translocated to the PSD in response to an acute cocaine exposure, without altering total protein expression (total homogenate) or

distribution to synaptosomal compartments in motor cortex, but not in PFC. p42-MAPK has been detected in neuronal and oligodendrocytes cell bodies and dendrites associated with microtubules proteins such as MAP-2 and myelin basic proteins, suggesting that p42-MAPK activation might be responsible for cellular structural changes associated with synaptic plasticity (Fiore et al., 1993). Our results suggest that the motor cortex is more responsive to the acute effects of cocaine as evidenced by the rapid translocation of p42-MAPK (and PSD-95) to the PSD compartment. This observation suggests that neuronal plasticity is taking place even after a single dose of cocaine (Wanat and Bonci, 2008).

Phosphorylation of p42-MAPK in motor cortex and PFC: Our data suggest no statistically significant changes in phospho-p42-MAPK following acute cocaine administration in either total homogenate, synaptosomal or PSD-enriched fractions in either motor cortex or PFC. These results were unexpected since a body of literature has demonstrated that cocaine promotes phosphorylation of p44/p42-MAPK (even after a single injection of cocaine) in a dose-dependent and brain area-dependent manner (Berhow et al., 1996; Valjent et al., 2000; Mattson et al., 2005; Valjent et al., 2006). In fact, a single injection of cocaine (20 mg/kg) induced phosphorylation of p44/p42-MAPK in the dorsal striatum, NAc, amygdala and in the deep layers of the PFC 5-10 min after the challenge injection (Valjent et al., 2004a; Valjent et al., 2006). In light of this, it is possible that these effects may be obscured in the present study since cocaine-induced phosphorylation of p44/p42-MAPK had been reported for a subdivision (Valjent et

al., 2004a) and not for the entire PFC. Furthermore, induction of p44/p42-MAPK phosphorylation has also been shown to be drug-dependent. For example, cocaine (Berhow et al., 1996) or morphine induced phosphorylation of p44/p42-MAPK in the VTA following repeated but not after a single injection (Jenab et al., 2005), whereas D-amphetamine-induced p44/p42-MAPK phosphorylation in the VTA occurred 15 min after a single but not repeated drug exposure (Rajadhyaksha et al., 2004; Valjent et al., 2006). Furthermore, it should be noted that in those series of experiments, p44/p42-MAPK phosphorylation was determined by immunocytochemistry (inmmunoreactive nuclei) (Rajadhyaksha et al., 2004; Valjent et al., 2006) and Western blot assays on total homogenate samples (Rajadhyaksha et al., 2004; Jenab et al., 2005). In our studies phospho-p42-MAPK was determined by Western blot analysis in specialized membranes and subcellular fractions, thus technical issues regarding method of detection, time of dissection or subcellular compartment investigated could account for the mentioned discrepancies. The kinetics of p44/p42-MAPK phosphorylation have been reported to be slightly modified following repeated cocaine exposure (20 mg/kg x 6 days) (Valjent et al., 2000), as phospho-p44/p42-MAPK immunostaining was detected 20 min after the challenge cocaine injection, but phospho-p44/42-MAPK was significantly reduced at this time-point following a single cocaine injection (Valjent et al., 2000). In light of this, our previous results with acute cocaine exposure could be explained by the fact that our rats were possibly sacrificed after the phosphorylation peak of phospho-p42-MAPK for these two brain areas.

p42-MAPK ratio in motor cortex and PFC: We observed that a challenge injection of cocaine increased the phosphorylation of p42-MAPK and therefore its activity (p42-MAPK ratio) in rats previously treated with a sensitizing cocaine regimen in motor cortex, but not in PFC. Our results agree with previous studies in which rats previously pretreated with cocaine (15 mg/kg/daily for 7 days) presented 90% higher levels of phospho-p44/p42-MAPK 20 min after cocaine challenge in NAc when compared to rats pretreated with saline and challenge with cocaine (Mattson et al., 2005). Furthermore, a challenge injection of cocaine significantly increased p44/p42-MAPK activity levels by 80% in NAc (Mattson et al., 2005) and by 37% in the VTA (Berhow et al., 1996) in rats repeatedly pretreated with cocaine when compare to rats pretreated with saline. It should be noted that the increase in p42-MAPK activity (p42-MAPK ratio) in total homogenate seen here is attributable to an increase in phosphorylation without a change in total p42-MAPK, in agreement with previous studies (Berhow et al., 1996). Since the changes in phospho-p42-MAPK expression and p42-MAPK ratio were limited to total homogenate and not to the synaptosomal or the PSD compartments in motor cortex, it is likely that the observed changes in p42-MAPK are restricted to the nuclei. It is well establish that the transcription factor cAMP response element binding (CREB) is a substrate for p44/p42-MAPK and that phosphorylated CREB in turn initiates the expression of immediate-early genes (*e.g.,* c-Fos and zif268). For example, *in situ* hybridization showed that immediate-early genes expression (Arc, zif268 and c-fos) were induced in the ACC, MOP and MOS in rats that were re-exposed to the self-administration

operant chamber previously associated with cocaine 22 hr after the end of cocaine administration (Hearing et al., 2008), thus demonstrating that cortical areas are implicated in drug-seeking behavior (Hearing et al., 2008). Furthermore, mice injected with the MEK inhibitor SL327 1 hr before an acute systemic cocaine injection showed a reduction in phospho-p44/p42-MAPK when compared to saline-cocaine control animals (Radwanska et al., 2005). In the same study, the expression of immediate-early genes cFos and JunB in NAc and amygdala was prevented when mice were pretreated with SL327 before acute cocaine administration (Radwanska et al., 2005). Altogether these results suggest that p42-MAPK plays an important role in the molecular adaptation associated with acute and repeated administration of cocaine.

Recently, PSD-95 has been shown to be a substrate for p42-MAPK. p42-MAPK phosphorylates PSD-95 at Thr287 and Ser290 when the p42-MAPK pathway is activated, suggesting a role of p42-MAPK in the regulation of synaptic plasticity (Sabio et al., 2004). Our data suggests a positive correlation between PSD-95 and p42-MAPK protein expression in the PSD of cocaine-treated rats (CS) in motor cortex. Interestingly, upon cocaine challenge we observed the same correlation in the PSD-enriched fraction in the PFC of rats previously treated with cocaine (**Fig. 4.19**). These results suggest even further the distinct responses of these two brain areas to the acute and repeated exposure to cocaine.

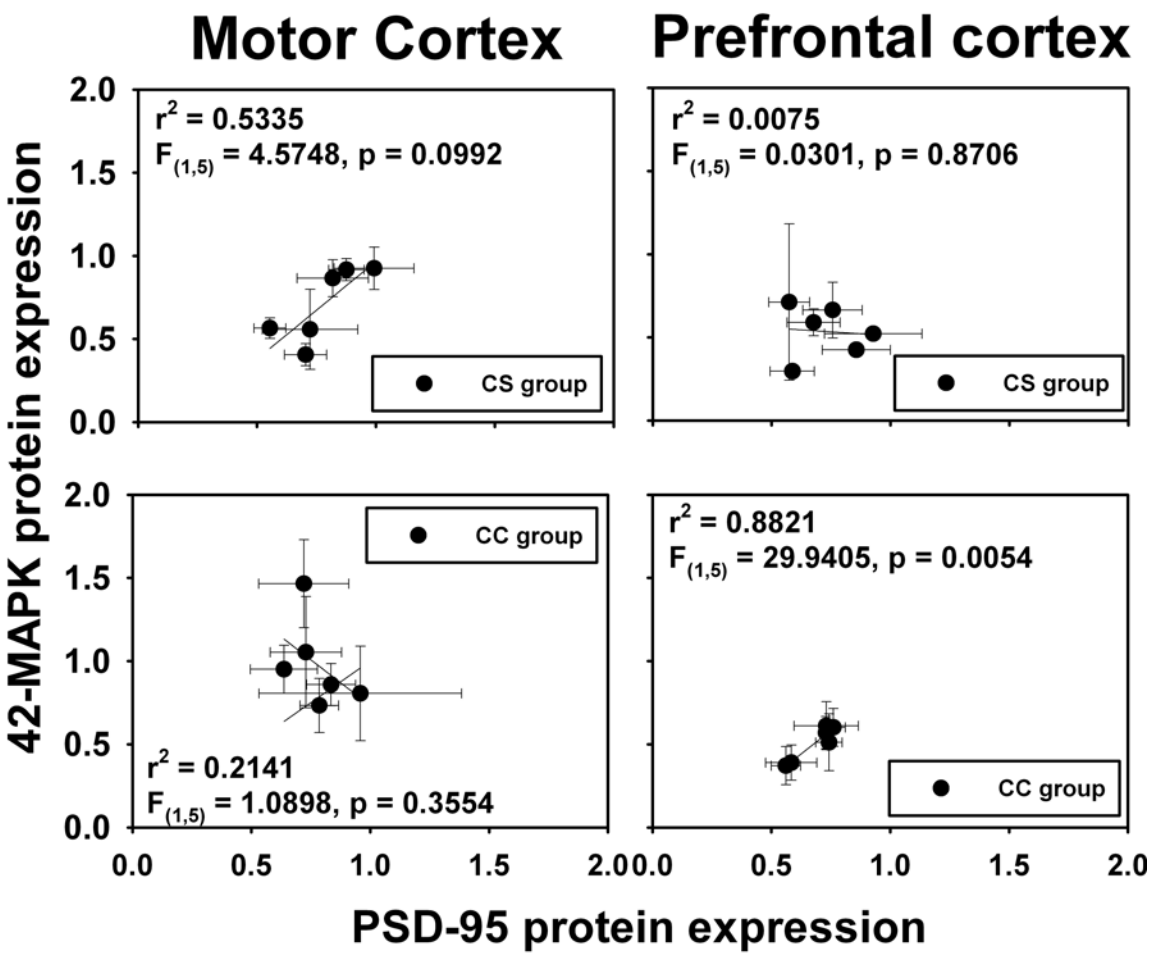

Figure 4.19. Correlation between PSD-95 and p42-MAPK expression in the PSD-enriched fraction from motor cortex and PFC. Rats were treated twice for 7 days with saline and challenged on day 10 with saline (CS; 1 ml/kg IP) or cocaine (CC; 15 mgk/kg IP). Graph represents the average normalized protein expression from 3-4 replicates. Results are expressed as mean ± SEM.

In summary, 5-HT_{2C}R function is regulated by a decrease in protein expression of the receptor in total homogenate and at the PSD compartment in motor cortex, whereas in the PFC, there is an apparent shift in edited 5-HT_{2C}R mRNA isoforms. Our results also suggest that acute and repeated cocaine administration increases the redistribution of two molecules involved in synaptic

plasticity, PSD-95 and p42-MAPK to the PSD in motor cortex, but not in the PFC. Increased phospho-p42-MAPK in total homogenate after cocaine challenge following a sensitizing cocaine regimen was only observed in motor cortex. Together our results suggest that motor cortex and PFC have different regulatory mechanisms for 5-HT_{2C}R function, with the motor cortex being more vulnerable to the pharmacological effects of cocaine.

CHAPTER 5: CONCLUSIONS AND PROJECTIONS TO THE FUTURE

Our objective was to identify the cortical molecular neuroadaptations of the 5-HT_{2C}R and intracellular signaling pathways associated with this receptor that may contribute to the reduced sensitivity of the 5-HT_{2C}R observed after repeated intermittent cocaine administration. Four possible neuroadaptations were explored in motor cortex and PFC: 1) changes in protein expression and subcellular localization of the 5-HT_{2C}R; 2) changes in expression and subcellular localization of PSD-95; 3) changes in expression, subcellular localization and phosphorylation of p44/p42-MAPK pathway; 4) changes in 5-HT_{2C}R mRNA editing.

To assess the effects of repeated intermittent cocaine administration on the protein expression and subcellular localization of the 5-HT_{2C}R in motor cortex and PFC, we first confirmed the expression of the 5-HT_{2C}R in cortical synaptosomal and PSD-enriched fractions using Western blot analysis and characterized four commercially-available 5-HT_{2C}R antibodies (Chapter 2). We found that the D-12 and N-19 anti-5-HT_{2C}R antibodies from Santa Cruz Biotechnology were suitable for Western blot analysis of the 5-HT_{2C}R. However, only the D-12 was suitable for immunoprecipitation studies. These observations pave the way for further quantitative analyses of subcellular localization and regulation of synaptic 5-HT_{2C}R protein following cocaine administration.

To study the effects of repeated intermittent cocaine administration on four edited 5-HT_{2C}R isoforms, we adapted qRT-PCR utilizing TaqMan® MGB probes (Chapter 3). Probes were developed for four 5-HT_{2C}R RNA isoforms and the sensitivity and specificity of these probes were validated systematically using standard templates. Relative expression of the four isoforms was measured in cDNAs from whole brain extracted from 129S6 and C57BL/6J mice. Rank order derived from this qRT-PCR analysis matched with that derived from DNA sequencing. In mutant mice solely expressing either non-edited or fully-edited 5-HT_{2C}R transcripts, only expected transcripts were detected. These findings suggested that this qRT-PCR method is suitable for the detection of closely-related mRNA sequences *ex vivo* without the necessity of characterizing the entire 5-HT_{2C}R profile.

In Chapter 4, we applied the findings obtained in Chapters 2 and 3 to investigate the role of molecular neuroadaptations in motor cortex and PFC in the induction and expression of behavioral sensitization. Our results suggested that repeated intermittent cocaine treatment reduced the expression of 5-HT_{2C}R protein in both total homogenate and in the PSD isolated from motor cortex, but not in PFC. With regards to the 5-HT_{2C}R editing profile, our data showed that the relative expression of the AD-edited, ABD-edited and fully-edited ABECD 5-HT_{2C}R mRNA isoforms was elevated only in the PFC when normalized to total 5-HT_{2C}R mRNA. It is possible that the combination of these minor changes could have an additive effect, resulting in a reduced 5-HT_{2C}R function following

repeated intermintent cocaine administration. These results suggest that the motor cortex and the PFC might have different regulatory mechanisms to downregulate 5-HT_{2C}R function. The combination of these two neuroadaptations might contribute to a strengthening of the cortico-striatal “habit” circuitry (*e.g.,* compulsive cocaine consumption, cocaine seeking), and to the activation of the reward pathway (**Fig. 5.1**).

Our findings suggest that the mechanisms of downregulation of 5-HT_{2C}R function in response to prolonged stimulation is brain-area dependent. In motor cortex, the function of the 5-HT_{2C}R is regulated by changing the actual amount of receptor expressed in the cell, whereas in the PFC there is an apparent shift in the edited 5-HT_{2C}R isoform profile. These two findings become important and useful when thinking about pharmacotherapeutic options for cocaine addiction. Ideally, the therapeutic drug should elevate the protein expression of 5-HT_{2C}R in brain areas where there is a decrease in 5-HT_{2C}R protein expression (*e.g.,* motor cortex), while shifting the profile of 5-HT_{2C}R mRNA edited isoforms to those isoforms that are efficiently coupled to G-proteins.

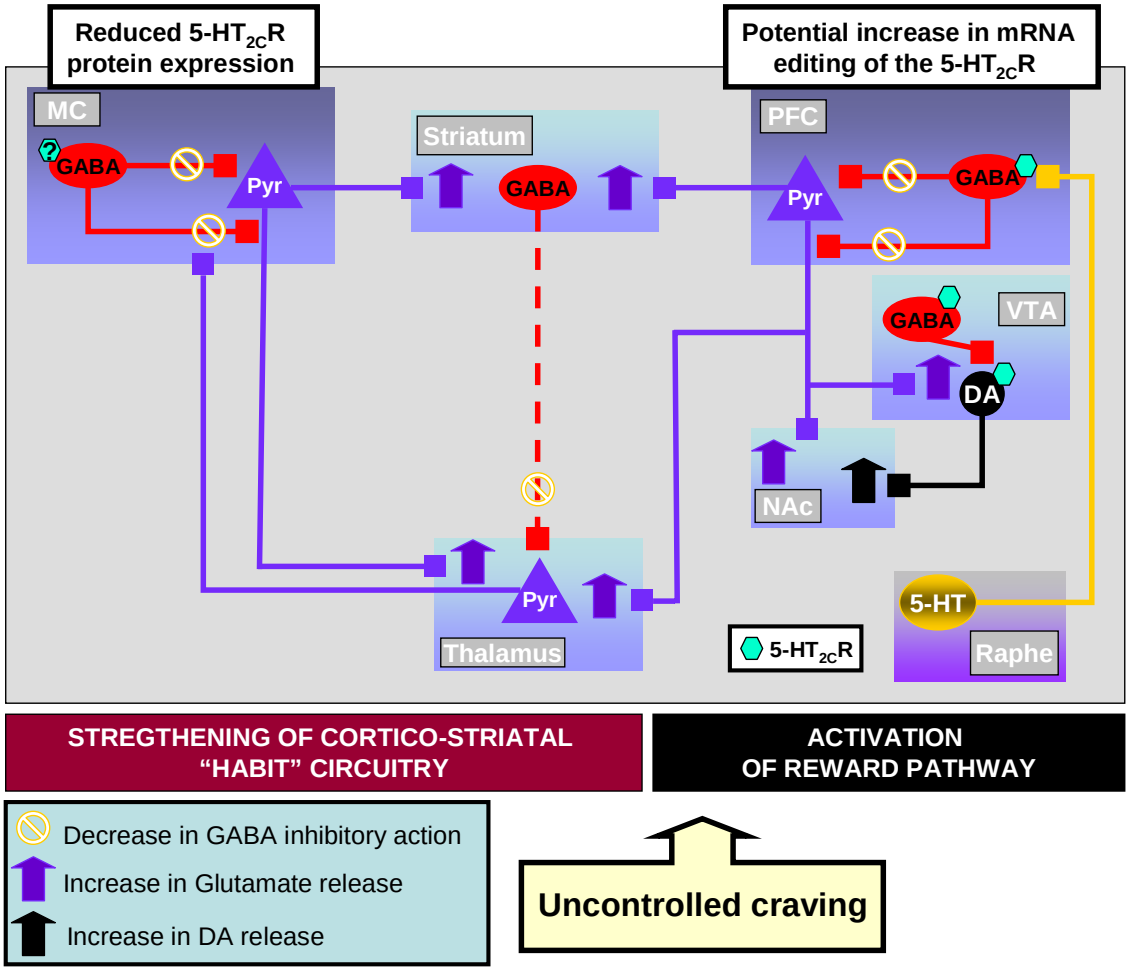

Figure 5.1. Schematic representation of the effects of repeated cocaine administration over 5-HT$_{2C}$R function.

One interesting pharmacotherapeutic option for cocaine addiction is the use of a 5-HT$_{2C}$R inverse agonist. Inverse agonists are ligands with negative efficacy at GPCR (or ligand that binds to the receptor at the same site of an agonist, but produces the opposite response). *In vitro* studies have shown that application of the 5-HT$_{2C}$R inverse agonist SB206553 induces translocation (or blocks internalization) of non-edited 5-HT$_{2C\text{-}INI}$R (Marion et al., 2004; Chanrion et

al., 2008) and partially-edited 5-HT_{2C}R isoforms (*e.g.,* 5-$HT_{2C\text{-}VSV}$R) to the plasma membrane (Marion et al., 2004). Atypical antipsychotic drugs that have inverse agonist properties at the 5-HT_{2C}R (*e.g.,* clozapine) and tetracyclic antidepressant mirtazapine have been shown to induce redistribution of the 5-$HT_{2C\text{-}INI}$R to the plasma membrane (Aloyo et al., 2008; Chanrion et al., 2008). Most importantly, primary cultured cortical neurons, which present a diverse population of 5-HT_{2C}R isoforms, previously pretreated with the 5-HT_{2C}R inverse agonist SB206553 (100 nM for 18 hrs) presented an increased Ca^{2+} response to the application of 5-HT compared to culture cortical neurons that did not receive the inverse agonist application (Chanrion et al., 2008). This enhanced response to 5-HT_{2C}R suggests that either a shift in the mRNA editing expression profile or an increase in receptor density occurs in response to long-term inverse agonist treatment. It is known that the ability of 5-HT_{2C}R agonists to activate PLC more efficiently is inversely proportional to the degree of mRNA editing of the 5-HT_{2C}R. The experiments mentioned above suggest that a 5-HT_{2C}R inverse agonists have the capacity of inducing a translocation of the non-edited 5-$HT_{2C\text{-}INI}$R isoforms (constitutively active receptor) to the plasma membrane enhancing 5-HT_{2C}R signaling. Thus, treatment with a 5-HT_{2C}R inverse agonist could modulate receptor downregulation mechanisms observed in motor cortex and PFC, which could in turn increase the 5-HT_{2C}R responsiveness to both ligand-dependent and ligand-independent (constitutive) signaling (**Fig. 5.2**).

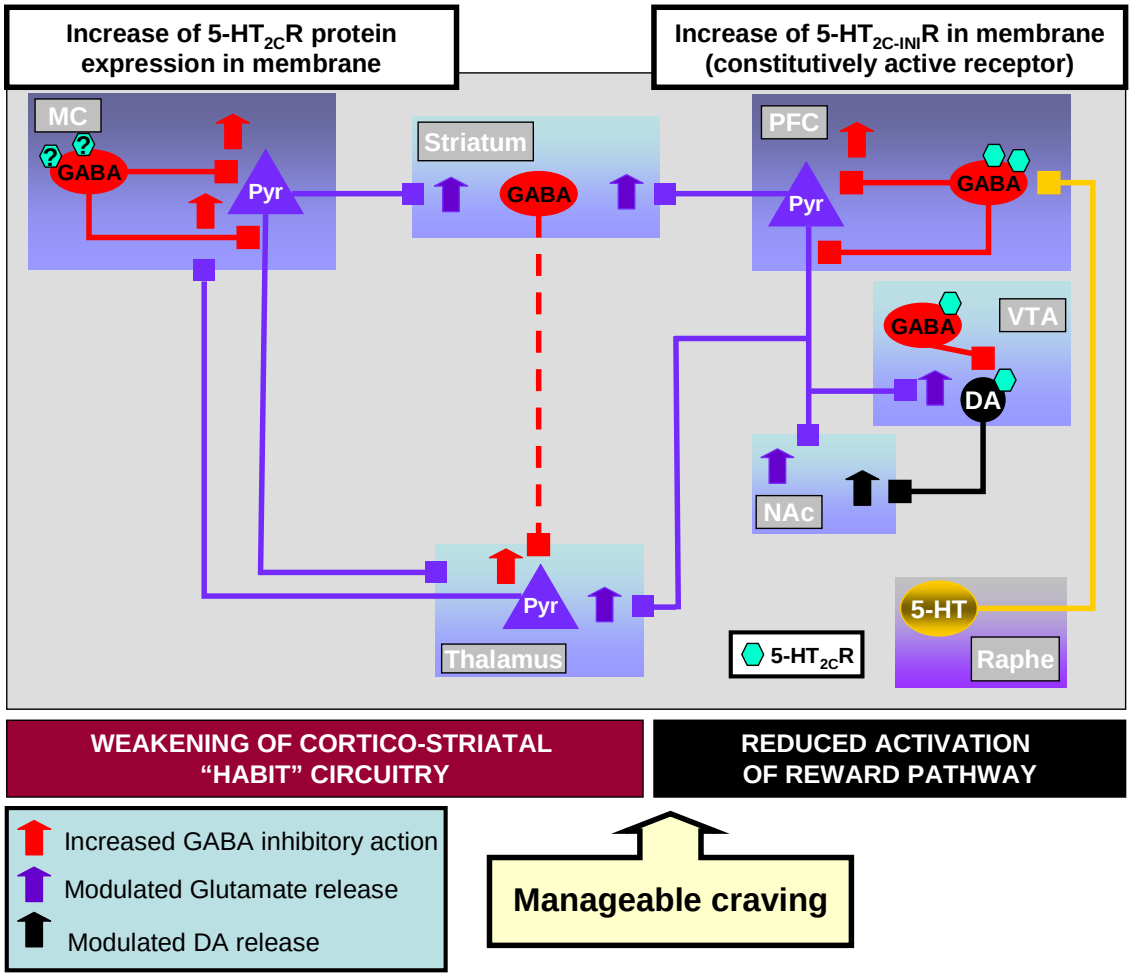

Figure 5.2. Schematic representation of the effects an 5-HT$_{2C}$R inverse agonist on 5-HT$_{2C}$R function previously disrupted by repeated cocaine administration.

In Chapter 4 we observed that the effects of acute and repeated cocaine exposure on PSD-95 and p44/42-MAPK are also brain-area dependent, illustrating even further the distinct adaptations in cortical circuits. p44/p42-MAPK is thought to integrate several cellular processes, and the near ubiquitous expression of these kinases make them unlikely therapeutic targets. However, protein-protein interactions such as the one observed between PSD-95 and the

5-HT_{2C}R could be disrupted to allow the receptor to remain activated in the plasma membrane (Gavarini et al., 2006). In support of this idea, siRNA knockdown of PSD-95 decreased the desensitization of the 5-HT_{2C}R Ca^{2+} response in cortical neurons (Gavarini et al., 2006). Additionally, the interaction between phosphatase and tensin homolog deleted at chromosome 10 (PTEN) and the 5-HT_{2C}R can be disrupted by a small Tat-3L4F peptide [a fragment of the 3rd intracellular loop of the 5-HT_{2C}R (Pro283-Arg297)]. The Tat-3L4F peptide acts as a decoy for PTEN, thus disrupting the 5-HT_{2C}R:PTEN complexes and allowing the 5-HT_{2C}R to remain in its phosphorylated form (active) in the plasma membrane (Ji et al., 2006). Similarly, disruption of the interaction between 5-HT_{2C}R and PSD-95 might allow the 5-HT_{2C}R to remain in the plasma membrane, thus making the receptor available for ligand stimulation. Thus, small molecules that disrupt protein-protein interactions could also be useful potential therapeutic targets for the treatment of addiction (Reilly et al., 2009).

In conclusion, the recovery of 5-HT_{2C}R inhibitory influence over the limbic-corticostriatal circuitry either by using a 5-HT_{2C}R inverse agoinst or a small peptide molecule that disrupts protein-protein interactions would be expected to modulate the activation of the limbic-corticostriatal circuitry thus reducing DA outflow from VTA (**Fig. 5.2**). Several 5-HT_{2C}R inverse agonists similar in structure to SB206553 are currently being tested in in clinical trials as therapeutic options for the treatment of depression, anxierty, psychosis, Parkinson's disease and obesity (Bubar and Cunningham, 2008). These compounds have potential as

treatments for cocaine addiction, since a key component for treating cocaine addiction is the the ability to convert compulsive drug-seeking (**Fig. 5.1**) into manageable craving (**Fig. 5.2**).

REFERENCES

Abramowski D, Rigo M, Duc D, Hoyer D, Staufenbiel M (1995) Localization of the 5-hydroxytryptamine2C receptor protein in human and rat brain using specific antisera. Neuropharmacology 34:1635-1645.

Abramowski D, Staufenbiel M (1995) Identification of the 5-hydroxytryptamine2C receptor as a 60-kDa N-glycosylated protein in choroid plexus and hippocampus. J Neurochem 65:782-790.

Afonso L, Mohammad T, Thatai D (2007) Crack whips the heart: a review of the cardiovascular toxicity of cocaine. Am J Cardiol 100:1040-1043.

Aloyo VJ, Berg KA, Spampinato U, Clarke WP, Harvey JA (2009) Current status of inverse agonism at serotonin(2A) (5-HT(2A)) and 5-HT(2C) receptors. Pharmacol Ther. *in press.*

Backstrom JR, Price RD, Reasoner DT, Sanders-Bush E (2000) Deletion of the serotonin 5-HT2C receptor PDZ recognition motif prevents receptor phosphorylation and delays resensitization of receptor responses. J Biol Chem 275:23620-23626.

Backstrom JR, Sanders-Bush E (1997) Generation of anti-peptide antibodies against serotonin 5-HT2A and 5-HT2C receptors. J Neurosci Methods 77:109-117.

Backstrom JR, Westphal RS, Canton H, Sanders-Bush E (1995) Identification of rat serotonin 5-HT2C receptors as glycoproteins containing N-linked oligosaccharides. Brain Res Mol Brain Res 33:311-318.

Baler RD, Volkow ND (2006) Drug addiction: the neurobiology of disrupted self-control. Trends Mol Med 12:559-566.

Ballesteros-Yanez I, Ambrosio E, avides-Piccione R, Perez J, Torres I, Miguens M, Garcia-Lecumberri C, DeFelipe J (2007) The effects of morphine self-administration on cortical pyramidal cell structure in addiction-prone lewis rats. Cereb Cortex 17:238-249.

Banker G, Churchill L, Cotman CW (1974) Proteins of the postsynaptic density. J Cell Biol 63:456-465.

Barker EL, Sanders-Bush E (1993) 5-hydroxytryptamine1C receptor density and mRNA levels in choroid plexus epithelial cells after treatment with

mianserin and (-)-1-(4-bromo-2,5-dimethoxyphenyl)-2-aminopropane. Mol Pharmacol 44:725-730.

Bass BL (2002) RNA editing by adenosine deaminases that act on RNA. Annu Rev Biochem 71:817-846.

Becamel C, Alonso G, Galeotti N, Demey E, Jouin P, Ullmer C, Dumuis A, Bockaert J, Marin P (2002) Synaptic multiprotein complexes associated with 5-HT(2C) receptors: a proteomic approach. EMBO J 21:2332-2342.

Becamel C, Gavarini S, Chanrion B, Alonso G, Galeotti N, Dumuis A, Bockaert J, Marin P (2004) The serotonin 5-HT2A and 5-HT2C receptors interact with specific sets of PDZ proteins. J Biol Chem 279:20257-20266.

Benne R (1996) RNA editing: how a message is changed. Curr Opin Genet Dev 6:221-231.

Benne R, van den BJ, Brakenhoff JP, Sloof P, Van Boom JH, Tromp MC (1986) Major transcript of the frameshifted coxII gene from trypanosome mitochondria contains four nucleotides that are not encoded in the DNA. Cell 46:819-826.

Bennett MK, Scheller RH (1994) A molecular description of synaptic vesicle membrane trafficking. Annu Rev Biochem 63:63-100.

Berg KA, Clarke WP, Cunningham KA, Spampinato U (2008a) Fine-tuning serotonin2c receptor function in the brain: molecular and functional implications. Neuropharmacology 55:969-976.

Berg KA, Cropper JD, Niswender CM, Sanders-Bush E, Emeson RB, Clarke WP (2001) RNA-editing of the 5-HT(2C) receptor alters agonist-receptor-effector coupling specificity. Br J Pharmacol 134:386-392.

Berg KA, Dunlop J, Sanchez T, Silva M, Clarke WP (2008b) A conservative, single-amino acid substitution in the second cytoplasmic domain of the human Serotonin2C receptor alters both ligand-dependent and -independent receptor signaling. J Pharmacol Exp Ther 324:1084-1092.

Berhow MT, Hiroi N, Nestler EJ (1996) Regulation of ERK (extracellular signal regulated kinase), part of the neurotrophin signal transduction cascade, in the rat mesolimbic dopamine system by chronic exposure to morphine or cocaine. J Neurosci 16:4707-4715.

Bonasera SJ, Tecott LH (2000) Mouse models of serotonin receptor function: toward a genetic dissection of serotonin systems. Pharmacol Ther 88:133-142.

Boudreau AC, Reimers JM, Milovanovic M, Wolf ME (2007) Cell surface AMPA receptors in the rat nucleus accumbens increase during cocaine withdrawal but internalize after cocaine challenge in association with altered activation of mitogen-activated protein kinases. J Neurosci 27:10621-10635.

Boudreau AC, Wolf ME (2005) Behavioral sensitization to cocaine is associated with increased AMPA receptor surface expression in the nucleus accumbens. J Neurosci 25:9144-9151.

Brown P, Gerfen CR (2006) Plasticity within striatal direct pathway neurons after neonatal dopamine depletion is mediated through a novel functional coupling of serotonin 5-HT2 receptors to the ERK 1/2 map kinase pathway. J Comp Neurol 498:415-430.

Brownlow HA, Pappachan J (2002) Pathophysiology of cocaine abuse. Eur J Anaesthesiol 19:395-414.

Bubar MJ, Cunningham KA (2006) Serotonin 5-HT2A and 5-HT2C receptors as potential targets for modulation of psychostimulant use and dependence. Curr Top Med Chem 6:1971-1985.

Bubar MJ, Cunningham KA (2007) Distribution of serotonin 5-HT2C receptors in the ventral tegmental area. Neuroscience 146:286-297.

Bubar MJ, Cunningham KA (2008) Prospects for serotonin 5-HT2R pharmacotherapy in psychostimulant abuse. Prog Brain Res 172:319-346.

Bubar MJ, Seitz PK, Thomas ML, Cunningham KA (2005) Validation of a selective serotonin 5-HT(2C) receptor antibody for utilization in fluorescence immunohistochemistry studies. Brain Res 1063:105-113.

Burmeister JJ, Lungren EM, Kirschner KF, Neisewander JL (2004) Differential roles of 5-HT receptor subtypes in cue and cocaine reinstatement of cocaine-seeking behavior in rats. Neuropsychopharmacology 29:660-668.

Burns CM, Chu H, Rueter SM, Hutchinson LK, Canton H, Sanders-Bush E, Emeson RB (1997) Regulation of serotonin-2C receptor G-protein coupling by RNA editing. Nature 387:303-308.

Callahan PM, Cunningham KA (1994) Involvement of 5-HT2C receptors in mediating the discriminative stimulus properties of m-chlorophenylpiperazine (mCPP). Eur J Pharmacol 257:27-38.

Callahan PM, Cunningham KA (1995) Modulation of the discriminative stimulus properties of cocaine by 5-HT1B and 5-HT2C receptors. J Pharmacol Exp Ther 274:1414-1424.

Canales JJ (2005) Stimulant-induced adaptations in neostriatal matrix and striosome systems: transiting from instrumental responding to habitual behavior in drug addiction. Neurobiol Learn Mem 83:93-103.

Canton H, Emeson RB, Barker EL, Backstrom JR, Lu JT, Chang MS, Sanders-Bush E (1996) Identification, molecular cloning, and distribution of a short variant of the 5-hydroxytryptamine2C receptor produced by alternative splicing. Mol Pharmacol 50:799-807.

Carroll FI, Howell LL, Kuhar MJ (1999) Pharmacotherapies for treatment of cocaine abuse: preclinical aspects. J Med Chem 42:2721-2736.

Carroll KM (2005) Recent advances in the psychotherapy of addictive disorders. Curr Psychiatry Rep 7:329-336.

Carta M, Allan AM, Partridge LD, Valenzuela CF (2003) Cocaine inhibits 5-HT3 receptor function in neurons from transgenic mice overexpressing the receptor. Eur J Pharmacol 459:167-169.

Chanrion B, Mannoury la CC, Gavarini S, Seimandi M, Vincent L, Pujol JF, Bockaert J, Marin P, Millan MJ (2008) Inverse agonist and neutral antagonist actions of antidepressants at recombinant and native 5-hydroxytryptamine2C receptors: differential modulation of cell surface expression and signal transduction. Mol Pharmacol 73:748-757.

Chevet E, Lemaitre G, Katinka MD (1995) Low concentrations of tetramethylammonium chloride increase yield and specificity of PCR. Nucleic Acids Res 23:3343-3344.

Childress AR, Mozley PD, McElgin W, Fitzgerald J, Reivich M, O'Brien CP (1999) Limbic activation during cue-induced cocaine craving. Am J Psychiatry 156:11-18.

Clemett DA, Punhani T, Duxon MS, Blackburn TP, Fone KC (2000) Immunohistochemical localisation of the 5-HT2C receptor protein in the rat CNS. Neuropharmacology 39:123-132.

Cotman CW (1974) Isolation of synaptosomal and synaptic plasma membrane fractions. Methods Enzymol 31:445-452.

Cruz-Reyes J, Rusche LN, Piller KJ, Sollner-Webb B (1998) T. brucei RNA editing: adenosine nucleotides inversely affect U-deletion and U-insertion reactions at mRNA cleavage. Mol Cell 1:401-409.

Cunningham KA, Bubar MJ, Filip M (2004) Localization of 5-HT2 receptors in the mesoaccumbens dopamine system and their behavioral significance. International J of Neuropsychopharm 7:S42-S43.

Cunningham KA, Callahan PM (1994) Neurobehavioral pharmacology of cocaine: role for serotonin in its locomotor and discriminative stimulus effects. NIDA Res Monogr 145:40-66.

Cunningham KA, Callahan PM, Appel JB (1986) Discriminative stimulus properties of the serotonin agonist MK 212. Psychopharmacology (Berl) 90:193-197.

Cunningham KA, Paris JM, Goeders NE (1992a) Chronic cocaine enhances serotonin autoregulation and serotonin uptake binding. Synapse 11:112-123.

Cunningham KA, Paris JM, Goeders NE (1992b) Serotonin neurotransmission in cocaine sensitization. Ann N Y Acad Sci 654:117-127.

Dalley JW, Cardinal RN, Robbins TW (2004) Prefrontal executive and cognitive functions in rodents: neural and neurochemical substrates. Neurosci Biobehav Rev 28:771-784.

De La Garza R, Cunningham KA (2000) The effects of the 5-hydroxytryptamine(1A) agonist 8-hydroxy-2-(di-n-propylamino)tetralin on spontaneous activity, cocaine-induced hyperactivity and behavioral sensitization: a microanalysis of ambulation. J Pharmacol Exp Ther 292:610-617.

De Deurwaerdere P, Navailles S, Berg KA, Clarke WP, Spampinato U (2004) Constitutive activity of the serotonin2C receptor inhibits in vivo dopamine release in the rat striatum and nucleus accumbens. J Neurosci 24:3235-3241.

Decker K, Trager T, Missel A, Heitz K, Kobsch S, Machura K, Loffert D (2002) Optimizing probe hybridization in real-time PCR for quantification and SNP genotyping. Qiagen News 4:13-16.

Di Matteo V, De Blasi A, Di Giulio C, Esposito E (2001) Role of 5 HT2C receptors in the control of central dopamine function. Trends Pharmacol Sci 22:229-232.

Di Giovanni G, De Deurwaerdere P, Di MM, Di M, V, Esposito E, Spampinato U (1999) Selective blockade of serotonin-2C/2B receptors enhances mesolimbic and mesostriatal dopaminergic function: a combined in vivo electrophysiological and microdialysis study. Neuroscience 91:587-597.

Di Matteo V, Di GG, Di MM, Esposito E (1999) SB 242084, a selective serotonin2C receptor antagonist, increases dopaminergic transmission in the mesolimbic system. Neuropharmacology 38:1195-1205.

Dracheva S, Chin B, Haroutunian V (2008a) Altered serotonin 2C receptor RNA splicing in suicide: association with editing. Neuroreport 19:379-382.

Dracheva S, Elhakem SL, Marcus SM, Siever LJ, McGurk SR, Haroutunian V (2003) RNA editing and alternative splicing of human serotonin 2C receptor in schizophrenia. J Neurochem 87:1402-1412.

Dracheva S, Patel N, Woo DA, Marcus SM, Siever LJ, Haroutunian V (2008b) Increased serotonin 2C receptor mRNA editing: a possible risk factor for suicide. Mol Psychiatry 13:1001-1010.

Du Y, Davisson MT, Kafadar K, Gardiner K (2006) A-to-I pre-mRNA editing of the serotonin 2C receptor: comparisons among inbred mouse strains. Gene 382:39-46.

Dubovsky SL, Thomas M (1995) Beyond specificity: effects of serotonin and serotonergic treatments on psychobiological dysfunction. J Psychosom Res 39:429-444.

Eberle-Wang K, Mikeladze Z, Uryu K, Chesselet MF (1997) Pattern of expression of the serotonin2C receptor messenger RNA in the basal ganglia of adult rats. J Comp Neurol 384:233-247.

Ehrlich I, Klein M, Rumpel S, Malinow R (2007) PSD-95 is required for activity-driven synapse stabilization. Proc Natl Acad Sci U S A 104:4176-4181.

El-Husseini AE, Schnell E, Chetkovich DM, Nicoll RA, Bredt DS (2000) PSD-95 involvement in maturation of excitatory synapses. Science 290:1364-1368.

El-Husseini A, Schnell E, Dakoji S, Sweeney N, Zhou Q, Prange O, Gauthier-Campbell C, guilera-Moreno A, Nicoll RA, Bredt DS (2002) Synaptic strength regulated by palmitate cycling on PSD-95. Cell 108:849-863.

Elorza A, Penela P, Sarnago S, Mayor F, Jr. (2003) MAPK-dependent degradation of G protein-coupled receptor kinase 2. J Biol Chem 278:29164-29173.

Englander MT, Dulawa SC, Bhansali P, Schmauss C (2005) How stress and fluoxetine modulate serotonin 2C receptor pre-mRNA editing. J Neurosci 25:648-651.

Everitt BJ, Robbins TW (2005) Neural systems of reinforcement for drug addiction: from actions to habits to compulsion. Nat Neurosci 8:1481-1489.

Ferguson SM, Fasano S, Yang P, Brambilla R, Robinson TE (2006) Knockout of ERK1 enhances cocaine-evoked immediate early gene expression and behavioral plasticity. Neuropsychopharmacology 31:2660-2668.

Filip M, Bubar MJ, Cunningham KA (2004) Contribution of serotonin (5-hydroxytryptamine; 5-HT) 5-HT2 receptor subtypes to the hyperlocomotor effects of cocaine: Acute and chronic pharmacological analyses. J Pharmacol Exp Ther 310:1246-1254.

Filip M, Bubar MJ, Cunningham KA (2006) Contribution of serotonin (5-HT) 5-HT2 receptor subtypes to the discriminative stimulus effects of cocaine in rats. Psychopharmacology (Berl) 183:482-489.

Filip M, Cunningham KA (2002) Serotonin 5-HT(2C) receptors in nucleus accumbens regulate expression of the hyperlocomotive and discriminative stimulus effects of cocaine. Pharmacol Biochem Behav 71:745-756.

Filip M, Cunningham KA (2003) Hyperlocomotive and discriminative stimulus effects of cocaine are under the control of serotonin(2C) (5-HT(2C)) receptors in rat prefrontal cortex. J Pharmacol Exp Ther 306:734-743.

Filip M, Nowak E, Papla I (2001) On the role of serotonin2A/2C receptors in the sensitization to cocaine. J Physiol Pharmacol 52:471-481.

Fiore RS, Bayer VE, Pelech SL, Posada J, Cooper JA, Baraban JM (1993) p42 mitogen-activated protein kinase in brain: prominent localization in neuronal cell bodies and dendrites. Neuroscience 55:463-472.

Fitzgerald LW, Iyer G, Conklin DS, Krause CM, Marshall A, Patterson JP, Tran DP, Jonak GJ, Hartig PR (1999) Messenger RNA editing of the human serotonin 5-HT2C receptor. Neuropsychopharmacology 21:82S-90S.

Fletcher PJ, Chintoh AF, Sinyard J, Higgins GA (2004) Injection of the 5-HT2C receptor agonist Ro60-0175 into the ventral tegmental area reduces cocaine-induced ambulation and cocaine self-administration. Neuropsychopharmacology 29:308-318.

Fletcher PJ, Grottick AJ, Higgins GA (2002) Differential effects of the 5-HT(2A) receptor antagonist M100907 and the 5-HT(2C) receptor antagonist SB242084 on cocaine-induced ambulation, cocaine self-administration and cocaine-induced reinstatement of responding. Neuropsychopharmacology 27:576-586.

Fone KC, Austin RH, Topham IA, Kennett GA, Punhani T (1998) Effect of chronic m-CPP on locomotion, hypophagia, plasma corticosterone and 5-HT2C receptor levels in the rat. Br J Pharmacol 123:1707-1715.

Fumagalli F, Molteni R, Calabrese F, Frasca A, Racagni G, Riva MA (2005) Chronic fluoxetine administration inhibits extracellular signal-regulated kinase 1/2 phosphorylation in rat brain. J Neurochem 93:1551-1560.

Fuster JM (1997) The Preforntal Cortex: Anatomy, Physiology and Neuropsychology of the frontal lobe. PA: Lippincott-Raven.

Gabbott PL, Warner TA, Jays PR, Salway P, Busby SJ (2005) Prefrontal cortex in the rat: projections to subcortical autonomic, motor, and limbic centers. J Comp Neurol 492:145-177.

Garavan H, Hester R (2007) The role of cognitive control in cocaine dependence. Neuropsychol Rev 17:337-345.

Garavan H, Kaufman JN, Hester R (2008) Acute effects of cocaine on the neurobiology of cognitive control. Philos Trans R Soc Lond B Biol Sci 363:3267-3276.

Garavan H, Pankiewicz J, Bloom A, Cho JK, Sperry L, Ross TJ, Salmeron BJ, Risinger R, Kelley D, Stein EA (2000) Cue-induced cocaine craving: neuroanatomical specificity for drug users and drug stimuli. Am J Psychiatry 157:1789-1798.

Gavarini S, Becamel C, Altier C, Lory P, Poncet J, Wijnholds J, Bockaert J, Marin P (2006) Opposite effects of PSD-95 and MPP3 PDZ proteins on serotonin 5-hydroxytryptamine2C receptor desensitization and membrane stability. Mol Biol Cell 17:4619-4631.

Gavarini S, Becamel C, Chanrion B, Bockaert J, Marin P (2004) Molecular and functional characterization of proteins interacting with the C-terminal

domains of 5-HT2 receptors: emergence of 5-HT2 "receptosomes". Biol Cell 96:373-381.

Gawin FH (1989) Cocaine abuse and addiction. J Fam Pract 29:193-197.

Gawin FH (1991) Cocaine addiction: psychology and neurophysiology. Science 251:1580-1586.

Ghasemzadeh MB, Mueller C, Vasudevan P (2008a) Behavioral sensitization to cocaine is associated with increased glutamate receptor trafficking to the postsynaptic density after extended withdrawal period. Neuroscience - *in press.*

Ghasemzadeh MB, Vasudevan P, Mueller C (2008b) Locomotor sensitization to cocaine is associated with distinct pattern of glutamate receptor trafficking to the postsynaptic density in prefrontal cortex: Early versus late withdrawal effects. Pharmacol Biochem Behav - *in press*.

Giorgetti M, Tecott LH (2004) Contributions of 5-HT(2C) receptors to multiple actions of central serotonin systems. Eur J Pharmacol 488:1-9.

Girault JA, Valjent E, Caboche J, Herve D (2007) ERK2: a logical AND gate critical for drug-induced plasticity? Curr Opin Pharmacol 7:77-85.

Gobert A, Rivet JM, Lejeune F, Newman-Tancredi A, dhumeau-Auclair A, Nicolas JP, Cistarelli L, Melon C, Millan MJ (2000) Serotonin(2C) receptors tonically suppress the activity of mesocortical dopaminergic and adrenergic, but not serotonergic, pathways: a combined dialysis and electrophysiological analysis in the rat. Synapse 36:205-221.

Gold MS (1992) Cocaine (and Crack): Clinical Aspoects. In: Substance abuse: A comprehensive textbook pp 205-221. Baltimore, MD: Williams & Wilkins.

Goldstein RA, DesLauriers C, Burda AM (2009) Cocaine: history, social implications, and toxicity--a review. Dis Mon 55:6-38.

Goldstein RZ, Tomasi D, Rajaram S, Cottone LA, Zhang L, Maloney T, Telang F, ia-Klein N, Volkow ND (2007) Role of the anterior cingulate and medial orbitofrontal cortex in processing drug cues in cocaine addiction. Neuroscience 144:1153-1159.

Goldstein RZ, Volkow ND (2002) Drug addiction and its underlying neurobiological basis: neuroimaging evidence for the involvement of the frontal cortex. Am J Psychiatry 159:1642-1652.

Grottick AJ, Fletcher PJ, Higgins GA (2000) Studies to investigate the role of 5-HT(2C) receptors on cocaine- and food-maintained behavior. J Pharmacol Exp Ther 295:1183-1191.

Gundelfinger ED, Tom DS (2000) Molecular organization of excitatory chemical synapses in the mammalian brain. Naturwissenschaften 87:513-523.

Gurevich I, Englander MT, Adlersberg M, Siegal NB, Schmauss C (2002a) Modulation of serotonin 2C receptor editing by sustained changes in serotonergic neurotransmission. J Neurosci 22:10529-10532.

Gurevich I, Tamir H, Arango V, Dwork AJ, Mann JJ, Schmauss C (2002b) Altered editing of serotonin 2C receptor pre-mRNA in the prefrontal cortex of depressed suicide victims. Neuron 34:349-356.

Haber SN, Calzavara R (2009) The cortico-basal ganglia integrative network: the role of the thalamus. Brain Res Bull 78:69-74.

Hannon J, Hoyer D (2008) Molecular biology of 5-HT receptors. Behav Brain Res 195:198-213.

Hearing MC, See RE, McGinty JF (2008) Relapse to cocaine-seeking increases activity-regulated gene expression differentially in the striatum and cerebral cortex of rats following short or long periods of abstinence. Brain Struct Funct 213:215-227.

Heffner TG, Hartman JA, Seiden LS (1980) A rapid method for the regional dissection of the rat brain. Pharmacol Biochem Behav 13:453-456.

Herrick-Davis K, Grinde E, Niswender CM (1999) Serotonin 5-HT2C receptor RNA editing alters receptor basal activity: implications for serotonergic signal transduction. J Neurochem 73:1711-1717.

Higgins GA, Fletcher PJ (2003) Serotonin and drug reward: focus on 5-HT2C receptors. Eur J Pharmacol 480:151-162.

Hoffman BJ, Mezey E (1989) Distribution of serotonin 5-HT1C receptor mRNA in adult rat brain. FEBS Lett 247:453-462.

Hooks MS, Duffy P, Striplin C, Kalivas PW (1994) Behavioral and neurochemical sensitization following cocaine self-administration. Psychopharmacology (Berl) 115:265-272.

Hoopengardner B, Bhalla T, Staber C, Reenan R (2003) Nervous system targets of RNA editing identified by comparative genomics. Science 301:832-836.

Hoyer D, Hannon JP, Martin GR (2002) Molecular, pharmacological and functional diversity of 5-HT receptors. Pharmacol Biochem Behav 71:533-554.

Hunt CA, Schenker LJ, Kennedy MB (1996) PSD-95 is associated with the postsynaptic density and not with the presynaptic membrane at forebrain synapses. J Neurosci 16:1380-1388.

Hurley JH, Bloem LJ, Pavalko F, Liu J, Tian M, Simon JR, Yu L (1999) Structure-function studies of the eighth hydrophobic domain of a serotonin receptor. J Neurochem 72:413-421.

Hyman SE, Malenka RC, Nestler EJ (2006) Neural Mechanisms of Addiction: The Role of Reward-Related Learning and Memory. Annu Rev Neurosci. 29: 565-598.

Igo RP, Jr., Weston DS, Ernst NL, Panigrahi AK, Salavati R, Stuart K (2002) Role of uridylate-specific exoribonuclease activity in Trypanosoma brucei RNA editing. Eukaryot Cell 1:112-118.

Itzhak Y, Martin JL (2002) Cocaine-induced conditioned place preference in mice: induction, extinction and reinstatement by related psychostimulants. Neuropsychopharmacology 26:130-134.

Iwamoto K, Kato T (2002) Effects of cocaine and reserpine administration on RNA editing of rat 5-HT2C receptor estimated by primer extension combined with denaturing high-performance liquid chromatography. Pharmacogenomics J 2:335-340.

Iwamoto K, Kato T (2003) RNA editing of serotonin 2C receptor in human postmortem brains of major mental disorders. Neurosci Lett 346:169-172.

Iwamoto K, Nakatani N, Bundo M, Yoshikawa T, Kato T (2005) Altered RNA editing of serotonin 2C receptor in a rat model of depression. Neurosci Res 53:69-76.

Jenab S, Festa ED, Nazarian A, Wu HB, Sun WL, Hazim R, Russo SJ, Quinones-Jenab V (2005) Cocaine induction of ERK proteins in dorsal striatum of Fischer rats. Brain Res Mol Brain Res 142:134-138.

Ji SP, Zhang Y, Van CJ, Jiang W, Liao M, Li L, Wan Q, Backstrom JR, Zhang X (2006) Disruption of PTEN coupling with 5-HT2C receptors suppresses behavioral responses induced by drugs of abuse. Nat Med 12:324-329.

Jog MS, Kubota Y, Connolly CI, Hillegaart V, Graybiel AM (1999) Building neural representations of habits. Science 286:1745-1749.

Julius D, MacDermott AB, Axel R, Jessell TM (1988a) Molecular characterization of a functional cDNA encoding the serotonin 1c receptor. Science 241:558-564.

Julius D, MacDermott AB, Jessel TM, Huang K, Molineaux S, Schieren I, Axel R (1988b) Functional expression of the 5-HT1c receptor in neuronal and nonneuronal cells. Cold Spring Harb Symp Quant Biol 53 Pt 1:385-393.

Kalivas PW (1995) Interactions between dopamine and excitatory amino acids in behavioral sensitization to psychostimulants. Drug Alcohol Depend 37:95-100.

Kalivas PW (2001) Drug addiction: to the cortex.and beyond! Am J Psychiatry 158:349-350.

Kalivas PW (2008) Addiction as a pathology in prefrontal cortical regulation of corticostriatal habit circuitry. Neurotox Res 14:185-190.

Kalivas PW, O'Brien C (2008) Drug addiction as a pathology of staged neuroplasticity. Neuropsychopharmacology 33:166-180.

Kalivas PW, Pierce RC, Cornish J, Sorg BA (1998) A role for sensitization in craving and relapse in cocaine addiction. J Psychopharmacol 12:49-53.

Kalivas PW, Stewart J (1991) Dopamine transmission in the initiation and expression of drug- and stress-induced sensitization of motor activity. Brain Res Brain Res Rev 16:223-244.

Karch SB (1999) Cocaine: history, use, abuse. J R Soc Med 92:393-397.

Kelley AE, Berridge KC (2002) The neuroscience of natural rewards: relevance to addictive drugs. J Neurosci 22:3306-3311.

Koob GF, Sanna PP, Bloom FE (1998) Neuroscience of addiction. Neuron 21:467-476.

Kosten TR, Scanley BE, Tucker KA, Oliveto A, Prince C, Sinha R, Potenza MN, Skudlarski P, Wexler BE (2006) Cue-induced brain activity changes and relapse in cocaine-dependent patients. Neuropsychopharmacology 31:644-650.

Kutyavin IV, Afonina IA, Mills A, Gorn VV, Lukhtanov EA, Belousov ES, Singer MJ, Walburger DK, Lokhov SG, Gall AA, Dempcy R, Reed MW, Meyer RB, Hedgpeth J (2000) 3'-minor groove binder-DNA probes increase sequence specificity at PCR extension temperatures. Nucleic Acids Res 28:655-661.

Le Moal M, Koob GF (2007) Drug addiction: pathways to the disease and pathophysiological perspectives. Eur Neuropsychopharmacol 17:377-393.

Li T, Yan CX, Hou Y, Cao W, Chen T, Zhu BF, Li SB (2008) Cue-elicited drug craving represses ERK activation in mice prefrontal association cortex. Neurosci Lett 448:99-104.

Liu S, Bubar MJ, Lanfranco MF, Hillman GR, Cunningham KA (2007) Serotonin2C receptor localization in GABA neurons of the rat medial prefrontal cortex: implications for understanding the neurobiology of addiction. Neuroscience 146:1677-1688.

Liu S, Cunningham KA (2006) Serotonin2C receptors (5-HT2C R) control expression of cocaine-induced conditioned hyperactivity. Drug Alcohol Depend 81:275-282.

Livak KJ, Schmittgen TD (2001) Analysis of relative gene expression data using real-time quantitative PCR and the 2(-Delta Delta C(T)) Method. Methods 25:402-408.

Lopez-Gimenez JF, Tecott LH, Palacios JM, Mengod G, Vilaro MT (2002) Serotonin 5- HT (2C) receptor knockout mice: autoradiographic analysis of multiple serotonin receptors. J Neurosci Res 67:69-85.

Mancia F, Brenner-Morton S, Siegel R, Assur Z, Sun Y, Schieren I, Mendelsohn M, Axel R, Hendrickson WA (2007) Production and characterization of monoclonal antibodies sensitive to conformation in the 5HT2c serotonin receptor. Proc Natl Acad Sci U S A 104:4303-4308.

Marion S, Weiner DM, Caron MG (2004) RNA editing induces variation in desensitization and trafficking of 5-hydroxytryptamine 2c receptor isoforms. J Biol Chem 279:2945-2954.

Matsumoto RR, Liu Y, Lerner M, Howard EW, Brackett DJ (2003) Sigma receptors: potential medications development target for anti-cocaine agents. Eur J Pharmacol 469:1-12.

Mattson BJ, Bossert JM, Simmons DE, Nozaki N, Nagarkar D, Kreuter JD, Hope BT (2005) Cocaine-induced CREB phosphorylation in nucleus accumbens

of cocaine-sensitized rats is enabled by enhanced activation of extracellular signal-related kinase, but not protein kinase A. Journal of Neurochemistry 95:1481-1494.

Maydanovych O, Beal PA (2006) Breaking the central dogma by RNA editing. Chem Rev 106:3397-3411.

McCreary AC, Cunningham KA (1999) Effects of the 5-HT2C/2B antagonist SB 206553 on hyperactivity induced by cocaine. Neuropsychopharmacology 20:556-564.

McFarland K, Davidge SB, Lapish CC, Kalivas PW (2004) Limbic and motor circuitry underlying footshock-induced reinstatement of cocaine-seeking behavior. J Neurosci 24:1551-1560.

McFarland K, Lapish CC, Kalivas PW (2003) Prefrontal glutamate release into the core of the nucleus accumbens mediates cocaine-induced reinstatement of drug-seeking behavior. J Neurosci 23:3531-3537.

McGrew L, Price RD, Hackler E, Chang MS, Sanders-Bush E (2004) RNA editing of the human serotonin 5-HT2C receptor disrupts transactivation of the small G-protein RhoA. Mol Pharmacol 65:252-256.

McMahon LR, Filip M, Cunningham KA (2001) Differential regulation of the mesoaccumbens circuit by serotonin 5-hydroxytryptamine (5-HT)2A and 5-HT2C receptors. J Neurosci 21:7781-7787.

Melikian HE (2004) Neurotransmitter transporter trafficking: endocytosis, recycling, and regulation. Pharmacol Ther 104:17-27.

Mengod G, Nguyen H, Le H, Waeber C, Lubbert H, Palacios JM (1990a) The distribution and cellular localization of the serotonin 1C receptor mRNA in the rodent brain examined by in situ hybridization histochemistry. Comparison with receptor binding distribution. Neuroscience 35:577-591.

Mengod G, Pompeiano M, Martinez-Mir MI, Palacios JM (1990b) Localization of the mRNA for the 5-HT2 receptor by in situ hybridization histochemistry. Correlation with the distribution of receptor sites. Brain Res 524:139-143.

Molineaux SM, Jessell TM, Axel R, Julius D (1989) 5-HT1c receptor is a prominent serotonin receptor subtype in the central nervous system. Proc Natl Acad Sci U S A 86:6793-6797.

Molnar Z, Cheung AF (2006) Towards the classification of subpopulations of layer V pyramidal projection neurons. Neurosci Res 55:105-115.

Moron JA, Devi LA (2007) Use of proteomics for the identification of novel drug targets in brain diseases. J Neurochem 102:306-315.

Navailles S, Moison D, Cunningham KA, Spampinato U (2008) Differential regulation of the mesoaccumbens dopamine circuit by serotonin2C receptors in the ventral tegmental area and the nucleus accumbens: an in vivo microdialysis study with cocaine. Neuropsychopharmacology 33:237-246.

Navailles S, Moison D, Ryczko D, Spampinato U (2006) Region-dependent regulation of mesoaccumbens dopamine neurons in vivo by the constitutive activity of central serotonin2C receptors. J Neurochem 99:1311-1319.

Nic Dhonnchadha BA, Cunningham KA (2008) Serotonergic mechanisms in addiction-related memories. Behav Brain Res 195:39-53.

Niswender CM (1998) Recent advances in mammalian RNA editing. Cell Mol Life Sci 54:946-964.

Niswender CM, Copeland SC, Herrick-Davis K, Emeson RB, Sanders-Bush E (1999) RNA editing of the human serotonin 5-hydroxytryptamine 2C receptor silences constitutive activity. J Biol Chem 274:9472-9478.

Niswender CM, Herrick-Davis K, Dilley GE, Meltzer HY, Overholser JC, Stockmeier CA, Emeson RB, Sanders-Bush E (2001) RNA editing of the human serotonin 5-HT2C receptor. alterations in suicide and implications for serotonergic pharmacotherapy. Neuropsychopharmacology 24:478-491.

Niswender CM, Sanders-Bush E, Emeson RB (1998) Identification and characterization of RNA editing events within the 5-HT2C receptor. Ann N Y Acad Sci 861:38-48.

Nutt D, Lingford-Hughes A (2008) Addiction: the clinical interface. Br J Pharmacol 154:397-405.

Ortiz J, Harris HW, Guitart X, Terwilliger RZ, Haycock JW, Nestler EJ (1995) Extracellular signal-regulated protein kinases (ERKs) and ERK kinase (MEK) in brain: regional distribution and regulation by chronic morphine. J Neurosci 15:1285-1297.

Paris JM, Callahan PM, Lee JM, Cunningham KA (1991) Behavioral sensitization to cocaine is not associated with changes in serotonin (5-HT) fiber immunoreactivity in rat forebrain. Brain Res Bull 27:843-847.

Parker LL, Backstrom JR, Sanders-Bush E, Shieh BH (2003) Agonist-induced phosphorylation of the serotonin 5-HT2C receptor regulates its interaction with multiple PDZ protein 1. J Biol Chem 278:21576-21583.

Pasqualetti M, Ori M, Castagna M, Marazziti D, Cassano GB, Nardi I (1999) Distribution and cellular localization of the serotonin type 2C receptor messenger RNA in human brain. Neuroscience 92:601-611.

Pazos A, Castro ME, Del OE, Romon T, del AC (1998) Autoradiographic characterization, anatomical distribution, and developmental pattern of a new 5-HT site in human brain. Ann N Y Acad Sci 861:262.

Pazos A, Hoyer D, Palacios JM (1984a) Mesulergine, a selective serotonin-2 ligand in the rat cortex, does not label these receptors in porcine and human cortex: evidence for species differences in brain serotonin-2 receptors. Eur J Pharmacol 106:531-538.

Pazos A, Hoyer D, Palacios JM (1984b) The binding of serotonergic ligands to the porcine choroid plexus: characterization of a new type of serotonin recognition site. Eur J Pharmacol 106:539-546.

Pazos A, Palacios JM (1985) Quantitative autoradiographic mapping of serotonin receptors in the rat brain. I. Serotonin-1 receptors. Brain Res 346:205-230.

Pazos A, Probst A, Palacios JM (1987) Serotonin receptors in the human brain--IV. Autoradiographic mapping of serotonin-2 receptors. Neuroscience 21:123-139.

Phillips GR, Huang JK, Wang Y, Tanaka H, Shapiro L, Zhang W, Shan WS, Arndt K, Frank M, Gordon RE, Gawinowicz MA, Zhao Y, Colman DR (2001) The presynaptic particle web: ultrastructure, composition, dissolution, and reconstitution. Neuron 32:63-77.

Pierce RC, Kalivas PW (1997) A circuitry model of the expression of behavioral sensitization to amphetamine-like psychostimulants. Brain Res Brain Res Rev 25:192-216.

Pierce RC, Reeder DC, Hicks J, Morgan ZR, Kalivas PW (1998) Ibotenic acid lesions of the dorsal prefrontal cortex disrupt the expression of behavioral sensitization to cocaine. Neuroscience 82:1103-1114.

Pitcher JA, Tesmer JJ, Freeman JL, Capel WD, Stone WC, Lefkowitz RJ (1999) Feedback inhibition of G protein-coupled receptor kinase 2 (GRK2) activity by extracellular signal-regulated kinases. J Biol Chem 274:34531-34534.

Pompeiano M, Palacios JM, Mengod G (1994) Distribution of the serotonin 5-HT2 receptor family mRNAs: comparison between 5-HT2A and 5-HT2C receptors. Brain Res Mol Brain Res 23:163-178.

Post RM, Rose H (1976) Increasing effects of repetitive cocaine administration in the rat. Nature 260:731-732.

Poyau A, Vincent L, Berthomme H, Paul C, Nicolas B, Pujol JF, Madjar JJ (2007) Identification and relative quantification of adenosine to inosine editing in serotonin 2c receptor mRNA by CE. Electrophoresis 28:2843-2852.

Pranzatelli MR, Murthy JN, Tailor PT (1993) Novel regulation of 5-HT1C receptors: downregulation induced both by 5-HT1C/2 receptor agonists and antagonists. Eur J Pharmacol 244:1-5.

Przegalinski E, Filip M, Papla I, Siwanowicz J (2001) Effect of serotonin (5-HT)1B receptor ligands on cocaine sensitization in rats. Behav Pharmacol 12:109-116.

Quirk K, Lawrence A, Jones J, Misra A, Harvey V, Lamb H, Revell D, Porter RH, Knight AR (2001) Characterisation of agonist binding on human 5-HT2C receptor isoforms. Eur J Pharmacol 419:107-112.

Radwanska K, Caboche J, Kaczmarek L (2005) Extracellular signal-regulated kinases (ERKs) modulate cocaine-induced gene expression in the mouse amygdala. Eur J Neurosci 22:939-948.

Rajadhyaksha A, Husson I, Satpute SS, Kuppenbender KD, Ren JQ, Guerriero RM, Standaert DG, Kosofsky BE (2004) L-type Ca2+ channels mediate adaptation of extracellular signal-regulated kinase 1/2 phosphorylation in the ventral tegmental area after chronic amphetamine treatment. J Neurosci 24:7464-7476.

Rauser L, Savage JE, Meltzer HY, Roth BL (2001) Inverse agonist actions of typical and atypical antipsychotic drugs at the human 5-hydroxytryptamine(2C) receptor. J Pharmacol Exp Ther 299:83-89.

Raymond JR, Mukhin YV, Gelasco A, Turner J, Collinsworth G, Gettys TW, Grewal JS, Garnovskaya MN (2001) Multiplicity of mechanisms of serotonin receptor signal transduction. Pharmacol Ther 92:179-212.

Rebrikov DV, Trofimov DI (2006) [Real-time PCR: approaches to data analysis (a review)]. Prikl Biokhim Mikrobiol 42:520-528.

Reilly MT, Cunningham KA, Natarajan A (2009) Protein-protein interactions as therapeutic targets in neuropsychopharmacology. Neuropsychopharmacology 34:247-248.

Ritz MC, Cone EJ, Kuhar MJ (1990) Cocaine inhibition of ligand binding at dopamine, norepinephrine and serotonin transporters: a structure-activity study. Life Sci 46:635-645.

Robinson TE, Becker JB (1986) Enduring changes in brain and behavior produced by chronic amphetamine administration: a review and evaluation of animal models of amphetamine psychosis. Brain Res 396:157-198.

Robinson TE, Berridge KC (1993) The neural basis of drug craving: an incentive-sensitization theory of addiction. Brain Res Brain Res Rev 18:247-291.

Roth BL, Willins DL, Kristiansen K, Kroeze WL (1998) 5-Hydroxytryptamine 2-Family Receptors (5-Hydroxytryptamine 2A, 5-Hydroxytryptamine 2B, 5-Hydroxytryptamine 2C): Where Structure Meets Function. Pharmacol Ther 79:231-257.

Sabio G, Reuver S, Feijoo C, Hasegawa M, Thomas GM, Centeno F, Kuhlendahl S, Leal-Ortiz S, Goedert M, Garner C, Cuenda A (2004) Stress- and mitogen-induced phosphorylation of the synapse-associated protein SAP90/PSD-95 by activation of SAPK3/p38gamma and ERK1/ERK2. Biochem J 380:19-30.

Samuel CE (2003) RNA editing minireview series. J Biol Chem 278:1389-1390.

Sanders-Bush E, Fentress H, Hazelwood L (2003) Serotonin 5-ht2 receptors: molecular and genomic diversity. Mol Interv 3:319-330.

Schaeffer HJ, Weber MJ (1999) Mitogen-activated protein kinases: specific messages from ubiquitous messengers. Mol Cell Biol 19:2435-2444.

Schefe JH, Lehmann KE, Buschmann IR, Unger T, Funke-Kaiser H (2006) Quantitative real-time RT-PCR data analysis: current concepts and the novel "gene expression's CT difference" formula. J Mol Med 84:901-910.

Schmauss C (2003) Serotonin 2C receptors: suicide, serotonin, and runaway RNA editing. Neuroscientist 9:237-242.

Schmittgen TD, Livak KJ (2008) Analyzing real-time PCR data by the comparative C(T) method. Nat Protoc 3:1101-1108.

Segal DS, Kuczenski R (1997) Behavioral alterations induced by an escalating dose-binge pattern of cocaine administration. Behav Brain Res 88:251-260.

Shippenberg T, Koob GF (2008) Chapter 97: Recent Advances in Animal Models of Drug Addiction. In: Neuropsychopharmacology: The Fifth Generation of Progress (Davis, K.L.; Charney, D.; Coyle, J.T.; Nemeroff, C. ed), pp 1381-1397. American College of Neuropsychopharmacology.

Sodhi MS, Airey DC, Lambert W, Burnet PW, Harrison PJ, Sanders-Bush E (2005) A rapid new assay to detect RNA editing reveals antipsychotic-induced changes in serotonin-2C transcripts. Mol Pharmacol 68:711-719.

Sodhi MS, Burnet PW, Makoff AJ, Kerwin RW, Harrison PJ (2001) RNA editing of the 5-HT(2C) receptor is reduced in schizophrenia. Mol Psychiatry 6:373-379.

Steketee JD (2003) Neurotransmitter systems of the medial prefrontal cortex: potential role in sensitization to psychostimulants. Brain Res Brain Res Rev 41:203-228.

Steketee JD (2005) Cortical mechanisms of cocaine sensitization. Crit Rev Neurobiol 17:69-86.

Suzuki T, Mitake S, Murata S (1999) Presence of up-stream and downstream components of a mitogen-activated protein kinase pathway in the PSD of the rat forebrain. Brain Res 840:36-44.

Suzuki T, Okumura-Noji K, Nishida E (1995) ERK2-type mitogen-activated protein kinase (MAPK) and its substrates in postsynaptic density fractions from the rat brain. Neurosci Res 22:277-285.

Thomas MJ, Kalivas PW, Shaham Y (2008) Neuroplasticity in the mesolimbic dopamine system and cocaine addiction. Br J Pharmacol 154:327-342.

Tohda M, Nomura M, Nomura Y (2006) Molecular pathopharmacology of 5-HT2C receptors and the RNA editing in the brain. J Pharmacol Sci 100:427-432.

Tzschentke TM (2000) The medial prefrontal cortex as a part of the brain reward system. Amino Acids 19:211-219.

Valjent E, Corvol JC, Pages C, Besson MJ, Maldonado R, Caboche J (2000) Involvement of the extracellular signal-regulated kinase cascade for cocaine-rewarding properties. J Neurosci 20:8701-8709.

Valjent E, Corvol JC, Trzaskos JM, Girault JA, Herve D (2006) Role of the ERK pathway in psychostimulant-induced locomotor sensitization. BMC Neurosci 7:20.

Valjent E, Pages C, Herve D, Girault JA, Caboche J (2004a) Addictive and non-addictive drugs induce distinct and specific patterns of ERK activation in mouse brain. Eur J Neurosci 19:1826-1836.

Valjent E, Pages C, Herve D, Girault JA, Caboche J (2004b) Addictive and non-addictive drugs induce distinct and specific patterns of ERK activation in mouse brain. Eur J Neurosci 19:1826-1836.

Van Oeleken D, Luyten WH, Leysen JE (2003) 5-HT2A and 5-HT2C receptors and their atypical regulation properties. Life Sci 72:2429-2449.

Vanderschuren LJ, Kalivas PW (2000) Alterations in dopaminergic and glutamatergic transmission in the induction and expression of behavioral sensitization: a critical review of preclinical studies. Psychopharmacology (Berl) 151:99-120.

Varadaraj K, Skinner DM (1994) Denaturants or cosolvents improve the specificity of PCR amplification of a G + C-rich DNA using genetically engineered DNA polymerases. Gene 140:1-5.

Vetulani J (2001) Drug addiction. Part II. Neurobiology of addiction. Pol J Pharmacol 53:303-317.

Volkow N (2004) Drug dependence and addiction, III: Expectation and brain function in drug abuse. Am J Psychiatry 161:621.

Volkow ND, Li TK (2004) Drug addiction: the neurobiology of behaviour gone awry. Nat Rev Neurosci 5:963-970.

Wanat MJ, Bonci A (2008) Dose-dependent changes in the synaptic strength on dopamine neurons and locomotor activity after cocaine exposure. Synapse 62:790-5.

Wang Q, O'Brien PJ, Chen CX, Cho DS, Murray JM, Nishikura K (2000) Altered G protein-coupling functions of RNA editing isoform and splicing variant serotonin2C receptors. J Neurochem 74:1290-1300.

Werry TD, Gregory KJ, Sexton PM, Christopoulos A (2005) Characterization of serotonin 5-HT2C receptor signaling to extracellular signal-regulated kinases 1 and 2. J Neurochem 93:1603-1615.

Werry TD, Loiacono R, Sexton PM, Christopoulos A (2008a) RNA editing of the serotonin 5HT2C receptor and its effects on cell signalling, pharmacology and brain function. Pharmacol Ther 119:7-23.

Werry TD, Stewart GD, Crouch MF, Watts A, Sexton PM, Christopoulos A (2008b) Pharmacology of 5HT(2C) receptor-mediated ERK1/2 phosphorylation: agonist-specific activation pathways and the impact of RNA editing. Biochem Pharmacol 76:1276-1287.

Wexler BE, Gottschalk CH, Fulbright RK, Prohovnik I, Lacadie CM, Rounsaville BJ, Gore JC (2001) Functional magnetic resonance imaging of cocaine craving. Am J Psychiatry 158:86-95.

White FJ, Kalivas PW (1998) Neuroadaptations involved in amphetamine and cocaine addiction. Drug Alcohol Depend 51:141-153.

Wolf ME (1998) The role of excitatory amino acids in behavioral sensitization to psychomotor stimulants. Prog Neurobiol 54:679-720.

Wolf ME, Sun X, Mangiavacchi S, Chao SZ (2004) Psychomotor stimulants and neuronal plasticity. Neuropharmacology 47 Suppl 1:61-79.

Wong ML, Medrano JF (2005) Real-time PCR for mRNA quantitation. Biotechniques 39:75-85.

Xie E, Zhu L, Zhao L, Chang LS (1996) The human serotonin 5-HT2C receptor: complete cDNA, genomic structure, and alternatively spliced variant. Genomics 35:551-561.

Yao WD, Gainetdinov RR, Arbuckle MI, Sotnikova TD, Cyr M, Beaulieu JM, Torres GE, Grant SG, Caron MG (2004) Identification of PSD-95 as a regulator of dopamine-mediated synaptic and behavioral plasticity. Neuron 41:625-638.

Yao Y, Nellaker C, Karlsson H (2006) Evaluation of minor groove binding probe and Taqman probe PCR assays: Influence of mismatches and template complexity on quantification. Mol Cell Probes 20:311-316.

VITA

María Fé Lanfranco Gallofré was born in Lima, Peru on March 22, 1978 to Luis Orlando Lanfranco Nosiglia and Ana María Gallofré Cassadó de Lanfranco. Ms. Lanfranco attended Universidad Peruana Cayetano Heredia for her Bachelor of Science degree in biology. She also obtained her degree of Licenciado en biologia at Universidad Peruana Cayetano Heredia. Ms. Lanfranco came to the University of Texas Medical Branch in Galveston, TX to pursue her Ph.D. in Pharmacology and Toxicology in the fall of 2003. Throughout her graduate career, Ms. Lanfranco received several honors including the Jason E. Perlman Research Award (2007) and the George Palmer Saunders II Memorial Scholarship (2008). Ms. Lanfranco, as the Pharmacology and Toxicology Program Student representative, was involved in several activities held by the Graduate School Organization (2004-2006). She was also a cofounder of the Pharmacology Student Organization (2006) where she served as secretary (2006-2007). She also served as a student representative on the Graduate School of Biological Sciences (GSBS) Curriculum Committee (2004-2008).

Education

2003-2009: Pharmacology and Toxicology, Ph.D. Program Candidate, University of Texas Medical Branch, Graduate School of Biomedical Science, Galveston, TX, USA.

2003: Biology, Licenciado in Science, mention in Biology, Universidad Peruana Cayetano Heredia, Facultad de Ciencias y Filosofía, Lima, Peru.

1997-2001: Science and Philosophy, B.Sc, Universidad Peruana Cayetano Heredia, Facultad de Ciencias y Filosofía, [Top 10%], Lima, Peru.

Publications

M.F. Lanfranco, P.K. Seitz, R.B. Emeson, E. Sanders-Bush and K.A. Cunningham (2008) “An Innovative Real-Time PCR Method to Measure Changes in RNA Editing of the Serotonin 2C Receptor (5-HT_{2C}R) in Brain” Journal of Neuroscience Methods – in press.

Liu S.; Bubar, M.J.; **Lanfranco M.F.**; Hillman, G.R.; Cunningham, K.A. (2007) Serotonin 2C Receptor (5-HT_{2C}R) Localization in GABA Neurons of the Rat Medial Prefrontal Cortex: Implications for Understanding the Neurobiology of Addiction, Neuroscience. 146:1677–1688.

This dissertation was typed by María Fé Lanfranco Gallofré